



**DEVELOPMENT AND APPLICATIONS OF
PROTON TRANSFER REACTION-MASS
SPECTROMETRY FOR HOMELAND
SECURITY: TRACE DETECTION OF
EXPLOSIVES**

by

Ramón González-Méndez, MSc

A thesis submitted to the University of Birmingham

for the degree of

DOCTOR OF PHILOSOPHY

School of Physics and Astronomy
The University of Birmingham, UK

February 2017

UNIVERSITY OF
BIRMINGHAM

University of Birmingham Research Archive

e-theses repository

This unpublished thesis/dissertation is copyright of the author and/or third parties. The intellectual property rights of the author or third parties in respect of this work are as defined by The Copyright Designs and Patents Act 1988 or as modified by any successor legislation.

Any use made of information contained in this thesis/dissertation must be in accordance with that legislation and must be properly acknowledged. Further distribution or reproduction in any format is prohibited without the permission of the copyright holder.

Abstract

This thesis investigates the challenging task of sensitive and selective trace detection of explosive compounds by means of proton transfer reaction mass spectrometry (PTR-MS). In order to address this, new analytical strategies and hardware improvements, leading to new methodologies and analytical tools, have been developed and tested. These are, in order of the Chapters presented in this thesis, the switching of reagent ions, the implementation of a novel thermal desorption unit, and the use of an ion funnel drift tube or fast reduced electric field switching to modify the ion chemistry. In addition to these, a more fundamental study has been undertaken to investigate the reactions of picric acid (PiA) with a number of different reagent ions. The novel approaches described in this thesis have improved the PTR-MS technique by making it more versatile in terms of its analytical performance, namely providing assignment of chemical compounds with high confidence. These techniques are going to be employed in the new generation of PTR-MS instruments being developed by KORE Technology Ltd. Although demonstrated for Homeland Security in this thesis, the developments made can be utilised for improved selectivity in areas such as atmospheric chemistry, and in the environmental, food and health sciences. These techniques have resulted in a more multidimensional and versatile instrument, providing a step change in the analytical applications of PTR-MS for either commercial or research exploitation.

Quiero dedicar esta tesis doctoral a mis padres, José Ramón y Marisol, a quienes les debo todo. No hay palabras suficientes para expresarles mi agradecimiento por su bondad y afecto incondicional mostrado a lo largo de todos estos largos años. Sin ellos nada hubiese sido posible. De todo corazón, ¡os quiero!

“That which does not destroy us makes us stronger”

Friedrich Nietzsche 1844-1900

“Life can only be understood backwards; but it must be lived forwards.”

Søren Kierkegaard 1813-1855

“Confía en el tiempo, que suele dar dulces salidas a muchas amargas dificultades”

Miguel de Cervantes Saavedra 1547-1616

Acknowledgements

It is my pleasure to thank here those individuals without whom this thesis would, undoubtedly, not be possible. I would firstly like to thank my supervisor, Dr. Chris. A. Mayhew, for giving me the opportunity to work within his research group. I thank you for all your support, trust and the opportunities for being attracted to the scientific world and, in a broader context, to a new life abroad from my home town. An immense cheers for all that.

I would also like to thank Dr. Peter Watts, particularly for his vast knowledge of chemistry and his scientific experience. His contributions and enthusiasm were instrumental in enhancing the quality of the science.

Thank you also to Kore Technology Ltd. and particularly to Dr. Fraser Reich for all his support, commitment and time put into the scientific collaboration and beyond. His insight and guidance greatly improved the quality of the research presented in this thesis. Besides that, I really appreciate Fraser very much for opening his home to me. I do not have words to express my gratitude.

I would like to thank all the work colleagues of the Molecular Physics Group: Raquel, Danny, Prema, Dave Howse, John Thompson and Kathleen Hynes, for all the laughs (and discussions) and anecdotes for the future.

I would also like to acknowledge financial support from the European Union (Proton Ionisation Molecular Mass Spectrometry-ITN Project) under FP7 Marie Skłodowska-Curie Actions (Grant Agreement Number 287382), the Innovative Research Call in Explosives and Weapons Detection 2010 (a Cross-Government programme sponsored by a number of Departments and Agencies under the UK Government's CONTEST strategy in partnership with the US Department of Homeland Security) and the Defence Science and Technology Laboratory.

List of publications

During the course of my postgraduate study within the School of Physics and Astronomy at the University of Birmingham, the following articles, conference abstracts and talks were accepted for publication and/or presentation at conferences.

Academic Journal papers

Published (in order of publication date)

1. P. Sulzer, B. Agarwal, S. Jürschik, M. Lanza, A. Jordan, E. Hartungen, G. Hanel, L.Märk, T. D. Märk, **R. González-Méndez**, P. Watts, C. A. Mayhew. **Applications of switching reagent ions in proton transfer reaction mass spectrometric instruments for the improved selectivity of explosive compounds.** *International Journal of Mass Spectrometry* 354–355 (2013), 123–128. <http://dx.doi.org/10.1016/j.ijms.2013.05.004>
2. Bishu Agarwal, **Ramón González-Méndez**, Matteo Lanza, Philipp Sulzer, Tilmann D. Märk, Neil Thomas and Chris A. Mayhew. **Sensitivity and Selectivity of Switchable Reagent-Ion Soft Chemical Ionisation Mass Spectrometry for the Detection of Picric Acid.** *The Journal of Physical Chemistry Part A*, 2014, 118 (37), pp 8229–8236. <http://dx.doi.org/10.1021/jp5010192>
3. Carolina Matias, Andreas Mauracher, Stefan E Huber, Stephan Denifl, Paulo Limão-Vieira, Paul Scheier, Tilmann D Märk, **Ramón González-Méndez**, and Chris Mayhew. **Dissociative electron attachment to the volatile anaesthetics enflurane and isoflurane and the chlorinated ethanes pentachloroethane and hexachloroethane.** *International Journal of Mass Spectrometry* 379 (2015) 179–186. <http://dx.doi.org/10.1016/j.ijms.2015.01.009>
4. **Ramón González-Méndez**, D. Fraser Reich, Stephen J. Mullock, Clive A. Corlett, Peter Watts and Chris A. Mayhew. **Development and use of a thermal desorption unit and proton transfer reaction mass spectrometry for trace explosive detection: determination of the limits of detection and an investigation of memory effects.** *International Journal of Mass Spectrometry* 385 (2015) 13–18. <http://dx.doi.org/10.1016/j.ijms.2015.05.003>

5. **Ramón González-Méndez**, Peter. Watts, David Olivenza-León, D. Fraser Reich, Stephen J. Mullock, Clive A. Corlett, Stuart Cairns, Peter Hickey, Matthew Brooks, and Chris A. Mayhew. **Enhancement of compound selectivity using a radio frequency ion-funnel proton transfer reaction mass spectrometer: improved specificity for explosive compounds.** *Analytical Chemistry*, 2016, 88 (21), 10624-10630. <http://dx.doi.org/10.1021/acs.analchem.6b02982>
6. Materić, D., Blenkhorn, D., **González-Méndez, R.**, Bruhn, D., Turner, C., Mason, N., Morgan, G., and Gauci, V. **Monoterpene emission from young scots pine may be influenced by nutrient availability.** *Applied Ecology and Environmental Research*. 2016, 14 (4), 667- 681. http://dx.doi.org/10.15666/aeer/1404_667681
7. **Ramón González-Méndez**, Peter Watts, David C. Howse, Immacolata Procino, Henry McIntyre and Chris A. Mayhew. **Ion mobility studies on the negative ion-molecule chemistry of isoflurane and enflurane.** *Journal of The American Society for Mass Spectrometry*, 2017, 28 (5), 939-946. <http://dx.doi.org/10.1007/s13361-017-1616-0>
8. **Ramón González-Méndez**, Peter Watts, David C. Howse, Immacolata Procino, Steven Taylor, Henry McIntyre and Chris A. Mayhew. **Ion mobility studies on the negative ion-molecule chemistry of pentachloroethane.** *International Journal of Mass Spectrometry* (2017) *In press*.

Submitted

1. Célia Lourenço, **Ramón González-Méndez**, Fraser Reich, Nigel Mason and Claire Turner. **A potential method for comparing instrumental analysis of breath gas volatile organic compounds using standards calibrated for the gas phase.** *Submitted to International Journal of Mass Spectrometry*.

In preparation

1. **Ramón González-Méndez**, Peter. Watts, D. Fraser Reich, Stephen J. Mullock, Stuart Cairns, Peter Hickey, Matthew Brooks, and Chris A. Mayhew. **Enhancing proton transfer reaction-mass spectrometry selectivity using rapid reduced electric field switching.**

2. **Ramón González-Méndez**, Peter Watts and Chris A. Mayhew. **Proton transfer reaction mass spectrometry and the detection of explosive taggants. A study of reactivity in the gas phase.**
3. **Ramón González-Méndez**, Peter Watts and Chris A. Mayhew. **Proton transfer reaction mass spectrometry and nitroanilines.**

Abstracts

1. **Ramón González-Méndez**, Bishu Agarwal, Matteo Lanza, Philipp Sulzer, Tilmann D. Mark, Neil Thomas and Chris A. Mayhew. **Sensitivity and selectivity of switchable reagent-ion soft chemical ionisation for the detection of picric acid.** Accepted for poster presentation at XIXth International Symposium on Atomic, Cluster and Surface Physics, 2014. Universitätszentrum Obergurgl, Austria
2. **Ramón González-Méndez**, Fraser Reich, Steve Mullock, Clive Corlett, Peter Watts and Chris A. Mayhew. **The application of a recently developed thermal desorption unit for the detection of traces of explosives using proton transfer reaction time of flight mass spectrometry.** Accepted for poster presentation at 20th International Mass Spectrometry Conference, 2014. Geneva, Switzerland
3. **Ramón González-Méndez**, Peter Watts, Fraser Reich and Chris A. Mayhew. **Proton Transfer reaction-mass spectrometry for trace explosive detection.** Accepted for poster presentation at Molecular Physics Workshop. Caen, France
4. **Ramón González-Méndez**, Peter Watts, Fraser Reich and Chris A. Mayhew. **Enhancing selectivity and sensitivity in the determination of TNT using an ion funnel and proton-transfer-reaction mass spectrometry.** Accepted for poster presentation at Spectrometry for Security Applications Workshop, 2015. Birmingham (UK)
5. **Ramón González-Méndez**, Peter Watts, David C. Howse, Immacolata Procino, Henry McIntyre, and Chris A. Mayhew. **Ion mobility studies on the negative ion-molecule chemistry of pentachloroethane.** Accepted for poster presentation at Spectrometry for Security Applications Workshop, 2016. Birmingham (UK)

Invited talks

1. **Ramón González-Méndez. Applications of PTR-MS to Homeland Security: trace detection of explosives.** June 2014. Talk at PIMMS Science Workshop, Jülich (Germany)
2. **Ramón González-Méndez. Improvements in sensitivity and selectivity using PTR-MS and its applications for Homeland Security.** July 2015. Talk at PIMMS Science Workshop, Caen (France)
3. **Ramón González-Méndez. Applications of Proton Transfer Reaction Mass Spectrometry for Explosive Detection** December 2016. Invited talk at Spectrometry for Security Applications. Workshop, Birmingham (UK)

List of abbreviations

‡	Denotes transition state	DT	Drift Tube
Δ	Denotes change (increment)	E	Electric Field Strength
1,3-DNB	1,3-dinitrobenzene	E/N	Reduced electric field (in Townsends)
2,4-DNT	2,4- dinitrotoluene	EGDN	Ethylene glycol dinitrate (1,2-dinitroxyethane)
2,6-DNT	2,6- dinitrotoluene	EI	Electron impact or electron ionisation
3,4-DNT	3,4- dinitrotoluene	ESI	Electrospray Ionisation
A ⁰	Amstrong (=10 ⁻¹⁰ m)	eV	electron-volt
amu	Atomic Mass Unit	Femto	Femto equals to 10 ⁻¹⁵
anti	Chemistry jargon for indicating two substituents are located “on opposite sides” of a reference plane	G	Gibbs free energy
AP	Amonium perchlorate (NH ₄ ClO ₄)	GB	Gas Basicity
APCI	Atmospheric Pressure Chemical Ionisation	GC	Gas Chromatography
B3LYP	Becke, 3-parameter, Lee-Yang-Parr (approximation used for DFT calculations)	GC-MS	Gas Chromatography-Mass Spectrometry
CI	Chemical Ionisation	H	Enthalpy (or hydrogen atom)
CID	Collision Induced Dissociation	H ₂ O ₂	Hydrogen peroxide
cps	counts per second	HC	Hollow cathode ion source
CWA	Chemical Warfare Agent	HCHO	Formaldehyde
DADP	Diacetone diperoxide	HCN	Hydrogen cyanide
DATB	Diaminotrinitrobenzene	HMTD	Hexamethylene triperoxide diamine
DC	Direct current	HMX	Octahydro-1,3,5,7-tetranitro-1,3,5,7-tetrazocine
DFT	Density Functional Theory	HNS	Hexanitrostilbene
DSTL	Defence Science and Technology Laboratory	IE	Ionization energy

IED	Improvised explosive device	NG	Nitroglycerine (1,2,3-Trinitroxypropane)
IF	Ion Funnel	NICI	Negative-ion-chemical ionization
IMS	Ion mobility Spectrometry	NIST	National Institute of Standards and Technology
IP	Ionisation Potential	NM	Nitromethane
K	Kelvin	NT	Nitrotoluene (2-NT, 3-NT or 4-NT)
k _B	Boltzmann constant = 1.3806488 × 10 ²³ J·K ⁻¹	°C	Celsius or centigrade degree
kHz	KiloHerzt (unit of frequency in the SI of units) = 10 ³ Hz	PA	Proton Affinity
kJ	Kilojoule	PDMS	polydimethylsilicone
kV	Kilovolt	PETN	Pentaerythritol tetranitrate
LC	Liquid Chromatography	Picric Acid (PA, PiA)	2,4,6-trinitrophenol
LoD	Limit of Detection	PID	Product Ion Distribution
m/z	mass to charge ratio	ppm	part per million
mbar	millibar (where bar stand for a metric unit of pressure, but not SI)	ppm _v	part per million per volume
MCP	Multichannel plate	ppq	parts per quadrillion
mm	millimetre	ppt	parts per trillion
MRI	Multiple Reagent Ion	PSU	Power Supply Unit
MS	Mass Spectrometry	PTFE	Polytetrafluoroethylene (also known as Teflon®)
MS ⁿ	Tandem Mass Spectrometry (where n indicates the number of mass spectrometry stages)	PTR	Proton Transfer Reaction
N	Number Density	PTR-MS	Proton Transfer Reaction-Mass Spectrometry
N _A	Avogadro's number =6.022·10 ²³ mol ⁻¹	Quad	Quadrupole mass analyser
ncps	normalised counts per second	r ²	regression coefficient for a linear fitting
ng	monogram (=10 ⁻⁹ gram)	RDX	1,3,5-trinitroperhydro-1,3,5-triazine
		RE	Recombination Energy

Rf or RF	Radiofrequency	TATP	Triacetone Triperoxide () (3,3,6,6,9,9-Hexamethyl- 1,4,7-cyclononatriperoxane
RF-IF	Radiofrequency-ion funnel		
RSD	Relative standard deviation	Td	Townsend
SCIMS	Soft Chemical Ionisation Mass Spectrometry	TDU	Thermal Desorption Unit
SD	Source drift region	Tetryl	Methyl-2,4,6- trinitrophenylnitramine
Sec	Seconds	TNB	1,3,5-Trinitrobenzene
SIFT	Selected Ion Flow Tube	TNM	Tetranitromethane
SPME	Solid-phase microextraction	TNT	2,4,6-trinitrotoluene
SRI	Switchable Reagent Ions	ToF	Time of flight
STP	Standard Temperature and Pressure (T= 273.15K, p= 1 atmosphere)	ToF-MS	Time of Flight-Mass Spectrometry
syn	Chemistry jargon for indicating two substituents are located “on the same side” of a reference plane	torr	Torricelli (a unit of pressure, not SI units)
TATB	Triaminotrinitrobenzene	V _{drift}	Voltage applied to the drift tube
		VOC	Volatile Organic compound

List of tables

T 1.1	Chemicals found in ambient air together with chemical formula, proton affinities (in $\text{kJ}\cdot\text{mol}^{-1}$) and protonated mass	9
T 1.2	Summary of the physical properties of the explosive compounds investigated in order of increasing molecular weight	17
T 2.1	Reactions of ions produced by EI of water vapour within a hollow cathode discharge and their corresponding rate coefficients	41
T 2.2	Reactions leading to the production of impurity ions in the HC	43
T 2.3	Ionization and reaction pathways occurring in the HC for O_2^+ reagent ion production.	45
T 2.4	Ionization and reaction pathways occurring in the glow discharge for NO^+ reagent ion production.	46
T 4.1	Enthalpy and free energy changes for the reactions of H_3O^+ , $\text{H}_3\text{O}^+\cdot\text{H}_2\text{O}$ and $\text{H}_3\text{O}^+\cdot 2\text{H}_2\text{O}$ with picric acid (PiA) at 298 K calculated at the B3LYP 6-31+G(d,p) level	92
T 4.2	Enthalpy and free energy changes for the reactions of $\text{PiAH}^+\cdot n\text{H}_2\text{O}$ ($n = 0, 1$ or 2) with H_2O at 298 K calculated at the B3LYP 6-31+G(d,p) level	93
T 4.3	Enthalpy and free energy changes for the reactions of $\text{PiA}^+\cdot n\text{H}_2\text{O}$ ($n = 0, 1$ or 2) with H_2O at 298 K calculated at the B3LYP 6-31+G(d,p) level	100
T 5.1	Calculated limits of detection (LoD) for EGDN, 1,3-DNB, 3,4-DNT, HMTD, 1,3,5-TNB, RDX, NG, 2,4,6-TNT and PETN, presented in order of increasing molar mass	117
T 6.1	Energetics for the proton transfer from H_3O^+ to TNT calculated using the	139

B3LYP functional and the 6-31+G(d,p) basis set

T 6.2	Energetics for the elimination of water from TNT following proton transfer from H_3O^+ for the three stable structures shown in figure 6.6	140
T 6.3	Energetics for the elimination of water from (a) 2,4-DNT and (b) 2,6-DNT following proton transfer from H_3O^+	143
T 6.4	Energetics for the elimination of water from 2-NT following proton transfer from H_3O^+	145

List of figures

F 1.1	Increase in PTR-MS publications since its conception until the end of 2016	3
F 1.2	The natural logarithm of the ratio of experimental rate coefficients k_{exp} to calculated collisional rate coefficients k_{coll} , $k_{\text{exp}}/k_{\text{coll}}$, and its dependence on exoergicity at 298K	12
F 1.3	Plots of the vapour pressure of several common high explosives versus temperature	16
F 1.4	Classification of trace explosive detection techniques and analysis methods	20
F 2.1	Schematic diagram of the Kore PTR-ToF-MS used for the work presented in this thesis showing the main components and vacuum achieved in the different regions of the instrument	37
F 2.2	Schematic representation of a glow discharge and associated components	40
F 2.3	Schematic section of a cylindrical hollow cathode used in PTR-MS and its electrostatic potential distribution	41
F 2.4	Schematic of hollow cathode (or glow discharge), source drift region (SD) and part of the drift tube (named as PTR) used in Kore PTR-MS instruments	42
F 2.5	Schematic of the extra set of lenses for minimising back-diffusion from the reactor into the GD region of the instrument	44
F 2.6	Photograph of a Kore drift tube showing the electrodes stack, alignment rods and push-in pins for electric contacts	47
F 2.7	Schematic of the processes occurring within a drift tube	49
F 2.8	Residence time of the H_3O^+ ions in the DT of a PTR-MS instrument	52
F 2.9	Percentage product ion distribution (PID) of the water reagent ions present in the drift tube as a function of reduced electric field for the range 80-200 Td	54

F 2.10	Schematic cross-section of the Thermal Desorption Unit (TDU)	55
F 2.11	(a) Circular PTFE swab mounted onto card -real scale. (b) Details of the “pepper pot” that forces gas through the swab to desorb the compound of interest	56
F 2.12	Image of the swab inserted into the TDU and the coupling of the TDU to the inlet of the PTR-ToF-MS	57
F 2.13	Schematic representation of the Kore Technology Ltd. radio frequency ion funnel drift tube	58
F 2.14	Photographs of an RF-IF drift tube from a lateral (a) and axial view (b)	59
F 2.15	(a) Computer model simulation showing the funnel effect and how ions are funnelled towards the exit aperture of the DT (b) Ion trajectory calculated using SIMION	60
F 2.16	Schematics depicting the electronics for the fast E/N switching hardware implemented on the Kore PTR-ToF-MS Series I	61
F 3.1	RDX.NO ⁺ signal intensity as a function of the reduced electric field	74
F 3.2	Product ion branching ratios in percentages as a function of <i>E/N</i> resulting from the reaction of O ₂ ⁺ with TNT	75
F 3.3	Dependence of normalised product ion signal intensities involving TNB as a function of <i>E/N</i>	76
F 3.4	Plots illustrating the (a) switching between water and oxygen chemistry at approximately 110 seconds and back again at approximately 300 seconds and (b) rapidity of the switching (fully achieved within 10 seconds)	78
F 3.5	Changes in actual mass spectra as a result of changing from water to oxygen chemistry for (a) TNT and (b) TNB	80
F 3.6	Switching between water and NO chemistry and the resulting product ions observed for the explosive RDX	82

F 4.1	Structures for protonated picric acid corresponding to two possible conjugate acids	94
F 4.2	Variation in ion signal intensities for (a) the reagent ion H_3O^+ , (b) the unnormalised protonated picric acid and (c) the normalised (10^6 cps of H_3O^+) protonated picric acid as a function of E/N	95
F 4.3	Relative variation in ion signal intensities for normalised PiAH^+ as a function of E/N using dry N_2 and N_2 at 10% humidity as carrier gases	96
F 4.4	Variation in ion signal intensities for (a) the reagent ion O_2^+ , (b) the unnormalised PiA^+ and (c) the normalised (10^6 cps of O_2^+) PiA^+ as a function of E/N	97
F 4.5	Variation in relative ion signal intensities for normalised PiA^+ as a function of E/N recorded using normal laboratory air compared to using laboratory air at 10% humidity as a carrier gas	99
F 4.6	Variation in ion signal intensities for (a) the unnormalised PiA^+ and (b) the normalised (10^6 cps of O_2^+) PiA^+ signal intensities resulting from the reaction of O_2^+ with picric acid as a function of E/N in a “dry” reaction chamber for which high purity N_2 was used as the carrier gas	101
F 4.7	Variation in (a) O_2^+ ion signal intensity as a function of E/N and (b) the normalised (10^6 cps of O_2^+) PiA^+ as a function of E/N in a dry reaction chamber for which high purity He was used as the carrier gas	101
F 4.8	Variation in ion signal intensities for (a) NO^+ , (b) unnormalised $\text{PiA}.\text{NO}^+$ and (c) normalised (10^6 cps of H_3O^+) $\text{PiA}.\text{NO}^+$ as a function of E/N recorded using a PTR-TOF 8000	102
F4.9	Variation in ion signal intensities for (a) Kr^+ , (b) unnormalised PiA^+ and (c) normalised (10^6 cps of Kr^+) PiA^+ as a function of E/N recorded using a PTR-TOF 8000 in an extremely “dry” reaction chamber	104
F 5.1	Schematic cross-section of the KORE Technology Ltd. thermal desorption unit	114
F 5.2	Illustrative calibration curve showing the normalised ion counts (relative to 10^6 H_3O^+ counts per second) of protonated TNT (m/z 228) versus mass (ng) spotted onto a swab prior to thermal desorption	118

F 5.3	Thermal desorption chromatographic spectrum for 1 ng DNT deposited onto a clean swab, showing the intensity of DNTH ⁺ as a function of time from just before and after insertion and compression of the swab	119
F 5.4	Thermal desorption chromatographic spectra for 100 ng of RDX showing the product ion intensities for <i>m/z</i> 75 and <i>m/z</i> 46 as a function of time	119
F 5.5	Logarithmic thermal desorption chromatographic spectra for 50 ng of NG, showing the intensities of the product ions at <i>m/z</i> 228 (NGH ⁺) and <i>m/z</i> 46 (NO ₂ ⁺) at <i>E/N</i> values of (a) 80 Td and (b) 180 Td	120
F 5.6	Logarithmic thermal desorption chromatographic spectra for 50 ng of TNT with channels <i>m/z</i> 228 and 46 being monitored at the <i>E/N</i> values of (a) 80 Td and (b) 180 Td	121
F 6.1	Schematic representation of the KORE Technology Ltd. radio frequency ion funnel drift tube (proton transfer reaction (PTR) region). Also shown is the ion source region (glow discharge GD), and a source drift (SD) region	132
F 6.2	Ion intensities in counts per second (cps) of the water reagent ions present in the drift as a function of drift tube voltage (a) in DC-only mode and (b) in RF-mode (ion funnel on)	135
F 6.3	Product ion intensities as a function of drift tube voltage in RF mode for 100 ng of TNT	138
F 6.4	Intensities in ncps of the product ion [TNT-H ₂ O]H ⁺ as a function of drift tube voltage and RF amplitude (volts) with the frequency kept at 760 kHz (± 3%)	138
F 6.5	Two possible configurations resulting from protonation of TNT in the 2 position	139
F 6.6	Stable structures of the [TNT-H ₂ O]H ⁺ ion	140
F 6.7	Percentage product ion distributions resulting from the reaction of H ₃ O ⁺ with 2,6-DNT in RF-mode including the secondary process resulting in the association of the protonated molecule with water as a function of	142

supplied drift tube voltage

F 6.8	Percentage product ion distributions resulting from the reaction of H_3O^+ with 2,6-DNT in DC-only mode including the secondary process resulting in the association of the protonated molecule with water as a function reduced electric field	142
F 6.9	Percentage product ion distributions resulting from the reaction of H_3O^+ with 2-NT in (a) RF-mode and (b) DC-only mode as a function drift tube voltage. Included are also the secondary ion-molecule processes resulting in the association of the protonated molecule with water	144
F 7.1	Changes in the protonated water and protonated water clusters intensities as E/N is switched between 180 Td and 90 Td at a frequency of 1 Hz	155
F 7.2	Percentage product ion distribution (PID) results for (a) 2,4-DNT and (b) 2,6-DNT as a function of reduced electric field (70 to 230 Td)	156
F 7.3	1 Hz E/N switching between 70 Td and 230 Td for (a) 2,4-DNT and (b) 2,6-DNT	157
F 7.4	(a) PID as a function of reduced electric field covering the range 70-210 Td and (b) reduced electric field 2 Hz switching plots for HMTD	158
F 7.5	(a) PID as a function of reduced electric field covering the range 70-210 Td and (b) reduced electric field 1 Hz switching plots for RDX	159
F 7.6	(a) PID as a function of reduced electric field covering the range 70-190 Td and (b) reduced electric field 1 Hz switching plots for PETN	160
F 7.7	Application of combining radio frequency and fast drift tube voltage switching at 0.5 Hz between 20 and 190 V (equivalent to 30 and 180 Td in DC-mode only) for TNT	161

Thesis outline

This thesis is structured in 3 parts:

- (i) Part I consists of the first two Chapters. Chapter 1 provides a general introduction of proton transfer reaction-mass spectrometry and its applications to Homeland Security (focused on explosives). Chapter 2 presents and summarizes the basic instrumental operational principles of PTR-MS.
- (i) Part II is the main body of this thesis consisting of Chapters 3-7 and provides details on the results obtained from each study. Where available the published papers have been used (Chapters 3-6). Chapter 7 presents a draft of a paper currently being prepared for publication. The following summarises the contents of each Chapter:
- Chapter 3: Applications of switching reagent ions in proton transfer reaction mass spectrometric instruments for the improved selectivity of explosive compounds - 2,4,6-trinitrotoluene (TNT), 1,3,5-trinitrobenzene (TNB), pentaerythritoltetranitrate (PETN), and cyclotrimethylenetrinitramine (RDX).
 - Chapter 4: Sensitivity and selectivity of switchable reagent ion soft chemical ionization mass spectrometry for the detection of picric acid.
 - Chapter 5: Development and use of a thermal desorption unit and proton transfer reaction-mass spectrometry for trace explosive detection: determination of the instrumental limits of detection and an investigation of memory effects.
 - Chapter 6: Enhancement of compound selectivity using a radio frequency ion-funnel proton transfer reaction mass spectrometer: improved specificity for explosive compounds.
 - Chapter 7: Enhancing proton transfer reaction-mass spectrometry selectivity using rapid reduced electric field switching.
- (ii) Finally, in Part III, which is formed of two Chapters, conclusions and future work are discussed. Chapter 8 basically summarises the concluding remarks for each study and Chapter 9 covers the (potential) research pathways for future work.

Three publications not directly associated with the theme of the thesis, but for which I was involved with, are added in appendices A-C. Appendix A presents a dissociative electron attachment study in collaboration with the University of Innsbruck and the Molecular and Atomic Collisions Laboratory in Portugal. This work is directly related to the ion mobility (IMS) studies given in appendices B and C. The studies presented were in collaboration with Smiths Detection (Smiths Group PLC). Although related to PTR-MS methods, IMS instruments are operated at much higher pressures than PTR-MS, making the occurring chemistry completely different. Besides, both of the IMS studies were carried out in negative ion mode, in contrast to the positive ion mode used in the PTR-MS studies.

TABLE OF CONTENTS

Abstract.....	i
Acknowledgements	iv
List of publications	v
Academic Journal papers.....	v
Published (in order of publication date)	v
Submitted.....	vi
In preparation.....	vi
Abstracts	vii
Invited talks	viii
List of abbreviations	ix
List of tables	xii
List of figures	xiv
Thesis outline.....	xix
PART I: INTRODUCTION	1
CHAPTER 1.....	2
1.1 Introduction	3
1.2 Chemical ionisation. Introduction and fundamentals	5
1.2.1 Chemical ionisation and proton transfer reaction-mass spectrometry (PTR-MS)	8
1.2.1.1 Thermodynamics of proton transfer reactions.....	8
1.2.1.2 Kinetics of proton transfer reactions	10
1.2.1.1 - Other chemical reagent ion systems (used in PTR-MS)	13
1.3 Homeland security	14
1.3.1 Explosives.....	14
1.3.2 Analytical technologies for explosives detection	18
1.3.2.1 Proton transfer reaction mass spectrometry and the detection of explosives	21
1.4 Aims of the thesis	22
References.....	24

CHAPTER 2.....	35
2.1 Introduction	36
2.2 Physics and chemistry involved in PTR systems	39
2.2.1 Reagent ions generation: Hollow Cathode (HC) and Source Drift (SD)	39
2.2.1.1 Other chemical reagent ion systems	45
2.2.2 Ion- molecule reactions: Drift Tube or PTR reactor.....	47
2.2.2.1 Neutral gas residence time.....	50
2.2.2.2 Ion mobilities and reaction times	50
2.2.2.3 Ion-Molecule Collisions, ion temperatures and ion cluster distributions...	52
2.3 New hardware developments.....	55
2.3.1 Thermal desorption unit.....	55
2.3.2 Drift tube with implemented radio-frequency ion funnel.....	57
2.3.3 Rapid switching of the reduced electric field	60
References.....	63
PART II: EXPERIMENTAL RESULTS	67
CHAPTER 3: APPLICATIONS OF SWITCHING REAGENT IONS IN PROTON TRANSFER REACTION MASS SPECTROMETRIC INSTRUMENTS FOR THE IMPROVED SELECTIVITY OF EXPLOSIVE COMPOUNDS.....	68
3.1. Abstract.....	69
3.2. Introduction.....	70
3.3. Experimental Details.....	72
3.4. Results and Discussions.....	73
3.4.1 NO ⁺ Reactions	73
3.4.2 O ₂ ⁺ Reactions.....	74
3.4.3 Sensitivity Details.....	77
3.4.4 Switching Reagent Ions	77
3.5. Conclusions.....	82
3.6. Acknowledgements.....	83
3.7. References.....	84

CHAPTER 4: SENSITIVITY AND SELECTIVITY OF SWITCHABLE REAGENT ION SOFT CHEMICAL IONIZATION MASS SPECTROMETRY FOR THE DETECTION OF PICRIC ACID	87
4.1. Abstract.....	88
4.2 Introduction.....	89
4.3. Experimental and Theoretical Details.....	90
4.3.1 Electronic Structure Calculations	90
4.3.2 Experimental Methods.....	91
4.4. Results.....	92
4.4.1 Electronic structure calculations.....	92
4.4.2 Experimental Results	94
4.4.2.1 H ₃ O ⁺ Measurements.....	94
4.4.2.2 O ₂ ⁺ Measurements.....	97
4.4.2.3. NO ⁺ Measurements	101
4.4.2.4. Kr ⁺ Measurements.....	103
4.5. Concluding remarks	104
4.6. Acknowledgements.....	105
4.7. References.....	105
CHAPTER 5: DEVELOPMENT AND USE OF A THERMAL DESORPTION UNIT AND PROTON TRANSFER REACTION-MASS SPECTROMETRY FOR TRACE EXPLOSIVE DETECTION: DETERMINATION OF THE INSTRUMENTAL LIMITS OF DETECTION AND AN INVESTIGATION OF MEMORY EFFECTS.....	109
5.1. Abstract.....	110
5.2. Introduction.....	111
5.3. Experimental Details and Methods.....	112
5.3.1 Proton Transfer Reaction Mass Spectrometry (PTR-MS).....	112
5.3.2 Thermal Desorption Unit (TDU).....	113
5.3.3 Operational Parameters.....	114
5.3.4 Explosive Compounds	115
5.3.5 Determining Instrumental Limits of Detection.....	115
5.4. Results.....	116

5.4.1 Product ions	116
5.4.2 Instrumental Limits of Detection	116
5.4.3 Memory Effects	118
5.5. Discussions	121
5.5.1 Product ions and improved selectivity	121
5.5.2 TDU/PTR-MS instrumental limits of detection and comparisons with other instruments	122
5.5.3 Cycle times	123
5.6. Conclusions	123
5.7. Acknowledgements	124
5.8. References	124

**CHAPTER 6: ENHANCEMENT OF COMPOUND SELECTIVITY USING A RADIO
FREQUENCY ION-FUNNEL PROTON TRANSFER REACTION MASS
SPECTROMETER: IMPROVED SPECIFICITY FOR EXPLOSIVE COMPOUNDS**

.....	128
6.1. Abstract	129
6.2. Introduction	130
6.3. Methods	131
6.3.1 Experimental Details	131
6.3.2 Electronic Structure Calculations	134
6.4. Results and Discussion	134
6.4.1 Reagent ions	134
6.4.2 2,4,6-trinitrotoluene (TNT)	136
6.4.3 Dinitrotoluenes	141
6.4.4 Nitrotoluenes	143
6.5. Conclusions	145
6.6. Acknowledgements	145
6.7. References	146

CHAPTER 7: ENHANCING PROTON TRANSFER REACTION-MASS SPECTROMETRY SELECTIVITY USING RAPID REDUCED ELECTRIC FIELD SWITCHING

SWITCHING	148
7.1. Abstract	149
7.2. Introduction	150
7.3. Experimental Details	151
7.3.1 Proton Transfer Reaction Mass Spectrometry (PTR-MS)	151
7.3.2 Fast reduced electric field switching	152
7.3.3 Operational parameters	153
7.3.4 Explosive compounds	154
7.4. Results and Discussion	154
7.4.1 Reagent ions	154
7.4.2 Explosive compounds	155
7.4.2.1 2,4- and 2,6-dinitrotoluene	155
7.4.2.2 HMTD	157
7.4.2.3 RDX	158
7.4.2.4 PETN	159
7.4.3 Combination of switching the drift tube DC voltage and the radio frequency ion funnel: an application to TNT	160
7.5. Conclusions	161
7.6. Acknowledgements	162
7.7. References	162

PART III: CONCLUSIONS AND FUTURE WORK..... **166**

CHAPTER 8: CONCLUDING REMARKS **167**

8.1. Summary of Research Findings and their Implications	169
8.1.1 Use of different reagent ions	169
8.1.2 New thermal desorption unit inlet system	170
8.1.3 Enhancing sensitivity and selectivity through changes to collisional induced dissociation processes	171
8.2. References	172

CHAPTER 9: FUTURE WORK.....	175
9.1. Potential new research lines.....	176
9.2. References.....	178
APPENDICES.....	181
Appendix A: Dissociative electron attachment to the volatile anaesthetics enflurane and isoflurane and the chlorinated ethanes pentachloroethane and hexachloroethane	182
Appendix B: Ion mobility studies on the negative ion-molecule chemistry of isoflurane and enflurane	183
Appendix C: Ion mobility studies on the negative ion-molecule chemistry of pentachloroethane.....	185

PART I:
INTRODUCTION

CHAPTER 1

GENERAL INTRODUCTION

1.1 Introduction

Proton Transfer Reaction Mass Spectrometry (PTR-MS) was originally developed by Werner Lindinger and his team at the Institut für Ionenphysik at the Leopold-Franzens University Innsbruck during the mid-1990s for monitoring organic trace gases.¹ Trace concentrations are defined as parts per million by volume (ppm_v ; $1\text{ppm}_v = 1 \cdot 10^{-6}$) and below.² Importantly, PTR-MS uses H_3O^+ as the reagent ion, which acts as a probe to the environment. The technique's main characteristics are robustness, little or no sample preparation needed, fast, sensitive and on-line measurement capabilities of organic trace components in the gas phase. As gases participate in innumerable processes, the uses of PTR-MS to the analytical sciences have found more and more applications since its conception. This can be exemplified in figure 1, showing the growth of PTR-MS scientific publications since its origin until the end of 2016.

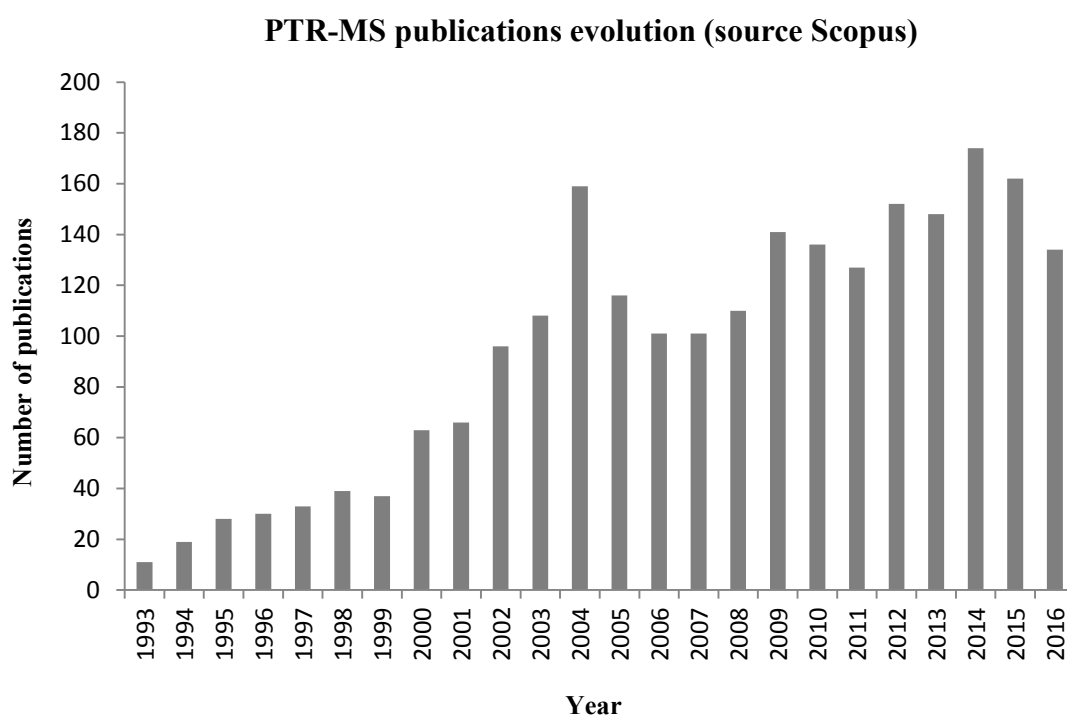


Figure 1.1: Increase in PTR-MS publications since its conception until the end of year 2016, illustrating the increase in the use of the technology. Source Scopus (words used “proton transfer reaction mass spectrometry” in Article Title, Abstract and Keywords). Last accessed 10/01/2017.

Currently, PTR-MS is mainly used in the environmental research field for the detection of anthropogenic and biogenic volatile organic compounds (VOCs), and particularly in atmospheric science. Food science is the second major field of application, closely followed by its use in the health sciences. A relatively new and growing application of PTR-MS is in the field of Homeland Security – the detection of traces of threat agents, e.g. explosives, chemical warfare agents and illicit drugs.³ A characteristic of the Homeland Security topic that makes it more challenging than when dealing with VOCs is that most of the analytes of interest are solids (at least at standard temperature and pressure). Therefore it is necessary to develop techniques to get explosives into the vapour phase and to keep them in this phase, so they are transferred effectively into the analytical instrument. This issue is dealt with in more detail in section 1.3 (page 14) and Chapters 2 (pages 35-66) and 5 (pages 109-127).

There are several analytical techniques designed to analyse compounds in trace quantities, and all have strengths and weaknesses. Among them all, probably, gas chromatography (GC) is the "gold-standard", and has been used for more than 50 years as a routine analytical technique in many laboratories around the world.^{4,5} Often GC is combined with mass spectrometry and an electron impact ionisation source. Users then make use of extensive mass spectral libraries to make identifications. The main weakness of GC is the long time necessary for an analysis, and even nowadays fast GCs require at least minutes for a complete separation. This is not fast enough for monitoring quick phenomena or where rapid analysis is needed, i.e. the quick chemical processes that can happen in the atmosphere or for use in security areas. Drift tube and/or flow tube based analytical techniques have a role to play here owing to the almost instantaneous analysis process. Provided that the analyte is in the gas phase in the drift tube the time resolution for PTR-MS is about 100 msec.³ Within this same category, a relevant technology is the Selected Ion Flow Tube (SIFT),^{6,7} which can easily achieve ppb_v (parts per billion by volume) sensitivity.⁶ An advantage of the SIFT technique is its ability to study reaction kinetics for a series of reagent ions unencumbered by other reagent ions being present. The main disadvantage of SIFT is the requirement to have an injection quadrupole mass spectrometer, which makes the instrument more complicated than a PTR-MS and which reduces the reagent ion intensity in the reaction region. Nevertheless, the company Syft Ltd. has developed and commercialised this technology and has designed the latest generation of instruments to be user friendly (improved and easy to use instrument

control and data analysis software) with claims of sensitivities down to 1 ppt_v within seconds.⁸

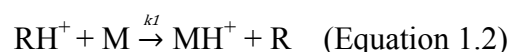
Atmospheric pressure chemical ionisation (APCI) is another approach to analyse ambient volatiles,⁹ where reagent ions are generated by means of a corona discharge and ionise the analyte sample by ion/molecule reactions. With the implementation of electrospray ionisation (ESI),¹⁰ APCI-MS has developed into a technique for the analysis of biological materials. A drawback for APCI is that it is high susceptible to chemical interferences, resulting in poor ionization efficiencies or excessive clustering.¹¹

Ion Mobility Spectrometry, introduced by Cohen and Kerasek in the 1970s,¹² is one of the most relevant drift tube technologies for security applications (drugs, explosives and chemical warfare agents, CWAs).^{13,14} IMS instruments rely solely on the mobility of the ions (mobility directly depending on various physical parameters including the size, shape, and charge of an ion, the type of buffer gas used) within the gas phase in a weak electric field of a drift tube at ambient pressure.¹⁵ IMS instruments are prone to false positives owing to their poor temporal resolution, thus, selectivity is one of the weaknesses of the technique.^{14,16} This is where PTR-MS has a role to play, as it shares some similarities with IMS and also APCI, but comes with its own distinctive advantages. When compared to IMS, the main technology used for security applications, limits of detection (LoDs) for most explosives are comparable. However, there is a higher confidence level in chemical compound assignment for PTR-MS owing to its mass spectrometric capabilities. Both techniques make use of a drift tube, but PTR-MS is operated at sub-atmospheric pressure whereas IMS is at atmospheric pressure. For explosives detection, IMS is usually run in negative ion mode, where association or hydride abstraction are common reaction mechanisms, whereas PTR-MS is operated in positive ion mode involving proton transfer reactions.

1.2 Chemical ionisation. Introduction and fundamentals

Chemical Ionisation (CI), is an ionisation method introduced by Munson and Field in 1966.¹⁷ Since then, the technique has been developed into a well-known and useful tool for analytical organic analysis, providing complementary information to other ionisation techniques.¹⁸⁻²⁰ In CI, the gas phase ionization of the analyte is achieved through an exothermic chemical reaction using positive or negative reagent ions (that can be atomic or molecular),³ typically

present at concentration levels $\leq 1\%$ of the reagent gas (present in large excess).²¹ Reagent ions are obtained, normally, by electron impact (or alternative methods such as photoionization or field ionization/desorption, to name a few), in an appropriate gas (equation 1.1). A simple chemical reaction for ionisation of an analyte molecule is proton transfer (the main process on which this Thesis is based), which can be written as in equation 1.2:



where R represents the reagent gas, RH^+ is the reagent ion in its positively charged form, M represents the analyte as a neutral, MH^+ the protonated parent ion and Z represents a third body; e^- represents an electron and k_I the bimolecular rate coefficient for the reaction.

MH^+ is susceptible to fragment to one or more product ions or even, although unlikely, react with the reagent gas R.²¹ When MH^+ , and/or its fragment ions, is mass analysed, this provides the CI mass spectrum for the analyte M and the reagent gas R.

In CI the reaction yield for the production of MH^+ depends on the kinetics of the ion/molecule reaction, on the concentration (partial pressures) of both RH^+ and M, and on the time available for both species to react.²¹ All these variables will be described shortly in the text.

Fast reactions, defined as the ones that proceed at the collisional rate, i.e. a reaction occurs with unit probability, are common for exothermic reactions, but only for proton transfer reactions is it true for every reaction. This makes proton transfer reaction mass spectrometry useful for analytical purposes.²¹

CI offers a series of advantages, namely:

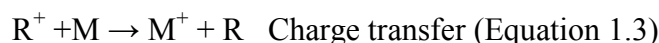
a) In comparison to other ionisation techniques, such as the most commonly used electron impact (EI), the lower energies involved during the ion/molecule reactions yields less fragmentation, often leaving the intact molecular species in its protonated parent ion form.^{1,3,21} EI makes uses of high energy electrons, about 70 eV, this being the optimum value to maximise collisional cross sections,²² and therefore producing high fragmentation yields. Most of the ionization potentials of organic molecules are around 8-12 eV,²³⁻²⁵ and a typical chemical bond energy is around 3 eV,^{25,26} thus when molecules are bombarded with such energetic electrons they tend to extensively fragment and subsequent processes such as rearrangements, transpositions and further fragmentation might happen, making the

interpretation of the mass spectra complicated. For comparison, PTR-MS, involves reaction processes whose energies are typically in the range of 0.1 to 0.4 eV (centre of mass frame).³

b) CI is a versatile ionization source suitable for different applications as it can be operated in either positive or negative ion modes. This is due to the fact that both positive and negative ions can be formed in the ion source plasma.²⁷ Only the polarity of the extraction voltages applied to the ion source would therefore dictate whether negative or positive ion mode is used.²⁸ This is slightly different for PTR-MS, where the reaction region is separated from the reagent ion source. Negative ion mode, or negative-ion-chemical ionization (NICI), is mostly used for explosive detection because explosives cannot often be detected in positive ion mode when using IMS. Among all the negative ion formation processes electron attachment or electron transfer are the most relevant, as most explosive compounds have high electron affinities.²⁹ An example of this work is shown in appendix A.

c) In CI the reagent gas, and hence the reagent ions, can be tailored to the particular chemical compound to be detected. The variety of reagent gases that has been successfully used is large.¹⁹ In positive ion mode examples include methane,²⁸ isobutene,^{30,31} acetone³² and ammonia,^{33,34} whilst for electron capture mode sulfur hexafluoride,³⁵ carbon dioxide,³⁶ and methane³⁷ are the most commonly used. In charge transfer processes singly ionised benzene,^{38,39} chlorobenzene,⁴⁰ Ar,⁴¹ and Xe,^{41,42} are frequently used as CI reagents.

Narrowing down all the possibilities mentioned, if we just refer to positive ion mode, depending on the type of reagent ion produced, different ion-molecule processes may take place. These are shown in equations 1.3 to 1.6:



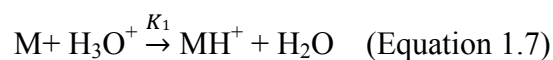
where X represents a third body to stabilise the adduct MR^+ .³

Charge transfer and proton transfer can both be dissociative or non-dissociative. Reactions 1.3 to 1.5 are usually very fast and, so they have been used to effectively ionise a given analyte.²¹

When referring to positive ion CI-MS, the most commonly used CI reagents are Brønsted acids, such as the RH^+ in equation 1.4. Those reagent ions are effective when the proton affinity of the acceptor molecule, M, exceeds that of the reagent species RH^+ , which makes the proton transfer thermodynamically feasible.

1.2.1 Chemical ionisation and proton transfer reaction-mass spectrometry (PTR-MS)

PTR-MS uses a variety of chemical ionization (CI), based upon equation 1.4, where the donor species is usually protonated water (also known as the hydronium ion, H_3O^+). We can therefore rewrite equation 1.4 to this specific case as:



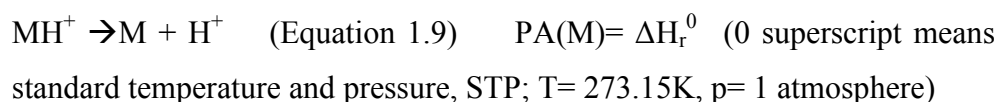
which always proceeds at the collisional rate providing the proton affinity (PA) of M is greater than that of H_2O , $\text{PA}(\text{M}) > \text{PA}(\text{H}_2\text{O})$.⁴³

1.2.1.1 Thermodynamics of proton transfer reactions

Equation 1.7 is thermodynamically feasible when $\Delta G < 0$ (Gibbs free energy). The thermodynamics for proton transfer reaction in the gas phase is influenced by two factors, namely the proton affinity (PA) - directly related to the enthalpy of the reaction - and gas phase basicity (GB) - related to the Gibbs free energy. The well-known Gibbs energy expression relates these factors according to equation 1.8:

$$\Delta G = \Delta H - T\Delta S \quad (\text{Equation 1.8})$$

The proton affinity of a molecule M in the gas phase is defined as the standard enthalpy (ΔH^0) for the reaction below

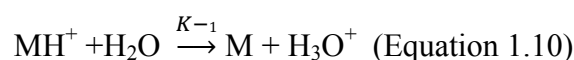


The gas phase basicity of a gaseous species is defined as the standard Gibbs free energy of the deprotonation for equation 1.7, so $\text{GB}(\text{M}) = \Delta G_r^0$.

Thus $GB(M) = PA(M) - T \cdot \Delta S_r^0$, where T is the temperature and ΔS_r^0 is the standard entropy change for the reaction, r . Changes in ΔS_r^0 are small for a proton transfer reaction, so we can approximate that $GB(M) \approx PA(M)$. Taking this into account, it is possible to use PA as a substitute for GB s when determining whether a reaction will be spontaneous.

For the generic proton transfer reaction shown in equation 1.7, $\Delta H_r^0 = -PA(M) + PA(H_2O)$, and $\Delta G_r^0 = -GB(M) + GB(H_2O)$. Proton transfer is exothermic when $\Delta H_r^0 < 0$ (that is $PA(H_2O) < PA(M)$), and is exoergic when $\Delta G_r^0 < 0$ (that is $GB(H_2O) < GB(M)$).

Considering equation 1.7, if $PA(M)$ is close to $PA(H_2O)$, the reverse reaction



will be significant. This reaction is endothermic, so the rate coefficient k_{-1} is much smaller than the forward reaction k_1 . However within the DT there is a high water excess plus an electric field, and in consequence this reaction, e.g. cases such as formaldehyde,⁴⁴ might be relevant.⁴⁵

Most organic species, M , fulfil the criterion $PA(M) > PA(H_2O)$,⁴³ whereas the main constituents of air, such as nitrogen, oxygen and carbon dioxide, do not (see Table 1.1 below). This implies that air can therefore be used as the buffer gas for the analysis of mixed samples because it does not interfere in the measurements. This is an extremely important advantage, as it simplifies the sampling and analysis. Moreover, the difference in proton affinities between analytes and reagent ions is generally small (less than 1 eV) and therefore the proton transfer ionisation process is regarded as soft -there is usually insufficient energy for bond breakage (although that is not always the case).

Table 1.1: Components found in ambient air with chemical formula, proton affinities (in kJ mol^{-1} (conversion factor, $96.485 \text{ kJ mol}^{-1} = 1 \text{ eV}$) and protonated mass.⁴⁶

Compound	Chemical Formula	PA (kJ mol^{-1})	Protonated mass (amu)
Oxygen	O_2	421.0	33
Hydrogen	H_2	422.3	3

Nitrogen	N ₂	493.6	29
Nitrogen Oxide	NO	531.8	31
Carbon dioxide	CO ₂	540.5	45
Methane	CH ₄	543.5	17
Nitrogen Dioxide	NO ₂	591.0	47
Sulfur Dioxide	SO ₂	672.3	65
Water	H ₂ O	691.0	19
Formaldehyde	CH ₂ O	712.9	31
Formic acid	CH ₂ O ₂	742.0	47
Benzene	C ₆ H ₆	750.4	79
Methanol	CH ₄ O	754.3	33
Acetic acid	C ₂ H ₄ O ₂	783.7	61
Acetone/propanal	C ₃ H ₆ O	812/786	59

1.2.1.2 Kinetics of proton transfer reactions

Owing to the long-distance electrostatic interaction between an ion and a molecule, ion-molecule reactions are among the fastest reactions known, and the resulting interaction energy at short range is often enough to overcome any energy barriers. This is in contrast to neutral molecule/molecule reactions that usually involve activation energies that have to be overcome for a reaction to take place.^{21,47}

For equation 1.7 we can write the rate equation as:

$$-\frac{d[H_3O^+]}{dt} = \frac{d[MH^+]}{dt} = k[H_3O^+][M] \quad (\text{Equation 1.11})$$

The reaction rate coefficient k can be measured or calculated. Several theoretical models have been used to determine the reaction rate coefficient of ion-molecule reactions, and these can be divided mainly in 2 classes:

1. non-polar reactants: the Langevin theory
2. polar reactants: the Average-Dipole-Orientation (ADO) or preferably classical trajectory theory.

Detailed mathematical models used to calculate rate coefficients are explained in depth in the book by Ellis and Mayhew³ or Emily House's thesis,⁴⁸ and an in depth explanation of those is not within the scope of this thesis. Nevertheless, it is important to give some details.

The ADO theory is the most used for collision rate calculations; in this theory k_{ADO} is given by the expression:^{3,48}

$$k_{ADO} = \sqrt{\frac{\pi\alpha e^2}{\mu\epsilon_0}} + \frac{C\mu_D e}{\epsilon_0} \sqrt{\frac{1}{2\pi\mu k_B T}} \quad (\text{Equation 1.12})$$

α : polarizability of the neutral reactant molecular

Q: charge of the ion

μ : reduced mass of the colliding reactants

ϵ_0 : permittivity of free space

μ_D : is the dipole moment of the reacting molecule

k_B : Boltzmann's constant

C: correction factor accounting for the average orientation of the neutral molecule's dipole moment. It is a function of α , μ_D and k_B .

Calculated k_{ADO} values underestimated the experimental rate constants by typically 10-20%.⁴⁸

Extensive set of thermal rate data for proton transfer reactions with hydronium as the reagent ion are available after studies using SIFT-MS and flowing afterglow measurements and can be found in the literature.^{6,49-54} To within experimental error, these values are in good agreement with theoretical calculations, so even an unknown reaction rate coefficient for a given analyte is not an issue, since this can be determined theoretically using the aforementioned methods cited above.³

It is relevant to highlight that most protonation reactions will be kinetically controlled, and the kinetically favoured site of protonation may differ from the thermodynamically favoured site.²¹ Examples of this are shown in this work for picric acid and the ion funnel TNT work (Chapters 4, pages 87-108, and 6, pages 128-147, respectively). Density Functional Theory (DFT) calculations (a quantum mechanical modelling method) can aid in identifying the most reactive site. In many cases the proton may interchange between the available basic sites in the molecule.^{21,24,27}

Exothermic bimolecular ion-molecule reactions (equations 1.3 to 1.6) are often spontaneous, i.e. a reaction usually occurs on every collision.³ However, this is not always the case, with the exception being proton transfer reaction processes.²¹ To date, not one

exothermic proton transfer reaction process has been found to occur at less than the collisional (maximum) rate. This is illustrated on figure 2, representing the correlation between the reaction efficiency of proton transfer, k_{exp}/k_{coll} , and its overall change in free energy at 298 K, where k_{exp} represents the experimental rate coefficients and k_{coll} the collisional coefficient.²⁷ What this figure shows is the high efficiency of exothermic proton transfer reactions up to a value of +2.5 kcal/mol,⁴³ and how as this reaction becomes thermoneutral the efficiency drops and becomes very low for endothermic or endoergic reactions.

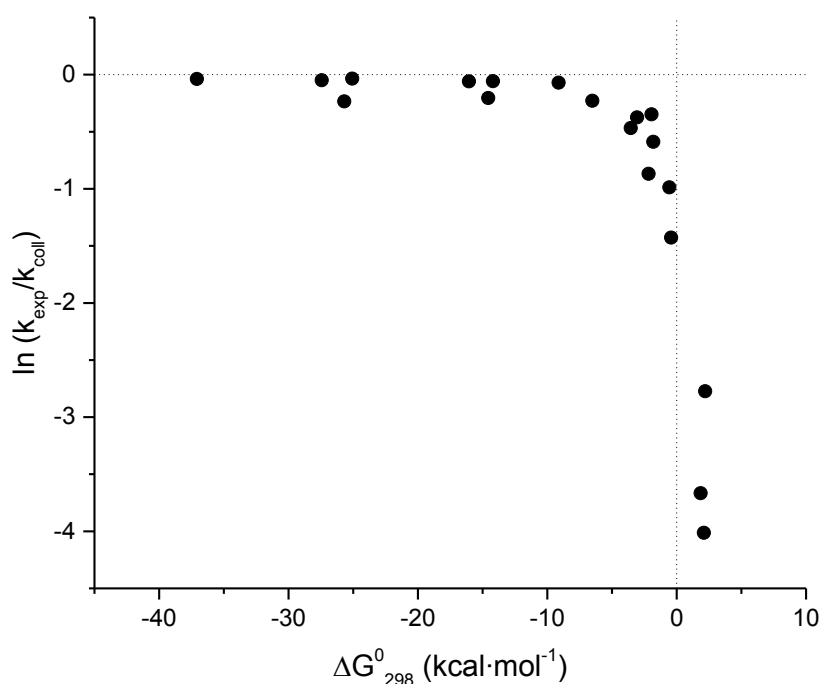


Figure 1.2: The natural logarithm of the experimental rate coefficients k_{exp} to the calculated collisional (reactions) coefficient k_{coll} , k_{exp}/k_{coll} , gives the value for the number of reactions per collision, i.e. when $k_{exp}/k_{coll} = 1$, we have unit efficiency. When it becomes endergonic, the efficiency drops sharply. Adapted from Bohme et al.⁴³

One issue is that the more exothermic the reaction is, the more fragmentation of MH^+ is likely to occur.²¹ Although in principle this might compromise the PTR-MS technique and limit the sensitivity, fragmentation (dissociative proton transfer) can also be used as an advantage in terms of selectivity (see experimental results Chapters).

1.2.1.1 - Other chemical reagent ion systems (used in PTR-MS)

Reagent ions other than H_3O^+ can be used for CI in the PTR-MS instrument. Technically speaking, when the proton transfer reaction is not the employed ionisation reaction, as in equation 1.7, the term PTR-MS should not apply, and the instrument is more accurately described as SCIMS (soft chemical ionisation mass spectrometry). Several examples for SCIMS can be found in the literature.⁵⁵⁻⁵⁷, where the use of alternative reagent ions have been focussed on the differentiation of isobaric and isomeric compounds,^{1,58-65} and the detection of compounds that do not react with H_3O^+ , such as ammonia with O_2^+ ,⁵⁶ alkanes with NO^+ ,⁶⁶ and methane and inorganic species, with Kr^+ ,⁶⁷ just to name a few examples.

Among all the possibilities O_2^+ and NO^+ have been routinely used with no further modification to the PTR-MS instrumentation apart from the reagent gases used. This is important, as no mass selection of the reagent ion is done, and hence a clean reagent ion signal is obtained. The usual reaction channel for these reagent ions are usually charge transfer (dominant for O_2^+) and adduct formation (dominant for NO^+), generically depicted in equations 1.3 and 1.6, respectively.

A positive ion colliding with a neutral molecule leading to charge exchange is defined as



With regards to the energetics for charge transfer we have to refer to the terms ionization energy of the neutral, $\text{IE}_{(\text{M})}$ and recombination energy of the reactant, $\text{RE}_{(\text{X}^{+\bullet})}$. Recombination energy of $\text{X}^{+\bullet}$ is defined as the gas phase exothermicity for the reaction



For atomic ions the recombination energy has the same numerical value as the ionization energy of the neutral (this is not necessarily the case for diatomic and polyatomic molecular ions due to energy storage in internal modes).^{21,27}

Ionization of the analyte through CT is possible only if the condition $\text{RE}_{(\text{X}^{+\bullet})} - \text{IE}_{(\text{M})} > 0$, and therefore no CT is possible if $\text{RE}_{(\text{X}^{+\bullet})}$ is lower than $\text{IE}_{(\text{M})}$. The exothermicity of the CT reaction remains as internal energy of the product ion $\text{M}^{+\bullet}$, and consequently if this energy is high enough $\text{M}^{+\bullet}$ can fragment. Following this, by an appropriate choice of the reagent gas, and thus the reagent ion, fragmentation can be limited.

When applying these concepts to O_2^+ and NO^+ what we have is:

- (i) O_2^+ : $RE(O_2^+) = 12.13 \text{ eV}$.⁶⁸ This is sufficiently high for many reactions with molecules to proceed via dissociative charge transfer, owing to the fact that most organic molecules have a first IE in the range 8-12eV.
- (ii) NO^+ : $RE(NO^+) = 9.26 \text{ eV}$.⁶⁸ Any organic molecule with IE below this value can undergo CT. When IE is above this value reaction channels based on hydride transfer (equation 1.5) and association (equation 1.6) are feasible.^{3,21} The channel that dominates depends upon the experimental conditions and the nature of the analyte.

1.3 Homeland security

This term was introduced during the 90s by the United States administration,⁶⁹ as an umbrella term referring to the national effort to prevent terrorist attacks, reduce the vulnerability to terrorism, and minimize the damage from attacks that do occur. Under this term are included all aspects related to the security of critical infrastructure, transportation security, biodefense, detection (and research on next-generation security technologies) of radioactive and radiological materials, drugs and explosives.

Within the Homeland Security topic this thesis will only focus on explosives detection, but chemical warfare agents (CWAs) and drugs are also important threats. In recent years PTR-MS has also been used for such purposes, and work on CWAs,⁷⁰⁻⁷² narcotics,⁷³ date rape drugs⁷⁴ and new psychoactive substances^{75,76} can be found in the literature.

1.3.1 Explosives

The accurate and reliable detection of explosive and/or explosive-like substances has become a crucial concern for the international community, affected not only by Homeland Security threats (as a result of the attacks perpetrated by terrorists and/or terrorist organisations in recent years⁷⁷), but military applications, land mine detection,⁷⁸ forensic investigations, environmental contamination (explosive compounds toxicity is well known and obsolete explosives and munitions can contaminate soil and water^{79,80}) and humanitarian concerns.⁸¹⁻⁸³ All of this has translated into research efforts to develop high analytical performance technologies for the detection of explosives.^{84,85}

Technically speaking, an explosive is a substance that, when subjected to an external stimulus (such as heat, impact, friction, static discharge or detonation), can initiate a very rapid, and self-propagating chemical reaction leading to the formation of more stable materials, whilst suddenly releasing a large amount of energy.⁸⁶ The energy generates a huge increase of temperature and pressure, so that all the materials present are predominantly converted into a hot gas phase.^{87,88} All these characteristics make explosives very useful both in military and civilian applications, with mining its largest commercial application.

Owing to their chemical and physical characteristics, explosives are quite difficult to detect.⁸⁹ One major problem is that most of the explosives have very low vapour pressures at room temperature,⁹⁰ so direct vapour detection is very difficult. It should be noted that vapour pressures of explosives increase quickly with temperature, but at the same time thermal decomposition of the compounds could occur resulting in the degradation of the substances.⁹¹ This is illustrated on figure 1.3, where vapour pressure of several common high explosives (materials which detonates at supersonic speeds, with values are between 3 and 9 km/sec.⁹²) as a function of temperature is shown. As a consequence of this low volatility many explosives tend to adsorb to cold surfaces very easily. On top of this, improvised explosive devices (IEDs) are concealed, lowering even more their concentrations. Therefore, trace sampling of explosives with very low vapour pressures is a challenging problem because of the low concentrations in a sampling volume. Moreover, the detection of explosive and explosive related compounds has to be done with high sensitivity and selectivity and in a reasonable time, adding an extra difficulty for analytical techniques.

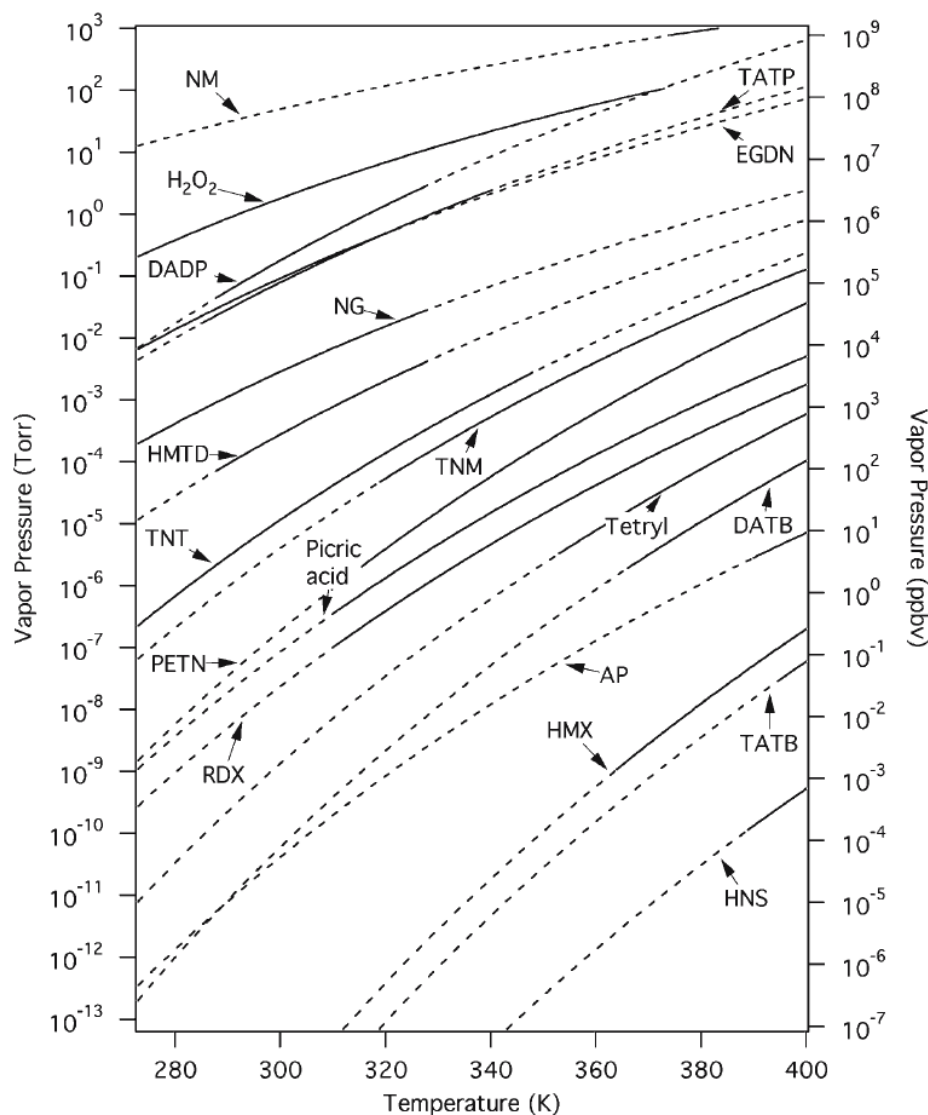
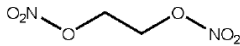
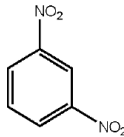
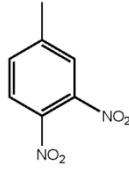
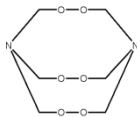
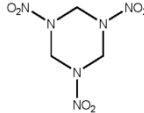
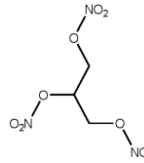
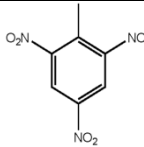
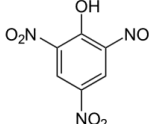
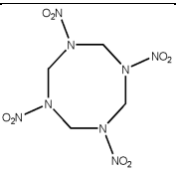
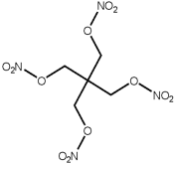


Figure 1.3: Plots of the vapour pressure of several common high explosives versus temperature. Solid lines are the experimentally measured temperature ranges; the dashed lines are extrapolations. Acronyms are defined in the list of abbreviations. Reproduced with permission from Reference 93. Copyright © 2007 Springer.

There are a large number of explosive compounds available either for military or civil use.⁹³ However, for the underlying work developed for this Thesis we have concentrated on the most common used ones (Table 1.2). Table 1.2 shows the name of the explosive, the chemical formula, the vapour pressure at 25°C (in mbar)⁹⁰, the protonated mass, the proton affinity and the structure of each of the explosives compounds.

Table 1.2: Summary of explosive compounds investigated in this thesis in order of increasing molecular weight.

Compound	Chemical Formula	Vapour Pressure at 25 °C (mbar)	Protonated Mass ^a	PA (kJ mol ⁻¹)	Structure
Ethylene glycol dinitrate (EGDN) (1,2-dinitroxyethane)	C ₂ H ₄ N ₂ O ₆	0.1	153.01	697 ^b	
1,3-dinitrobenzene (1,3-DNB)	C ₆ H ₄ N ₂ O ₄	6.0E·10 ⁻⁵ (1,2 DNB) 2.7·10 ⁻⁴ (1,3 DNB)	169.02	757 ^b	
3,4- dinitrotoluene (3,4-DNT)	C ₆ H ₃ CH ₃ N ₂ O ₄	4.2·10 ⁻⁴ (2,4- DNT) 2.1·10 ⁻⁴ (2,6- DNT) N/A (3,4- DNT)	183.04	-	
Hexamethylene triperoxide diamine (HMTD)	C ₆ H ₁₂ N ₂ O ₆	0.13	209.08	-	
1,3,5-trinitroperhydro- 1,3,5-triazine (RDX)	C ₃ H ₆ N ₆ O ₆	4.9·10 ⁻⁹	223.04	771 ^b	
Nitroglycerine (1,2,3- Trinitroxypropane) (NG)	C ₃ H ₅ N ₃ O ₉	6.5·10 ⁻⁴	228.01	-	
2,4,6-trinitrotoluene (TNT)	C ₇ H ₅ N ₃ O ₆	9.3·10 ⁻⁶	228.03	744 ^b	
2,4,6-trinitrophenol (picric acid, PiA)	C ₆ H ₃ N ₃ O ₇	9.84·10 ⁻⁷	230	764, 756, 711 ^c	

Octahydro-1,3,5,7-tetranitro-1,3,5,7-tetrazocine (HMX) (Not detected)	$C_4H_8N_8O_8$	$2.4 \cdot 10^{-14}$	297.05	765 ²	
Pentaerythritol tetranitrate (PETN)	$C_5H_8N_4O_{12}$	$1.1 \cdot 10^{-08}$	317.02	739 ²	

- Most abundant isotopes used (note that the protonated parent is not necessarily the most dominant product ion resulting from the reaction of H_3O^+ with an explosive).
- Determined by us using density functional theory (DFT) calculations (B3LYP functional with 6-31+G(d,p) basis set; software employed was GAUSSIAN09). Data unpublished from Molecular Physics Research Group (University of Birmingham).
- Depending upon the protonation site (see Chapter 4 for more information).

1.3.2 Analytical technologies for explosives detection

Traditionally there have been two approaches for explosives detection, namely direct vapour detection (only suitable for volatile compounds - and these are a minority -, although recent instrumental advances have renewed the interest in this methodology^{29,94-96}) and particle-based sampling where traces of explosive compound are collected from surfaces and/or materials with the help of a “collecting item” or vacuuming.^{89,90,97} Swiping relies on the adsorption of an analyte to the surface of a swab material. For swipe-based particle collection, swabs are the most used item, and are manufactured in a wide variety of materials, designed specifically for a given instrument, such as PTFE, Nomex[®], Teflon[®], Teflon[®]-coated fiberglass, paper, cotton wool, among many others.⁹⁸⁻¹⁰⁰ After the crucial sampling step, the analyte is usually desorbed from the swab and vaporised as a preliminary step in the detection process.¹⁶ This approach, as explained in section 2.3.1 (pages 54-57) and Chapter 5 (pages 109-127) is the approach used in the work presented in this thesis with PTR-MS.

When we refer to the detection technology itself, there is a wide variety of analytical techniques used, from the basic use of canines and electronic noses,¹⁰¹⁻¹⁰³ to very modern, sensitive and complex technologies.⁹⁵ Some of the current technologies make use of a pre-separation by means of a chromatographic system (either liquid or gas), limiting the overall speed of detection.¹⁰⁴⁻¹⁰⁹

A wide variety of analytical techniques are used for the trace detection of explosives, and several reviews in recent years have covered most of them in depth.^{84,110-113} There are almost as many classifications as reviews, but a possible classification (not exhaustive) is shown in figure 1.4 based on the physical principle the technique is founded on.

Many of the analytical techniques described in the reviews show impressive performance LoDs, in the region of ppt or even ppq, with high selectivity.^{105,106} This, however, comes at a cost, e.g. expensive hardware, need for qualified personnel, long analysis cycle times and are only suitable for research laboratory use. These limit their usability in the field.¹¹⁴ As will be explained in the next section PTR-MS overcomes most of these drawbacks.

Among the most promising detection schemes are those based on the ionization of explosives and the subsequent detection of the ions formed. Based on this principle, Ion Mobility Spectrometry (IMS), has become the most used analytical technique in security areas, e.g. airports, due to the ease of use, rapid response time, low cost and relative high sensitivity.^{14,16} In the field, more than 10,000 IMS systems have been deployed at security checkpoints worldwide as a tool to aid in reducing drugs smuggling or national security threats detection, and more than 50,000 handheld IMS analyzers have been deployed for chemical-weapons monitoring within the armed forces around the world.^{14,115} As explained at the end of section 1.1, IMS drawbacks are the poor selectivity as they solely rely on the mobility (or reduced mobility when normalised to temperature and pressure) of the ions as the identification parameter. An IMS approach to enhance explosives detection selectivity is the use of dopant agents, such as dichloromethane.^{116,117} If these substances are present in excess compared with the analyte, they are ionized first by electron transfer from the reactant ions before undergoing a reaction with the analyte molecules (usually by association or adduct formation). Nevertheless, this in some cases is not enough and the technology is prone to false positives and/or negatives, so higher selectivity in the analysis is needed. Ideally new technologies preserving all the IMS advantages, namely sensitivity and fast cycle analysis time, with an added increase in selectivity would benefit the end user. Here is where PTR-MS can compete with its inherent advantages.

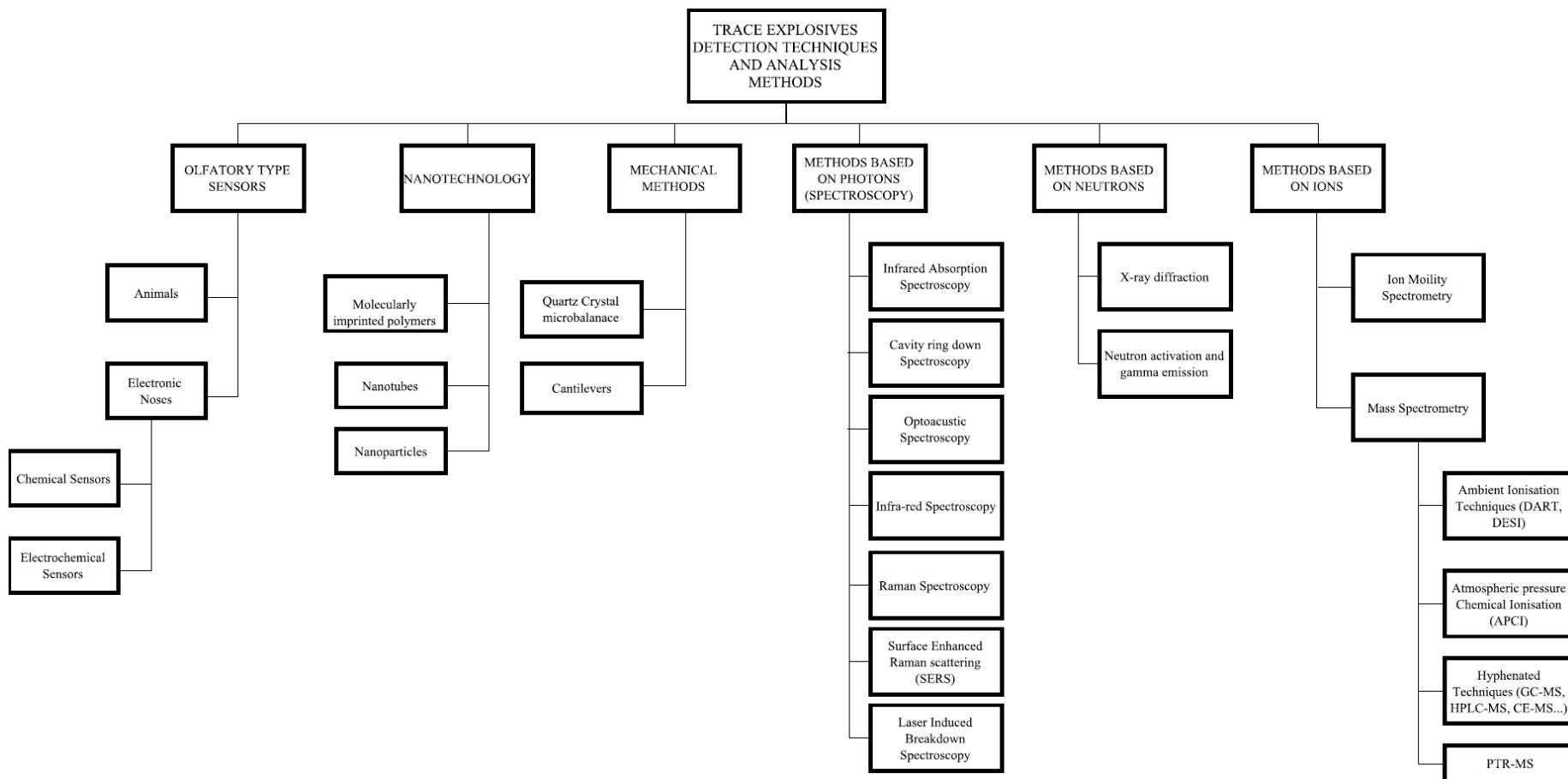


Figure 1.4: Trace explosives detection methods, arranged according to their operative principle.

1.3.2.1 Proton transfer reaction mass spectrometry and the detection of explosives

For a mass spectrometric technique to be considered as useful for the detection of explosives, it should be as sensitive and as rapid as IMS but with MS comes much improved selectivity. The major problems are that MS instrumentation is not cheap and is not handheld, compromising its suitability in applications where these features are needed.⁶⁴ All of the techniques used for trace explosive detection have advantages and limitations.

In the past few years PTR-MS has emerged as a useful analytical tool for the detection of explosives.¹¹⁸⁻¹²² However, PTR-MS is arguably the most broad-based platform analytical technology available. For any technology to be adopted as an analytical tool, it is necessary for it to be able to detect quickly trace quantities with high selectivity. Another important factor to consider is the whole of the detection process (comprising of sampling, analysis and recovery), which needs to be executed within tens of seconds if it is to be acceptable for use in security areas where large number of people are present. Until now this has not been achieved with PTR-MS, but, as will be explained in the experimental section, with the latest hardware development, namely a thermal desorption unit (TDU), these requirements can be completely fulfilled.

The work developed during this thesis has been focussed on the development of the instrumentation as well as analytical protocols that allow sensitive, selective and fast identification of explosive compounds. Most of the explosive compounds show very low volatility, and therefore the first step to overcome for PTR to be useful as an analytical technique for the analysis of explosives is to get trace particulate matter into the vapour phase. This is a crucial step and would compromise the outcome of the overall analysis process. For this instrumental development was needed. Using standard swabs, the same as used by the security forces in airports, a bespoke thermal desorption unit was developed in collaboration with Kore Technology Ltd. This thermal desorption unit allowed us to have a temporal concentration pulse of material in a very short period of time without thermally degrading the explosive molecules – thermolability is an important issue for explosive compounds, as already stated.

Then, there is the high confidence level in assignment. This is particularly needed for areas of security. The detection of an ion at a given m/z for an explosive does not guarantee that that explosive is present. There is still some ambiguity associated with assignment. New

instrumental developments can overcome this issue. Rapid switching of reagent ions is one way to improve selectivity. This alters the ion chemistry and hence the m/z of the product ion(s) detected. Another way is to alter the reduced electric field, either by using an RFIF or by quickly modifying the electric field. The use of reduced electric field switching and/or using a radio frequency ion-funnel (RFIF) in the reaction region (drift tube) of a PTR-MS can be used to enhance specificity by manipulating the ion-molecule chemistry through inducing collisional induced dissociation.

1.4 Aims of the thesis

This thesis aims to contribute to the current knowledge and understanding of ion/molecule processes for PTR-MS and explosive compounds detection. Particular emphasis has been placed on investigating a number of new methodologies and tools to improve selectivity and sensitivity in the assignment.

Chapter 3 describes a study where a switchable reagent ion source is used to improve PTR-MS selectivity for the detection of a series of explosive compounds, namely TNT, TNB, PETN and RDX. Selectivity is improved owing to the production of different product ions resulting from changes in the reagent ion-molecule chemistry.

Chapter 4 describes a study where a switchable reagent-ion source is used to investigate the reactions of NO^+ , H_3O^+ , O_2^+ and Kr^+ with picric acid (2,4,6- trinitrophenol, $\text{C}_6\text{H}_3\text{N}_3\text{O}_7$, PiA) . For H_3O^+ and O_2^+ , PiA shows an unusual behaviour that can be used to aid assignment.

Chapter 5 describes a study in which a novel thermal desorption unit (TDU) has been developed and specifically designed for the detection of trace quantities of explosives using PTR-MS. Details on recovery times and instrumental limits of detection for the screening of the most common explosive compounds are provided.

Chapter 6 describes a study where the use of a radio frequency ion-funnel in the reaction region (drift tube) of a PTR-MS instrument has been used to enhance specificity by manipulating the ion-molecule chemistry through collisional induced processes. This is applied to trinitrotoluene, dinitrotoluenes and nitrotoluenes to demonstrate the advantages of this new RFIF-PTR-ToF-MS for analytical chemical purposes.

Chapter 7 describes a study where fast changes in the reduced electric field in a PTR-MS instrument led to changes in collisional induced dissociation, resulting in different product ion distributions that can be used to identify a compound of interest with higher specificity. This is applied to 2,4- and 2,6-dinitrotoluene, HMTD, RDX, and PETN. Finally, the combined operation of a radio frequency ion-funnel PTR-MS and fast drift tube voltage switching is exemplified for TNT.

References

1. Lindinger, W.; Hansel, A.; Jordan, A., On-line monitoring of volatile organic compounds at pptv levels by means of proton-transfer-reaction mass spectrometry (PTR-MS) medical applications, food control and environmental research. *International Journal of Mass Spectrometry and Ion Processes* **1998**, *173* (3), 191-241.
2. A. D. McNaught, A. Wilkinson. Blackwell Scientific Publications, O., *IUPAC. Compendium of Chemical Terminology, 2nd ed. (the "Gold Book")*. 2006.
3. Andrew M. Ellis, Chris A. Mayhew, *Proton Transfer Reaction Mass Spectrometry: Principles and Applications*. 1st ed.; Wiley: 2014.
4. Grob, R. L.; Barry, E. F., *Modern practice of gas chromatography*. John Wiley & Sons: 2004.
5. Jennings, W.; Mittlefehldt, E.; Stremple, P., *Analytical gas chromatography*. Academic Press: 1997.
6. Smith, D.; Španěl, P., Selected ion flow tube mass spectrometry (SIFT-MS) for on-line trace gas analysis. *Mass Spectrometry Reviews* **2005**, *24* (5), 661-700.
7. Španěl, P.; Smith, D., Progress in SIFT-MS: Breath analysis and other applications. *Mass Spectrometry Reviews* **2011**, *30* (2), 236-267.
8. Syft Technologies, What is SIFT-MS? <http://www.syft.com/what-is-sift-ms/> (accessed 18-10-2016).
9. Lane, D. A.; Thomson, B. A., Monitoring a chlorine spill from a train derailment. *Journal of the Air Pollution Control Association* **1981**, *31* (2), 122-127.
10. Whitehouse, C. M.; Dreyer, R.; Yamashita, M.; Fenn, J., Electrospray ionization for mass-spectrometry of large biomolecules. *Science* **1989**, *246* (4926), 64-71.
11. McLuckey, S. A.; Glish, G. L.; Asano, K. G.; Grant, B. C., Atmospheric sampling glow discharge ionization source for the determination of trace organic compounds in ambient air. *Analytical Chemistry* **1988**, *60* (20), 2220-2227.
12. Cohen, M. J.; Karasek, F. W., Plasma Chromatography™—A New Dimension for Gas Chromatography and Mass Spectrometry. *Journal of Chromatographic Science* **1970**, *8* (6), 330-337.
13. Fetterolf, D.; Clark, T., Detection of Trace Explosive Evidence by Ion Mobility Spectrometry. *Journal of Forensic Sciences* **1993**, *38* (1), 28-39.

14. Eiceman, G. A.; Karpas, Z.; Hill Jr, H. H., *Ion mobility spectrometry*. CRC press: 2013.
15. Collins, D.; Lee, M., Developments in ion mobility spectrometry–mass spectrometry. *Anal Bioanal Chem* **2002**, *372* (1), 66-73.
16. Ewing, R. G.; Atkinson, D. A.; Eiceman, G. A.; Ewing, G. J., A critical review of ion mobility spectrometry for the detection of explosives and explosive related compounds. *Talanta* **2001**, *54* (3), 515-529.
17. Munson, M. S. B.; Field, F. H., Chemical Ionization Mass Spectrometry. I. General Introduction. *Journal of the American Chemical Society* **1966**, *88* (12), 2621-2630.
18. Richter, W. J.; Schwarz, H., Chemical Ionization—A Mass-Spectrometric Analytical Procedure of Rapidly Increasing Importance. *Angewandte Chemie International Edition in English* **1978**, *17* (6), 424-439.
19. Munson, B., Development of chemical ionization mass spectrometry. *International Journal of Mass Spectrometry* **2000**, *200* (1–3), 243-251.
20. Munson, B., CIMS, Chemistry in Mass Spectrometry. *International Journal of Mass Spectrometry* **2015**, *377*, 502-506.
21. Harrison, A. G., *Chemical Ionization Mass Spectrometry*. CRC Press: 1982.
22. Mark, T. D., Fundamental aspects of electron impact ionization. *International Journal of Mass Spectrometry and Ion Physics* **1982**, *45*, 125-145.
23. Zhan, C.-G.; Nichols, J. A.; Dixon, D. A., Ionization Potential, Electron Affinity, Electronegativity, Hardness, and Electron Excitation Energy: Molecular Properties from Density Functional Theory Orbital Energies. *The Journal of Physical Chemistry A* **2003**, *107* (20), 4184-4195.
24. Vollhardt, P.; Schore, N., *Organic Chemistry*. 2011.
25. Lias, S. G., Gas-phase ion and neutral thermochemistry. *J. Phys. Chem. Ref Data* **1988**, *17* (1).
26. Blanksby, S. J.; Ellison, G. B., Bond dissociation energies of organic molecules. *Accounts of chemical research* **2003**, *36* (4), 255-263.
27. Gross, J. H., *Mass Spectrometry. A textbook*. 2nd ed.; Springer: 2011; p 754.
28. Hunt, D. F.; Stafford, G. C.; Crow, F. W.; Russell, J. W., Pulsed positive negative ion chemical ionization mass spectrometry. *Analytical Chemistry* **1976**, *48* (14), 2098-2104.

29. Takats, Z.; Cotte-Rodriguez, I.; Talaty, N.; Chen, H.; Cooks, R. G., Direct, trace level detection of explosives on ambient surfaces by desorption electrospray ionization mass spectrometry. *Chemical Communications* **2005**, (15), 1950-1952.
30. Milne, G.; Fales, H.; Axenrod, T., Identification of dangerous drugs by isobutane chemical ionization mass spectrometry. *Analytical chemistry* **1971**, *43* (13), 1815-1820.
31. McGuire, J. M.; Munson, B., Comparison of isopentane and isobutane as chemical ionization reagent gases. *Analytical chemistry* **1985**, *57* (3), 680-683.
32. Hunt, D. F.; Ryan, J. F., Chemical ionization mass spectrometry studies. I. Identification of alcohols. *Tetrahedron Letters* **1971**, *12* (47), 4535-4538.
33. Keough, T.; DeStefano, A., Factors affecting reactivity in ammonia chemical ionization mass spectrometry. *Organic Mass Spectrometry* **1981**, *16* (12), 527-533.
34. Lawrence, D. L., Accurate mass measurement of positive ions produced by ammonia chemical ionization. *Rapid Communications in Mass Spectrometry* **1990**, *4* (12), 546-549.
35. Laramee, J. A.; Arbogast, B. C.; Deinzer, M. L., Electron capture negative ion chemical ionization mass spectrometry of 1,2,3,4-tetrachlorodibenzo-p-dioxin. *Analytical Chemistry* **1986**, *58* (14), 2907-2912.
36. Ong, V. S.; Hites, R. A., Electron capture mass spectrometry of organic environmental contaminants. *Mass Spectrometry Reviews* **1994**, *13* (3), 259-283.
37. Williamson, D. H.; Knighton, W. B.; Grimsrud, E. P., Effect of buffer gas alterations on the thermal electron attachment and detachment reactions of azulene by pulsed high pressure mass spectrometry¹. *International Journal of Mass Spectrometry* **2000**, *195-196*, 481-489.
38. Subba Rao, S.; Fenselau, C., Evaluation of benzene as a charge exchange reagent. *Analytical Chemistry* **1978**, *50* (3), 511-515.
39. Allgood, C.; Ma, Y. C.; Munson, B., Quantitation using benzene in gas chromatography/chemical ionization mass spectrometry. *Analytical chemistry* **1991**, *63* (7), 721-725.
40. Sieck, L. W., Determination of Molecular weight distribution of aromatic components in petroleum products by chemical ionization mass spectrometry with chlorobenzene as reagent gas. *Analytical Chemistry* **1983**, *55* (1), 38-41.
41. Li, Y. H.; Herman, J. A.; Harrison, A. G., Charge exchange mass spectra of some C₅H₁₀ isomers. *Canadian Journal of Chemistry* **1981**, *59* (12), 1753-1759.

42. Herman, J. A.; Li, Y. H.; Harrison, A., Energy dependence of the fragmentation of some isomeric $[C_6H_{12}]^+$ ions. *Organic Mass Spectrometry* **1982**, *17* (3), 143-150.
43. Bohme, D. K.; Mackay, G. I.; Schiff, H. I., Determination of proton affinities from the kinetics of proton transfer reactions. VII. The proton affinities of O_2 , H_2 , Kr, O, N_2 , Xe, CO_2 , CH_4 , N_2O , and CO. *The Journal of Chemical Physics* **1980**, *73* (10), 4976-4986.
44. Hansel, A.; Singer, W.; Wisthaler, A.; Schwarzmann, M.; Lindinger, W., Energy dependencies of the proton transfer reactions $H_3O^+ + CH_2O \rightleftharpoons CH_2OH^+ + H_2O$. *International journal of mass spectrometry and ion processes* **1997**, *167*, 697-703.
45. de Gouw, J.; Warneke, C.; Karl, T.; Eerdekens, G.; van der Veen, C.; Fall, R., Sensitivity and specificity of atmospheric trace gas detection by proton-transfer-reaction mass spectrometry. *International Journal of Mass Spectrometry* **2003**, *223-224*, 365-382.
46. Hunter, E. P. L.; Lias, S. G., Evaluated Gas Phase Basicities and Proton Affinities of Molecules: An Update. *Journal of Physical and Chemical Reference Data* **1998**, *27* (3), 413-656.
47. Crespo Gonzalez, E. Proton transfer reaction-mass spectrometry, applications in life sciences. Radboud University, 2012.
48. House, E. Refinement of ptr-ms methodology and application to the measurement of (o) vocs from cattle slurry. Doctoral Thesis, University of Edinburgh, 2008.
49. Anicich, V. G., An index of the literature for bimolecular gas phase cation-molecule reaction kinetics. **2003**.
50. Arnold, S. T.; Thomas, J. M.; Viggiano, A., Reactions of $H_3O^+(H_2O)_n$ and $H^+(H_2O)_n$ (CH_3COCH_3)_m with CH_3SCH_3 . *International journal of mass spectrometry* **1998**, *179*, 243-251.
51. Arnold, S. T.; Viggiano, A.; Morris, R. A., Rate constants and product branching fractions for the reactions of H_3O^+ and NO^+ with C2-C12 alkanes. *The Journal of Physical Chemistry A* **1998**, *102* (45), 8881-8887.
52. Midey, A. J.; Arnold, S. T.; Viggiano, A., Reactions of $H_3O^+(H_2O)_n$ with Formaldehyde and Acetaldehyde. *The Journal of Physical Chemistry A* **2000**, *104* (12), 2706-2709.
53. Schoon, N.; Amelynck, C.; Vereecken, L.; Coeckelberghs, H.; Arijs, E., A selected ion flow tube study of the reactions of H_3O^+ , NO^+ and O_2^+ with some monoterpene oxidation products. *International Journal of Mass Spectrometry* **2004**, *239* (1), 7-16.

54. Amelynck, C.; Schoon, N.; Kuppens, T.; Bultinck, P.; Arijs, E., A selected ion flow tube study of the reactions of H_3O^+ , NO^+ and O_2^+ with some oxygenated biogenic volatile organic compounds. *International Journal of Mass Spectrometry* **2005**, *247* (1), 1-9.
55. Blake, R. S.; Wyche, K. P.; Ellis, A. M.; Monks, P. S., Chemical ionization reaction time-of-flight mass spectrometry: Multi-reagent analysis for determination of trace gas composition. *International Journal of Mass Spectrometry* **2006**, *254* (1–2), 85-93.
56. Norman, M.; Hansel, A.; Wisthaler, A., O_2^+ as reagent ion in the PTR-MS instrument: Detection of gas-phase ammonia. *International Journal of Mass Spectrometry* **2007**, *265* (2–3), 382-387.
57. Jordan, A.; Haidacher, S.; Hanel, G.; Hartungen, E.; Herbig, J.; Märk, L.; Schottkowsky, R.; Seehauser, H.; Sulzer, P.; Märk, T. D., An online ultra-high sensitivity Proton-transfer-reaction mass-spectrometer combined with switchable reagent ion capability (PTR + SRI – MS). *International Journal of Mass Spectrometry* **2009**, *286* (1), 32-38.
58. Wyche, K. P.; Blake, R. S.; Willis, K. A.; Monks, P. S.; Ellis, A. M., Differentiation of isobaric compounds using chemical ionization reaction mass spectrometry. *Rapid Communications in Mass Spectrometry* **2005**, *19* (22), 3356-3362.
59. Blake, R. S.; Patel, M.; Monks, P. S.; Ellis, A. M.; Inomata, S.; Tanimoto, H., Aldehyde and ketone discrimination and quantification using two-stage proton transfer reaction mass spectrometry. *International Journal of Mass Spectrometry* **2008**, *278* (1), 15-19.
60. Inomata, S.; Tanimoto, H., Differentiation of Isomeric Compounds by Two-Stage Proton Transfer Reaction Time-of-Flight Mass Spectrometry. *Journal of the American Society for Mass Spectrometry* **2008**, *19* (3), 325-331.
61. Karl, T.; Hansel, A.; Cappellin, L.; Kaser, L.; Herdinger-Blatt, I.; Jud, W., Selective measurements of isoprene and 2-methyl-3-buten-2-ol based on NO^+ ionization mass spectrometry. *Atmospheric Chemistry and Physics* **2012**, *12* (24), 11877-11884.
62. Karl, T.; Kaser, L.; Turnipseed, A., Eddy covariance measurements of isoprene and 232-MBO based on NO^+ time-of-flight mass spectrometry. *International Journal of Mass Spectrometry* **2014**, *365–366*, 15-19.
63. Lanza, M.; Acton, W. J.; Jürschik, S.; Sulzer, P.; Breiev, K.; Jordan, A.; Hartungen, E.; Hanel, G.; Märk, L.; Mayhew, C. A.; Märk, T. D., Distinguishing two isomeric

mephedrone substitutes with selective reagent ionisation mass spectrometry (SRI-MS). *Journal of Mass Spectrometry* **2013**, *48* (9), 1015-1018.

64. González-Méndez, R.; Reich, D. F.; Mullock, S. J.; Corlett, C. A.; Mayhew, C. A., Development and use of a thermal desorption unit and proton transfer reaction mass spectrometry for trace explosive detection: Determination of the instrumental limits of detection and an investigation of memory effects. *International Journal of Mass Spectrometry* **2015**, *385*, 13-18.

65. Koss, A. R.; Coggon, M. M.; Veres, P. R.; de Gouw, J. A., Evaluation of NO⁺ reagent ion chemistry for online measurements of atmospheric volatile organic compounds. *Atmospheric Measurement Techniques* **2016**, *9* (7), 2909.

66. Inomata, S.; Tanimoto, H.; Yamada, H., Mass Spectrometric Detection of Alkanes Using NO⁺ Chemical Ionization in Proton-transfer-reaction Plus Switchable Reagent Ion Mass Spectrometry. *Chemistry Letters* **2014**, *43* (4), 538-540.

67. Sulzer, P.; Edtbauer, A.; Hartungen, E.; Jürschik, S.; Jordan, A.; Hanel, G.; Feil, S.; Jaksch, S.; Märk, L.; Märk, T. D., From conventional proton-transfer-reaction mass spectrometry (PTR-MS) to universal trace gas analysis. *International Journal of Mass Spectrometry* **2012**, *321–322*, 66-70.

68. Linstrom P. J., Mallard, W. G. (Eds.), National Institute of Standards and Technology, Gaithersburg MD, 20899, <http://webbook.nist.gov>.

69. Government, U. S., To establish the Department of Homeland Security, and for other purposes. Defense, D. O., Ed. 2002.

70. Kassebacher, T.; Sulzer, P.; Jürschik, S.; Hartungen, E.; Jordan, A.; Edtbauer, A.; Feil, S.; Hanel, G.; Jaksch, S.; Märk, L.; Mayhew, C. A.; Märk, T. D., Investigations of chemical warfare agents and toxic industrial compounds with proton-transfer-reaction mass spectrometry for a real-time threat monitoring scenario. *Rapid Communications in Mass Spectrometry* **2013**, *27* (2), 325-332.

71. Petersson, F.; Sulzer, P.; Mayhew, C. A.; Watts, P.; Jordan, A.; Märk, L.; Märk, T. D., Real-time trace detection and identification of chemical warfare agent simulants using recent advances in proton transfer reaction time-of-flight mass spectrometry. *Rapid Communications in Mass Spectrometry* **2009**, *23* (23), 3875-3880.

72. Cordell, R. L.; Willis, K. A.; Wyche, K. P.; Blake, R. S.; Ellis, A. M.; Monks, P. S., Detection of Chemical Weapon Agents and Simulants Using Chemical Ionization Reaction Time-of-Flight Mass Spectrometry. *Analytical Chemistry* **2007**, *79* (21), 8359-8366.
73. Agarwal, B.; Petersson, F.; Jürschik, S.; Sulzer, P.; Jordan, A.; Märk, T. D.; Watts, P.; Mayhew, C. A., Use of proton transfer reaction time-of-flight mass spectrometry for the analytical detection of illicit and controlled prescription drugs at room temperature via direct headspace sampling. *Anal Bioanal Chem* **2011**, *400* (8), 2631-2639.
74. Jürschik, S.; Agarwal, B.; Kassebacher, T.; Sulzer, P.; Mayhew, C. A.; Märk, T. D., Rapid and facile detection of four date rape drugs in different beverages utilizing proton transfer reaction mass spectrometry (PTR-MS). *Journal of Mass Spectrometry* **2012**, *47* (9), 1092-1097.
75. Lanza, M.; Acton, W. J.; Sulzer, P.; Breiev, K.; Jürschik, S.; Jordan, A.; Hartungen, E.; Hanel, G.; Märk, L.; Märk, T. D.; Mayhew, C. A., Selective reagent ionisation-time of flight-mass spectrometry: a rapid technology for the novel analysis of blends of new psychoactive substances. *Journal of Mass Spectrometry* **2015**, *50* (2), 427-431.
76. Acton, W. J.; Lanza, M.; Agarwal, B.; Jürschik, S.; Sulzer, P.; Breiev, K.; Jordan, A.; Hartungen, E.; Hanel, G.; Märk, L.; Mayhew, C. A.; Märk, T. D., Headspace analysis of new psychoactive substances using a Selective Reagent Ionisation-Time of Flight-Mass Spectrometer. *International Journal of Mass Spectrometry* **2014**, *360* (0), 28-38.
77. Burke, J., Al Qaeda. *Foreign Policy* **2004**, 18-26.
78. Jenkins, T. F.; Leggett, D. C.; Miyares, P. H.; Walsh, M. E.; Ranney, T. A.; Cragin, J. H.; George, V., Chemical signatures of TNT-filled land mines. *Talanta* **2001**, *54* (3), 501-513.
79. Gorontzy, T.; Drzyzga, O.; Kahl, M. W.; Bruns-nagel, D.; Breitung, J.; Loew, E. v.; Blotevogel, K. H., Microbial Degradation of Explosives and Related Compounds. *Critical Reviews in Microbiology* **1994**, *20* (4), 265-284.
80. Rodgers, J. D.; Bunce, N. J., Treatment methods for the remediation of nitroaromatic explosives. *Water Research* **2001**, *35* (9), 2101-2111.
81. Germain, M. E.; Knapp, M. J., Optical explosives detection: from color changes to fluorescence turn-on. *Chemical Society Reviews* **2009**, *38* (9), 2543-2555.
82. Salinas, Y.; Martínez-Máñez, R.; Marcos, M. D.; Sancenón, F.; Costero, A. M.; Parra, M.; Gil, S., Optical chemosensors and reagents to detect explosives. *Chemical Society Reviews* **2012**, *41* (3), 1261-1296.

83. Yang, L.; Li, X.; Qin, C.; Shao, K.-Z.; Su, Z.-M., A fluorescent sensor for highly selective sensing of nitro explosives and Hg (ii) ions based on a 3D porous layer metal-organic framework. *CrystEngComm* **2016**.
84. Mäkinen, M.; Nousiainen, M.; Sillanpää, M., Ion spectrometric detection technologies for ultra-traces of explosives: A review. *Mass Spectrometry Reviews* **2011**, *30* (5), 940-973.
85. Fainberg, A., Explosives Detection for Aviation Security. *Science* **1992**, *255* (5051), 1531-1537.
86. Rudolf Meyer, J. K., Axel Homburg *Explosives*. Sixth ed.; Wiley-VCH Verlag GmbH: 2007; p 433.
87. Singh, S., Sensors—An effective approach for the detection of explosives. *Journal of Hazardous Materials* **2007**, *144* (1-2), 15-28.
88. Senesac, L.; Thundat, T. G., Nanosensors for trace explosive detection. *Materials Today* **2008**, *11* (3), 28-36.
89. Steinfeld, J. I.; Wormhoudt, J., Explosives detection: a challenge for physical chemistry. *Annual Review of Physical Chemistry* **1998**, *49* (1), 203-232.
90. Ewing, R. G.; Waltman, M. J.; Atkinson, D. A.; Grate, J. W.; Hotchkiss, P. J., The vapor pressures of explosives. *TrAC Trends in Analytical Chemistry* **2013**, *42* (0), 35-48.
91. Moore, D. S., Instrumentation for trace detection of high explosives. *Review of Scientific Instruments* **2004**, *75* (8), 2499-2512.
92. Cooper, P. W., *Explosives engineering*. Wiley-VCH: 1996.
93. Moore, D., Recent Advances in Trace Explosives Detection Instrumentation. *Sens Imaging* **2007**, *8* (1), 9-38.
94. Agrawal, J. P., *High energy materials: propellants, explosives and pyrotechnics*. John Wiley & Sons: 2010.
95. Martínez-Lozano, P.; Rus, J.; Fernández de la Mora, G.; Hernández, M.; Fernández de la Mora, J., Secondary Electrospray Ionization (SESI) of Ambient Vapors for Explosive Detection at Concentrations Below Parts Per Trillion. *Journal of the American Society for Mass Spectrometry* **2009**, *20* (2), 287-294.
96. Nilles, J. M.; Connell, T. R.; Stokes, S. T.; Dupont Durst, H., Explosives Detection Using Direct Analysis in Real Time (DART) Mass Spectrometry. *Propellants, Explosives, Pyrotechnics* **2010**, *35* (5), 446-451.

97. Ewing, R. G.; Clowers, B. H.; Atkinson, D. A., Direct Real-Time Detection of Vapors from Explosive Compounds. *Analytical Chemistry* **2013**, *85* (22), 10977-10983.
98. DeTata, D. A.; Collins, P. A.; McKinley, A. J., A Comparison of Common Swabbing Materials for the Recovery of Organic and Inorganic Explosive Residues. *Journal of Forensic Sciences* **2013**, *58* (3), 757-763.
99. Staymates, J. L.; Grandner, J.; Gillen, G., Fabrication of adhesive coated swabs for improved swipe-based particle collection efficiency. *Analytical Methods* **2011**, *3* (9), 2056-2060.
100. Verkouteren, J. R.; Coleman, J. L.; Fletcher, R. A.; Smith, W. J.; Klouda, G. A.; Gillen, G., A method to determine collection efficiency of particles by swipe sampling. *Measurement Science and Technology* **2008**, *19* (11), 115101.
101. Harper, R. J.; Almirall, J. R.; Furton, K. G., Identification of dominant odor chemicals emanating from explosives for use in developing optimal training aid combinations and mimics for canine detection. *Talanta* **2005**, *67* (2), 313-327.
102. Furton, K. G.; Myers, L. J., The scientific foundation and efficacy of the use of canines as chemical detectors for explosives. *Talanta* **2001**, *54* (3), 487-500.
103. Yinon, J., Peer Reviewed: Detection of Explosives by Electronic Noses. *Analytical Chemistry* **2003**, *75* (5), 98 A-105 A.
104. DeTata, D.; Collins, P.; McKinley, A., A fast liquid chromatography quadrupole time-of-flight mass spectrometry (LC-QToF-MS) method for the identification of organic explosives and propellants. *Forensic Science International* **2013**, *233* (1-3), 63-74
105. Xu, X.; Van de Craats, A. M.; de Bruyn, P. C., Highly sensitive screening method for nitroaromatic, nitramine and nitrate ester explosives by high performance liquid chromatography-atmospheric pressure ionization-mass spectrometry (HPLC-API-MS) in forensic applications. Wiley: Hoboken, NJ, ETATS-UNIS, 2004; Vol. 49, p 10.
106. Xu, X.; Koeberg, M.; Kuijpers, C.-J.; Kok, E., Development and validation of highly selective screening and confirmatory methods for the qualitative forensic analysis of organic explosive compounds with high performance liquid chromatography coupled with (photodiode array and) LTQ ion trap/Orbitrap mass spectrometric detections (HPLC-(PDA)-LTQOrbitrap). *Science & Justice* **2014**, *54* (1), 3-21.

107. Zhao, X.; Yinon, J., Identification of nitrate ester explosives by liquid chromatography–electrospray ionization and atmospheric pressure chemical ionization mass spectrometry. *Journal of Chromatography A* **2002**, 977 (1), 59-68.
108. Mathis, J. A.; McCord, B. R., The analysis of high explosives by liquid chromatography/electrospray ionization mass spectrometry: multiplexed detection of negative ion adducts. *Rapid communications in mass spectrometry* **2005**, 19 (2), 99-104.
109. Buryakov, I. A., Express analysis of explosives, chemical warfare agents and drugs with multicapillary column gas chromatography and ion mobility increment spectrometry. *Journal of Chromatography B* **2004**, 800 (1), 75-82.
110. Brown, K.; Greenfield, M.; McGrane, S.; Moore, D., Advances in explosives analysis—part I: animal, chemical, ion, and mechanical methods. *Anal Bioanal Chem* **2015**, 1-13.
111. Brown, K.; Greenfield, M.; McGrane, S.; Moore, D., Advances in explosives analysis—part II: photon and neutron methods. *Anal Bioanal Chem* **2015**, 1-17.
112. Tourné, M., Developments in explosives characterization and detection. *Journal of Forensic Research* **2013**, 2014.
113. Caygill, J. S.; Davis, F.; Higson, S. P. J., Current trends in explosive detection techniques. *Talanta* **2012**, 88 (0), 14-29.
114. Rämpke, A.; Palma-Cando, A.; Shkura, E.; Teckhausen, P.; Polywka, A.; Görrn, P.; Scherf, U.; Riedl, T., Highly sensitive gas-phase explosive detection by luminescent microporous polymer networks. *Scientific Reports* **2016**, 6, 29118.
115. Eiceman, G. A.; Stone, J. A., Peer Reviewed: Ion Mobility Spectrometers in National Defense. *Analytical Chemistry* **2004**, 76 (21), 390 A-397 A.
116. Daum, K. A.; Atkinson, D. A.; Ewing, R. G.; Knighton, W. B.; Grimsrud, E. P., Resolving interferences in negative mode ion mobility spectrometry using selective reactant ion chemistry. *Talanta* **2001**, 54 (2), 299-306.
117. Daum, K. A.; Atkinson, D. A.; Ewing, R. G., Formation of halide reactant ions and effects of excess reagent chemical on the ionization of TNT in ion mobility spectrometry. *Talanta* **2001**, 55 (3), 491-500.
118. Jürschik, S.; Sulzer, P.; Petersson, F.; Mayhew, C. A.; Jordan, A.; Agarwal, B.; Haidacher, S.; Seehauser, H.; Becker, K.; Märk, T. D., Proton transfer reaction mass

spectrometry for the sensitive and rapid real-time detection of solid high explosives in air and water. *Anal Bioanal Chem* **2010**, 398 (7-8), 2813-2820.

119. Mayhew, C. A.; Sulzer, P.; Petersson, F.; Haidacher, S.; Jordan, A.; Märk, L.; Watts, P.; Märk, T. D., Applications of proton transfer reaction time-of-flight mass spectrometry for the sensitive and rapid real-time detection of solid high explosives. *International Journal of Mass Spectrometry* **2010**, 289 (1), 58-63.

120. Sulzer, P.; Petersson, F.; Agarwal, B.; Becker, K. H.; Jürschik, S.; Märk, T. D.; Perry, D.; Watts, P.; Mayhew, C. A., Proton Transfer Reaction Mass Spectrometry and the Unambiguous Real-Time Detection of 2,4,6 Trinitrotoluene. *Analytical Chemistry* **2012**, 84 (9), 4161-4166.

121. Sulzer, P.; Agarwal, B.; Jürschik, S.; Lanza, M.; Jordan, A.; Hartungen, E.; Hanel, G.; Märk, L.; Märk, T. D.; González-Méndez, R.; Watts, P.; Mayhew, C. A., Applications of switching reagent ions in proton transfer reaction mass spectrometric instruments for the improved selectivity of explosive compounds. *International Journal of Mass Spectrometry* **2013**, 354–355 (0), 123-128.

122. Agarwal, B.; González-Méndez, R.; Lanza, M.; Sulzer, P.; Märk, T. D.; Thomas, N.; Mayhew, C. A., Sensitivity and Selectivity of Switchable Reagent Ion Soft Chemical Ionization Mass Spectrometry for the Detection of Picric Acid. *The Journal of Physical Chemistry A* **2014**, 118 (37), 8229-8236.

CHAPTER 2

INSTRUMENTAL

This Chapter covers the technical details dealing with the instrumentation used to perform the work presented in this thesis. All of the experiments, with the exception of picric acid (Chapter 4, pages 87-108), were undertaken using a commercial Kore PTR-ToF-MS (either a first generation instrument or a Series I). For the picric acid work, published results were undertaken using an IONICON Analytik GmbH SRI-PTR-ToF-MS 8000, although for reproducibility purposes measurements were repeated with a first generation Kore PTR-ToF-MS based at the Molecular Physics Research Group at The University of Birmingham. In addition to this, bespoke instrumentation manufactured by Kore Technology was also used. This involved the use of a thermal desorption unit (Chapter 5, pages 109-127), a drift tube implemented with an ion-funnel (Chapter 6, pages 128-147) and a fast switching of reduced electric field technology (Chapter 7, pages 148-165).

2.1 Introduction

Figure 2.1 illustrates the basic layout for the key components of a PTR-MS instrument, showing the main components and different vacuum levels achieved in the different regions of the instrument. These regions are:

- glow discharge source (GD) to create reagent ions (the ion source)
- a reaction region (the drift tube, DT)
- a mass analyzer to separate the ions according to their mass to charge (m/z) ratio (a time of flight (ToF) with a reflectron configuration)
- an ion detector (multichannel plate type, MCP)
- data acquisition system
- electronics to control all the above components
- vacuum system to achieve the necessary vacuum regimes for the different sections of the instrument

Besides these main components, transfer lenses (named as Transfer Optics and Deflectors), and ToF source (used to pulse ions into the time of flight tube) are also shown for completeness.

All these sections are at different pressures, from approximately 1 mbar in the discharge ion source and drift tube, down to about 10^{-7} mbar in the mass spectrometric region (figure 2.1 shows the different and progressive vacuum steps). The vacuum is achieved by means of two turbomolecular and one rotary pumps.

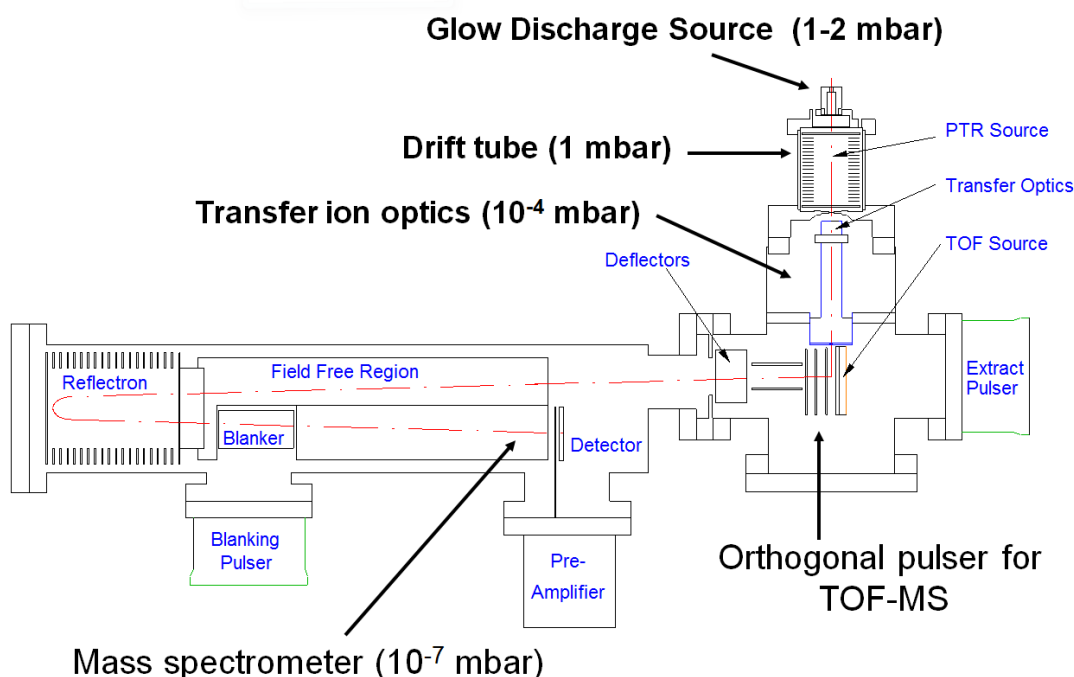


Figure 2.1 Schematic diagram of the Kore PTR-ToF-MS used for this work showing the main components and typical pressures achieved in each region. The lines schematically illustrate the trajectories of the ions from the inlet to the detector. Adapted with permission from Kore Technology Ltd. Manual Z-5851-M.

Water vapour from a distilled water reservoir is introduced into a hollow cathode electrical discharge where, after ionisation via electron impact and subsequent ion-molecule processes, the terminal reagent ion is H_3O^+ . These ions are then transferred to the DT of the instrument where H_3O^+ donates its proton to an analyte M whose proton affinity (PA) is greater than that of water following equation 1.7 (page 8). This process can be non-dissociative (resulting in the protonated parent molecule MH^+) and/or dissociative. Fragmentation may be spontaneous upon proton transfer or may require additional energy which is supplied through collisions with the buffer gas during the migration of the product ions down the drift tube under the influence of the electric field, E .

Once a charged analyte reaches the end of the drift tube it is transferred into the mass spectrometer region via a series of transfer optics, arriving at the extract pulser where all ions are given the same kinetic energy and pulsed in packages into the field-free region of the time of flight tube. Within this region ions fly towards the back of the tube, where a series of electrodes, known as a reflectron, reflect the ions towards the MCP detector. Ions are separated according to their drift time, which is directly related with their mass-to-charge ratio (m/z) - the time of arrival at the detector is proportional to $\sqrt{m/z}$. Ions arriving at the detector are pulse counted, amplified and converted into a digital signal for subsequent data treatment with the help of computer software that displays them onto a mass spectrum.

Once the ions are pulsed into the mass analyser, there are two pairs of spectrometer deflector plates, which force the direction of the ions. These deflectors allow the steering of the ion beam into the field free region of the mass analyser to be optimised. It is important to highlight that the low pressures in the mass spectrometric regions leads to a considerable increase in the mean free path λ of the ions. This can be calculated using the expression:¹

$$\lambda = \frac{RT}{\sqrt{2}\pi d^2 N_A p} \quad (\text{Equation 2.1})$$

R: Universal constant gas $R = k_B \cdot N_A = 8.3144621 \text{ J}\cdot\text{mol}^{-1}\cdot\text{K}^{-1}$ (NIST²)

T: temperature (100°C = 373K)

d: diameter of air molecules (considering ideal gases) $d_{\text{loschmidt}} = 3.61 \cdot 10^{-10} \text{ m}$ (A°)

p: pressure

The result is a change from $\lambda_{\text{drift}} \approx 75 \text{ }\mu\text{m}$ to $\lambda_{\text{ToF}} = 930 \text{ m}$. This increase in λ means that it is unlikely that anymore collisions with the vanishingly small remaining air molecules present in that region might happen, so therefore the analyte's composition (in the form of protonated parent molecule or product ions) at the exit of the DT is preserved.³ It has however, been observed that collisional processes in the transfer region between the drift tube and ion transfer optics do occur leading to product ions such as N_2H^+ and CO_2H^+ .³ It is important to mention that in this region collisional induced dissociation (CID) could also occur. Fine tuning of the voltages is needed to minimise this.

The blanking pulser shown in figure 2.1 is a characteristic feature for the first generation instrument used and is not present in newer instruments from KORE. Its purpose is to stop the majority of the m/z 19 (hydronium) ions reaching the detector in order to preserve its lifetime. It provides an electric pulse that deviate ions flying down the time of flight tube at a given pre-set time.⁴

A commonly used detector in conjunction with ToF mass analysers is the dual micro-channel plate type electron multiplier (MCP). This is due to the fact that MCP show high time resolution (<1 ns), which means that the ions arriving at the detector (at least theoretically) are not overlapped (although this might not be always the case and saturation of the detector is possible).

Historically, and due to the high cost of time of flight mass analysers, quadrupoles were used as the standard mass spectrometer. Nowadays, with the drop in cost for the technology almost all the commercial PTR-MS systems are equipped with ToF mass analysers. The main advantages for using a quadrupole based system are higher sensitivity and smaller size/weight (this is quite relevant in terms of portability). However, ToF mass spectrometers offer higher resolution, no m/z limit (theoretically) and acquisition of the complete mass spectrum without scanning.⁵

The several physics and chemistry processes involved in the main parts of a PTR-MS are described in the next section 2.2, whereas the newly designed and implemented hardware, namely the thermal desorption unit, ion funnel drift tube and fast reduced electric field switching are briefly described in section 2.3 (pages 54- 62) and explained in more depth in the corresponding results Chapters (see Chapters 5-7).

2.2 Physics and chemistry involved in PTR systems

2.2.1 Reagent ions generation: Hollow Cathode (HC) and Source Drift (SD)

Hollow cathode (HC) discharges are classified according to their voltage-current characteristics, and one class of them is known as glow discharges (GD) when are between 1 μ A and 1 A.⁶ They receive this name because a visible luminous glow is observed.⁵ A schematic of a generic glow discharge and associated electronic components is shown in figure 2.2.

Low pressure gas discharges in cylindrical hollow cathodes for the determination of ion-molecule reaction rate constants were investigated during the 1970s, proving that they could be used as sources of secondary and tertiary ions, including hydronium among many others.⁷⁻¹⁰ When such HCs were implemented in the first PTR-MS instruments, a very pure hydronium beam was achievable with no need for a mass filter and thus simplifying the instrumentation required.¹¹

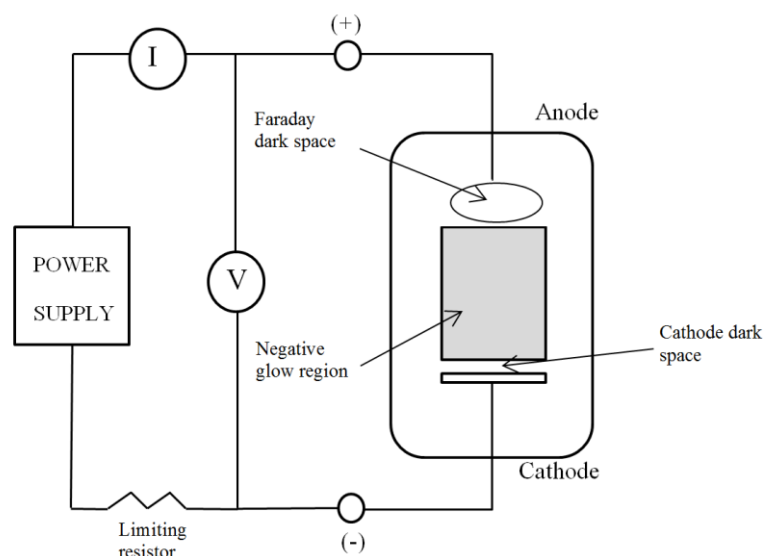


Figure 2.2: Schematic representation of a glow discharge and associated components. Adapted from Harrison *et al.*¹²

The structure of a glow discharge and the processes occurring within are complex, and an in depth explanation is not the purpose of this thesis, so only the salient points relevant to this work are provided here (in depth discussions are available by Marcus *et al.*¹³ and Pillow *et al.*¹⁴). As reported by Howorka *et al.*,¹⁰ the cylindrical HC configuration confines the plasma into a cylinder along the axis of the cathode (see figure 2.3) known as the negative glow (with a potential close to the anode potential),⁸ where a high density of electrons and positive ions are located.¹⁵ Between this region and the cathode there is a potential of a few hundred volts – the so-called cathode fall region - where energetic electrons collide with neutrals forming the primary ion products H_2O^+ , H_2^+ , H^+ , O^+ and OH^+ .^{10,11} These species are very reactive, so they react rapidly with neutral water molecules to lead to hydronium (equations 2.2-2.8). The chemical reactions happening within a HC leading to H_3O^+ , together with their rate coefficients are summarised in table 2.1.

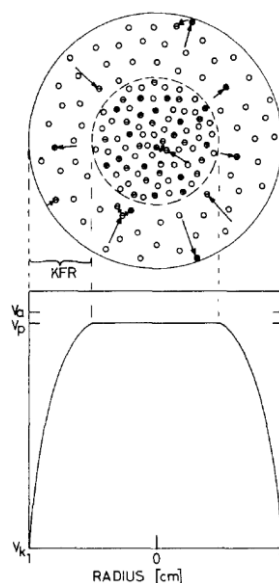


Figure 2.3: Schematic section of a cylindrical hollow cathode used in PTR-MS and its potential distribution. V_A , V_p and V_k represent the anode potential, negative glow potential and cathode potential, respectively. Reproduced with permission from Reference 10. Copyright © 1974 American Institute of Physics.

Once the plasma strikes, it is self-sustained as positive gas ions gain speed in the cathode dark space colliding with the cathode surface and sputtering new secondary particles, mainly as neutral atoms and a small percentage as ions.¹⁶ Positive ions return to the cathode surface, but neutrals diffuse into the negative glow region where they collide with energetic electrons, ions and metastable atoms leading finally after a series of ion-molecule processes to the aforementioned ion products and finally to H_3O^+ .^{12,16}

Table 2.1: Reactions of ions produced by EI of water vapour within a hollow cathode discharge and their corresponding rate coefficients k at 300 K. Bold letters represent the final products. Rate coefficients taken from Ikezoe *et al.*¹⁷

Reactions		Rate coefficient k [10^{-9} ($\text{cm}^3 \cdot \text{s}^{-1}$)] at 300K	
$\text{OH}^+ + \text{H}_2\text{O} \rightarrow$	$\text{H}_3\text{O}^+ + \text{O}$	1.3	Equation 2.2
	$\text{H}_2\text{O}^+ + \text{OH}$	1.8	Equation 2.3

$O^+ + H_2O \rightarrow$	$H_2O^+ + O$	2.6	Equation 2.4
$H_2^+ + H_2O \rightarrow$	$H_3O^+ + H$	3.4	Equation 2.5
	$H_2O^+ + H_2$	3.9	Equation 2.6
$H^+ + H_2O \rightarrow$	$H_2O^+ + H$	8.2	Equation 2.7
$H_2O^+ + H_2O \rightarrow$	$H_3O^+ + OH$	1.8	Equation 2.8

Figure 2.4 shows the hollow cathode (HC) discharge source, source drift region (SD) and partially the drift tube used in the PTR-MS instruments manufactured by Kore Technology. The hollow cathode used on Kore instruments has an operational pressure range of 1 to 2 mbar. It is formed of 2 aluminium (material whose secondary electron coefficient is very high) electrodes, an anode and a cathode, that generate an electrical discharge in a gas between them whilst a high potential (800volts) is applied between both electrodes, thus a plasma is generated.

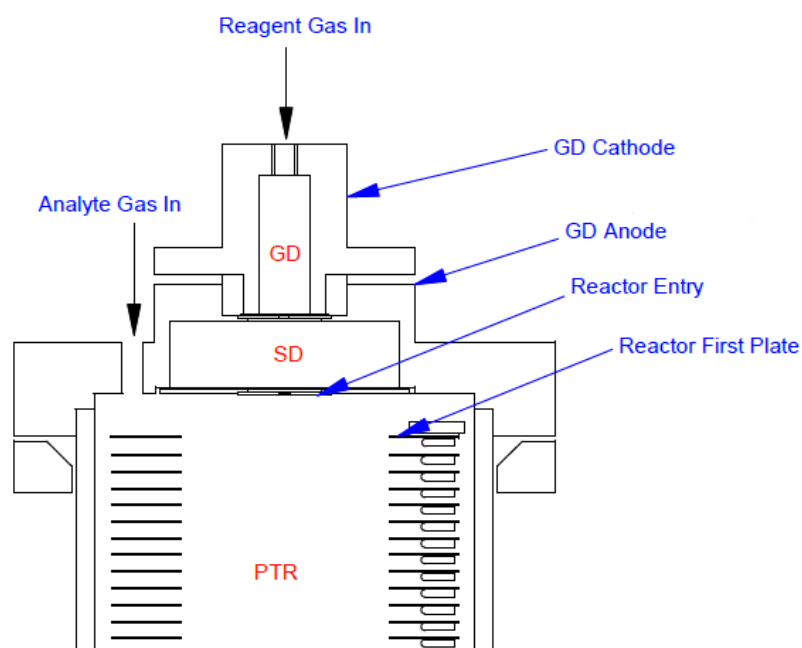


Figure 2.4: Schematic of hollow cathode (or glow discharge), source drift region (SD) and part of the drift tube (named as PTR) used in Kore PTR-MS instruments. Reagent and analyte gas inlets are also shown. Adapted with permission from Kore Technology Ltd. Manual Z-9831-M.

Rate coefficients, k , on table 2.1 show that these reactions are very fast. So, in order to facilitate them to completely take place and maximise the intensity of the terminal ion H_3O^+ the SD region is added at the end of the HC. This also aids to extract ions from the GD and enhances H_3O^+ production through breaking-up protonated water clusters and via additional ion-molecule reactions involving ions that can react with water. As result of all this, at the end of the SD region a very pure beam, 99.5%, of H_3O^+ is obtained without the additional need for a mass filter.^{11,15} The advantage of that is that a less complex experimental set-up is required, but limiting the capability of selecting other reagent ions. This is a different approach to SIFT-MS, where an injection quadrupole is added after this region (microwave plasma is used instead of a HC) so the ability to select the reagent ion is possible. As will be described later, in section 2.2.1.1 (page 45), the selection of different reagent ions is also possible if different reagent gases are used (O_2^+ and NO^+ being the best options for SCIMS). Complications arise because it is not only H_3O^+ which is produced in the ion source region. Owing to the back streaming of air from the drift tube into the discharge region other “terminal” (impurity) ions, shown in table 2.2, are produced. These are NO^+ , NO_2^+ and O_2^+ . Their recombination energies (RE) are less than the ionisation energy of water (12.6 eV). (NO^+ (RE = 9.3 eV), O_2^+ (RE = 12.1 eV) and NO_2^+ (RE = 9.6 eV)). Operating conditions can be adjusted so that the total ion signal level of these impurity ions is typically less than 2-3% of the H_3O^+ intensity. Therefore, they usually are of little consequence for compounds whose proton affinities are greater than that of water. However, m/z 46, NO_2^+ , is of special relevance for explosives detection as this is a fragment ion coming from compounds with a nitro-oxy (-O- NO_2) substituent on their structures.

Table 2.2: Reactions leading to the production of reagent ions that do not react with H_2O - NO^+ , NO_2^+ and O_2^+ . Rate coefficients taken from Anicich.¹⁸

Reactions		Rate constants k [10^{-9} ($\text{cm}^3 \cdot \text{s}^{-1}$)] at 300K	Impurity ion	
$\text{N}_2^+ + \text{O}_2 \rightarrow$	$\text{NO}^+ + \text{O}$	2.6	NO^+	Equation 2.9
$\text{NO}^+ + \text{O} \rightarrow$	NO_2^+	2.3	NO_2^+	Equation 2.10
$\text{O}_2 + \text{e}^- \rightarrow$	O_2^+	N/A	O_2^+	Equation 2.11

New Kore instruments incorporate an extra set of lenses (shown in figure 2.5),¹⁹ which minimise back-diffusion of air from the reactor through the SD and into the GD and thus minimising the O_2^+ , NO^+ and NO_2^+ signals. The aim of this new electrode is to change the exit of the SD from an aperture to (effectively) a ‘pipe’ through to the PTR, restricting back-diffusion from the reactor.

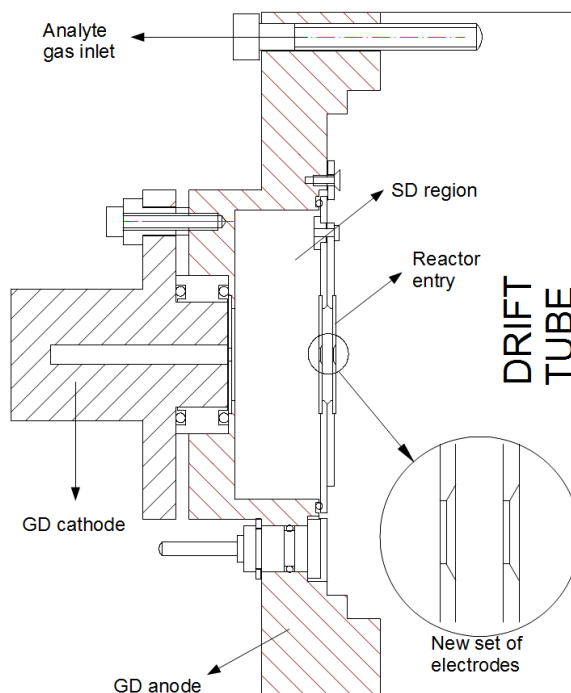


Figure 2.5: Schematic of the extra set of lenses for minimising back-diffusion from the reactor into the GD region of the instrument. Adapted with permission from Kore Technology Ltd.

By using this new SD electrode the H_3O^+/O_2^+ (m/z 21/34) ratio has improved by a factor of ~ 4 compared to data taken without the electrode. Use of this set of electrodes does not affect the sensitivity whatsoever; if anything there has been a slight improvement of the signals obtained due to the fact that the proton transfer reaction channel is enhanced versus charge transfer.¹⁹

2.2.1.1 Other chemical reagent ion systems

Routinely PTR-MS instruments employ H_3O^+ as the reagent ion, but it is also possible to use other reagent ions, e.g. O_2^+ and NO^+ , which are arguably the most useful in terms of soft chemical ionisation. Tables 2.3 and 2.4 show the ion-molecule processes happening in the HC to obtain both O_2^+ and NO^+ respectively. Although the instrument should technically be called SCIMS rather than PTR-MS, traditionally the same nomenclature is used independently of the reagent ion. Switchable Reagent Ions (SRI[®]) is Ionicon's commercial name given to this implemented technology within a normal PTR-MS instrument, where different reagent source gases are used to produce O_2^+ and NO^+ .²⁰ In order to generate them, the source gases for the HC are pure oxygen and ambient air passed through a charcoal filter or a mixture of pure nitrogen and oxygen, respectively. High intensity (10^6 cps) and purity (> 95%) reagent ions signal are observed for both O_2^+ and NO^+ under such conditions.²¹

Table 2.3. Ionization and reaction pathways occurring in the HC for O_2^+ reagent ion production. Pure oxygen is used as the source gas. Rate coefficients taken from Anicich.¹⁸

Reactions		Rate constants k ($\text{cm}^3 \cdot \text{s}^{-1}$) at 300K	
$\text{O}_2 + \text{e}^- \rightarrow$	$\text{O}_2^+ + 2\text{e}^-$	N/A	Equation 2.12
	$\text{O}^+ + \text{O} + 2\text{e}^-$	N/A	Equation 2.13
$\text{O}^+ + \text{O}_2 \rightarrow$	$\text{O}_2^+ + \text{O}$	2.1×10^{-11}	Equation 2.14

Generation of NO^+ requires a more complex reaction pathway, and requires longer residence times of ions in the HC and SD region. This requires applying lower voltages and lowering the inlet pressure for the HC gas.²²

Table 2.4. Ionization and reaction pathways occurring in the glow discharge for NO^+ reagent ion production. Rate coefficients taken from Anicich.¹⁸

Reactions		Rate constants k	
		$(\text{cm}^3 \cdot \text{s}^{-1})$ at 300K	
$\text{O}_2 + \text{e}^- \rightarrow$	$\text{O}_2^+ + \text{O} + 2\text{e}^-$	N/A	Equation 2.15
	$\text{O}^+ + \text{O} + 2\text{e}^-$	N/A	Equation 2.16
$\text{N}_2 + \text{e}^- \rightarrow$	$\text{N}_2^+ + 2\text{e}^-$	N/A	Equation 2.17
	$\text{N}^+ + \text{N} + 2\text{e}^-$	N/A	Equation 2.18
$\text{N}_2 + \text{O}^+ \rightarrow$	$\text{NO}^+ + \text{N}$	1.20×10^{-12}	Equation 2.19
$\text{N}^+ + \text{O}_2 \rightarrow$	$\text{NO}^+ + \text{O}$	5.8×10^{-10}	Equation 2.20

Among other source gases that can be used in SCIMS, tailored to solve a particular problem, Kr^+ has been used within PTR-MS instrumentation for some applications,^{23,24} and also for explosives (see picric acid work, Chapter 4).²⁵ Kr^+ is formed through electron impact $\text{Kr} + \text{e}^- \rightarrow \text{Kr}^+$ (equation 2.21). Pure Kr is used as the precursor gas feeding the HC and only after ensuring that all the remaining traces of water have been removed, as the $\text{RE}(\text{Kr}^+) = 14.00 \text{ eV}$,² and should any water traces remain in the DT of the instrument the terminal reagent ion would always be H_3O^+ ($\text{IE}(\text{H}_2\text{O}) = 12.62 \text{ eV}$),² therefore long cleaning times with nitrogen are needed before using this reagent gas. Kr^+ has been applied to the detection of inorganic substances such as CH_4 , CO , CO_2 , NO_x and SO_2 .²³

Xe^+ is other exotic reagent ion that can be used. Pure Xe is fed into the HC and through the ionisation process $\text{Xe} + \text{e}^- \rightarrow \text{Xe}^+$ (equation 2.22) a Xe^+ beam is obtained. $\text{RE}(\text{Xe}^+) = 12.13 \text{ eV}$,² is very similar than that of O_2^+ , so it wouldn't be expected advantages in terms of the range of accessible substances that can be ionized. However, an important advantage is its use as an alternative to pure oxygen.

2.2.2 Ion- molecule reactions: Drift Tube or PTR reactor

The drift tube (DT) is the heart of the instrument. It provides a fixed reaction length (important for quantitative analysis) where the ion-molecule reactions occur and minimises water clustering, thus maximise the ionisation of the analyte of interest, mainly whilst ensuring that H_3O^+ is the dominant reagent ion, by changes in operational parameters,^{11,15} and thus minimising water clustering.

Drift tubes have been used since the 1960s, when Earl W. McDaniel of the Georgia Institute of Technology started the construction of a revolutionary low voltage applied drift cell for the study of gas phase ion mobilities.²⁶ Since then, drift tubes have been used mainly in IMS, and more recently in PTR-MS. Although drift tubes used in IMS and PTR-MS are similar in many ways, they also show distinctive characteristics, mainly in the way they are operated -atmospheric pressure for IMS and at low pressures for PTR-MS. A typical Kore drift tube for PTR-MS, as seen in figure 2.6, consists of a 9.36 cm series of 26 ring electrodes, made of stainless steel, separated equally from each other by an insulating material as Teflon® or ceramic, and housed in a 10 cm cylindrical glass chamber. Usually the ring electrodes are located in the outer part of the glass, just because it is easier to manufacture, but it is also possible to place them internally.

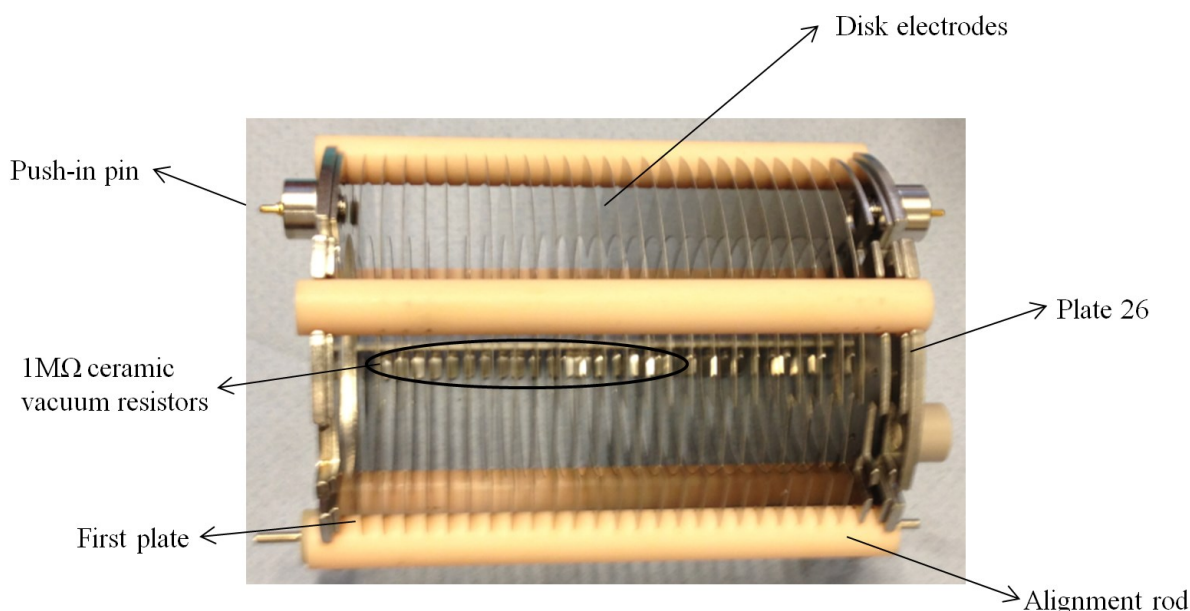


Figure 2.6. Photograph of a Kore drift tube showing the electrodes stack, alignment rods and push-in pins for electric contacts.

An interconnected chain of 1 MΩ ceramic vacuum resistors attached to the ring electrodes define a homogenous electric field when a voltage is applied between the uppermost electrode and the bottom plate. Thus, a linearly decreasing potential ($\Delta V_{first \rightarrow last}$) is generated within the DT. Typical operating values for standard conditions provide an electric field strength E (expressed in $V \cdot cm^{-1}$) of:

$$E = \frac{\Delta V_{first \rightarrow last}}{l_{drift\ tube}} \quad (\text{Equation 2.23})$$

$$\cong 24 V \cdot cm^{-1}$$

$\Delta V_{first \rightarrow last}$:Potential difference between first and last plate is 225volts.

The gas number density, N , can be obtained using the ideal gas law, $p \cdot V = n \cdot R \cdot T = N \cdot k_B \cdot T$, where n is the number of moles $n = N/N_A$ (where N_A is the Avogadro's number $= 6.022 \cdot 10^{23} \text{ mol}^{-1}$), R is the Universal gas constant ($= 8.3144621 \text{ J} \cdot \text{mol}^{-1} \cdot \text{K}^{-1}$) and k_B is the Boltzmann constant ($= 1.3806488 \times 10^{-23} \text{ J} \cdot \text{K}^{-1}$).² In terms of standard temperature and pressure, N can be calculated from

$$N = \left(\frac{p_{drift}}{T_{drift}} \right) \cdot \left(\frac{T_0}{p_0} \right) \cdot \left(\frac{N_A}{V_{mol}} \right) \quad (\text{Equation 2.24})$$

where

p_{drift} is the DT pressure (normally set at 1mbar)

T_{drift} is the DT temperature (normally set at $= 100^\circ\text{C}$)

V_{mol} is the molar gas volume ($1 \text{ mol} = 22.14 \text{ L} = 22.414 \cdot 10^3 \text{ cm}^3$, STP conditions).

$T_0 = 273.15 \text{ K}$
 $p_0 = 1013.25 \text{ mbar}$

For the conditions given this gives $N = 1.94 \times 10^{16} \text{ cm}^{-3}$.

Now we can derive the ratio $E/N = 22.2 V \cdot cm^{-1} / 1.94 \cdot 10^{16} \text{ cm}^{-3} \cong 124 \text{ Td}$.

The calculated $E/N \cong 124$ Td lays within the range 120-140 Td, which provide a good compromise between low clustering and reasonable reaction times without excessive fragmentation, and therefore it is the typical selected value for operating PTR-MS instruments.^{5,27}

The ratio E/N , is usually given in non SI units of Townsend (Td) ($1 \text{ Td} = 10^{-17} \text{ V cm}^2$); to give an idea of value, 100 Td corresponds to a centre of mass collisional energy of 0.15 eV for H_3O^+ with a nitrogen molecule.⁵

A graphical overview of what happens in the drift tube is schematically shown in figure 2.7. It illustrates as a reactant ion (represented by the blue coloured sphere) travelling along the DT at a constant drift velocity, encounters and collides with a reactant neutral (represented by the green coloured sphere), reacting (represented by the red arrow) via an either non-dissociative or dissociative proton transfer reaction, producing a product ion (represented by the red coloured sphere). Collisions with the buffer gas molecules (represented by the grey coloured spheres), the most numerous ones, do not produce any product ions although they might have an effect on the whole reaction process and also (potentially) affect the product ions fragmentation distribution.

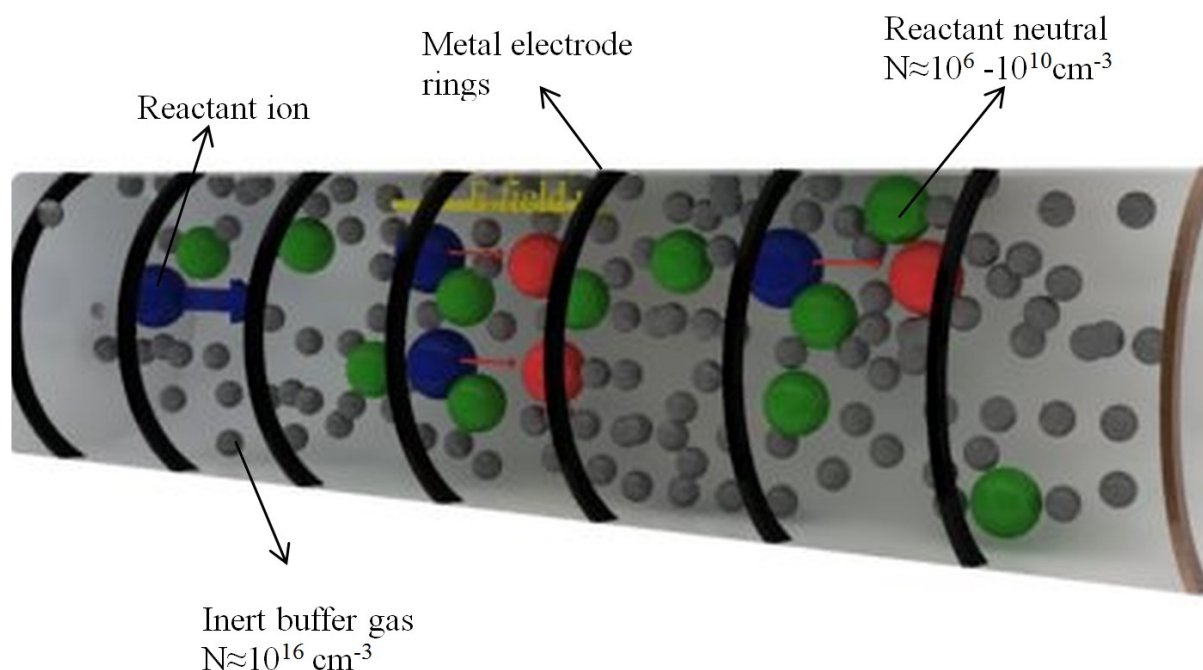


Figure 2.7: Schematic of the processes occurring within a drift tube. The reactant ion (blue colour) migrates under the effect of the E field (in yellow) towards the exit of the DT. In its

way mostly non-dissociative proton transfer reaction occurs from hydronium when that collides with a reactant neutral (green coloured sphere) resulting in a product ion (red colour). Inert buffer gas molecules are represented by the grey spheres.

2.2.2.1 Neutral gas residence time

Residence time is defined as the time that a “slice” of gas would take to travel along the DT of the instrument. The volumetric flow rate for a DT operated at non-STP conditions, F_{DT} , can be related to the STP flow conditions, F^0 , from the expression:⁵

$$F_{DT} = F^0 \cdot (p^0/p_{drift}) \cdot (T_{drift}/T^0) \quad \text{Equation 2.25}$$

where the 0 superscript means STP (1 atm and 0°C); (1atm = 760 torr = 1013.25mbar).

Considering a standard Kore DT of 9.36cm long and 7.2 cm diameter, and the typical operational values of 100°C and 1.5 mbar pressure receiving an STP air flow rate, F^0 , into the instrument of $1.35 \text{ cm}^3 \cdot \text{s}^{-1}$, we can derive that $F_{DT} = (1.35 \text{ cm}^3 \cdot \text{s}^{-1}) \cdot (1013.25\text{mbar}/1.5\text{mbar}) \cdot (373 \text{ K}/273\text{K}) = 1246 \text{ cm}^3 \cdot \text{s}^{-1}$.

Therefore, the average residence time for a neutral is given by the expression $t_{\text{residence neutrals}} = V_{\text{reactor}}/F_{DT} = (\pi \cdot 3.6^2 \text{ cm}^2 \cdot 10 \text{ cm}) / (1246 \text{ cm}^3 \cdot \text{s}^{-1}) = 0.33\text{s}$.

2.2.2.2 Ion mobilities and reaction times

The reaction time (defined as the time it takes for an H_3O^+ ion to travel down the length of the DT) can be calculated from the expression $t_{drift} = l_{drift} / v_{drift}$, where t_{drift} is the residence time of H_3O^+ ions in the drift tube (in seconds), l_{drift} is the drift tube length and v_{drift} is the drift velocity of the ions within the DT.

Assuming low electric fields (E) within the DT the relationship between v_{drift} of the ion swarm and the E applied is given by the expression,²⁸

$$v_{drift} = \mu \cdot E \quad \text{(Equation 2.26)}$$

where μ is the ion mobility and E is the electric field strength. μ is a function of the temperature, pressure, size and structure of the ion and the neutral gas molecules. To make it

independent from (T,p) a new term, referred to as μ^0 , the so-called reduced mobility, is introduced and if we normalise the mobility for STP conditions we get that:

$$\mu^0 = \left(\frac{p}{p^0}\right) \cdot \left(\frac{T^0}{T}\right) \cdot \mu = \left(\frac{N}{N^0}\right) \cdot \mu \quad (\text{Equation 2.27})$$

where p is the pressure, T the temperature and N the gas number density in the DT at the operational conditions. The 0 superscript indicates STP conditions.

Combining this expression into the drift velocity we have that

$$v_{\text{drift}} = N^0 \cdot \mu^0 \cdot \left(\frac{E}{N}\right) \quad (\text{Equation 2.28})$$

Finally we can derive that

$$t_{\text{drift}} = \left(\frac{l_{\text{drift}}}{\mu^0 \cdot N^0}\right) \cdot \left(\frac{E}{N}\right)^{-1} \quad (\text{Equation 2.29})$$

$\mu^0(\text{H}_3\text{O}^+)$ in nitrogen as the buffer gas is $2.81 \text{ cm}^2 \cdot \text{V}^{-1} \cdot \text{s}^{-1}$,²⁹ and $N^0 = 2.687 \cdot 10^{19} \text{ cm}^{-3}$.⁵ For the previous 124 Td we can derive that $t_{\text{drift}} = \left(9.36 \text{ cm} / 2.81 \text{ cm}^2 \text{V}^{-1} \text{s}^{-1} \times 2.7 \cdot 10^{19} \text{ cm}^{-3}\right) \cdot (1.24 \cdot 10^{15} \text{ V} \cdot \text{cm}^2) = 153 \mu\text{s}$ for a mean $v_{\text{drift}} = 941 \text{ m} \cdot \text{s}^{-1}$.

De Gouw *et al.*,³⁰ have proved that this calculation is in good agreement with the experimentally measured values for $E/N > 100 \text{ Td}$, where H_3O^+ is the most abundant ion populating the DT. At lower values, the water clusters, $\text{H}_3\text{O}^+ \cdot (\text{H}_2\text{O})_n$ ($n=1,2$), dominate and their lower mobilities alter the calculation.

Within comparison to the residence time for neutrals this value is around 2 orders of magnitude shorter.³¹

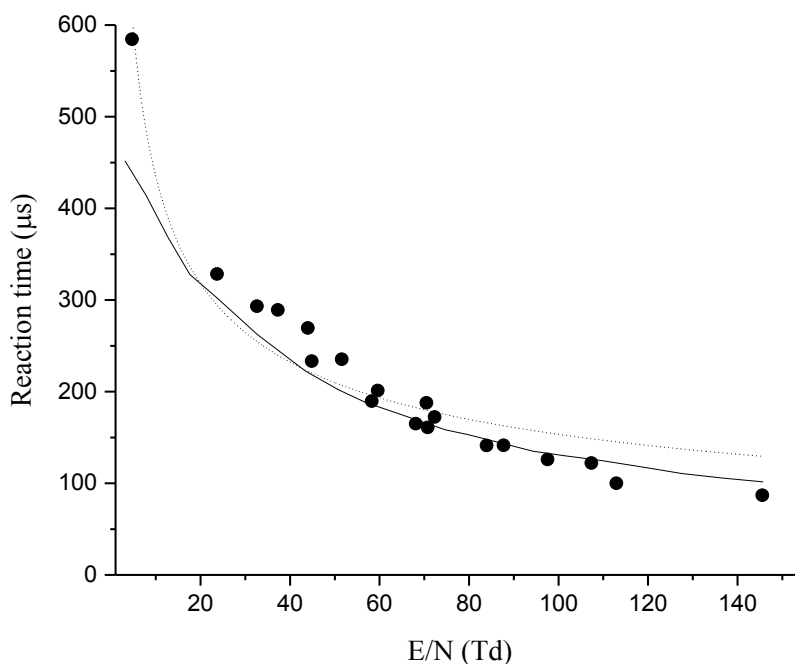


Figure 2.8. Residence time of H_3O^+ ions in the DT of a PTR-MS instrument. The solid circles are experimental results, the solid curve is calculated using equation 2.29 and the dotted line represents an inversely proportional fit to the experimental results. Adapted from de Gouw *et al.*³⁰

2.2.2.3 Ion-Molecule Collisions, ion temperatures and ion cluster distributions

It is not within the scope of this thesis to make an in depth description of the energetics for the ion-molecule collision; discussions about this can be seen elsewhere in the literature.^{3,5,30} Nevertheless, it is important to highlight the effect that these can have in terms of the types of product ions.

The basics of the kinetic theory behind proton transfer reactions was obtained in flow tube instruments that operate at thermal energies (room temperature).³² However, the DT of a PTR-MS instrument operates at supra-thermal energies,⁵ as ions are affected by an electric field whilst travelling along the length of the DT and thus $T_{\text{ions}} > T_{\text{drift tube}}$.³⁰ This is a consequence of the selective heating of the ions by the electric field E . The mean ion kinetic energy has been derived by Warnier,^{33,34} and factors that contribute to it are thermal contribution, ion's kinetic energy (at v_{drift}) and additionally a contribution from collisions between the ions and the buffer gas molecules (of mass m_{buffer}).

$$KE_{ion} = \frac{3}{2}k_B T + \frac{1}{2}m_{ion} v_{drift}^2 + \frac{1}{2}m_{buffer} v_{drift}^2 \quad (\text{Equation 2.30})$$

Equation 2.30 refers to the ion kinetic energy in the laboratory frame of reference. However, when referring to ion-molecule reactions what is relevant is the collision energy. Thus, the relative kinetic energy of the colliding species is required.^{3,33,34} For ion-molecule reactions there is conservation of linear momentum, i.e. inelastic collisions, so the kinetic energy given by equation 2.30 is not the same as the collision energy. We have to refer to the centre of mass frame (CoM). CoM is the frame in which we are travelling along with the centre of mass, considering only the interactions between particles, and thus giving us the energy available for the reaction:

$$KE_{CoM} = \frac{1}{2} \left(\frac{m_{neutral} \cdot m_{ion}}{m_{neutral} + m_{ion}} \right) \cdot (v_{ion}^2 + v_{neutral}^2) \quad (\text{Equation 2.31})$$

where

$$KE_{ion} = \frac{1}{2}m_{ion} v_{ion}^2 \quad (\text{Equation 2.32}) \quad \text{and} \quad \frac{3}{2}k_B T = \frac{1}{2}m_{neutral} v_{neutral}^2 \quad (\text{Equation 2.33})$$

$m_{neutral}$ refers to the neutral molecule involve in the collision. This can be a non-reactive collision with a buffer gas molecule or a reactive collision with an analyte molecule.

Combining equations we can finally derive that:

$$KE_{CoM} = \frac{m_{neutral}}{m_{ion} + m_{neutral}} (KE_{ion} - \frac{3}{2}k_B T) + \frac{3}{2}k_B T \quad (\text{Equation 2.34})$$

Taken the previously calculated value of $v_{drift}=941 \text{ m}\cdot\text{s}^{-1}$ at 124 Td and supposing a molecule of 2,4,6-trinitrotoluene (molecular mass of 227) using equation 2.34 we can calculate the centre-of-mass collision energy between TNT and H_3O^+ . The buffer gas (air) has a relative molecular mass of 28.8 (weighted average of N_2 and O_2). The calculation gives a number of $\sim 0.24 \text{ eV}$ at 300 K, that is almost an order of magnitude higher than the average thermal kinetic energy at 300 K. This clearly shows the extra energy the electric field provides in PTR-MS.⁵

An important consequence of all this is that ions have an effective collisional temperature, T_{eff} . In addition their internal energies will be non-thermal. This is directly related to the fact

that upon collision with other molecules, kinetic energy is partially converted into internal energy and if enough, this would lead to a higher fragmentation.²² Higher kinetic energies - or what is the same, high E/N values - reduce the reaction time, lower water clusters formation and, decreases sensitivity.^{3,30}

A clear effect of this can be appreciated in figure 2.9, where protonated water H_3O^+ (m/z 19) and the dimer and trimer water clusters, $\text{H}_3\text{O}^+\cdot\text{H}_2\text{O}$ (m/z 37) and $\text{H}_3\text{O}^+\cdot(\text{H}_2\text{O})_2$ (m/z 55), respectively, are represented versus the reduced electric field. For example at 90 Td (under the operational temperature and pressure values used) protonated water clusters are the dominant reagent ions, whereas at 180 Td these have negligible intensities because the collisions occurring in the drift tube are sufficient to break-up protonated water clusters to the H_3O^+ monomer. The actual percentage of protonated water clusters for fixed E/N is also strongly dependent on the humidity of the buffer gas in the drift tube.

It is important to run PTR-MS experiments at a high enough E/N to avoid excessive water clustering, but low enough to avoid fragmentation and to have higher sensitivity. Therefore, a compromise is needed, which depends mainly on the nature of the analyte to study.

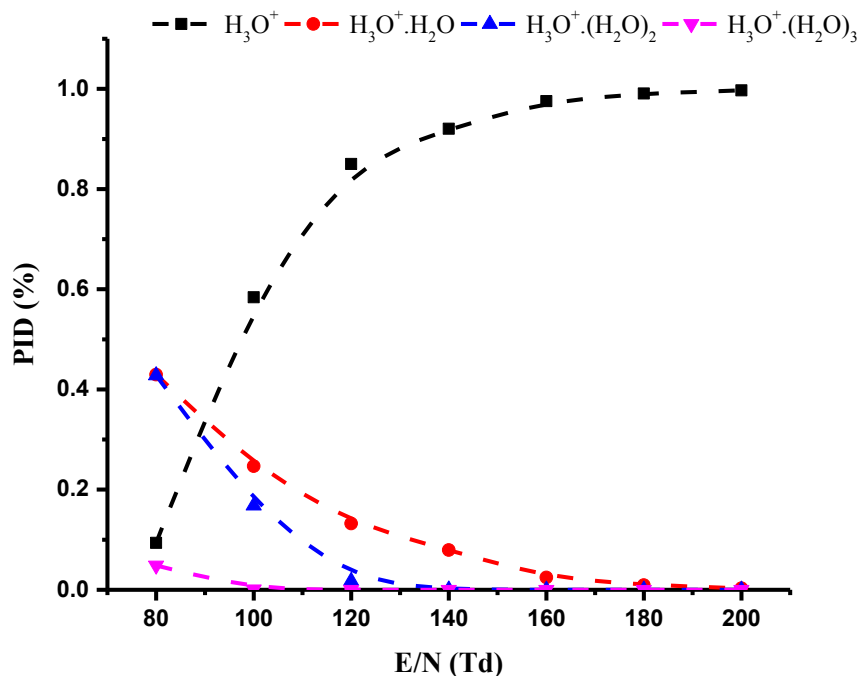


Figure 2.9. Percentage product ion distribution (PID) of the water reagent ions present in the drift tube as a function of reduced electric field for the range 80-200Td.

2.3 New hardware developments

2.3.1 Thermal desorption unit

To overcome any memory effects,³⁵ and to ensure that a concentration pulse of an explosive material is driven to the DT of a PTR-MS instrument, Kore specifically designed and built a thermal desorption unit (TDU). A characteristic feature of this unit is that it creates a real seal between two anvils and the swab, forcing all the material deposited onto the swab to be directed into the PTR-MS and not being lost sideways. A schematic representation of this new TDU and “anvil” system is provided in figure. 2.10. The force is sufficiently high to plastically deform the PTFE swab and convert it into a gas tight circular seal around the rim of the swab.³⁶ The TDU is connected directly to the inlet of the PTR-MS instrument making use of a short (10cm) passivated (SilcoNert[®]2000) heated stainless steel.

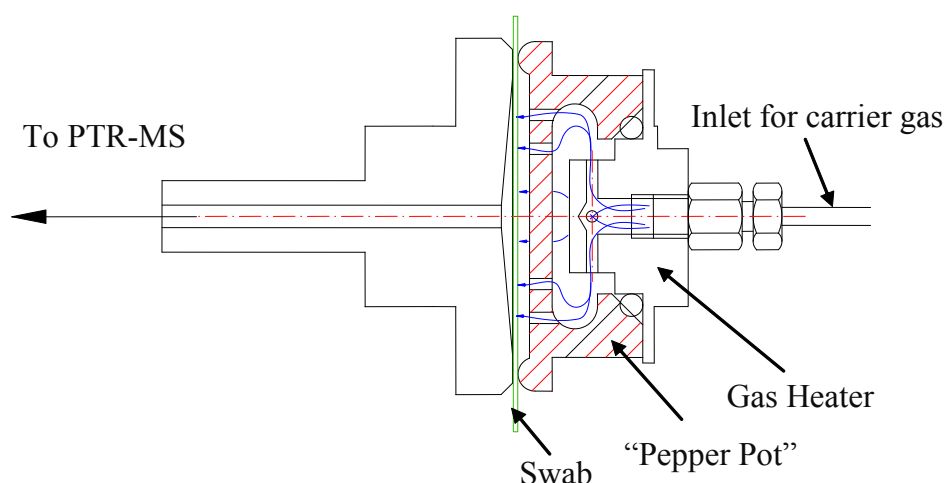


Figure 2.10. Schematic cross-section of the TDU. Laboratory air is heated as it passes through the gas heater section and then is equally distributed onto the swab's surface via the “pepper pot”, which is a series of holes directing the heated air towards the swab. Adapted with permission from Kore Technology Ltd.

This unit uses polytetrafluoroethylene (PTFE) circular swabs (ThermoFisher Scientific, Cheshire, UK) - see figure 2.11(a)- of 3.5 cm of diameter, presented in a cardboard mount for easy handling. A seal is created by bringing together the two heated anvils that apply a high force (and temperature) to the swab. Once a seal is created, laboratory air used as carrier gas heated within the TDU to the desire temperature (maximum operational specification is 200

°C) flows through a series of holes in a heated metal plate (the “pepper pot”). A detailed view of the “pepper pot” is shown on figure 2.11 (b). This air then passes through the swab and into the inlet system driving any thermally desorbed material through to the drift tube. As soon as the swab is crushed any trace material present on its surface will be thermally desorbed in a very short time. However, the actual temporal duration of this “pulse” of a compound will depend on many factors, such as the desorption, inlet and drift tube temperatures, carrier flow rate and analyte’s nature (mainly volatility and ease of adsorption to surfaces). This concentrated temporal pulse is thus observed by monitoring an appropriate m/z channel as a function of time.

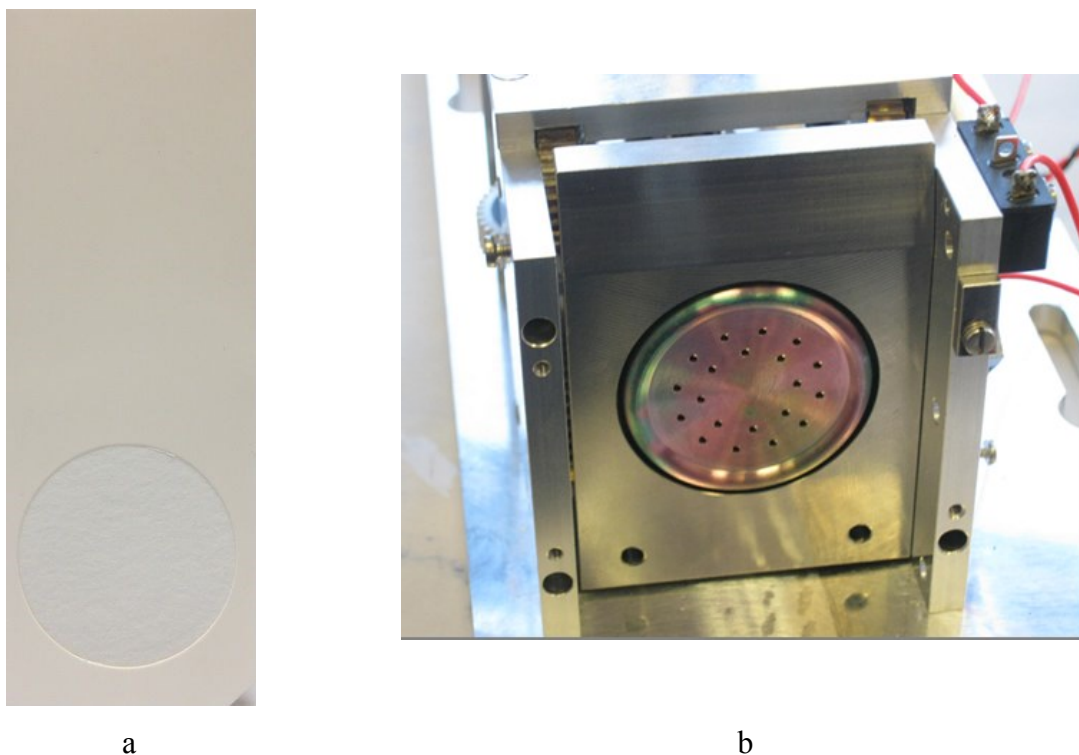


Figure 2.11. (a) Circular PTFE swab mounted onto card -real scale. (b) Detail of the “pepper pot” that forces gas through the swab to desorb the compound of interest. The flow is distributed equally all around the surface of the anvil, so it flows through the whole surface of the swab.

Being a bespoke unit the connection to the inlet of the PTR instrument is quite straight forward and makes use of Swagelok standard connections. The only caution is ensuring to avoid any cold spots on the analytes pathway into the DT. This is shown in figure 2.12, where

the inlet between the TDU outlet and the PTR inlet is externally heated (to the same temperature of the TDU and to that of the PTR oven) and thermally insulated.

With the use of this TDU, as shown in Chapter 5, memory effects are reduced, and for all the compounds investigated, 30 seconds after insertion the base line was recovered, with the exception of RDX (that took around 60 seconds).

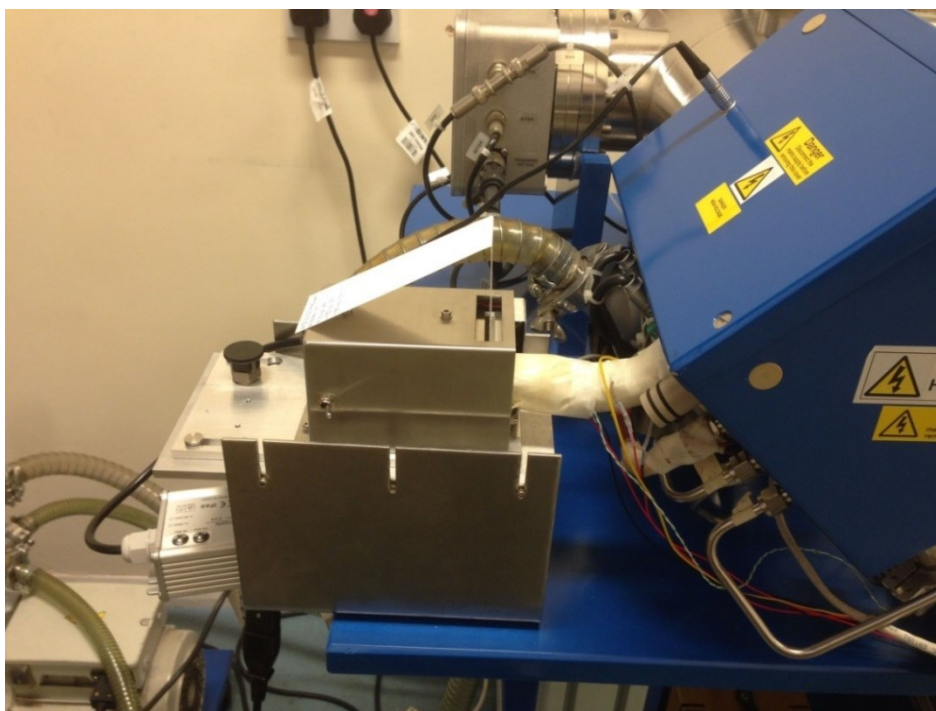


Figure 2.12. Image of the swab inserted into the TDU and the coupling of the TDU to the inlet of the PTR-ToF-MS.

2.3.2 *Drift tube with implemented radio-frequency ion funnel*

Although ion funnels (IFs) were originally developed to link different regions of mass spectrometers kept at different pressure regimes, therefore increasing ion transmission efficiency and hence instrumental sensitivity and dynamic range,³⁷⁻⁴⁰ its implementation on a PTR-MS drift tube is something novel, and developed and implemented by Kore Technology in around 2011.⁴¹ It was originally designed to increase sensitivity by enhancing the proportion of ions extracted from the DT into the MS region of the instrument – in DC-only mode about 99% of the ions do not make it through the final aperture of the DT (inferred from ion current measurements).

The IF drift tube - schematically shown in figures 2.13 and 2.14 - replaces the standard drift tube in the PTR-MS. It consists of a tube ~ 9.04 cm in length formed of 29 stainless steel plates of 0.2 mm thickness, mounted on precision-machined ceramic rods at an even spacing of 3.2 mm per plate.⁴¹ Tabs on the electrodes permit a resistor chain on a ceramic strip to be connected in addition to two capacitor stacks which allow the radio frequency (RF) to be applied to the second half of the reactor. The orifice diameters of the plates through the first half of the stack is 40 mm, as used in the standard drift tube reactor. In the second half of the drift tube the orifice diameter steadily decreases to 6 mm at the final plate before the exit orifice.⁴¹ Across the complete ion-funnel a DC voltage is applied driving ions axially. In addition to this, to the second part of the drift tube an AC electric field, provided at a radio frequency (RF), can be applied. This RF field is such that adjacent electrodes have opposite voltage polarities in the AC component. The frequency was set at 760 kHz and the amplitude selected for the majority of the studies (peak-to-peak) was 200 V, which is superimposed on the DC voltage gradient across the drift tube.

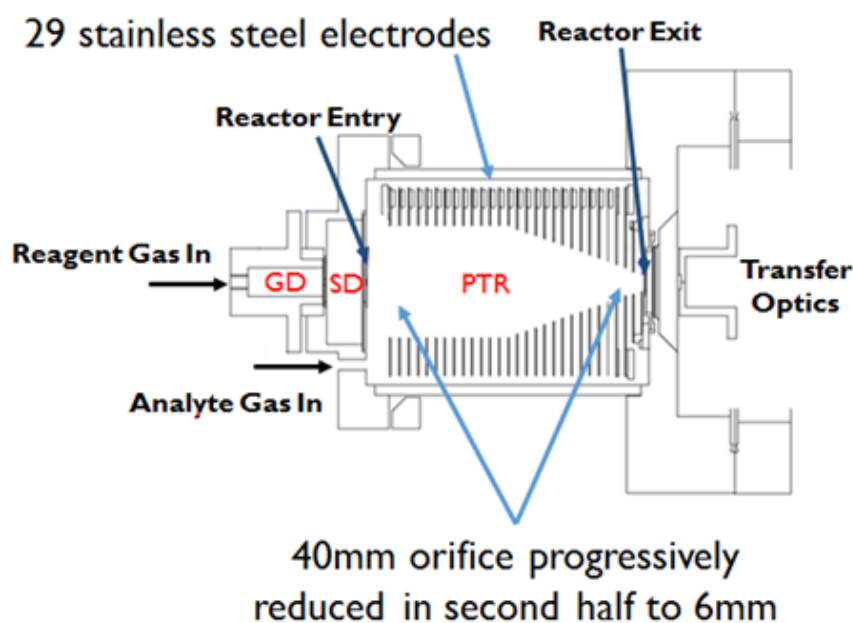


Figure 2.13: Schematic representation of the Kore Technology Ltd. radio frequency ion funnel drift tube (proton transfer reaction (PTR) region) used in this investigation. Also shown is the ion source region (glow discharge GD) and a source drift (SD) region. After

exiting the drift tube the transfer optics guide the ions into the ToF-MS region. Adapted with permission from Kore Technology internal documentation.

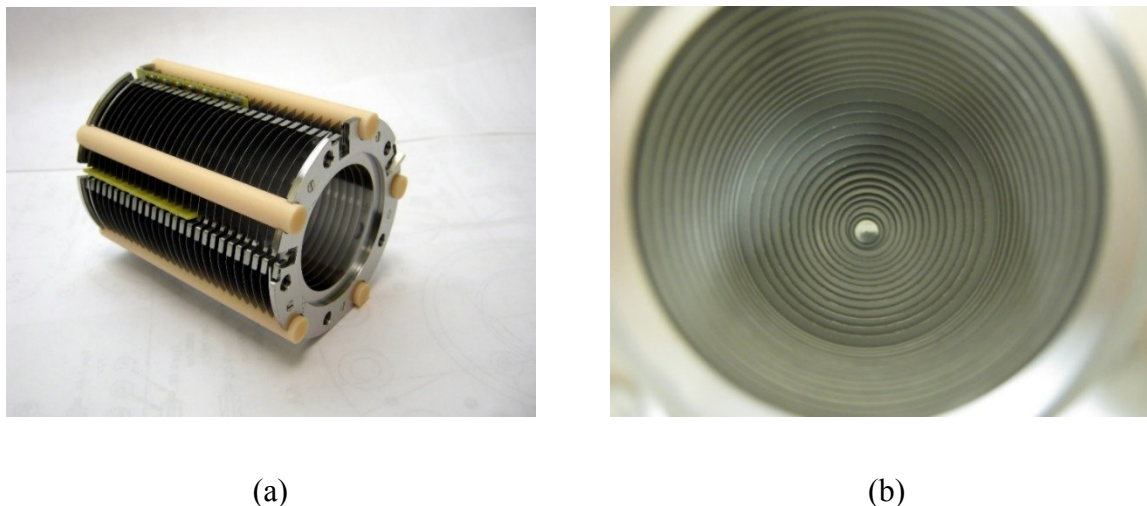


Figure 2.14: Photographs of an RF-IF drift tube from a lateral (a) and axial view (b)

The main purpose of the RF field is to focus ions radially by creating repulsive effective potentials at the edges of the electrodes, thus focussing the ions towards the 400 μm aperture orifice at the end of the DT (as illustrated in figure 2.15(a) and (b)),^{40,43} through which ions enter the ion transfer region for ToF-MS. However, in addition to this intended purpose, the RF results in ions oscillating between electrodes as they drift down the reactor. This gives ions higher collisional energies, enhancing collisional induced dissociation of product ions and potentially used for improved selectivity –as explained in Chapter 6.

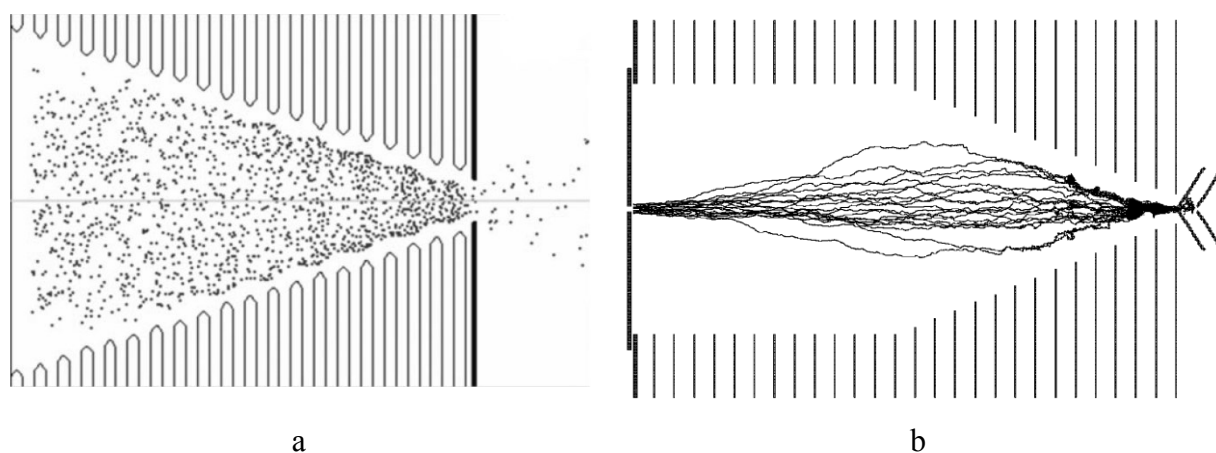


Figure 2.15: (a) Computer model simulation showing the funnel effect and how ions (represented by dots) are funnelled towards the exit aperture of the DT, thus enhancing the number of ions extracted from the DT into the mass spectrometer region of the instrument. Reproduced with permission from reference 40. Copyright © 2010 John Wiley & Sons, Ltd. (b) Ion trajectory calculated using SIMION 8.0.4 for m/z 107 with $RF = 240V$, $f = 820$ kHz, $dc = 60$ V and buffer gas pressure 1.80 mbar. Reproduced with permission from reference 43. Copyright © 2017 Elsevier

2.3.3 Rapid switching of the reduced electric field

Although PTR-MS is considered to be a soft chemical ionisation technique, fragmentation can still occur and it would be, in DC-only mode, dictated mainly by the nature of the analyte and the reduced electric field. As previously explained in section 2.2.2 (page 47), a key parameter on the operation of PTR-MS is the reduced electric field strength, E/N . This parameter is selected by the operator beforehand when running the PTR instrument, and modifying it would affect the resulting products ion branching ratios.^{15,44} Fragmentation, in most cases is not desirable. However it can be used advantageously as a way to enhance selectivity.

The simplest way to provide a rapid change in E/N is to quickly alter the E field by rapidly changing the voltage applied across the drift tube. For such purpose, new electronics hardware and software were developed by Kore Technology for the purpose of providing fast reduced electric field switching that could be retrofitted onto the Kore PTR-ToF-MS (see figure 2.16).

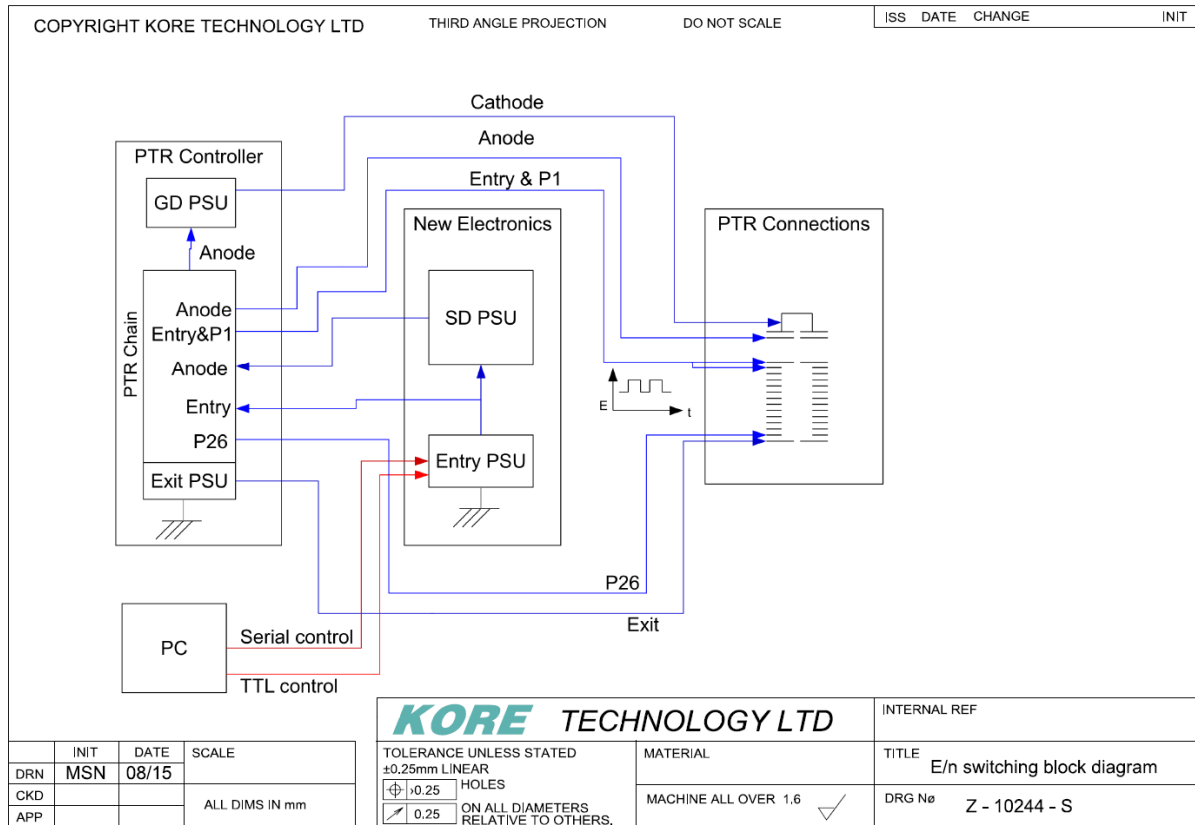


Figure 2.16: Schematics depicting the electronics for the fast E/N switching hardware implemented on the Kore PTR-ToF-MS Series I. Adapted with permission from Kore Technology Ltd. internal document Z-10244-S.

The fast reduced electric field switching is accomplished by software control of a programmable +500 volts power supply unit (PSU) which can be controlled over the range 50 to 450 volts (covering typically the E/N range of between approximately 10 and 250Td). It is possible to switch the amplitude of the output voltage according to the two required E/N values. The electric field strength within the DT is therefore computer controlled by using a serial digital-to-analog converter to convert the binary signal from the computer into a control voltage for the power supply. In addition to the voltage control, the software also provides the facility to alter the frequency of switching between the two voltages, whereby the first E/N value initially appears as a binary number on the serial port of the computer. This is then converted by the serial digital-to-analog converter to the control voltage required to cause the output voltage of the PSU to give the first required E/N value. After a time delay, set by the switching frequency value (in the Hz region), a second binary value is then output onto the serial port to similarly provide the second E/N value. In addition to this, a floating +300 volts

PSU provides the voltage gradient for the SD region of the PTR source. The software automatically switches between two pre-set E/N values, and the data acquisition system automatically records the intensity of the selected ions at the E/N values as a function of time. This new development can be used to improve chemical compound selectivity as detailed in Chapter 7.

References

1. Rohlf, J. W., *Modern Physics from α to Z^0* . Wiley, 1994
2. Linstrom P. J., Mallard, W. G. (Eds.), National Institute of Standards and Technology, Gaithersburg MD, 20899, <http://webbook.nist.gov>.
3. Geiger, F. Fast-response measurements of organic trace species in the Earth's atmosphere. Karlsruhe, KIT Scientific Publishing, Karlsruhe, 2014.
4. Kore, Technology Ltd., Manual Z-5851-M, 2006.
5. Andrew M. Ellis, Chris A. Mayhew, *Proton Transfer Reaction Mass Spectrometry: Principles and Applications*. 1st ed.; Wiley: 2014; p 336.
6. Mavrodineanu, R., Hollow cathode discharges. *J. Res. Nat. Bureau Standards* **1984**, *89* (2), 143.
7. Märk, T.; Lindinger, W.; Howorka, F.; Egger, F.; Varney, R.; Pahl, M., A simple bakeable hollow cathode device for the direct study of plasma constituents. *Review of Scientific Instruments* **1972**, *43* (12), 1852-1853.
8. Howorka, F.; Lindinger, W.; Pahl, M., Ion sampling from the negative glow plasma in a cylindrical hollow cathode. *International Journal of Mass Spectrometry and Ion Physics* **1973**, *12* (1), 67-77.
9. Lindinger, W., Reaction-Rate Constants in Steady-State Hollow-Cathode Discharges: Ar+ H₂O Reactions. *Physical Review A* **1973**, *7* (1), 328.
10. Howorka, F.; Lindinger, W.; Varney, R. N., Reaction rate constants in steady-state hollow cathode discharges: N₂+H₂O reactions. *The Journal of Chemical Physics* **1974**, *61* (3), 1180-1188.
11. Hansel, A.; Jordan, A.; Holzinger, R.; Prazeller, P.; Vogel, W.; Lindinger, W., Proton transfer reaction mass spectrometry: on-line trace gas analysis at the ppb level. *International Journal of Mass Spectrometry and Ion Processes* **1995**, *149–150* (0), 609-619.
12. Harrison, W. W.; Hess, K. R.; Marcus, R. K.; King, F. L., Glow discharge mass spectrometry. *Analytical Chemistry* **1986**, *58* (2), 341A-356A.
13. Marcus, R. K., *Glow discharge spectroscopies*. Plenum Press, New York, NY 1993.
14. Pillow, M. E., A critical review of spectral and related physical properties of the hollow cathode discharge. *Spectrochimica Acta Part B: Atomic Spectroscopy* **1981**, *36* (8), 821-843.

15. Lindinger, W.; Hansel, A.; Jordan, A., On-line monitoring of volatile organic compounds at pptv levels by means of proton-transfer-reaction mass spectrometry (PTR-MS) medical applications, food control and environmental research. *International Journal of Mass Spectrometry and Ion Processes* **1998**, *173* (3), 191-241.
16. Westwood, W., Glow discharge sputtering. *Progress in Surface Science* **1976**, *7* (2), 71-111.
17. Ikezoe, Y.; Matsuoka, S.; Takebe, M., *Gas phase ion-molecule reaction rate constants through 1986*. Ion reaction research group of the Mass spectroscopy society of Japan: 1987.
18. Anicich, V. G., *An index of the literature for bimolecular gas phase cation-molecule reaction kinetics*. Jet Propulsion Lab., California Inst. of Tech.; Pasadena, CA.. **2003**.
19. Kore, Technology., Internal document: Initial results from the new SD electrode in PTR-TOF-MS. 2016.
20. Smith, D.; Adams, N. G.; Miller, T. M., A laboratory study of the reactions of N^+ , N_2^+ , N_3^+ , N_4^+ , O^+ , O_2^+ , and NO^+ ions with several molecules at 300 K. *The Journal of Chemical Physics* **1978**, *69* (1), 308-318.
21. Jordan, A.; Haidacher, S.; Hanel, G.; Hartungen, E.; Herbig, J.; Märk, L.; Schottkowsky, R.; Seehauser, H.; Sulzer, P.; Märk, T. D., An online ultra-high sensitivity Proton-transfer-reaction mass-spectrometer combined with switchable reagent ion capability (PTR + SRI – MS). *International Journal of Mass Spectrometry* **2009**, *286* (1), 32-38.
22. Dunne, E. Measurement of atmospheric volatile organic compounds with proton transfer reaction-mass spectrometry. Monash University. Faculty of Science. School of Chemistry, 2016.
23. Sulzer, P.; Edtbauer, A.; Hartungen, E.; Jürschik, S.; Jordan, A.; Hanel, G.; Feil, S.; Jaksch, S.; Märk, L.; Märk, T. D., From conventional proton-transfer-reaction mass spectrometry (PTR-MS) to universal trace gas analysis. *International Journal of Mass Spectrometry* **2012**, *321–322*, 66-70.
24. Edtbauer, A.; Hartungen, E.; Jordan, A.; Hanel, G.; Herbig, J.; Jürschik, S.; Lanza, M.; Breiev, K.; Märk, L.; Sulzer, P., Theory and practical examples of the quantification of CH_4 , CO , O_2 , and CO_2 with an advanced proton-transfer-reaction/selective-reagent-ionization instrument (PTR/SRI-MS). *International Journal of Mass Spectrometry* **2014**, *365–366*, 10-14.

25. Agarwal, B.; González-Méndez, R.; Lanza, M.; Sulzer, P.; Märk, T. D.; Thomas, N.; Mayhew, C. A., Sensitivity and Selectivity of Switchable Reagent Ion Soft Chemical Ionization Mass Spectrometry for the Detection of Picric Acid. *The Journal of Physical Chemistry A* **2014**, *118* (37), 8229-8236.
26. McDaniel, E. W.; Martin, D. W.; Barnes, W. S., Drift Tube-Mass Spectrometer for Studies of Low-Energy Ion-Molecule Reactions. *Review of Scientific Instruments* **1962**, *33* (1), 2-7.
27. Blake, R. S.; Monks, P. S.; Ellis, A. M., Proton-Transfer Reaction Mass Spectrometry. *Chemical Reviews* **2009**, *109* (3), 861-896.
28. Mason, E. A.; McDaniel, E. W., *Transport properties of ions in gases*. 1988; Vol. 89.
29. Dotan, I.; Albritton, D. L.; Lindinger, W.; Pahl, M., Mobilities of CO_2^+ , N_2H^+ , H_3O^+ , $\text{H}_3\text{O}^+\cdot\text{H}_2\text{O}$, and $\text{H}_3\text{O}^+\cdot(\text{H}_2\text{O})_2$ ions in N_2 . *The Journal of Chemical Physics* **1976**, *65* (11), 5028-5030.
30. de Gouw, J.; Warneke, C.; Karl, T.; Eerdekens, G.; van der Veen, C.; Fall, R., Sensitivity and specificity of atmospheric trace gas detection by proton-transfer-reaction mass spectrometry. *International Journal of Mass Spectrometry* **2003**, *223–224*, 365-382.
31. Fujii, T., *Ion/Molecule Attachment Reactions: Mass Spectrometry*. Springer: 2015.
32. Smith, D.; Španěl, P., Selected ion flow tube mass spectrometry (SIFT-MS) for on-line trace gas analysis. *Mass Spectrometry Reviews* **2005**, *24* (5), 661-700.
33. Wannier, G. H., On the motion of gaseous ions in a strong electric field. I. *Physical Review* **1951**, *83* (2), 281.
34. Wannier, G. H., Motion of gaseous ions in strong electric fields. *Bell System Technical Journal* **1953**, *32* (1), 170-254.
35. Mayhew, C. A.; Sulzer, P.; Petersson, F.; Haidacher, S.; Jordan, A.; Märk, L.; Watts, P.; Märk, T. D., Applications of proton transfer reaction time-of-flight mass spectrometry for the sensitive and rapid real-time detection of solid high explosives. *International Journal of Mass Spectrometry* **2010**, *289* (1), 58-63.
36. González-Méndez, R.; Reich, D. F.; Mullock, S. J.; Corlett, C. A.; Mayhew, C. A., Development and use of a thermal desorption unit and proton transfer reaction mass spectrometry for trace explosive detection: Determination of the instrumental limits of detection and an investigation of memory effects. *International Journal of Mass Spectrometry* **2015**, *385*, 13-18.

37. Shaffer, S. A.; Tang, K.; Anderson, G. A.; Prior, D. C.; Udseth, H. R.; Smith, R. D., A novel ion funnel for focusing ions at elevated pressure using electrospray ionization mass spectrometry. *Rapid Communications in Mass Spectrometry* **1997**, *11* (16), 1813-1817.
38. Mayer, T.; Borsdorf, H., Ion transfer from an atmospheric pressure ion funnel into a mass spectrometer with different interface options: Simulation-based optimization of ion transmission efficiency. *Rapid Communications in Mass Spectrometry* **2016**, *30* (3), 372-378.
39. Meier, L.; Berchtold, C.; Schmid, S.; Zenobi, R., Sensitive detection of drug vapors using an ion funnel interface for secondary electrospray ionization mass spectrometry. *Journal of Mass Spectrometry* **2012**, *47* (5), 555-559.
40. Kelly, R. T.; Tolmachev, A. V.; Page, J. S.; Tang, K.; Smith, R. D., The ion funnel: Theory, implementations, and applications. *Mass Spectrometry Reviews* **2010**, *29* (2), 294-312.
41. Barber, S.; Blake, R. S.; White, I. R.; Monks, P. S.; Reich, F.; Mullock, S.; Ellis, A. M., Increased Sensitivity in Proton Transfer Reaction Mass Spectrometry by Incorporation of a Radio Frequency Ion Funnel. *Analytical Chemistry* **2012**, *84* (12), 5387-5391.
42. González-Méndez, R.; Watts, P.; Olivenza-León, D.; Reich, D. F.; Mullock, S. J.; Corlett, C. A.; Cairns, S.; Hickey, P.; Brookes, M.; Mayhew, C. A., Enhancement of compound selectivity using a radio frequency ion-funnel proton transfer reaction mass spectrometer: improved specificity for explosive compounds. *Analytical Chemistry* **2016**, *88* (21), 10624-10630.
43. Brown, P. A.; Cristescu, S. M.; Mullock, S. J.; Reich, D. F.; Lamont-Smith, C. S.; Harren, F. J. M., Implementation and characterization of an RF ion funnel ion guide as a proton transfer reaction chamber. *International Journal of Mass Spectrometry* **2017**. In press.
44. Brown, P.; Watts, P.; Mark, T. D.; Mayhew, C. A., Proton transfer reaction mass spectrometry investigations on the effects of reduced electric field and reagent ion internal energy on product ion branching ratios for a series of saturated alcohols. *International Journal of Mass Spectrometry* **2010**, *294* (2-3), 103-111.

PART II: EXPERIMENTAL RESULTS

CHAPTER 3

APPLICATIONS OF SWITCHING REAGENT IONS IN PROTON TRANSFER REACTION MASS SPECTROMETRIC INSTRUMENTS FOR THE IMPROVED SELECTIVITY OF EXPLOSIVE COMPOUNDS

This chapter is a reformatted copy of my published article:

International Journal of Mass Spectrometry 354–355 (2013), 123–128.

Philipp Sulzer,¹ Bishu Agarwal,¹ Simone Jürschik,¹ Matteo Lanza,¹ Alfons Jordan,¹ Eugen Hartungen,¹ Gernot Hanel,¹ Lukas Märk,¹ Tilmann D. Märk,² Ramón González-Méndez,³ Peter Watts,³ and Chris A. Mayhew.^{3,*}

1. IONICON Analytik Gesellschaft m.b.H., Eduard-Bodem-Gasse 3, A-6020 Innsbruck, Austria
2. Institut für Ionenphysik und Angewandte Physik, Leopold-Franzens Universität Innsbruck, Technikerstr. 25, 6020 Innsbruck, Austria
3. School of Physics and Astronomy, University of Birmingham, Edgbaston, Birmingham, B15 4TT, UK

* Corresponding author: Tel.:+441214144729; fax:+441214144577. E-mail address: c.mayhew@bham.ac.uk

Declaration of contribution

My contribution to the study described on this Chapter was in the editing (writing, proof reading and discussions process) of the manuscript. I also took measurements with the Molecular Physics Research Group's KORE PTR-ToF at the University of Birmingham, for reproducibility purposes.

3.1. Abstract

Here we demonstrate the use of a switchable reagent ion proton transfer reaction mass spectrometer (SRI-PTR-MS) instrument to improve the instrument's selectivity for the detection of the explosive compounds 2,4,6-trinitrotoluene (TNT), 1,3,5-trinitrobenzene (TNB), pentaerythritol tetranitrate (PETN), and cyclotrimethylenetrinitramine (RDX). Selectivity is improved owing to the production of different product ions resulting from changes in the reagent ion-molecule chemistry. To be of use as an analytical tool for homeland security applications, it is important that the reagent ions (and hence product ions) can be rapidly changed (seconds) if the technology is to be acceptable. This paper presents measurements which show how it is possible to rapidly switch the reagent ion from H_3O^+ to either O_2^+ or NO^+ to enhance selectivity for the detection of four explosives. That switching reagents ion can be done quickly (in seconds) results from the fact that the recombination energies of O_2^+ and NO^+ are less than the ionisation potential of H_2O . Reaction processes observed are non-dissociative charge transfer (O_2^+ with TNT and TNB), dissociative charge transfer (O_2^+ with TNT) and adduct formation (NO^+ with PETN and RDX). O_2^+ is found to be unreactive with PETN and RDX, and under the conditions operating in the reaction region of the PTR-MS only a low signal associated with $\text{NO}^+\cdot\text{TNT}$ was observed. No $\text{NO}^+\cdot\text{TNB}$ was detected.

3.2. Introduction

The potential of terrorists to use explosives and chemical warfare agents focus our attention on the need to detect dangerous agents in low concentrations reliably, in real-time and with high sensitivity and selectivity. This is a particularly challenging task when only trace concentrations of threat compounds with low vapour pressure, such as explosives, are present on exposed surfaces in complex chemical environments.

In the response to recent failed terrorists' attacks involving explosives, the United States installed so-called "Full Body Scanners" as a security measure at selected airports to detect bulk quantities of threat agents concealed on a person. In addition to uncertainties about the ability of such scanners to detect explosives in places not accessible in routine physical pat-down searches, concerns have been raised about radiation doses in the case of X-ray scanners.¹ Furthermore, questions have been raised with regard to privacy issues. In March 2010 a Muslim woman became the first passenger to be barred from boarding a flight from Manchester Airport (UK) to Islamabad (Pakistan) because she refused to undergo a full body scan for religious reasons (her companion also declined the scan for "medical reasons" and was also not allowed to board the plane).² This was in accordance with the UK's government directive on scanners; passengers are not permitted to fly if they refuse body scanning – and passengers are not offered any alternative security procedure (*e.g.* a pat-down search). This case serves to highlight public sensitivities surrounding emerging counter-terrorism technologies, and illustrates the difficulties in balancing the need for security with the rights of privacy.

Independent of the rights and wrongs for adopting counter terrorism technology, it is becoming increasingly obvious that all techniques have their own advantages and limitations, and hence no approach relying on a single technology will be able to provide complete security or meet all needs. It is, therefore, prudent to explore a wide range of suitable technologies for the detection of threat agents beyond imaging techniques, and in particular approaches based on chemical analysis that do not infringe on any civil right issues.

The most commonly deployed chemical analysis technology for the detection of threat agents in security areas is Ion Mobility Spectrometry (IMS).^{3,4} Despite its sensitivity and robustness, IMS has certain disadvantages; the most critical is its limited chemical specificity. This can cause false positive signals resulting from the erroneous identification of harmless interferences as a threat agent. The rapid detection of traces of threat agents adhered to people

or objects with a high level of confidence (low rate of false positives) in ambient air with a sensitivity that equals or surpasses that of IMS, but has a superior selectivity requires a new analytical approach.

In a series of recent papers we have highlighted the potential of the platform technology proton transfer reaction mass spectrometry (PTR-MS) for the detection of explosives,⁵⁻⁸ in addition to other threat agents.⁹⁻¹² Having mass spectrometric capabilities, this technology of course has improved selectivity compared to IMS owing to its ability to generate protonated parent species, *i.e.* an ion is produced with an m/z which is observed at one atomic mass unit above that of the neutral species. Although, an observed m/z at where MH^+ is expected (M being the neutral analyte) provides a greater confidence in an assignment, an m/z does not provide a unique indicator for the identity of trace gases in an air sample, because for low resolution mass spectrometers, *i.e.* those using quadrupole filtering, it can only provide a nominal m/z value. This causes problems if isomeric or isobaric compounds are present in the environment because they have the same nominal mass (isobaric) or identical mass (isomeric). High resolution mass spectrometers can be used to separate out isobaric compounds. However this adds considerably to the cost of an analytical instrument. Furthermore, it is not just isobaric/isomeric compounds that can cause problems in the interpretation of mass spectra. Product ions resulting from fragmentation, clustering, and secondary ion-molecule reactions can also cause complications for accurate assignments and hence in the unambiguous detection of a compound.

To improve selectivity of PTR-MS, we have recently shown that H_3O^+ drift-tube ion-molecule chemistry for the explosives 2,4,6-trinitrotoluene (TNT: $C_7H_5N_3O_6$, m/z 227) and 1,3,5-trinitrobenzene (TNB: $C_6H_3N_3O_6$, m/z 213), can be discriminated by changing E/N .⁸ The aim of this paper is to demonstrate how the switching of reagent ions from H_3O^+ to NO^+ or O_2^+ can also be used to enhance selectivity, not only for TNT and TNB, but also for cyclotrimethylenetrinitramine (RDX: $C_3H_6N_6O_6$, m/z 222) and pentaerythritol tetranitrate (PETN: $C_5H_8N_4O_{12}$, m/z 316). However, an important practical aspect for analytical detection in real-world environments is that to be applicable, a switchable reagent ion source used to enhance the selectivity must be able to change from one reagent ion to another rapidly (within seconds). We shall show that this is possible for switching between H_3O^+ , NO^+ and O_2^+ .

Prior to this work, two other studies have appeared in the literature based on the use of ion-molecule reactions in low-pressure reaction environments for the detection of explosives

using reagent ions other than H_3O^+ .^{13,14} Both of these earlier studies have focused on the unstable explosive triacetone triperoxide (TATP), $\text{C}_9\text{H}_{18}\text{O}_6$. A selected ion flow tube – mass spectrometer (SIFT-MS) study by Wilson *et al.*,¹³ using thermal H_3O^+ , O_2^+ , and NO^+ as the reagent ions, claimed that only NO^+ reactions with TATP showed product ions that provided “unequivocal evidence” for the presence of a TATP-based explosive. Shen *et al.*,¹⁴ using a proton transfer reaction quadrupole mass spectrometer with either H_3O^+ or NH_4^+ as the reagent ions, showed that TATP could be detected by either identifying (weakly) TATP.H^+ (proton transfer from H_3O^+) or TATP.NH_4^+ (association reaction with NH_4^+) by using a suitable reduced electric field in the drift tube.

3.3. Experimental Details

A high resolution PTR-TOF-MS (PTR-TOF 8000, IONICON Analytik GmbH) was used for this study. Details on the technology can be found in previous publications,^{8,15} and therefore only details on the experimental procedures used in this study will be provided. The measurement procedure for the explosives involved drawing air through a charcoal filter into a glass vial (through a septum in the lid), which contained a small amount of the solid explosive (typically 1-3 milligrams). The air passed over the sample and was drawn into a tube connected to the inlet system of the PTR-TOF-MS. The glass vial, sample inlet line and the drift tube of the PTR-TOF 8000 were maintained at approximately 100 °C. The uniform heating of the inlet lines and PTR chamber is critical to measurements involving solid explosives because of their condensable nature.

NO^+ or O_2^+ reagent ions were produced by flowing air or oxygen, respectively, via a computer controlled mass flow controller into a hollow cathode discharge source. These reagent ions, under the influence of a voltage gradient, passed through a small orifice from the hollow cathode ion source into an adjacent drift tube reaction section, where the explosive analyte under investigation was introduced via the gas inlet system mentioned above. In addition to producing either ions NO^+ and O_2^+ , H_3O^+ was also produced owing to residual water vapour on the surfaces of tubing going to and in the hollow cathode ion source, but this always resulted in an ion intensity of less than 5% found for that of the dominant reagent ion signal. For O_2^+ another contaminant ion observed was NO_2^+ . Although this was less than 1% of the O_2^+ signal intensity, and its intensity decreased with increasing reduced electric field, E/N (the ratio of the electric field applied down the drift tube to the air number density in the

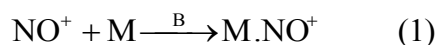
drift tube), this still represented a significant signal intensity in comparison to the product ion signal intensities resulting from reactions with trace explosives in the reaction region, and therefore care must be taken when detecting nitro aromatic compounds because NO_2^+ is often used as a marker for such explosives.

3.4. Results and Discussions

Before investigating the capabilities of fast switching, we first investigated the reaction of the reagent ions NO^+ and O_2^+ with each of the explosives as a function of E/N , and therefore this will be described first.

3.4.1 NO^+ Reactions

With the possible exception of RDX, the ionisation potentials of the explosives investigated in this study are higher than the recombination energy of NO^+ (9.6 eV). TNB has the highest ionisation potential at 10.96 ± 0.02 ,¹⁶ and all others have ionisation potentials at or below approximately 10.5 eV, *i.e.* TNT is at 10.5 eV, PETN is at 10.4 eV and RDX is at 9.8 eV.¹⁷ In the case of PETN and RDX the values given correspond to appearance energies for ions observed at m/z 46 (presumably NO_2^+) and m/z 128 (which is unassigned in the paper), respectively. Given the values for the ionisation potentials of the explosives, other than perhaps for RDX, electron charge transfer from the explosives is not to be expected, and indeed none is observed. Even for RDX, which has an ionisation potential close to that of NO, no ions at m/z 128 that may result from dissociative charge transfer are observed. Instead we find that NO^+ only reacts with PETN and RDX via adduct formation, *i.e.*



where M = PETN or RDX and B represents the buffer gas (air). Under the operational conditions we used in the PTR device, we only observed weak association of NO^+ with TNT and none at all with TNB. Therefore, the reagent ion NO^+ does not provide a sufficiently sensitive ion probe for the detection of TNT or TNB in the PTR-MS. We also note that in order to observe the $\text{M}.\text{NO}^+$ adduct for M = PETN or RDX, it is necessary to operate the drift tube at relatively low E/N values (*e.g.* below 100 Td), because the $\text{M}.\text{NO}^+$ signal intensity drops dramatically with increasing E/N . Above approximately an E/N value of 140 Td, little

adduct formation is observed owing to it being quickly returned back to NO^+ and M through a collisional induced dissociation process. To illustrate this, figure 3.1 presents the signal intensity for $\text{RDX}\cdot\text{NO}^+$ as a function of E/N (a similar result was obtained for the signal intensity of $\text{PETN}\cdot\text{NO}^+$ as a function of E/N).

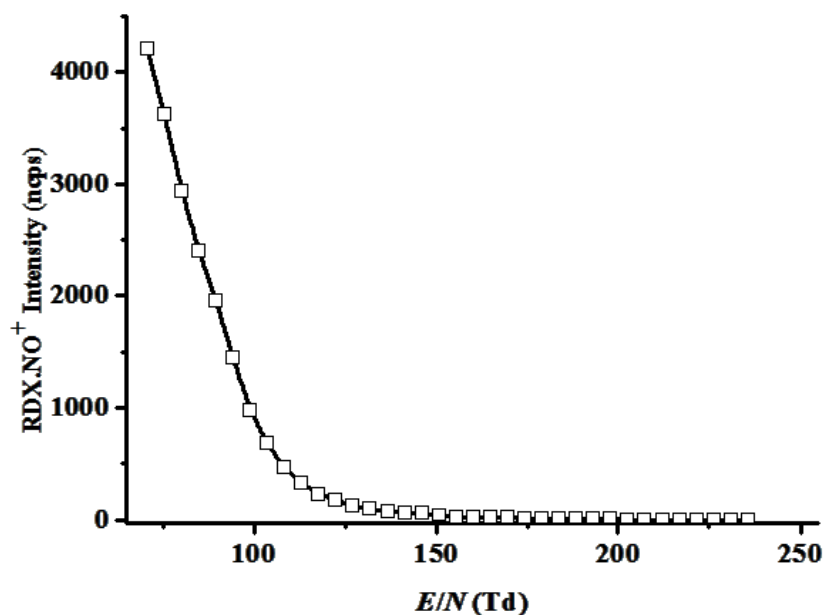
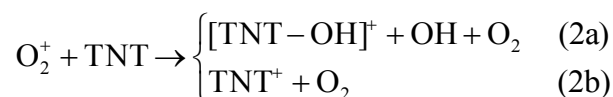


Figure 3.1. $\text{RDX}\cdot\text{NO}^+$ signal intensity (normalised counts per second) as a function of the reduced electric field (E/N). The unit for E/N is given in Townsend (Td), where $1 \text{ Td} = 10^{-21} \text{ V m}^2$. The dramatic drop in intensity is a result of collisional induced dissociation of $\text{RDX}\cdot\text{NO}^+$ to RDX and NO^+ .

3.4.2 O_2^+ Reactions

Unlike NO^+ , the recombination energy of O_2^+ (12.07 eV) is more than sufficient for charge transfer to be an energetically feasible reaction pathway for all of the explosives investigated in this study. Although charge transfer is thermodynamically allowed, interestingly no such reaction is observed with either PETN or RDX. However, just because a charge transfer reaction pathway is exoergic it does not necessarily have to occur.¹⁸ There could be a number of reasons to cause the rate coefficients for these reactions to be significantly below the collisional value, such as a lack of an energy resonance. This is in stark contrast to exoergic proton transfer reactions which proceed with high efficiency when $\Delta G \leq -20 \text{ kJ mol}^{-1}$,¹⁹ which certainly applies to the explosives reported in this study.⁸

In contrast to PETN and RDX, O_2^+ does react with TNT and TNB by charge transfer. In the case of TNT this occurs predominantly via dissociative charge transfer with a product ion being observed at an m/z of 210, which results from the loss of a hydroxyl radical from TNT^+ . In addition to that channel, non-dissociative transfer is also observed with a product ion being observed at m/z 227:



A study of the branching ratios of these two pathways as a function of E/N shows a small dependence on E/N . Unsurprisingly the branching ratio associated with pathway (2b) decreases with increasing E/N owing to either more collisional energy in the reaction process or collisional induced dissociation of the TNT^+ with the buffer gas, or both. At the lowest E/N used in this study, 70 Td, reaction pathways (2a) and (2b) have percentage branching ratios of approximately 93% and 7%, respectively. By 150 Td, the branching ratio associated with reaction pathway (2b) is less than 1%. This is illustrated in figure 3.2, which provides the percentage product ion branching ratios for the reaction of O_2^+ with TNT as a function of E/N .

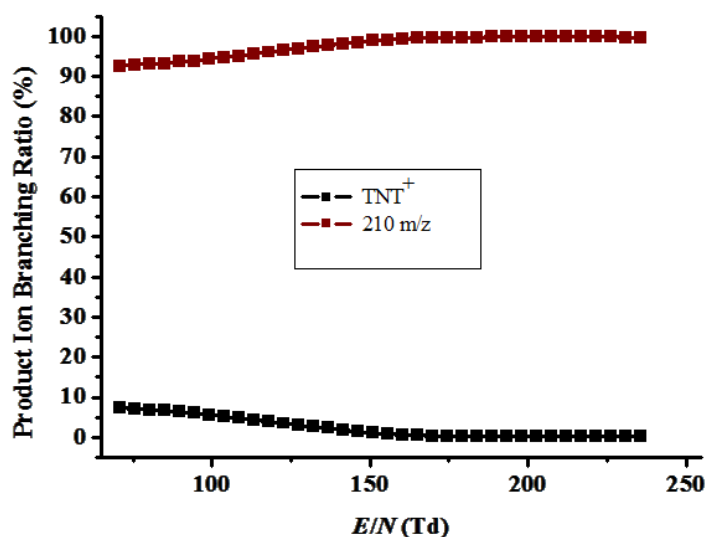


Figure 3.2. Product ion branching ratios in percentages as a function of E/N resulting from the reaction of O_2^+ with TNT. Only two reaction channels have been identified, one is non-dissociative charge transfer resulting in an ion at m/z 227 (TNT^+) and the other, and most

dominant channel, is an ion observed at m/z 210 caused by dissociative charge transfer resulting from the loss of a hydroxyl radical from TNT^+ .

In comparison to TNT, the reaction of O_2^+ with TNB proceeds only via a non-dissociative charge transfer pathway:



However, this is not the only ion observed which contains TNB, because at low E/N values association of TNB^+ with water was observed to occur. This is illustrated in figure 3.3, which also shows the E/N sensitivity dependence of the TNB^+ signal intensity.

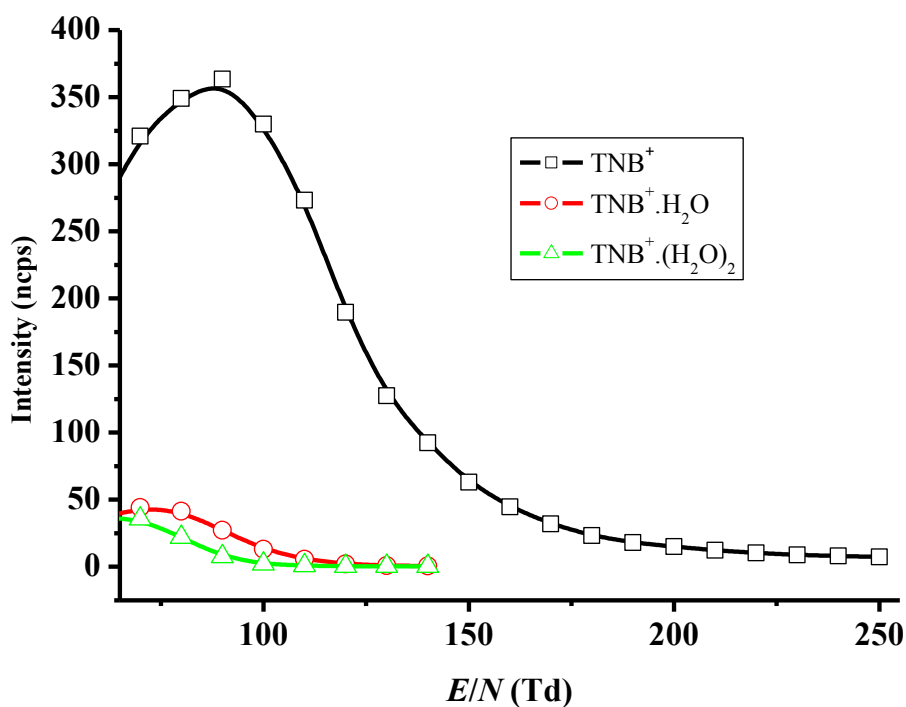


Figure 3.3. Dependence of normalised product ion signal intensities involving TNB as a function of E/N . The only ion resulting from the reaction with O_2^+ is TNB^+ , but with decreasing E/N , secondary ion-molecule reactions occur leading to the association of TNB^+ with residual water in the system resulting in the formation of $\text{TNB}^+ \cdot (\text{H}_2\text{O})_n$ ($n = 1$ and 2).

3.4.3 Sensitivity Details

It is generally found in PTR-MS work, with a few reported exceptions,^{5,8} that when using H_3O^+ as a reagent ion the sensitivity for detection of an analyte decreases with increasing E/N as a result of factors such as decreased reaction time and fragmentation of the protonated parent molecule. The intensities of the product ions produced from reactions with O_2^+ and NO^+ with all of the explosives investigated in this study have been found to follow this trend. The main difference when using reagent ions other than H_3O^+ is that the drift tube may be operated at even lower E/N values than can be used when relying on water chemistry, which results in improved sensitivity in terms of normalised counts per second (ncps). (ncps refers to the intensity obtained for an ion at a given m/z by integrating over the spectral line, dividing by the integrated reagent ion signal and multiply by 10^6 .) In the case of H_3O^+ , its signal intensity drops dramatically for E/N values much below 90 Td (depending on humidity) owing to the formation of protonated water clusters ($\text{H}_3\text{O}^+(\text{H}_2\text{O})_n$ ($n \geq 1$)), thereby limiting the E/N values that can be used. However, it must be appreciated that the actual value of E/N to be used is a competition between strong reagent ion signal, reaction time and limiting fragmentation. To decide on the most appropriate E/N value for a given instrument it is necessary to review the cps (not ncps) and select the E/N that provides the most intense product ion signal.

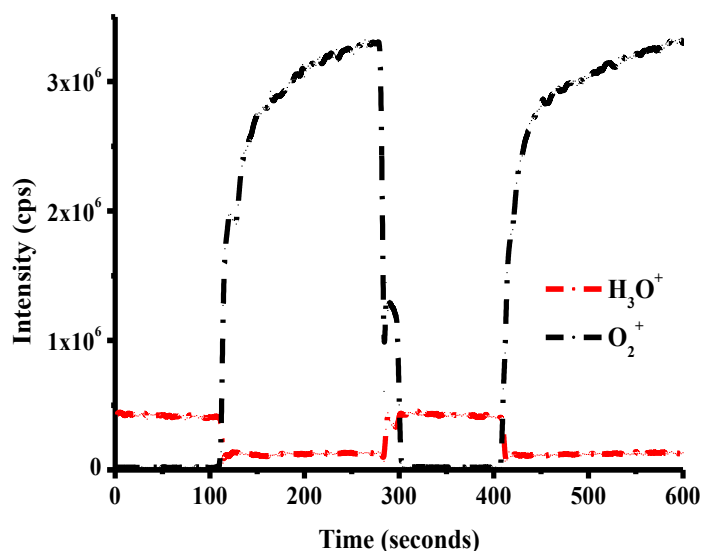
3.4.4 Switching Reagent Ions

For real-world applications detection of threat agents with high levels of confidence is needed rapidly (within tens of seconds). With just a nominal m/z to identify a compound it is impossible to be unambiguous in an assignment. A way forward to improve selectivity is to rapidly change reagent ions in order to change the product ions produced via an ion-molecule reaction, *e.g.* from the protonated parent resulting from a reaction with H_3O^+ to a charged ion resulting from a charge transfer reaction or an association process. We have therefore investigated how quickly the reagent ion can be switched from H_3O^+ to NO^+ or O_2^+ and back again. To achieve this we have used two computer controlled mass flow units. One of these flow controllers was used for water vapour and another was either used for air for NO^+ production, or O_2 for O_2^+ production. Of course it is relatively straightforward to have any number of flow controllers connected to the inlet of the hollow cathode if one wishes to switch between various other gases for introduction into the hollow cathode discharge source. However, when using humid air as a buffer gas, rapid switching from water dominated

chemistry to another type of chemistry is only possible for reagent ions produced that do not react with water, otherwise ion-molecule reactions in the drift chamber and hollow cathode ion source will ultimately result in H_3O^+ becoming the terminal and dominant reagent ion. With their recombination energies being less than the ionisation potential of water, O_2^+ and NO^+ are ideal reagent ions. Of course any reagent ion must also not be able to react with the major components of air. In addition to the recombination energies of O_2^+ and NO^+ being less than the ionisation potential of H_2O (12.6 eV), they are also less than that for N_2 (15.6 eV), and therefore they cannot react with this major air constituent. In comparison if, for example, Kr^+ is used as a reagent ion, its recombination energy of 14.0 eV is higher than the ionisation potentials of O_2 (12.1 eV) and H_2O . That its recombination energy is greater than that of water means that rapid switching from water to Kr chemistry in a PTR-MS is not possible. Furthermore, owing to its reaction with O_2 little of the Kr^+ reagent ions would be left to react with trace compounds even in a dry reaction chamber. A recent investigation has shown how this can be limited by diluting the buffer gas with helium when sampling from air.²⁰

Figure 3.4 (a) shows the reagent ion signal intensities of O_2^+ and H_3O^+ as a function of time as the reagent ions are being switched, with the drift tube being operated at an E/N of 120 Td. It can be seen from this figure that the intensity and hence production of O_2^+ is greater than that for H_3O^+ and that rapid switching of reagent ions is possible. This latter point is highlighted further in figure 3.4 (b), which shows an expanded region over a switching cycle. From figure 3.4 (b) it can be seen that within approximately 10 seconds in switching from water to oxygen chemistry the H_3O^+ signal intensity has dramatically reduced and the O_2^+ signal intensity is high.

(a)



(b)

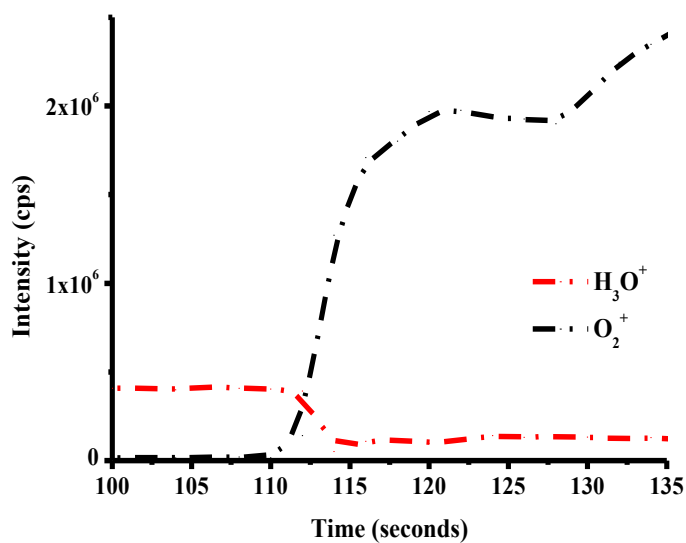
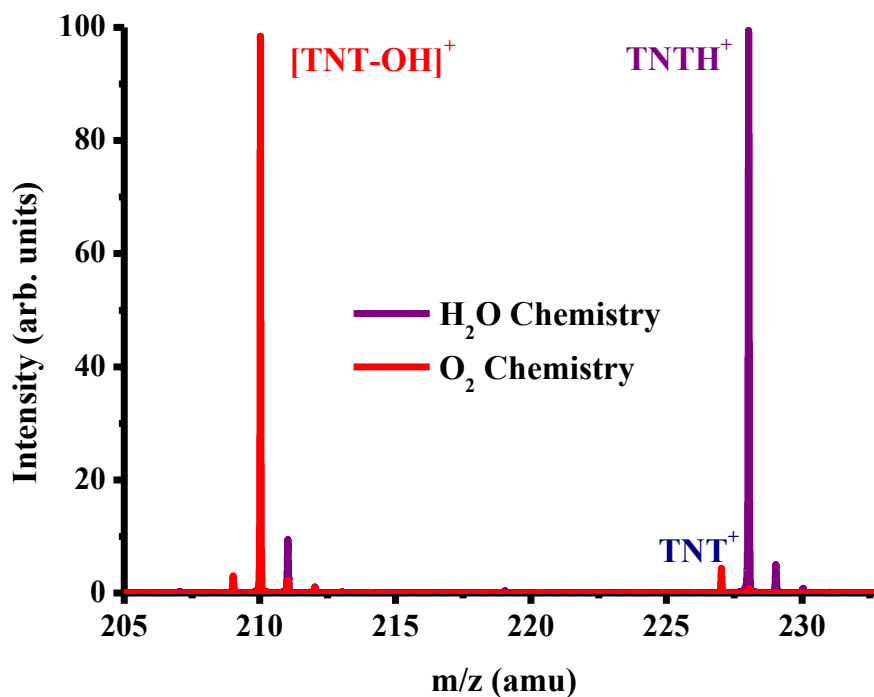


Figure 3.4. Plots illustrating the (a) switching between water and oxygen chemistry at approximately 110 seconds and back again at approximately 300 seconds and (b) rapidity of the switching (fully achieved within 10 seconds), although we comment that the O₂⁺ ion signal has not reached its highest intensity.

Figure 3.5 shows what happens to the mass spectra in switching between water and oxygen chemistry for (a) TNT and (b) TNB. For these mass spectra the intensity of the most intense product ion (m/z 210 for O₂⁺ reactions and m/z 228 for H₃O⁺ reactions) has been normalised to 100 for the sake of clarity.

(a)



(b)

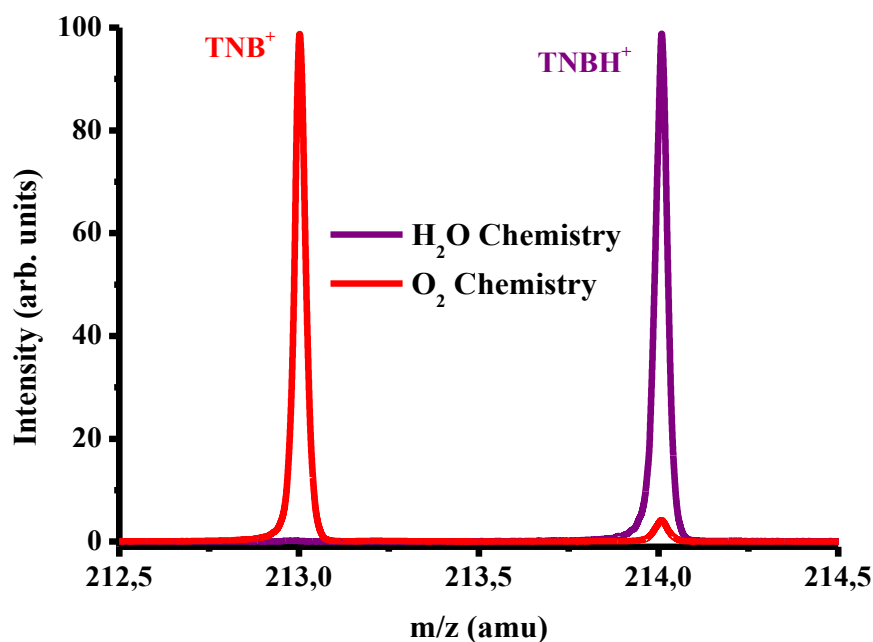


Figure 3.5. Changes in actual mass spectra as a result of changing from water to oxygen chemistry for (a) TNT and (b) TNB. H_3O^+ reacts with both TNT and TNB via non-dissociative proton transfer whereas O_2^+ reacts via a charge transfer processes with the

dominant channel being dissociative for TNT and non-dissociative for TNB. These spectra were recorded at an E/N value of 180 Td.

The lack of a reaction with O_2^+ with either PETN or RDX can also be used in a discriminatory way, *i.e.* simply switching from water to oxygen chemistry with no product ions being observed helps in the assignment of these explosives in a complex environment. Alternatively, or in addition, it is possible to rapidly switch to NO chemistry, which results in the adducts $M.NO^+$ ($M = PETN$ or RDX) providing the E/N used is kept low, *e.g.* 90 Td. This is illustrated in figure 3.6 for the explosive RDX whilst operating the drift tube at 90 Td. The signal intensities for the formation of $RDX.NO^+$ relative to that for $RDXH^+$ resulting from the reaction of H_3O^+ are shown. Although the signal intensities are comparable, in a recent study we have found that the dominant reaction channels for the reaction of H_3O^+ with RDX result from dissociative proton transfer (with a branching ratio of greater than 99%), with the dominant product ion being an ion at m/z 176, which we assign to a loss of HONO from the protonated parent molecule. Given that the non-dissociative proton transfer channel to form $RDX.H^+$ from the reaction of H_3O^+ with RDX has a very small branching ration (less than 1%), figure 3.6 suggests that the sensitivity for detection of $RDX.NO^+$ is rather small. This is not to be unexpected, because adduct formation relies on a third body to stabilise the complex, and in the low pressure environment of the drift tube of a PTR-MS, this will be inefficient in comparison to a bimolecular reaction process.

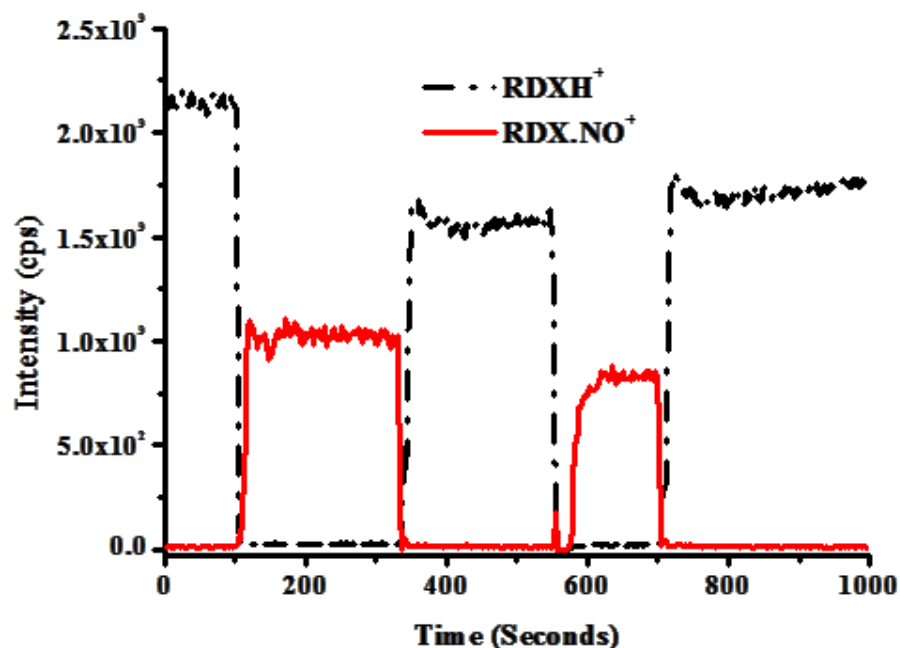


Figure 3.6. Switching between water and NO chemistry and the resulting product ions observed for the explosive RDX.

3.5. Conclusions

Using a rapid switching procedure we have demonstrated that it is possible to change the reagent ion in the reaction chamber of a PTR-MS instrument in order to alter the ion-molecule reaction processes, which leads to the production of different but highly assignable product ions. This switching can therefore be used to significantly enhance the selectivity of the PTR-MS instruments to aid in Homeland Security areas, where high sensitivity and high selectivity real-time detection of threat agents are required. The enhancement of selectivity can be easily controlled by a relatively simple automatic computer procedure to provide rapid switching of gases/vapours entering the hollow cathode discharge ion source, and hence rapid switching of the reagent ions. If needed this could be done in conjunction with a rapid change in the E/N to enhance the selectivity for compounds such as TNT and TNB, which demonstrate an anomalous behaviour in protonated parent ion signal intensity as E/N is increased from approximately 90 Td up to 200 Td.⁸ Although these are relatively simple methods to enhance selectivity, and hence to provide a much higher level of confidence for the real-time and rapid analytical detection of explosives and threat agents in general, their importance lies in the fact

that low resolution mass spectrometric techniques (and hence relatively low-cost systems) may be used in a PTR-MS instrument, rather than the high resolution (and hence relatively expensive) time-of-flight mass spectrometers used in this study.

We have shown that O_2^+ and NO^+ are ideal reagent ions for rapid switching from water chemistry in a PTR, because their recombination energies are less than that of the ionisation potential of water, and therefore conversion from proton transfer reactions to charge transfer (O_2^+) or association (NO^+) reactions with the explosives investigated in this study can be rapid (within seconds). This is not possible for reagent ions whose recombination energies are greater than that of water and the major constituents in air (N_2 and/or O_2). For example, Kr^+ would react with residual water vapour present in the drift tube/ion source, leading ultimately to the production of H_3O^+ ions through secondary reaction processes with a signal intensity that can be higher than the Kr^+ signal for a considerable time after the initial switching from water to Kr chemistry. This places a limiting factor on fast switching to Kr^+ from H_3O^+ . Furthermore, Kr^+ would also react with O_2 via non-dissociative charge transfer resulting in substantial intensities of O_2^+ in the reaction region, which are also much higher than those for Kr^+ . Only by using a dry system and the inlet air heavily diluted with He would it be possible to generate Kr^+ as the dominant reagent ion.

To conclude, in our opinion the results presented here, and in our other studies dealing with the detection of explosives,⁵⁻⁸ demonstrate the capabilities of providing a better selectivity for the detection of explosives than that of IMS systems currently used in homeland security applications, thereby reducing dramatically, but not necessarily eliminating, false positives. The identification of threat agents with a high level of confidence in real-time and in trace quantities is of great importance to the military, to emergency responders, and for applications in checkpoint security areas such as airports, harbours, and train stations.

3.6. Acknowledgements

This project was in part funded under the Innovative Research Call in Explosives and Weapons Detection 2010 initiative (CAM and PW). This is a Cross-Government programme sponsored by a number of Departments and Agencies under the UK Government's CONTEST strategy in partnership with the US Department of Homeland Security. The Early

Stage Researchers (ML and RGM) acknowledge the support of the PIMMS Initial Training Network which in turn is supported by the European Commission's 7th Framework Programme under Grant Agreement Number 287382.

3.7. References

1. E. Zolfagharifard "Full-body scanners spark concerns" the ENGINEER 5th January 2010 (www.theengineer.co.uk/news/).
2. www.timesonline.co.uk/tol/news/uk/article7048576.ece March 3 2010.
3. Eiceman G.A., Karpas Z., *Ion Mobility Spectrometry*, 2nd Edition, Taylor and Francis (2005).
4. Watts, P. In Use of ion mobility for the detection and analysis of vapours. *Analytical proceedings*, Royal Society of Chemistry: **1991**, 28 (10), 328-331.
5. Mayhew, C. A.; Sulzer, P.; Petersson, F.; Haidacher, S.; Jordan, A.; Märk, L.; Watts, P.; Märk, T. D., Applications of proton transfer reaction time-of-flight mass spectrometry for the sensitive and rapid real-time detection of solid high explosives. *International Journal of Mass Spectrometry* **2010**, 289 (1), 58-63.
6. Jürschik, S.; Sulzer, P.; Petersson, F.; Mayhew, C. A.; Jordan, A.; Agarwal, B.; Haidacher, S.; Seehauser, H.; Becker, K.; Märk, T. D., Proton transfer reaction mass spectrometry for the sensitive and rapid real-time detection of solid high explosives in air and water. *Anal Bioanal Chem* **2010**, 398 (7-8), 2813-2820.
7. Sulzer, P.; Jordan, A.; Märk, L.; Mayhew, C. A.; Becker, K.; Märk, T. D., Technical advances in proton transfer reaction-mass spectrometry and new fields of application. *American Laboratory* **2011**, 43 (9), 13-15.
8. Sulzer, P.; Petersson, F.; Agarwal, B.; Becker, K. H.; Jürschik, S.; Märk, T. D.; Perry, D.; Watts, P.; Mayhew, C. A., Proton Transfer Reaction Mass Spectrometry and the Unambiguous Real-Time Detection of 2,4,6 Trinitrotoluene. *Analytical Chemistry* **2012**, 84 (9), 4161-4166.
9. Petersson, F.; Sulzer, P.; Mayhew, C. A.; Watts, P.; Jordan, A.; Märk, L.; Märk, T. D., Real-time trace detection and identification of chemical warfare agent simulants using

- recent advances in proton transfer reaction time-of-flight mass spectrometry. *Rapid Communications in Mass Spectrometry* **2009**, *23* (23), 3875-3880.
10. Agarwal, B.; Petersson, F.; Jürschik, S.; Sulzer, P.; Jordan, A.; Märk, T. D.; Watts, P.; Mayhew, C. A., Use of proton transfer reaction time-of-flight mass spectrometry for the analytical detection of illicit and controlled prescription drugs at room temperature via direct headspace sampling. *Anal Bioanal Chem* **2011**, *400* (8), 2631-2639.
 11. Jürschik, S.; Agarwal, B.; Kassebacher, T.; Sulzer, P.; Mayhew, C. A.; Märk, T. D., Rapid and facile detection of four date rape drugs in different beverages utilizing proton transfer reaction mass spectrometry (PTR-MS). *Journal of Mass Spectrometry* **2012**, *47* (9), 1092-1097.
 12. Kassebacher, T.; Sulzer, P.; Jürschik, S.; Hartungen, E.; Jordan, A.; Edtbauer, A.; Feil, S.; Hanel, G.; Jaksch, S.; Märk, L.; Mayhew, C. A.; Märk, T. D., Investigations of chemical warfare agents and toxic industrial compounds with proton-transfer-reaction mass spectrometry for a real-time threat monitoring scenario. *Rapid Communications in Mass Spectrometry* **2013**, *27* (2), 325-332.
 13. Wilson, P. F.; Prince, B. J.; McEwan, M. J., Application of Selected-Ion Flow Tube Mass Spectrometry to the Real-Time Detection of Triacetone Triperoxide. *Analytical Chemistry* **2005**, *78* (2), 575-579.
 14. Shen, C.; Li, J.; Han, H.; Wang, H.; Jiang, H.; Chu, Y., Triacetone triperoxide detection using low reduced-field proton transfer reaction mass spectrometer. *International Journal of Mass Spectrometry* **2009**, *285* (1-2), 100-103.
 15. Jordan, A.; Haidacher, S.; Hanel, G.; Hartungen, E.; Märk, L.; Seehauser, H.; Schottkowsky, R.; Sulzer, P.; Märk, T. D., A high resolution and high sensitivity proton-transfer-reaction time-of-flight mass spectrometer (PTR-TOF-MS). *International Journal of Mass Spectrometry* **2009**, *286* (2-3), 122-128.
 16. Kotov, B.V.; Potapov, V.K., Ionization potentials of strong organic electron acceptors, *Khim. Vys. Energ.*, **1972**, *6*, 375.
 17. Schramm, E.; Mühlberger, F.; Mitschke, S.; Reichardt, G.; Schulte-Ladbeck, R.; Pütz, M.; Zimmermann, R., Determination of the ionization potentials of security-relevant substances with single photon ionization mass spectrometry using synchrotron radiation. *Applied spectroscopy* **2008**, *62* (2), 238-247.

18. Jarvis, G.; Kennedy, R.; Mayhew, C.; Tuckett, R., Charge transfer from neutral perfluorocarbons to various cations: long-range versus short-range reaction mechanisms. *International Journal of Mass Spectrometry* **2000**, *202* (1), 323-343.
19. Bouchoux, G.; Salpin, J.-Y.; Leblanc, D., A relationship between the kinetics and thermochemistry of proton transfer reactions in the gas phase. *International journal of mass spectrometry and ion processes* **1996**, *153* (1), 37-48.
20. Sulzer, P.; Edtbauer, A.; Hartungen, E.; Jürschik, S.; Jordan, A.; Hanel, G.; Feil, S.; Jaksch, S.; Märk, L.; Märk, T. D., From conventional proton-transfer-reaction mass spectrometry (PTR-MS) to universal trace gas analysis. *International Journal of Mass Spectrometry* **2012**, *321–322*, 66-70.

CHAPTER 4

SENSITIVITY AND SELECTIVITY OF SWITCHABLE REAGENT ION SOFT CHEMICAL IONIZATION MASS SPECTROMETRY FOR THE DETECTION OF PICRIC ACID

This chapter is a reformatted copy of my published article:

The Journal of Physical Chemistry Part A, 2014, 118 (37), 8229–8236.

Bishu Agarwal,^{1,2} Ramón González-Méndez,³ Matteo Lanza,¹ Philipp Sulzer,¹ Tilmann D. Märk,^{1,2} Neil Thomas,³ and Chris A. Mayhew^{3*}

1. Ionicon Analytik Gesellschaft m.b.H., Eduard-Bodem-Gasse 3, A-6020 Innsbruck, Austria
2. Institut für Ionenphysik und Angewandte Physik, Leopold Franzens Universität Innsbruck, Technikerstr. 25, A-6020 Innsbruck, Austria
3. School of Physics and Astronomy, University of Birmingham, Edgbaston, Birmingham, B15 2TT, UK

* Corresponding author: Tel.:+441214144729; fax:+441214144577. E-mail address: c.mayhew@bham.ac.uk

Declaration of contribution

My contribution to the study described in this Chapter is the experimental work performed on the Ionicon PTR-ToF 8000 (Ionicon Analytik GmbH, Austria) during a secondment done at their facilities in August 2013. I also took the same measurements with

the Molecular Physics Research Group's KORE PTR-ToF at the University of Birmingham, for reproducibility purposes, although that data was not included on the published article. I also contributed to the elaboration of the graphs, data analysis and the elaboration of the manuscript jointly with the other co-authors.

The Density Functional Theory (DFT) calculations used to aid in the interpretation of the data were made by Dr. Peter Watts (Molecular Physics Research Group, University of Birmingham).

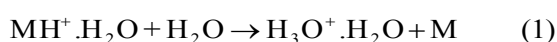
4.1. Abstract

We have investigated the reactions of NO^+ , H_3O^+ , O_2^+ and Kr^+ with picric acid (2,4,6-trinitrophenol, $\text{C}_6\text{H}_3\text{N}_3\text{O}_7$, PiA) using a time-of-flight mass spectrometer with a switchable reagent-ion source. NO^+ forms a simple adduct ion $\text{PiA}\cdot\text{NO}^+$, whilst H_3O^+ reacts with PiA via non-dissociative proton transfer to form PiAH^+ . In contrast, both O_2^+ and Kr^+ react with PiA by non-dissociative charge transfer to produce PiA^+ . For Kr^+ , we also observe dissociation of PiA, producing NO_2^+ with a branching percentage of approximately 40%. For the reagent ions H_3O^+ and O_2^+ (and operating the drift tube with normal laboratory air), we find that the intensities of the PiAH^+ and PiA^+ ions both exhibit a peak at a given drift-tube voltage (which is humidity dependent). This unusual behaviour implies a peak in the detection sensitivity of PiA as a function of the drift-tube voltage (and hence E/N). Aided by electronic-structure calculations and our previous studies of trinitrotoluene and trinitrobenzene, we provide a possible explanation for the observed peak in the detection sensitivity of PiA.

4.2 Introduction

A number of our recent publications have demonstrated the use of switchable reagent ion soft chemical ionisation mass spectrometric instrumentation for the detection of various threat agents including explosives,¹⁻⁵ drugs,^{4,6-9} chemical warfare agents,^{10,11} and toxic industrial compounds.¹¹ The explosive studies have included the reactions of H_3O^+ with trinitrotoluene (TNT), trinitrobenzene (TNB), pentaerythritoltetranitrate (PETN), cyclotrimethylene-trinitramine (RDX), 1,3-dinitrobenzene (DNB) and 2,4-dinitrotoluene (DNT),¹⁻⁴ and O_2^+ and NO^+ with TNT, TNB, PETN and RDX.⁵ The aim of our studies into different reagent ions is to investigate whether rapid switching between them could enhance the selectivity of detection, i.e. whether it is possible to distinguish isobaric and isomeric compounds.

A particularly interesting finding from the H_3O^+ studies with explosives was the dependence of the detection sensitivity of TNTH^+ and TNBH^+ on reduced electric field (the ratio of the electric field strength E and the gas number density N in the drift tube).³ For the majority of PTR-MS studies it has been found that the signal intensity for the protonated parent decreases with increasing E/N (e.g. in the case of the explosives this is observed to occur dramatically for RDX and PETN). A decrease in the protonated parent ion signal with increasing E/N is the expected behaviour owing to reduced reaction times and increased collisional induced dissociation. A decrease in the protonated parent ion signal is also observed for low E/N if association of the protonated parent with water present in the drift tube occurs. If this association occurs at a given E/N then it will be observed that the protonated signal intensity would initially increase as E/N is increased owing to the reduction in association, reach a maximum and then begin to decrease owing to the two factors already mentioned above. It can normally be expected that any decrease with the protonated parent (AH^+) as a result of association with water would be mirrored by an increase in the $\text{AH}^+ \cdot \text{H}_2\text{O}$ signal intensity, so that the parent molecule of interest would still be involved in a product ion (e.g. this has been observed for 1,3-DNB and 2,4-DNT),³ and hence an identifiable m/z in the mass spectrum. However, this is not always the case. For TNTH^+ and TNBH^+ no significant increase in the $\text{MH}^+ \cdot \text{H}_2\text{O}$ ion signals were observed at low E/N because of a ligand switching process:



Given that the terminal ion does not contain the explosive and is one that is already abundant

in the drift tube so that the contribution from the secondary reactions cannot be detected, reaction (1) results in a loss of sensitivity for the detection of TNTH^+ and TNBH^+ as E/N is reduced.

Reaction (1) is not common, and an aim of our recent studies has been to investigate whether any other explosives or explosive related compounds behave in a similar fashion. The importance of this relates to the appropriate conditions needed to enhance sensitivity (correct E/N) and selectivity (rapid switching of E/N) of detection. Therefore, we have investigated a large number of compounds, including nitrobenzene, nitromethane, nitrotoluenes, dinitrobenzenes, dinitrotoluenes and picric acid (PiA). Only the trinitroaromatic compound picric acid ($\text{C}_6\text{H}_3\text{N}_3\text{O}_7$) was found to behave in a similar way to TNT and TNB, and this compound is therefore the subject of this paper.

In addition to using H_3O^+ as a reagent ion, in this study we have extended this investigation by looking at the reaction of picric acid with NO^+ , O_2^+ and Kr^+ to determine what product ions are produced, so that we can not only determine if selectivity can be enhanced for picric acid detection by switching the reagent ions, but also to investigate the sensitivity of detection as a function of E/N for these three reagent ions. Of particular interest here is that we have found that the intensity of the product ion resulting from the reaction of O_2^+ with picric acid behaves in a similar way to that observed for protonated picric acid with E/N , although over a different E/N range.

To aid in the interpretation of the experimental results, DFT calculations have been undertaken to determine thermochemical values for picric acid and its reaction with various ions. These calculations are also reported in this paper.

4.3. Experimental and Theoretical Details

4.3.1 Electronic Structure Calculations

Density Functional Theory calculations using the GAUSSIAN09 PROGRAM with the GaussView 5 interface have been undertaken to determine the proton affinity of picric acid, heats of formation of various ions and reaction processes at 298 K.¹² Although it is appreciated that the drift tube temperature used in our experiments is greater than 298 K, the thermochemical calculations at 298 K provide a useful indication as to whether a reaction

pathway is energetically possible or not. The B3LYP functional with the 6-31+G(d,p) basis set was used for this study.

4.3.2 Experimental Methods

For this study we have used the recently developed switchable reagent ion PTR-TOF 8000 (manufactured by Ionicon Analytik GmbH, Austria).¹³ A full description of this instrument has already been published,¹⁴ and hence only brief details will be provided here.

Carrier gas was passed through a septum into a glass vial containing picric acid. The carrier gas passed over the sample and was drawn into a tube connected to the inlet system of the PTR-TOF 8000. The glass vial was kept at approximately 70 °C, whereas the sample inlet line and the drift tube were maintained at approximately 120 °C. For those H_3O^+ and O_2^+ experiments where we wished to keep the humidity in the drift tube to a minimum value, high purity nitrogen was used as a carrier gas, otherwise normal laboratory air was used after it had been passed through a hydrocarbon trap. For the Kr^+ experiments the drift tube was operated under extremely dry conditions (defined as the case when the H_3O^+ signal intensity is less than approximately 3% of the total Kr^+ ion signal at any given E/N) and the carrier gas used was helium as described by Sulzer *et al.*¹⁵ As both Kr^+ and O_2^+ react with picric acid via charge transfer we have also investigated the reactions of O_2^+ with picric acid using the carrier gas (He) used in the krypton experiments to allow a direct comparison between the two studies. When operating using helium in the drift tube, the drift tube voltage is limited such that the maximum E/N that can be used is 110 Td because above this value an electrical discharge occurs making the system unstable.

H_3O^+ , NO^+ , Kr^+ or O_2^+ reagent ions were produced by flowing water vapour, nitrogen/oxygen mix (3:1), krypton or oxygen, respectively, into a hollow cathode discharge ion source. The reagent ions, under the influence of a voltage gradient, passed through a small orifice from the hollow cathode ion source into an adjacent drift (reaction) tube section, where the picric acid in trace amounts was introduced via the gas inlet system mentioned above. When using NO^+ and O_2^+ as the reagent ions, H_3O^+ was also produced owing to some residual water vapour on the surfaces of tubing going to and in the hollow cathode ion source, but this always resulted in an ion intensity of less than 5% found for that of the dominant reagent ion signal after several seconds and much less when running in pure nitrogen.

For the series of investigations presented in this study picric acid was purchased from Sigma Aldrich with a stated purity of $\geq 98\%$. Owing to its susceptibility to explode through

friction or shock, picric acid is supplied wet, *i.e.* under a layer of water, which renders picric acid safe to handle. Therefore, before any measurements were taken a small quantity of wet picric acid was placed in the glass vial and allowed to air-dry.

4.4. Results

4.4.1 Electronic structure calculations

Since much of the thermochemistry of the reaction processes involved in this study is unknown, a series of electronic structure calculations have been undertaken. These provide crucial information which can be used to determine which reaction pathways are energetically possible. The thermochemical calculations for various reaction processes involving protonated species of importance to the study presented here are summarized in tables 4.1 and 4.2. Table 4.1 presents the changes in the enthalpies and free energies for the reactions of H_3O^+ , $\text{H}_3\text{O}^+\cdot\text{H}_2\text{O}$ and $\text{H}_3\text{O}^+\cdot 2\text{H}_2\text{O}$ with picric acid. Table 4.2 provides the changes in the enthalpies and free energies for the reactions of $\text{PiAH}^+\cdot n\text{H}_2\text{O}$ ($n = 0-2$) with H_2O .

Table 4.1. Enthalpy and free energy changes for the reactions of H_3O^+ , $\text{H}_3\text{O}^+\cdot\text{H}_2\text{O}$ and $\text{H}_3\text{O}^+\cdot 2\text{H}_2\text{O}$ with picric acid (PiA) at 298 K calculated at the B3LYP 6-31+G(d,p) level.

Reactants	Product(s)	ΔH_{298} kJ mol ⁻¹	ΔG_{298} kJ mol ⁻¹
PiA + H_3O^+	PiA1H ⁺ ·H ₂ O	-139	-97
	PiA1H ⁺ + H ₂ O	-80	-75
	PiA4H ⁺ ·H ₂ O	-124	-86
	PiA4H ⁺ + H ₂ O	-27	-27
PiA + $\text{H}_3\text{O}^+\cdot\text{H}_2\text{O}$	PiA1H ⁺ ·2H ₂ O	-66	-27
	PiA1H ⁺ ·H ₂ O + H ₂ O	+19	+27
	PiA4H ⁺ ·2H ₂ O	-74	-28
	PiA4H ⁺ ·H ₂ O + H ₂ O	+34	+37
PiA + $\text{H}_3\text{O}^+\cdot 2\text{H}_2\text{O}$	PiA1H ⁺ ·3H ₂ O	-58	-11
	PiA1H ⁺ ·2H ₂ O + H ₂ O	+29	+37
	PiA4H ⁺ ·3H ₂ O	-55	-7
	PiA4H ⁺ ·2H ₂ O + H ₂ O	+21	+37

Table 4.2. Enthalpy and free energy changes for the reactions of $\text{PiAH}^+ \cdot n\text{H}_2\text{O}$ ($n = 0, 1$ or 2) with H_2O at 298 K calculated at the B3LYP 6-31+G(d,p) level.

Reactants	Product(s)	$\Delta H_{298} \text{ kJ mol}^{-1}$	$\Delta G_{298} \text{ kJ mol}^{-1}$
$\text{PiA1H}^+ + \text{H}_2\text{O}$	$\text{PiA1H}^+ \cdot \text{H}_2\text{O}$	-59	-22
$\text{PiA1H}^+ \cdot \text{H}_2\text{O} + \text{H}_2\text{O}$	$\text{PiA1H}^+ \cdot 2\text{H}_2\text{O}$	-85	-54
	$\text{PiA} + \text{H}_3\text{O}^+ \cdot \text{H}_2\text{O}$	-19	-27
$\text{PiA1H}^+ \cdot 2\text{H}_2\text{O} + \text{H}_2\text{O}$	$\text{PiA1H}^+ \cdot 3\text{H}_2\text{O}$	-86	-48
	$\text{PiA} + \text{H}_3\text{O}^+ \cdot 2\text{H}_2\text{O}$	-29	-37
$\text{PiA4H}^+ + \text{H}_2\text{O}$	$\text{PiA4H}^+ \cdot \text{H}_2\text{O}$	-97	-59
$\text{PiA4H}^+ \cdot \text{H}_2\text{O} + \text{H}_2\text{O}$	$\text{PiA4H}^+ \cdot 2\text{H}_2\text{O}$	-108	-65
	$\text{PiA} + \text{H}_3\text{O}^+ \cdot \text{H}_2\text{O}$	-34	-37
$\text{PiA4H}^+ \cdot 2\text{H}_2\text{O} + \text{H}_2\text{O}$	$\text{PiA4H}^+ \cdot 3\text{H}_2\text{O}$	-76	-44
	$\text{PiA} + \text{H}_3\text{O}^+ \cdot 2\text{H}_2\text{O}$	-21	-37

To our knowledge the proton affinity of picric acid is not available in the literature. The actual value depends on to which site on the picric acid the proton attaches. We have undertaken DFT calculations for the proton attaching to either the 2 or the 4 nitro groups. The calculated proton affinities corresponding to PiA1H^+ , PiA2H^+ and PiA4H^+ are 764, 756 and 711 kJ mol^{-1} , respectively. There is only one possible structure for the 4-nitro group PiA4H^+ with the proton sitting on a nitro group. However, for the nitrogroups adjacent to the hydroxyl group, there are two possible configurations when a proton is attached, PiA1H^+ and PiA2H^+ , and these are shown in figure 4.1. Transition state energies for PiA1H^+ to PiA2H^+ are calculated to be $\Delta H +47 \text{ kJ mol}^{-1}$ and $\Delta G +45 \text{ kJ mol}^{-1}$, and , it is thus likely that PiA1H^+ is the stable structure when the proton is transferred to the 2 nitro group. The proton affinities determined for picric acid are all greater than the proton affinity of H_2O , but less than that for $(\text{H}_2\text{O})_2$. This means that whilst H_3O^+ is thermodynamically allowed to transfer a proton to picric acid, $\text{H}_3\text{O}^+ \cdot \text{H}_2\text{O}$ cannot. Ligand switching from $\text{H}_3\text{O}^+ \cdot \text{H}_2\text{O}$ to PiA to form $\text{PiA} \cdot \text{H}_3\text{O}^+$ and H_2O is thermodynamically also not possible. The value for the proton affinity corresponding to the conjugate acid PiA4H^+ is relatively close to water ($\text{PA}(\text{H}_2\text{O}) = 691 \text{ kJ mol}^{-1}$).¹⁶ Based on the studies of other molecules whose proton affinities are close to water, e.g. hydrogen cyanide ($\text{PA}(\text{HCN}) = 713 \text{ kJ mol}^{-1}$) and formaldehyde ($\text{PA}(\text{HCHO}) = 712 \text{ kJ$

mol^{-1}),¹⁷⁻¹⁹ we can expect that if formed substantial back reaction of PiA4H^+ with water will occur owing to the large abundance of neutral water in the reaction region.

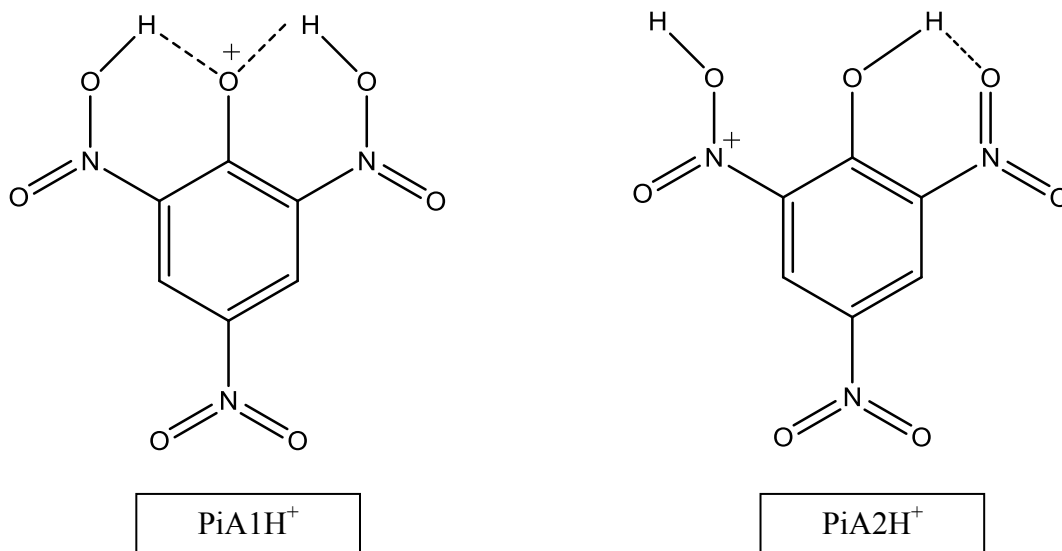


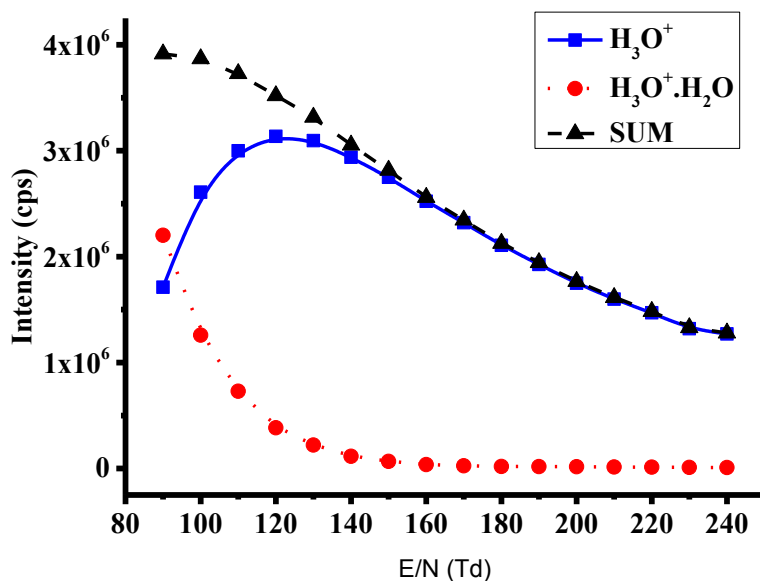
Figure 4.1. Structures for protonated picric acid corresponding to two possible conjugate acids.

4.4.2 Experimental Results

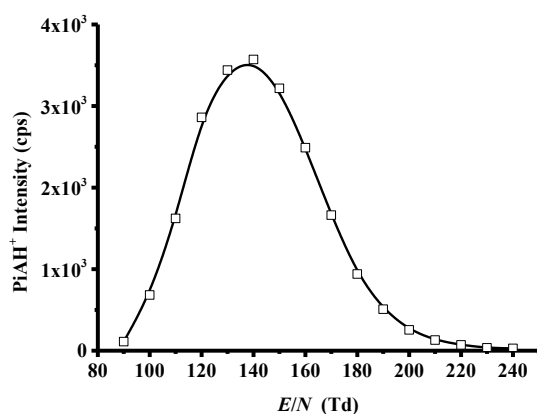
4.4.2.1 H_3O^+ Measurements

Figure 4.2(a) provides information on the $\text{H}_3^{16}\text{O}^+$ reagent ion signal (as determined in the normal way by recording the signal intensity for $\text{H}_3^{18}\text{O}^+$ to avoid detection saturation issues) as a function of E/N over the range 90 – 240 Td as measured on the PTR-TOF 8000. The overall reagent ion signal intensity is excellent, being around 3×10^6 cps. However, there is an obvious dependence on intensity on E/N , which we attribute to transmission factors and at low E/N water clustering. Figure 4.2(a) shows that as H_3O^+ decreases at low E/N values (< 120 Td) a comparable increase in $\text{H}_3\text{O}^+ \cdot \text{H}_2\text{O}$ occurs. Below approximately 100 Td, m/z 37 ($\text{H}_3\text{O}^+ \cdot \text{H}_2\text{O}$) becomes the dominant reagent ion.

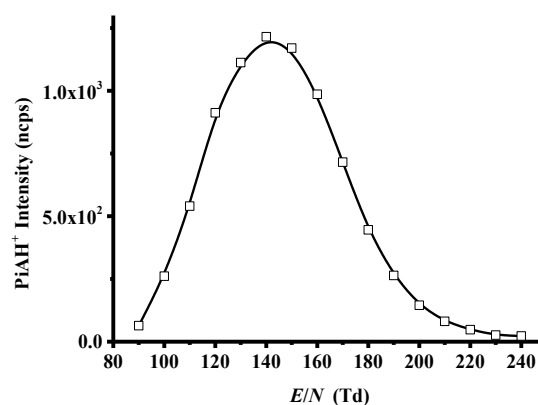
Reaction of H_3O^+ with picric acid is via non-dissociative proton transfer leading to PiAH^+ . Figures 4.2 (b) and (c) graphically represent the dependence of the detection efficiency for PiAH^+ on E/N for the raw and normalised (to $10^6 \text{H}_3\text{O}^+$) counts per second, respectively, using laboratory air as the carrier gas.



(a)



(b)

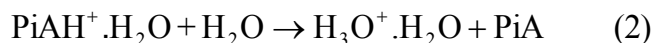


(c)

Figure 4.2. The variation in ion signal intensities for (a) the reagent ion H_3O^+ , (b) the unnormalised protonated picric acid and (c) the normalised (10^6 cps of H_3O^+) protonated picric acid as a function of E/N . Purified laboratory air was used as the carrier gas.

The E/N dependence observed for $PiAH^+$ follows a similar pattern to one we have observed for two other trinitroaromatic compounds, TNT and TNB [3]. A simple chemical mechanism explains the observations for TNT and TNB, as described briefly in the introduction above and in more detail by Sulzer *et al.*³ From the DFT calculations provided in table 4.2, we propose a similar process is taking place with picric acid. That is as E/N is

reduced adduct formation of PiAH^+ with H_2O occurs. However, we observe only small quantities of $\text{PiAH}^+\cdot\text{H}_2\text{O}$. Therefore, as proposed for TNT and TNB, $\text{PiAH}^+\cdot\text{H}_2\text{O}$ reacts with water leading to the formation of PiA and $\text{H}_3\text{O}^+\cdot\text{H}_2\text{O}$, *i.e.*



The (298 K) DFT calculations show that for reaction (2) $\Delta G = -27 \text{ kJ mol}^{-1}$ for PiA1H^+ and $\Delta G = -37 \text{ kJ mol}^{-1}$ for PiA4H^+ (table 4.2). Even if instead of reaction (1) $\text{PiAH}^+\cdot\text{H}_2\text{O}$ forms a higher hydrate through adduct formation, the reaction of $\text{PiAH}^+\cdot 2\text{H}_2\text{O}$ with H_2O leading to the products $\text{H}_3\text{O}^+\cdot 2\text{H}_2\text{O} + \text{PiA}$ is also exoergonic with $\Delta G = -37 \text{ kJ mol}^{-1}$. Thus ion-molecule reactions of $\text{PiAH}^+\cdot n(\text{H}_2\text{O})$ with H_2O can explain the low intensity observed for the $\text{PiAH}^+\cdot n(\text{H}_2\text{O})$ ions and hence the reduction in the PiAH^+ signal at low E/N . In confirmation of this proposal, figure 4.3 presents the normalised signal intensities (with the maxima set at 100 for ease of comparison) for a dry N_2 and for the case where N_2 has added water leading to a relative humidity of 10%. (Note that even when using N_2 as a buffer gas in the drift tube, there will still be water diffusing into the drift tube from the ion source.) In agreement with expectations the peak intensity shifts to higher E/N as the humidity of the carrier gas in the drift tube increase.

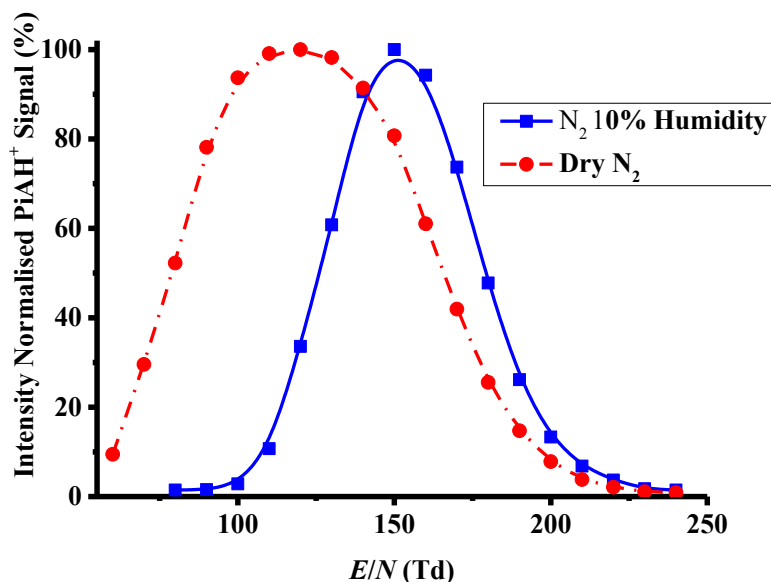
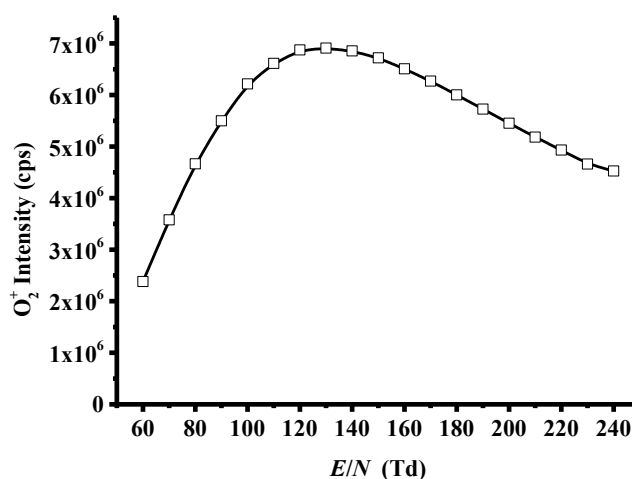


Figure 4.3. The relative variation in ion signal intensities for normalised PiAH^+ as a function of E/N using dry N_2 and N_2 at 10% humidity as carrier gases. The maximum intensity has been set at 100 for both sets of data to ease comparison.

4.2.2 O₂⁺ Measurements

Unlike H₃O⁺ studies, which are limited to E/N of greater than approximately 90 Td owing to clustering with H₂O, which dramatically reduces the H₃O⁺ intensity below 90 Td (see figure 4.2(a)), there is no such restriction for the O₂⁺ measurements because there is no observable adduct formation with H₂O. Thus for these studies we were able to start measurements at lower E/N values. Figure 4.4(a) gives details on the O₂⁺ reagent ion signal intensity as a function of E/N (60 – 240 Td) using laboratory air passed through a hydrocarbon trap as the buffer gas in the drift tube. This reagent ion signal had to be determined by using the molecular oxygen isotope at m/z 34 (¹⁶O¹⁸O⁺), owing to detection saturation at m/z 32. It can be seen that even at 60 Td the signal intensity is relatively high at approximately 2×10^6 cps and then steadily increases as E/N increases reaching a maximum of approximately 7×10^6 cps at about 120 Td and then decreases with increasing E/N . Thus the signal intensity of O₂⁺ as a function of E/N follows a similar behaviour as found for H₃O⁺. Given that none of the decrease observed in the O₂⁺ intensity for $E/N < 120$ Td can be attributed to cluster formation we assume it is a result of extraction issues from the ion source. Although the change in intensity of the reagent ions over the E/N range covered in this study is not dramatic (approximately a factor of three) it is important that any product ion signal is normalised to the reagent ion signal (we have used 10^6 cps of O₂⁺).



(a)

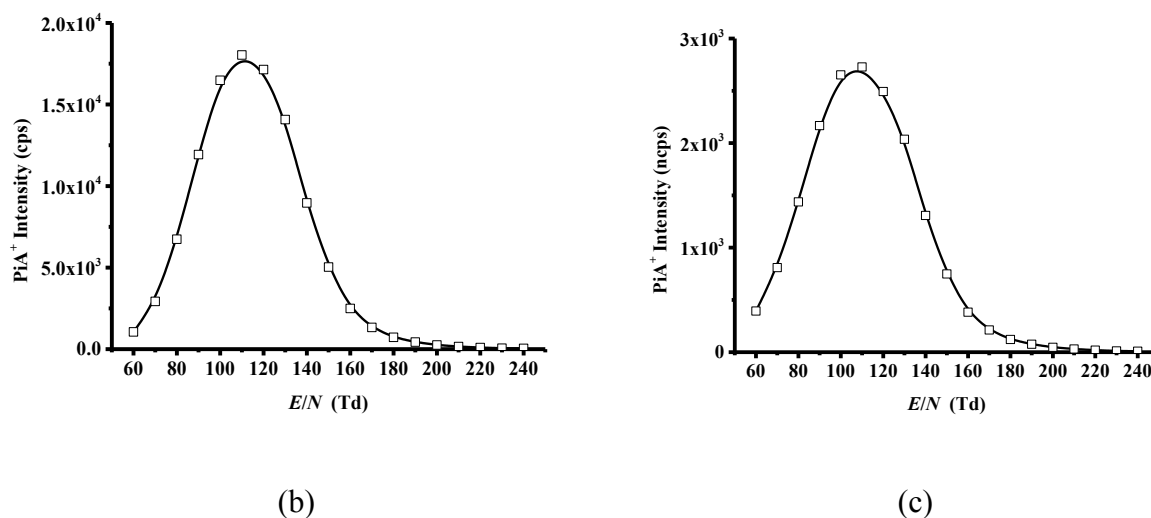


Figure 4.4. The variation in ion signal intensities for (a) the reagent ion O_2^+ , (b) the unnormalised PiA^+ and (c) the normalised (10^6 cps of O_2^+) PiA^+ as a function of E/N . Purified laboratory air was used as the carrier gas.

For all E/N values, O_2^+ is found to react with picric acid by non-dissociative charge transfer:



No other ions could be identified in the mass spectra that could be associated with the reaction of O_2^+ with PiA. For reaction (3) to be observed the ionisation potential of picric acid must be less than that of oxygen (12.07 eV). This agrees with an experimental value of the ionisation potential of picric acid of 10.1 eV obtained from single photoionisation mass spectrometric measurements.²⁰ The dependence of PiA^+ unnormalised and normalised signal intensities as a function of E/N is shown in figure 4.4(b) and (c), respectively. We find that the PiA^+ signal intensity follows a similar dependence to that found for the PiAH^+ signal (although over a different E/N range). (Compare figure (4.2(c)) with figure 4.4(c)). To determine whether this is humidity dependent we investigated how the peak position changes in going from using normal laboratory air to laboratory air at 10% humidity. This is shown in figure 4.5, which should be compared with figure 4.3.

A comparison of figures 4.4(c) and 4.5 with figures 4.2(c) and 4.3, respectively, implies that a similar process proposed for the reaction of $\text{PiAH}^+\cdot\text{H}_2\text{O}$ with water (reaction (2)) is occurring for $\text{PiA}^+\cdot\text{H}_2\text{O}$ and water resulting in neutral PiA and a protonated water cluster:

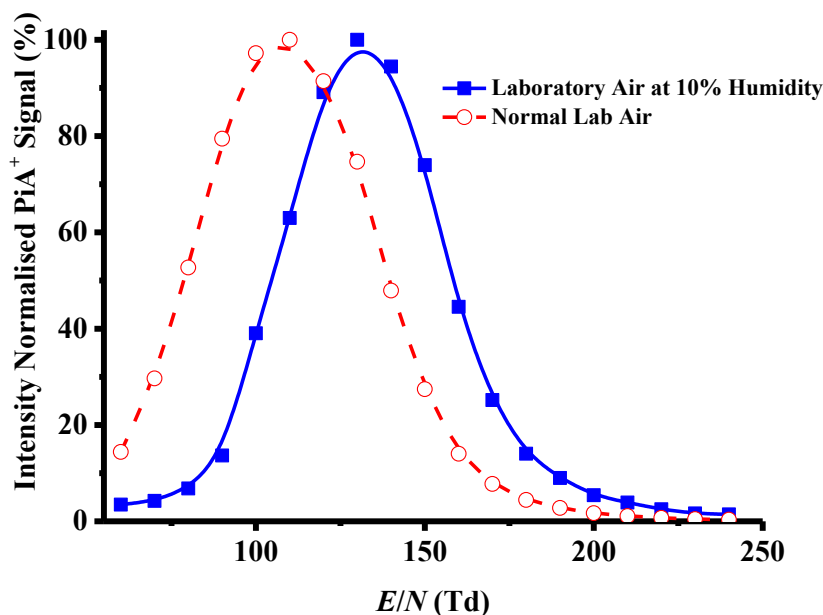


Figure 4.5. The variation in relative ion signal intensities for normalised PiA^+ as a function of E/N recorded using normal laboratory air compared to using laboratory air at 10% humidity as a carrier gas.

Table 4.3 presents enthalpy and free energy changes for the reactions of $\text{PiA}^+\cdot n\text{H}_2\text{O}$ ($n = 0, 1$ or 2) with H_2O at 298 K calculated at the B3LYP 6-31+G(d,p) level. From this table it can be seen that the proposed reaction route (4) is endoergic with $\Delta G = +17 \text{ kJ mol}^{-1}$. This leads to a problem, because we have suggested in an earlier publication that an endoergic of $+17 \text{ kJ mol}^{-1}$ is too high for $\text{DNBH}^+\cdot\text{H}_2\text{O}$ to react with water via a ligand switching mechanism within the drift tube environment.³ However, it could be argued that PiA^+ is formed with a significant amount of internal energy following the charge transfer (approximately 2 eV), which is far more than PiAH^+ would have following proton transfer from H_3O^+ to DNB, and that after associating with H_2O there is sufficient energy to drive reaction (4). This raises the question as to whether excited PiA^+ would readily associate with water.

Table 4.3. Enthalpy and free energy changes for the reactions of $\text{PiA}^+ \cdot n\text{H}_2\text{O}$ ($n = 0, 1$ or 2) with H_2O at 298 K calculated at the B3LYP 6-31+G(d,p) level.

Reactants	Product(s)	ΔH_{298} kJ mol ⁻¹	ΔG_{298} kJ mol ⁻¹
$\text{PiA}^+ + \text{H}_2\text{O}$	$\text{PiA}^+ \cdot \text{H}_2\text{O}$	-77	-43
$\text{PiA}^+ \cdot \text{H}_2\text{O} + \text{H}_2\text{O}$	$\text{PiA}^+ \cdot 2\text{H}_2\text{O}$	-90	-55
	$\text{PiA-H} + \text{H}_3\text{O}^+ \cdot \text{H}_2\text{O}$	+15	+17
$\text{PiA}^+ \cdot 2\text{H}_2\text{O} + \text{H}_2\text{O}$	$\text{PiA}^+ \cdot 3\text{H}_2\text{O}$	-79	-41
	$\text{PiA-H} + \text{H}_3\text{O}^+ \cdot 2\text{H}_2\text{O}$	+10	+8

To further investigate the humidity dependence of the PiA^+ intensity, we replaced laboratory air with either pure nitrogen or helium (used also to compare later with the Kr^+ study). Figures 4.6 (a) and (b) shows the unnormalised and the normalised measurements for PiA^+ obtained when using nitrogen as the carrier gas, respectively, and figure 4.7 (b) the results when using He as the buffer gas. (Figure 4.7(a) shows the O_2^+ signal intensity as a function of E/N in a He buffer gas, which is considerably less than obtained when using air or nitrogen (figure 4.4(a)) but still of sufficient intensity for our study.) It can be seen that the shape of the PiA^+ intensity curves (compare figure 4.4(c) with figures 4.6(b) and 4.7(b)) has dramatically changed and behaves more like the normal behaviour (*i.e.* decreasing intensity with increasing E/N), except for an unexplained kink in the curve of figure 4.6(b) which approximately occurs at the position where the maximum is observed for those measurements taken using a more humid reaction chamber.

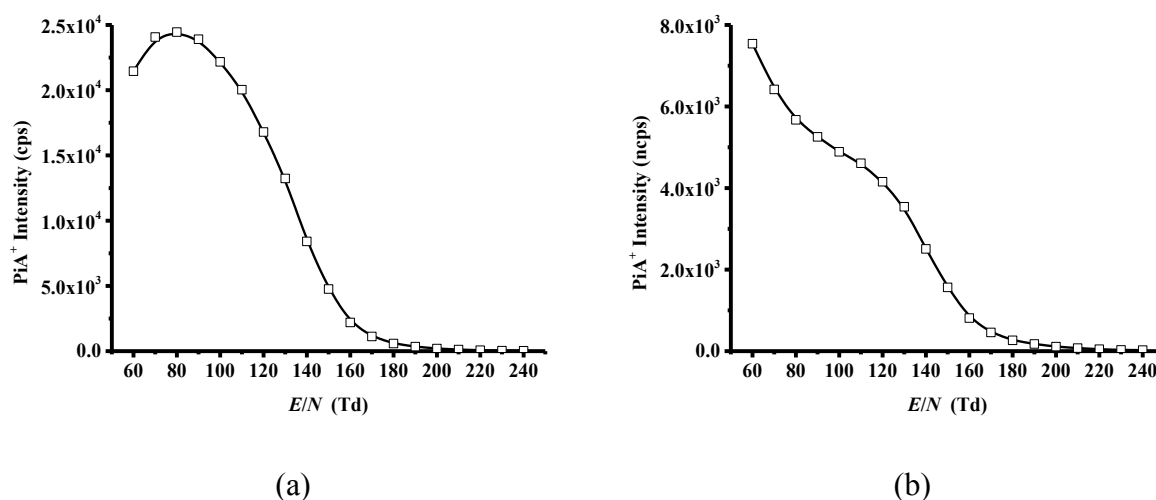


Figure 4.6. The variation in ion signal intensities for (a) the unnormalised PiA^+ and (b) the normalised (10^6 cps of O_2^+) PiA^+ signal intensities resulting from the reaction of O_2^+ with picric acid as a function of E/N in a "dry" reaction chamber for which high purity N_2 was used as the carrier gas.

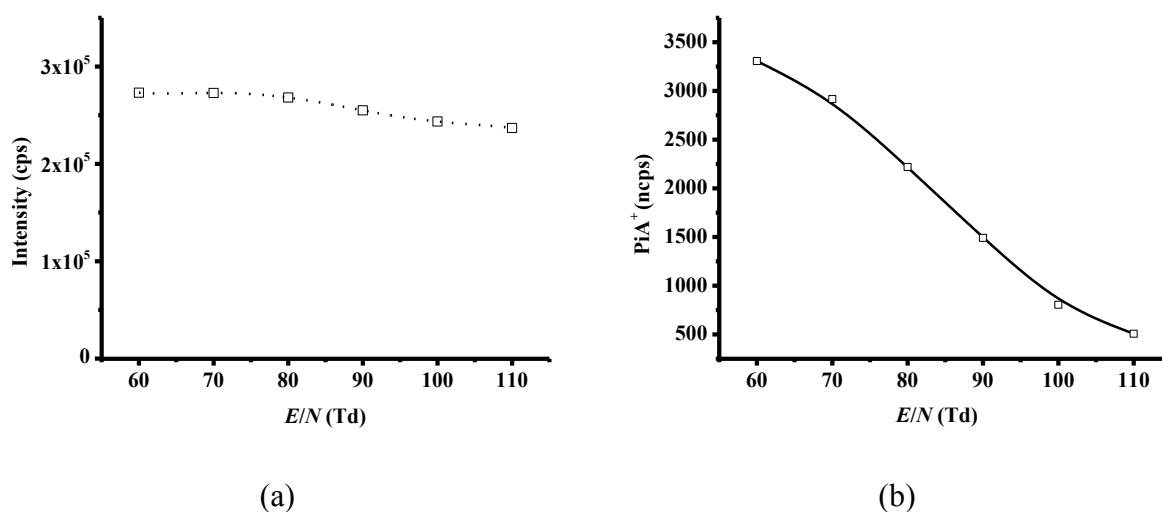


Figure 4.7. The variation in (a) O_2^+ ion signal intensity as a function of E/N and (b) the normalised (10^6 cps of O_2^+) PiA^+ as a function of E/N in a dry reaction chamber for which high purity He was used as the carrier gas.

4.4.2.3. NO^+ Measurements

The NO^+ reactions with picric acid were studied to see whether they could be used for improving the selectivity. Figure 4.8 provides a summary of the results for the reactions of

NO^+ with picric acid. As found for the production of O_2^+ reagent ions, owing to the lack of association with water we can be operate the drift tube at lower E/N values than is possible when using water vapour in the ion source. Figure 4.8(a) gives the N^{16}O^+ reagent ion signal intensity (calculated using the $^{15}\text{N}^{16}\text{O}^+$ signal intensity) as a function of E/N over the range of 60-180 Td.

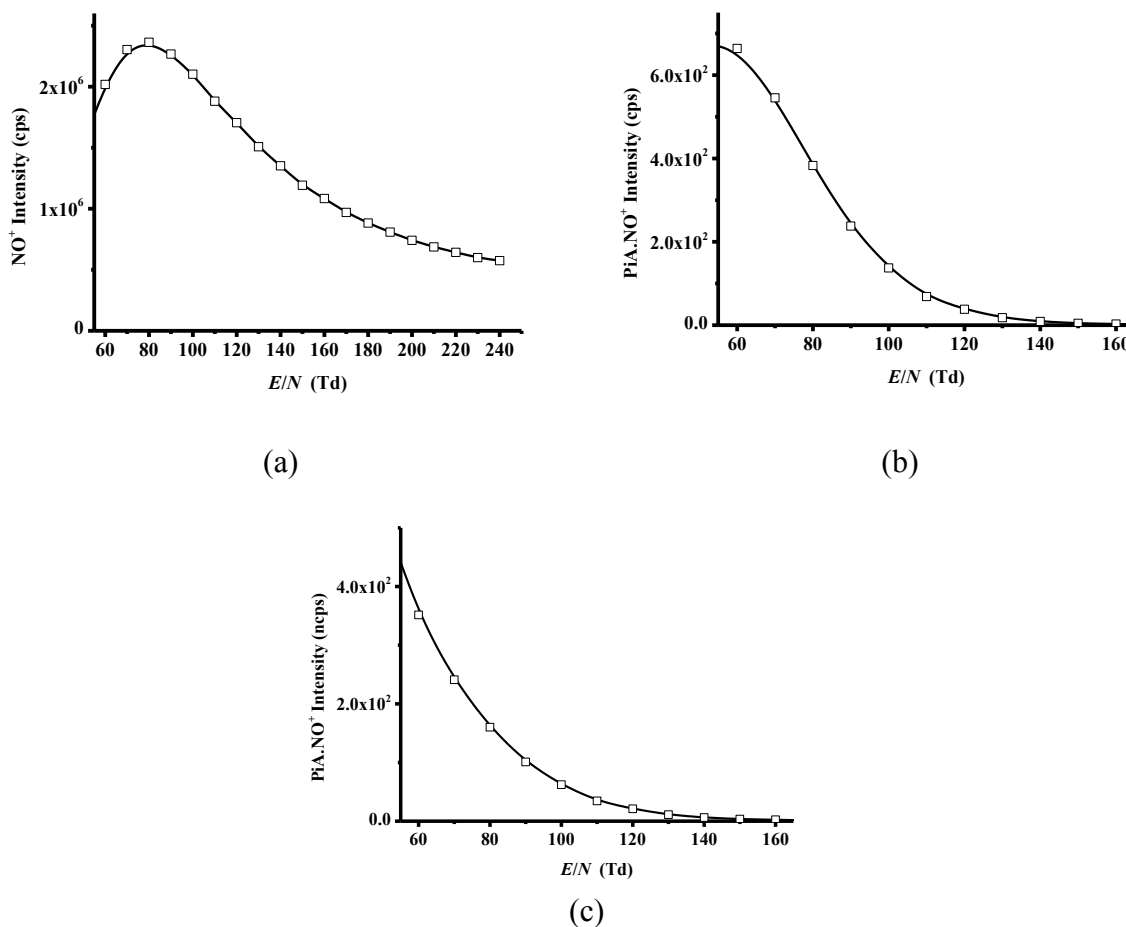


Figure 4.8. The variation in ion signal intensities for (a) NO^+ , (b) unnormalised $\text{PiA} \cdot \text{NO}^+$ and (c) normalised (10^6 cps of H_3O^+) $\text{PiA} \cdot \text{NO}^+$ as a function of E/N recorded using a PTR-TOF 8000. Purified laboratory air was used as the carrier gas.

Given that the ionisation potential of picric acid is greater than the recombination energy of NO^+ (9.6 eV); NO^+ reagent ions cannot react with picric acid via charge transfer processes and only adduct formation is observed ($\text{PiA} \cdot \text{NO}^+$). DFT calculations show that this is a strong complex ($\Delta G = -81 \text{ kJ mol}^{-1}$). However, it only observed to be readily formed at

low E/N values, as illustrated in figures 4.8(b) and (c), which give the unnormalised and normalised (to 10^6 NO^+ reagent ions per second) signal intensities, respectively, as a function of E/N .

4.4.2.4. Kr^+ Measurements

Figure 4.9 (a) shows the total Kr^+ reagent ion signal intensity (cps) as a function of E/N over the range 60-110 Td. To determine the signal intensity, only the signal intensity at $^{78}\text{Kr}^+$ is used to determine the overall Kr^+ counts, owing to detection saturation at the m/z values corresponding to the more dominant isotopes. From figure 4.9 (a) it can be seen that the reagent ion intensity increases with increasing E/N , starting at approximately 1.3×10^6 cps at 30 Td going up to about 3.3×10^6 cps at 110 Td. Given that Kr^+ is highly reactive, it is possible that this increase in reagent signal is associated with a reduced reaction time as E/N increases.

Kr^+ has a recombination energy of 14.0 eV, which is much higher than that for O_2^+ . Therefore, we may expect that in addition to non-dissociative charge transfer, dissociative charge transfer to picric acid could occur. In agreement with this we have observed two product ions. One is PiA^+ and the other is NO_2^+ , with branching percentages of approximately 60% and 40%, respectively, across the range of E/N values investigated, i.e. there is no major E/N dependence (at 110 Td the branching ratio of NO_2^+ has increased to about 50%). Figures 4.9 (b) and (c) gives raw and normalised signal intensities, respectively, for PiA^+ as a function E/N . In this case the PiA^+ follows a normal behaviour of decreasing intensity with increasing E/N .

There is one final point with the Kr^+ reactions. It can be seen from figure 4.9 (c) that the maximum normalised counts per second of the product ion are significantly less than the maximum value obtained for the reactions H_3O^+ or O_2^+ , although identical concentrations of picric acid in the drift tube were used for all of the experiments. This implies that the reaction efficiency is less than unity. This is entirely possible. Although, exergonic proton transfer reactions generally occur with unit efficiency,²¹ the same cannot be said for exergonic charge transfer processes. Factors other than energetics, such as an energy resonance connecting the neutral molecule to an ionic state at the recombination energy of the reagent ion, play a role in determining the efficiency of simple charge transfer reactions.²²

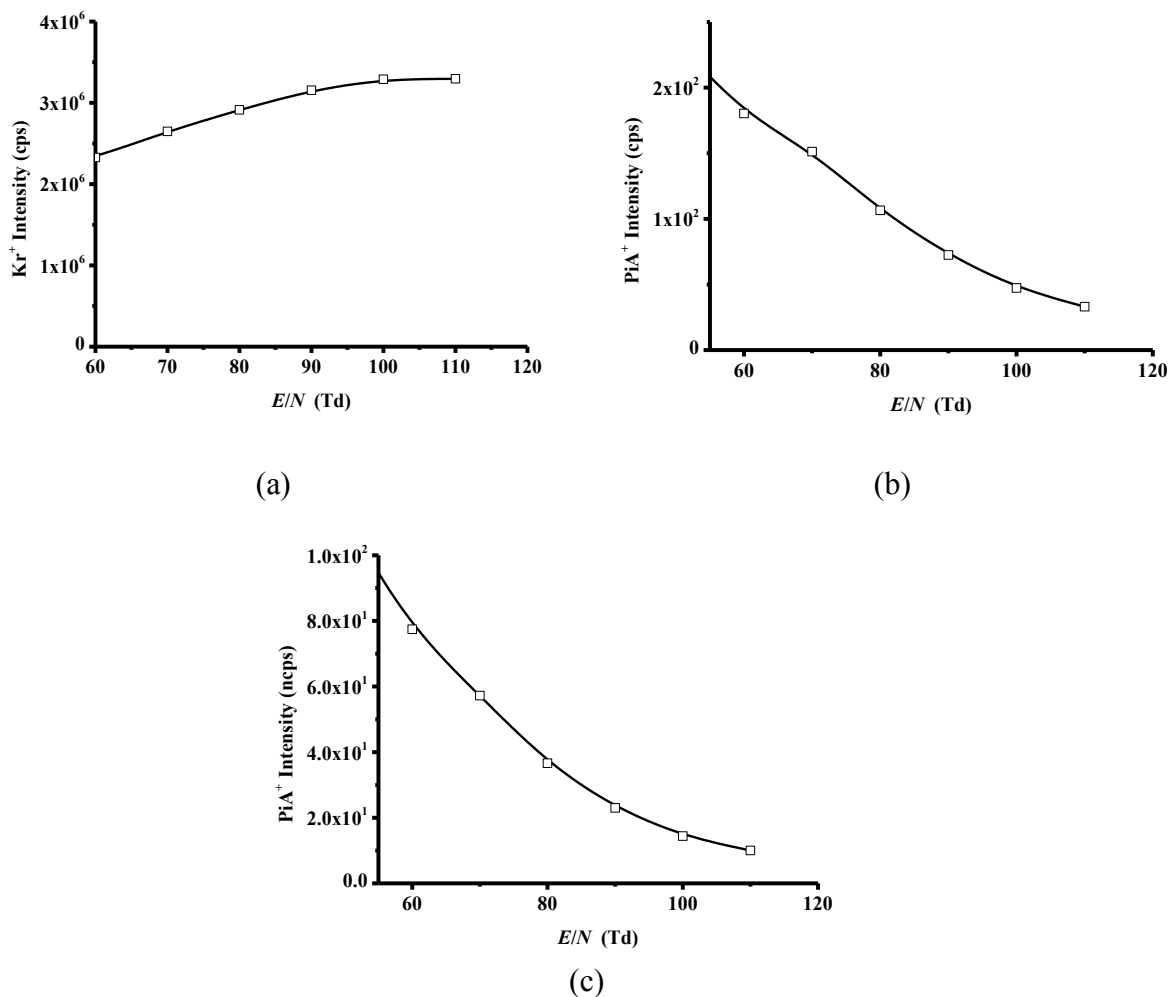


Figure 4.9. The variation in ion signal intensities for (a) Kr^+ , (b) unnormalised PiA^+ and (c) normalised (10^6 cps of Kr^+) PiA^+ as a function of E/N recorded using a PTR-TOF 8000 in an extremely “dry” reaction chamber. High purity He was used as the carrier gas.

4.5. Concluding remarks

Using the recently developed switchable reagent ion source PTR-TOF 8000, we have investigated the reactions of H_3O^+ , NO^+ , O_2^+ and Kr^+ with picric acid (PiA) over a range of E/N values. The H_3O^+ investigation was undertaken to see if PiA mirrored our earlier work with TNT and TNB. The other reagent ions were investigated to see if the reaction processes leads to product ions which could be used to improve selectivity. The reaction processes are non-dissociative proton transfer for reaction with H_3O^+ , non-dissociative charge transfer for

reaction with O_2^+ , non-dissociative and dissociative charge transfer for reaction with Kr^+ and adduct formation for reaction with NO^+ . However, the actual final product ion in a humid reaction system when either $PiAH^+$ or PiA^+ are the product ions has been found to be highly dependent on the E/N used. Once $PiAH^+ \cdot H_2O$ and $PiA^+ \cdot H_2O$ are able to be formed, we propose that secondary ion reactions with water lead to a product ion that no longer contains picric acid. As found for protonated TNT and TNB, the behaviour of the intensity of protonated picric acid parent as E/N is changed by rapidly changing the drift tube voltage has the potential for use as a powerful discriminatory analytical probe to detect picric acid. This drift tube voltage bias, coupled with switching from water to oxygen chemistry, which can be done within seconds, followed again by changing E/N provides an analytical procedure for the identification of picric acid with a high level of confidence in the assignment.

For PTR-MS to be useful in security areas special procedures need to be adopted to achieve a high level of confidence in the assignment of a compound, which is not possible just based on a nominal m/z value. Rapid switching of reagent ions is one way to improve selectivity. This alters the ion chemistry and hence the m/z of the product ion(s) detected. The combination of an unusual E/N dependence on ion signal intensity, which in the case of picric acid occurs for PiA^+ and $PiAH^+$ product ions, and rapid switching reagent ions (as demonstrated by Sulzer *et al.*),⁵ results in a powerful and multidimensional analytical tool for the screening of picric acid in complex chemical environments providing higher confidence levels in assignment than possible when simply relying on a nominal m/z value.

4.6. Acknowledgements

We acknowledge the support of the PIMMS Initial Training Network which in turn is supported by the European Commission's 7th Framework Programme under Grant Agreement Number 287382.

4.7. References

1. Mayhew, C. A.; Sulzer, P.; Petersson, F.; Haidacher, S.; Jordan, A.; Märk, L.; Watts, P.; Märk, T. D., Applications of proton transfer reaction time-of-flight mass spectrometry for

- the sensitive and rapid real-time detection of solid high explosives. *International Journal of Mass Spectrometry* **2010**, *289* (1), 58-63.
- Jürschik, S.; Sulzer, P.; Petersson, F.; Mayhew, C. A.; Jordan, A.; Agarwal, B.; Haidacher, S.; Seehauser, H.; Becker, K.; Märk, T. D., Proton transfer reaction mass spectrometry for the sensitive and rapid real-time detection of solid high explosives in air and water. *Anal Bioanal Chem* **2010**, *398* (7-8), 2813-2820.
 - Sulzer, P.; Petersson, F.; Agarwal, B.; Becker, K. H.; Jürschik, S.; Märk, T. D.; Perry, D.; Watts, P.; Mayhew, C. A., Proton Transfer Reaction Mass Spectrometry and the Unambiguous Real-Time Detection of 2,4,6 Trinitrotoluene. *Analytical Chemistry* **2012**, *84* (9), 4161-4166P.
 - Sulzer, P.; Jürschik, S.; Agarwal, B.; Kassebacher, T.; Hartungen, E.; Edtbauer, A.; Petersson, F.; Warmer, J.; Holl, G.; Perry, D.; Mayhew, C.; Märk, T., Designer Drugs and Trace Explosives Detection with the Help of Very Recent Advancements in Proton-Transfer-Reaction Mass Spectrometry (PTR-MS). In *Future Security*, Aschenbruck, N.; Martini, P.; Meier, M.; Tölle, J., Eds. Springer Berlin Heidelberg: 2012; Vol. 318, pp 366-375.
 - Sulzer, P.; Agarwal, B.; Jürschik, S.; Lanza, M.; Jordan, A.; Hartungen, E.; Hanel, G.; Märk, L.; Märk, T. D.; González-Méndez, R.; Watts, P.; Mayhew, C. A., Applications of switching reagent ions in proton transfer reaction mass spectrometric instruments for the improved selectivity of explosive compounds. *International Journal of Mass Spectrometry* **2013**, *354–355* (0), 123-128.
 - Agarwal, B.; Petersson, F.; Jürschik, S.; Sulzer, P.; Jordan, A.; Märk, T. D.; Watts, P.; Mayhew, C. A., Use of proton transfer reaction time-of-flight mass spectrometry for the analytical detection of illicit and controlled prescription drugs at room temperature via direct headspace sampling. *Anal Bioanal Chem* **2011**, *400* (8), 2631-2639.
 - Jürschik, S.; Agarwal, B.; Kassebacher, T.; Sulzer, P.; Mayhew, C. A.; Märk, T. D., Rapid and facile detection of four date rape drugs in different beverages utilizing proton transfer reaction mass spectrometry (PTR-MS). *Journal of Mass Spectrometry* **2012**, *47* (9), 1092-1097.
 - Lanza, M.; Acton, W. J.; Jürschik, S.; Sulzer, P.; Breiev, K.; Jordan, A.; Hartungen, E.; Hanel, G.; Märk, L.; Mayhew, C. A.; Märk, T. D., Distinguishing two isomeric mephedrone substitutes with selective reagent ionisation mass spectrometry (SRI-MS).

- Journal of Mass Spectrometry* **2013**, *48* (9), 1015-1018.
9. Acton, W. J.; Lanza, M.; Agarwal, B.; Jürschik, S.; Sulzer, P.; Breiev, K.; Jordan, A.; Hartungen, E.; Hanel, G.; Märk, L.; Mayhew, C. A.; Märk, T. D., Headspace analysis of new psychoactive substances using a Selective Reagent Ionisation-Time of Flight-Mass Spectrometer. *International Journal of Mass Spectrometry* **2014**, *360* (0), 28-38.
 10. Petersson, F.; Sulzer, P.; Mayhew, C. A.; Watts, P.; Jordan, A.; Märk, L.; Märk, T. D., Real-time trace detection and identification of chemical warfare agent simulants using recent advances in proton transfer reaction time-of-flight mass spectrometry. *Rapid Communications in Mass Spectrometry* **2009**, *23* (23), 3875-3880.
 11. Kassebacher, T.; Sulzer, P.; Jürschik, S.; Hartungen, E.; Jordan, A.; Edtbauer, A.; Feil, S.; Hanel, G.; Jaksch, S.; Märk, L.; Mayhew, C. A.; Märk, T. D., Investigations of chemical warfare agents and toxic industrial compounds with proton-transfer-reaction mass spectrometry for a real-time threat monitoring scenario. *Rapid Communications in Mass Spectrometry* **2013**, *27* (2), 325-332.
 12. DFT calculations were performed using the Gaussian 09 programme with the GaussView interface.(Gaussian 09, Revision A.02, M. J. Frisch, G. W. Trucks, H. B. Schlegel, G. E. Scuseria, M. A. Robb, J. R. Cheeseman, G. Scalmani, V. Barone, B. Mennucci, G. A. Petersson, H. Nakatsuji, M. Caricato, X. Li, H. P. Hratchian, A. F. Izmaylov, J. Bloino, G. Zheng, J. L. Sonnenberg, M. Hada, M. Ehara, K. Toyota, R. Fukuda, J. Hasegawa, M. Ishida, T. Nakajima, Y. Honda, O. Kitao, H. Nakai, T. Vreven, J. A. Montgomery, Jr., J. E. Peralta, F. Ogliaro, M. Bearpark, J. J. Heyd, E. Brothers, K. N. Kudin, V. N. Staroverov, R. Kobayashi, J. Normand, K. Raghavachari, A. Rendell, J. C. Burant, S. S. Iyengar, J. Tomasi, M. Cossi, N. Rega, J. M. Millam, M. Klene, J. E. Knox, J. B. Cross, V. Bakken, C. Adamo, J. Jaramillo, R. Gomperts, R. E. Stratmann, O. Yazyev, A. J. Austin, R. Cammi, C. Pomelli, J. W. Ochterski, R. L. Martin, K. Morokuma, V. G. Zakrzewski, G. A. Voth, P. Salvador, J. J. Dannenberg, S. Dapprich, A. D. Daniels, O. Farkas, J. B. Foresman, J. V. Ortiz, J. Cioslowski, and D. J. Fox, Gaussian, Inc., Wallingford CT, 2009.)
 13. <http://www.ionicon.com> (last accessed January 2014).
 14. Jordan, A.; Haidacher, S.; Hanel, G.; Hartungen, E.; Märk, L.; Seehauser, H.; Schottkowsky, R.; Sulzer, P.; Märk, T. D., A high resolution and high sensitivity proton-

- transfer-reaction time-of-flight mass spectrometer (PTR-TOF-MS). *International Journal of Mass Spectrometry* **2009**, *286* (2–3), 122-128.
15. Sulzer, P.; Edtbauer, A.; Hartungen, E.; Jürschik, S.; Jordan, A.; Hanel, G.; Feil, S.; Jaksch, S.; Märk, L.; Märk, T. D., From conventional proton-transfer-reaction mass spectrometry (PTR-MS) to universal trace gas analysis. *International Journal of Mass Spectrometry* **2012**, *321–322*, 66-70.
 16. Hunter E. P., Lias, S. G., “Proton Affinity Evaluation” in NIST Chemistry WebBook, NIST Standard Reference Database Number 69, Eds. Linstrom P. J., Mallard, W. G., National Institute of Standards and Technology, Gaithersburg MD, 20899, <http://webbook.nist.gov>.
 17. Christian, T. J.; Kleiss, B.; Yokelson, R. J.; Holzinger, R.; Crutzen, P.; Hao, W. M.; Shirai, T.; Blake, D. R., Comprehensive laboratory measurements of biomass-burning emissions: 2. First intercomparison of open-path FTIR, PTR-MS, and GC-MS/FID/ECD. *Journal of Geophysical Research: Atmospheres* **2004**, *109* (D2).
 18. Karl, T.; Christian, T. J.; Yokelson, R. J.; Artaxo, P.; Hao, W. M.; Guenther, A., The Tropical Forest and Fire Emissions Experiment: method evaluation of volatile organic compound emissions measured by PTR-MS, FTIR, and GC from tropical biomass burning. *Atmospheric Chemistry and Physics* **2007**, *7* (22), 5883-5897.
 19. Knighton, W. B.; Fortner, E. C.; Midey, A. J.; Viggiano, A. A.; Herndon, S. C.; Wood, E. C.; Kolb, C. E., HCN detection with a proton transfer reaction mass spectrometer. *International Journal of Mass Spectrometry* **2009**, *283* (1–3), 112-121.
 20. Schramm, E.; Mühlberger, F.; Mitschke, S.; Reichardt, G.; Schulte-Ladbeck, R.; Pütz, M.; Zimmermann, R., Determination of the ionization potentials of security-relevant substances with single photon ionization mass spectrometry using synchrotron radiation. *Applied spectroscopy* **2008**, *62* (2), 238-247.
 21. Bohme, D. K.; Mackay, G. I.; Schiff, H. I., Determination of proton affinities from the kinetics of proton transfer reactions. VII. The proton affinities of O₂, H₂, Kr, O, N₂, Xe, CO₂, CH₄, N₂O, and CO. *The Journal of Chemical Physics* **1980**, *73* (10), 4976-4986.
 22. Jarvis, G.; Kennedy, R.; Mayhew, C.; Tuckett, R., Charge transfer from neutral perfluorocarbons to various cations: long-range versus short-range reaction mechanisms. *International Journal of Mass Spectrometry* **2000**, *202* (1), 323-343.

CHAPTER 5

DEVELOPMENT AND USE OF A THERMAL DESORPTION UNIT AND PROTON TRANSFER REACTION-MASS SPECTROMETRY FOR TRACE EXPLOSIVE DETECTION: DETERMINATION OF THE INSTRUMENTAL LIMITS OF DETECTION AND AN INVESTIGATION OF MEMORY EFFECTS

This chapter is a reformatted copy of my published article:

International Journal of Mass Spectrometry 385 (2015), 13–18.

Ramón González-Méndez,¹ D. Fraser Reich,² Stephen J. Mullock,² Clive A. Corlett,² and
Chris A. Mayhew^{1*}

1. School of Physics and Astronomy, University of Birmingham, Edgbaston, Birmingham, B15 2TT, UK
2. KORE Technology Limited, Cambridgeshire Business Park, Ely, Cambridgeshire CB7 4EA, UK

* Corresponding author: Tel.:+441214144729; fax:+441214144577. E-mail address: c.mayhew@bham.ac.uk

Declaration of contribution

My contribution to the study described in this Chapter was conceiving and designing the experiments, performing the experiments, interpreting the data and elaborating the manuscript jointly with the other co-authors.

5.1. Abstract

A novel thermal desorption unit (TDU) has been developed and specifically designed for the detection of trace quantities of explosives using a proton transfer reaction mass spectrometer (PTR-MS). For the first time details on recovery times and instrumental limits of detection for the screening of explosives with this TDU/PTR-MS system are reported. We demonstrate that traces (nanograms or less) of explosives deposited on swabs are desorbed within less than a second upon insertion into the TDU. For a short period of time (seconds) a concentration “pulse” of an explosive enters the drift (reaction) tube of the PTR-MS. This temporal concentration pulse of material is monitored in real-time by recoding the product ion intensities for a given explosive as a function of time. By changing the reduced electric field in the drift tube region of the PTR-MS, we demonstrate how selectivity can be improved. This study demonstrates that the TDU/PTR-MS instrument meets security application criteria in terms of sensitivity, selectivity and recovery times.

5.2. Introduction

Highly selective and sensitive screening for traces of explosives in complex chemical environments is important in many areas of security. A number of analytical techniques are available for use in the detection of explosives. These are highlighted and compared in a recent review,¹ and includes ion mobility spectrometry (IMS), atmospheric pressure chemical ionisation mass spectrometry and desorption electrospray ionisation-mass spectrometry. IMS is the most commonly used technique found in security areas, owing to its compactness and ease of operation. Its use has been critically reviewed by Ewing et al.² A limitation of IMS is its reliance on the temporal separation of ions in a high-pressure drift tube for its selectivity. In comparison to IMS, the technique known as proton transfer reaction mass spectrometry (PTR-MS) has a better selectivity owing to the use of a mass spectrometer. PTR-MS has been shown to be a useful platform technology capable of detecting a range of explosives,³⁻⁷ (in addition to other threat agents).⁸⁻¹¹ Identification of explosives with a high level of confidence minimises false positives and is therefore beneficial for applications in security areas. However, for PTR-MS to be adopted as an analytical tool, it is not sufficient to be able to detect explosives present in trace quantities with high levels of confidence, it is also necessary to do so with limited memory effects. Crucially, the whole process of sampling, analysis and recovery needs to be completed within tens of seconds if it is to be acceptable to security personnel and the travelling public. Until now that has not been achieved with PTR-MS.⁴

The detection of many explosives is challenging because of their low vapour pressures.¹² Without any sample preparation, low vapour pressure makes it very difficult to introduce sufficient vapour concentrations of an explosive into the reaction region (the drift tube) of a PTR-MS to make it detectable. An approach to remedy this problem was adopted in this investigation. For this we have adopted a similar technique routinely used in IMS, namely a pre-concentration technique followed by thermal desorption. An earlier attempt of pre-concentration and thermal desorption of explosives with PTR-MS resulted in limited success.⁴ That study used a suction device that drew air through a fine wire mesh to trap particulates of an explosive. This mesh was then ohmically heated to evaporate that trapped material. A simple heated inlet tube placed close to the wire mesh carried some of the desorbed material into the drift tube reactor. Although this successfully resulted in much higher characteristic ion signals than had been previously obtained it suffered from a long recovery times, with

memory effects being observed of tens of minutes. No quantification in terms of the instrumental limits of detection (LoD) was possible in that previous study.

In order to overcome problems associated with memory effects and to determine instrumental LoD for the detection of trace explosives, we have developed a novel variable temperature thermal desorption unit (TDU) for use with PTR-MS. Recovery times and instrumental limits of detection (LoD) for the combined TDU/PTR-MS system are reported for a number of explosive compounds. In order of increasing molecular mass, these are ethylene glycol dinitrate (EGDN, m/z 152, $C_2H_4N_2O_6$), 1,3-dinitrobenzene (DNB, m/z 168, $C_6H_4N_2O_4$), 3,4-dinitrotoluene (DNT, m/z 182, $C_7H_6N_2O_4$), hexamethylene triperoxide diamine (HMTD, m/z 208, $C_6H_{12}N_2O_6$), 1,3,5-trinitrobenzene (TNB, m/z 213, $C_6H_3N_3O_6$), 1,3,5-trinitroperhydro-1,3,5-triazine (RDX, m/z 222, $C_3H_6N_6O_6$), nitroglycerin (NG, m/z 227, $C_3H_5N_3O_9$), 2,4,6-trinitrotoluene (TNT, m/z 227, $C_7H_5N_3O_6$), and pentaerythritol tetranitrate (PETN, m/z 316, $C_5H_8N_4O_{12}$). The selection of explosives reported have been chosen because they cover a wide range of vapour pressures, ranging from the 4.9×10^{-9} mbar (RDX) to 0.1 mbar (EGDN) at 25 °C.¹² Mass spectrometric m/z analysis of the product ions provides good selectivity. However, this paper illustrates how this selectivity can be enhanced by changing operational parameters in the drift (reaction) region.

5.3. Experimental Details and Methods

5.3.1 Proton Transfer Reaction Mass Spectrometry (PTR-MS)

A first generation KORE Technology Ltd. Proton Transfer Reaction - Time of Flight - Mass Spectrometer (PTR-ToF-MS), manufactured in 2006, was used in this study. Details on this instrument have already been published.¹³⁻¹⁵ and hence only a brief description is provided here. Using a needle valve, water vapour is introduced into a hollow cathode discharge where, after ionisation via electron impact and subsequent ion-molecule processes, the terminal reagent ions are H_3O^+ .¹⁶ These ions are transferred from the ion source into the drift tube (reaction region) of the PTR-ToF-MS. H_3O^+ ions donate their protons to compounds (M) present in the drift tube whose proton affinities are greater than that of water ($PA(H_2O) = 691 \text{ kJ mol}^{-1}$). This process can be non-dissociative (resulting in the protonated parent molecule MH^+) and/or dissociative. Dissociative proton transfer results in product ions which,

depending on their m/z values, may or may not be useful for the identification of a compound with a high level of confidence. Complications other than dissociation arise because it is not only H_3O^+ ions that are produced in the ion source region. Back streaming of air from the drift tube into the ion source results in the production of other “terminal” (impurity) ions. These cannot react with water because their recombination energies (RE) are less than the ionisation energy of water (12.6 eV), and include NO^+ (RE = 9.3 eV), O_2^+ (RE = 12.1 eV) and NO_2^+ (RE = 9.6 eV), respectively. Operating conditions are such that the total impurity ion signal level is typically less than 3% of the H_3O^+ intensity. Therefore usually these ions are of little consequence. However, we have found that NO_2^+ is a product ion from the reaction of H_3O^+ with explosives that contains a nitrate group, i.e. EGDN, NG and PETN, and with RDX. That must be taken into account when calculating the LoD using NO_2^+ .

5.3.2 Thermal Desorption Unit (TDU)

The TDU designed and developed for use with PTR-MS is better described as a swab crusher, which makes it unique. Unlike some other TDUs where often a poor seal is made between the inlet and outlet carrier gas flows, this design features a high-force annular “anvil” that compresses the PTFE in a ring around the edge of a swab. A schematic representation of this new TDU and “anvil” system is provided in figure 5.1. The force is sufficiently high to plastically deform the PTFE and convert it into a gas tight circular seal around the rim of the swab, thereby improving the transfer of material from the swab into the inlet line. The TDU is connected to a short heated stainless steel inlet system, the surfaces of which are passivated (SilcoNert® 2000 treated) to minimise adsorption, leading to the reaction chamber. Once a seal is created, a carrier gas (in this study laboratory air) is heated to the temperature of the TDU before it flows through a series of holes in a heated metal plate. This heated air then passes through the swab and into the inlet system driving any desorbed material through to the drift tube. The actual temporal duration of a “pulse” of concentration of a compound will depend on many factors including the compound’s volatility and chemical nature, the temperature of the inlet system, the carrier gas flow rate and the temperature of the inlet lines. The inlet line from the TDU to the drift tube of the PTR-MS was kept as short as possible and heated during measurements to further minimise losses onto the surfaces.

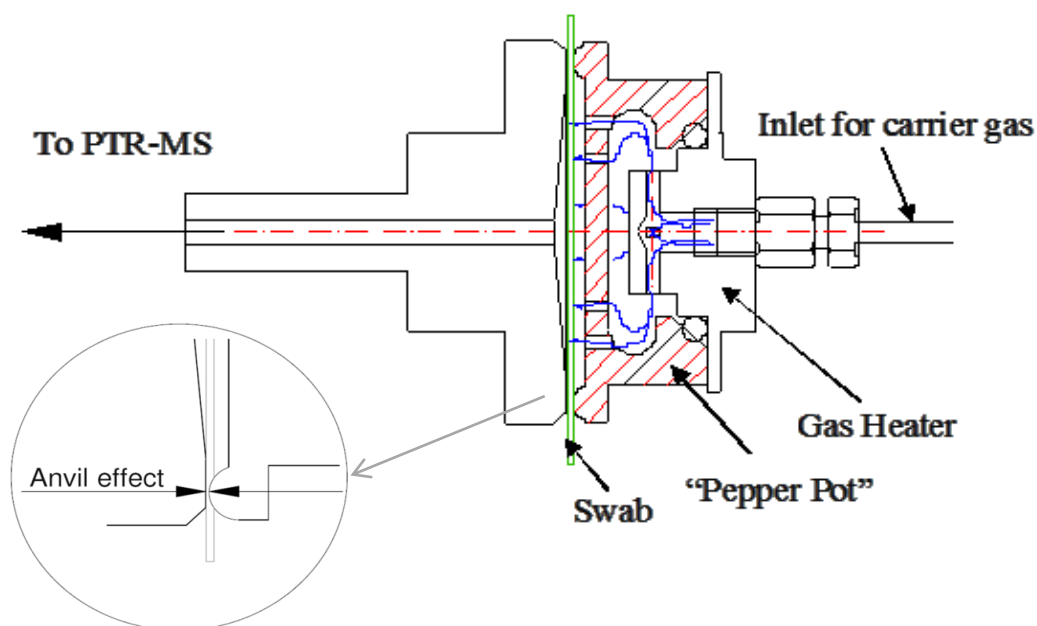


Figure 5.1. Schematic cross-section of the KORE Technology Ltd. thermal desorption unit. The laboratory air is heated as it travels through the heating block to the temperature of the block. This heated air is then dispersed across the surface area of the swab via a series of equally spaced holes (the pepper pot) directed towards the swab. The passage of the air heats the swab resulting in thermal desorption of material placed on it. This material is carried through by the gas flow to the drift tube reactor.

5.3.3 Operational Parameters

All measurements were taken under the same operational conditions, namely the TDU, inlet tubing and drift tube were maintained at temperatures of 140 °C, 150 °C and 100 °C (maximum possible with the current drift tube heating system), respectively. The drift tube pressure was set at 1.1 mbar. The only variable was the operating drift tube voltage, which was adjusted to provide an appropriate reduced electric field which resulted in the best sensitivity for each explosive investigated. (The reduced electric field value is the ratio of the electric field strength (E) and the gas number density (N), and is given in units of Townsend (Td) ($1 \text{ Td} = 10^{-17} \text{ V cm}^2$).

5.3.4 Explosive Compounds

Single component standards for the explosives used in this study were purchased from AccuStandard Inc., New Haven, CT. Typically, these standards contained 1 mg of an explosive placed in 1 ml of either acetonitrile (AcN) or a mix of AcN and methanol (MeOH). RDX and TNT came in an AcN: MeOH (1:1) mix. PETN and DNT were delivered in MeOH. EGDN and HMTD (both at 0.1 mg) were supplied in AcN. NG (0.1 mg) came supplied in a 1 ml solution of ethanol. However, O_2^+ reacts with ethanol to form an ion at m/z 46 via dissociative charge transfer, which complicates the analysis. Therefore, we purchased a sample of NG (100 μ g) dissolved in AcN (1 ml) from Dr. Ehrenstorfer GmbH, Ausburg, Germany. The results for NG presented in this paper are all taken using that sample. Samples were diluted in the appropriate solvent(s) (HPLC grade) to provide the required quantity of an explosive. Typically 1 μ l of a solvent containing the required mass of an explosive was spotted onto a PTFE swab of diameter 3.5 cm. This swab came prepared from the manufacturer (ThermoFisher Scientific) and was mounted on rectangular cardboard for easy insertion into our TDU.

5.3.5 Determining Instrumental Limits of Detection

The instrumental limit of detection (LoD) for a given m/z is taken to be the situation when the signal intensity in that channel exceeds the background noise level by factor of three. The background signal will be m/z dependent, because of ion signals resulting from various chemical impurities in different concentrations present in the instrument and/or as a result of unreactive ions coming from the hollow cathode ion source. To calculate the LoD for a compound M we have used the expression:

$$\text{LoD} = \frac{3\sigma_{\text{Background}}}{\epsilon_M},$$

where $\sigma_{\text{Background}}$ is the standard deviation of a blank swab and ϵ_M is the instrument's sensitivity for compound M in counts per second (determined by integrating the ion signal over the temporal peak) per ng of explosive placed on a swab. To test for linearity, the amount of explosive deposited on a swab was varied from as low as 0.06 ng up to 1000 ng (the actual range depended on the explosive being investigated.). Precision of the technique was evaluated in terms of repeatability and reproducibility. Repeatability determinations involved measurements of 5 replicates consecutively, while reproducibility determinations were 5

replicates over 5 different days, with each replicate being the mean of three measurements. We used five times the limit of detection for each of the compounds to evaluate these parameters.

5.4. Results

5.4.1 Product ions

Table 5.1 provides a list of product ions detected at a given E/N for each explosive. For the majority of the explosives investigated the protonated parent was detected (EGDN, DNB, DNT, HMTD, NG, TNB, TNT and PETN). However, in addition to the protonated parent for the nitrate esters (EGDN, NG and PETN) a more dominant product ion at m/z 46 (NO_2^+) was also observed. RDX was the only explosive compound in this study for which no protonated parent signal was observed, instead the product ions NO_2^+ , $\text{CH}_3\text{N}_2\text{O}_2^+$ (m/z 75 (dominant at the E/N used)) and ($[\text{RDX-HONO}]\text{H}^+$) (m/z 176) were detected.

5.4.2 Instrumental Limits of Detection

Table 5.1 also presents the instrumental LoD values. These have been obtained from calibration plots of the type shown in figure 5.2, which is for TNT. Large variations in LoD are found. The lowest LoD obtained is for DNT at 0.07 ± 0.01 ng. This is followed by DNB (0.13 ± 0.02 ng), TNB (0.14 ± 0.02 ng) and TNT (0.15 ± 0.01 ng). For RDX, a LoD of 6 ± 2 ng is obtained using the product ion at m/z 75. The calculated LoD for NG is found to be 2.0 ± 0.2 ng when using the protonated parent signal at m/z 228, but somewhat higher when using the fragment ion signal at m/z 46 (12 ± 2 ng).

Table 5.1. Calculated limits of detection (LoD) for the explosives investigated in this study presented in order of increasing molar mass. The product ions resulting from the reaction of H_3O^+ with a given explosive and their corresponding nominal m/z values are presented at given E/N values. The E/N value used for a given explosive was found to provide the best sensitivity. The linear dynamic range in nanograms (ng) is given for each explosive and the corresponding regression coefficient (r^2) provided. The precision of the method was evaluated by the determination of the repeatability and reproducibility in terms of relative standard deviation (RSD).

Explosive	Product Ion, nominal m/z	E/N (Td)	Linear dynamic range (ng)	r^2	LoD (ng)	Repeatability (RSD %) (n=5)	Reproducibility (RSD %) (n=5)
EGDN	EGDNH^+ , 153	110	10-300	0.9982	4.4 ± 0.5	13.8	19.0
	NO_2^+ , 46			0.9910	7.2 ± 0.6	9.2	16.1
1,3-DNB	DNBH^+ , 169	170	0.5-25	0.9981	0.13 ± 0.02	2.9	7.7
3,4-DNT	DNTH^+ , 183	140	0.3-25	0.9982	0.07 ± 0.01	5.0	3.7
HMTD	HMTDH^+ , 209	90	1-500	0.9996	0.74 ± 0.08	3.8	5.2
1,3,5-TNB	TNBH^+ , 214	210	0.2-25	0.9980	0.14 ± 0.02	3.9	6.5
RDX	$[\text{RDX-HONO}]\text{H}^+$, 176	110	50-1000	0.8938	36 ± 6	0.5	17.7
	$\text{CH}_3\text{N}_2\text{O}_2^+$, 75			0.9974	6 ± 2	2.8	23.1
	NO_2^+ , 46			0.9993	14.9 ± 0.8	3.1	7.1
NG	NGH^+ , 228	80	15-500	0.9763	2.0 ± 0.2	9.6	10.8
	NO_2^+ , 46			0.9849	12 ± 2	6.6	6.5
2,4,6-TNT	TNTH^+ , 228	180	0.25-50	0.9974	0.15 ± 0.01	1.2	2.9
PETN	PETNH^+ , 317	110	15-500	0.9996	0.6 ± 0.1	2.0	3.9
	NO_2^+ , 46			0.9953	14 ± 1	12.4	16.4

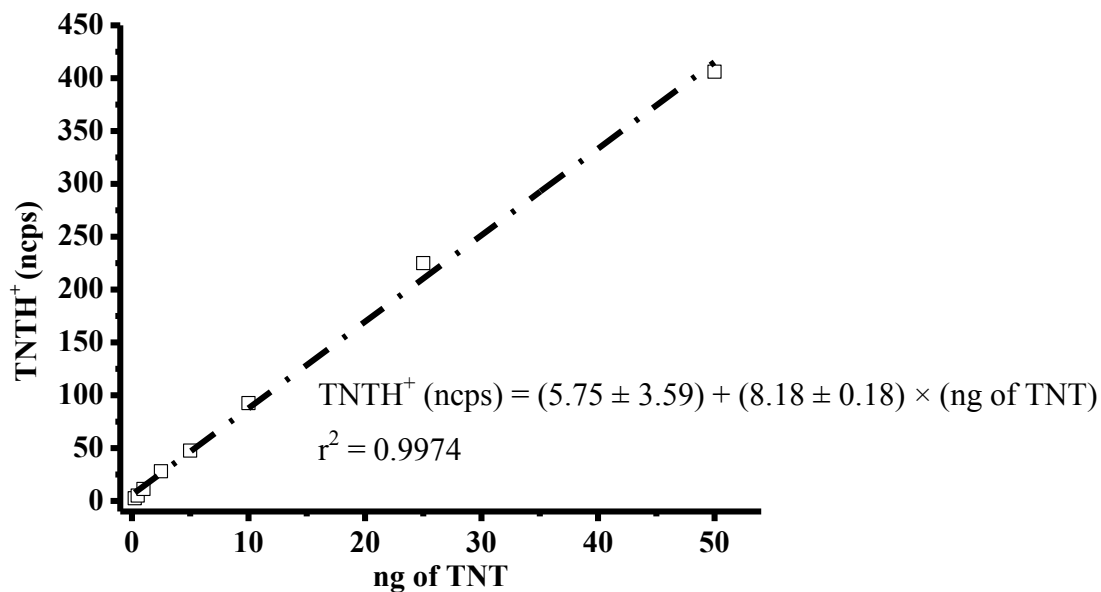


Figure 5.2. Illustrative calibration curve. This shows the normalised ion counts (relative to 10^6 H_3O^+ counts per second) of protonated TNT (m/z 228) versus mass (ng) spotted onto a swab prior to thermal desorption. The linear fit shown has $r^2 = 0.9974$.

5.4.3 Memory Effects

For the majority of compounds investigated it was found that the ion signal at the m/z being used to identify an explosive had returned to background levels within tens of seconds. EGDN, DNT and HMTD showed the least memory effects. This is illustrated for DNT in figure 5.3. This figure shows a chromatographic spectrum (product ion intensity versus time) for the protonated parent signal that resulted from 1 ng of DNT desorbed from a swab. For comparison, figure 5.4 shows the temporal intensity profiles of the dominant product ions at m/z 46 and 75 resulting from RDX. Although the product ion signals for RDX do not return to background values as quickly as those obtained for the other explosives, by approximately 60 seconds the ion signal intensities have dropped to approximately 5% of their peak values.

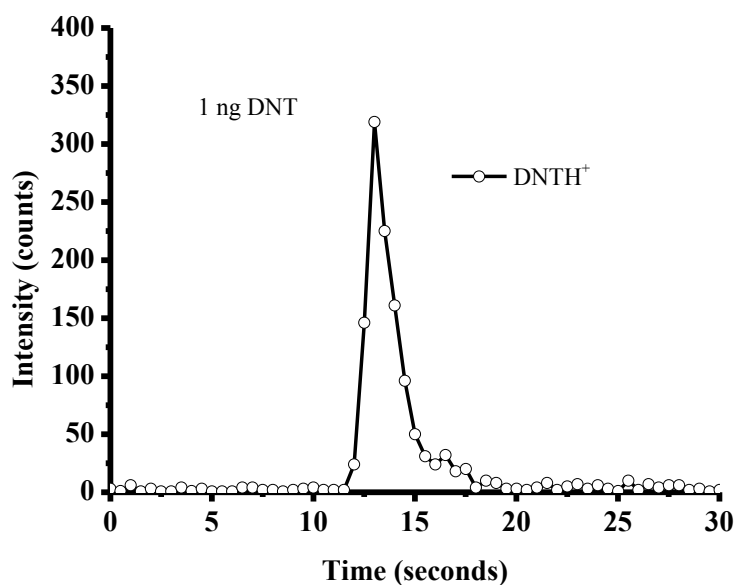


Figure 5.3. Thermal desorption chromatographic spectrum for 1 ng DNT deposited onto a clean swab. This is a plot shows the intensity of DNTH⁺ as a function of time from just before and after insertion and compression of the swab.

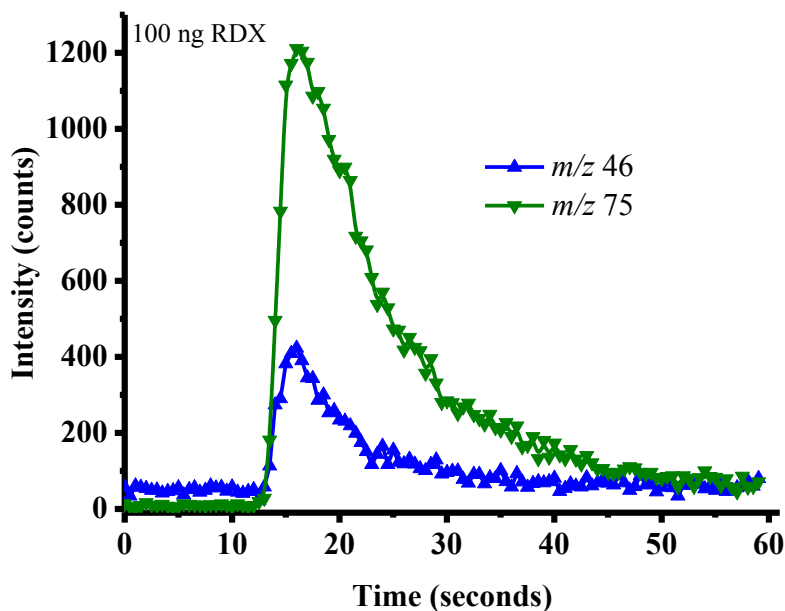


Figure 5.4. Thermal desorption chromatographic spectra for 100 ng of RDX. The product ion intensities for m/z 75 and m/z 46 as a function of time are shown.

For the other compounds studied, DNB, TNB, NG, TNT and PETN, memory effects were found to be slightly greater than those found for explosives such as DNT, but significantly less than that observed for RDX. Typically background levels were reached in approximately 20 seconds. To illustrate this, figure 5.5 (a) shows the temporal profiles of NGH^+ and NO_2^+ for 50 ng of NG taken at an E/N of 80 Td, which is the best value of the reduced electric field in terms of sensitivity for detecting the protonated parent. To demonstrate the effect of E/N on the product ion branching ratios, figure 5.5 (b) shows the identical NG product ions being monitored, but this time taken at a higher reduced electric field of 180 Td. Figures 5.6 (a) and (b) show the corresponding results for TNT at E/N values of 80 Td and 180 Td, respectively, using a swab onto which 50 ng of TNT was placed.

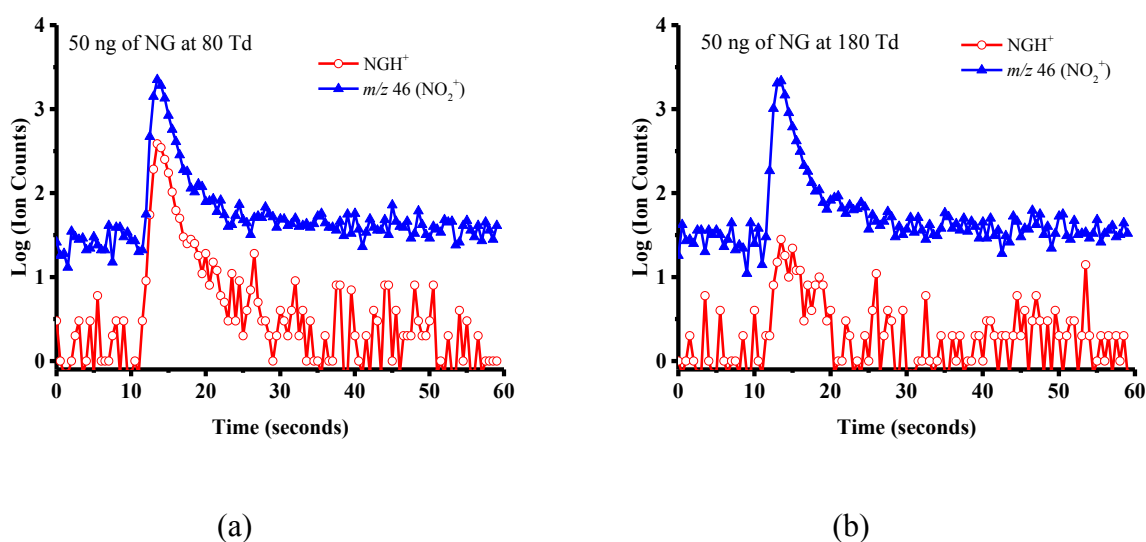


Figure 5.5. Logarithmic thermal desorption chromatographic spectra for 50 ng of NG. The intensities of the product ions at m/z 228 (NGH^+) and m/z 46 (NO_2^+) are shown at E/N values of (a) 80 Td and (b) 180 Td.

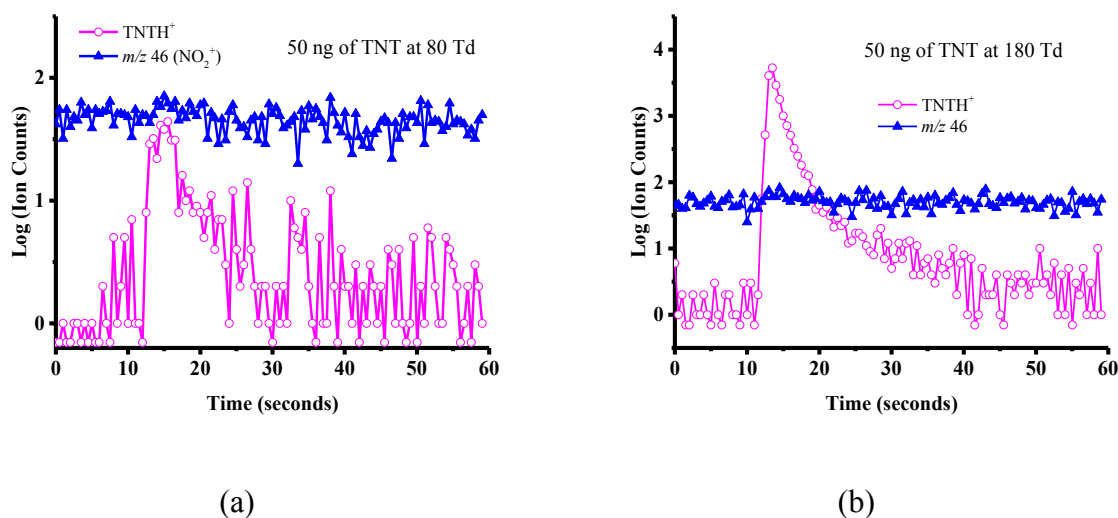
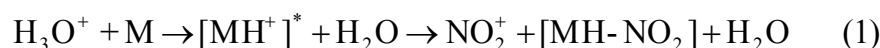


Figure 5.6. Logarithmic thermal desorption chromatographic spectra for 50 ng of TNT with channels m/z 228 and 46 being monitored at the E/N values of (a) 80 Td and (b) 180 Td. Only one product ion results from the reaction of H_3O^+ with TNT, TNTH^+ at m/z 228.

5.5. Discussions

5.5.1 Product ions and improved selectivity

Compared to IMS, PTR-MS provides more selectivity because of the mass spectral analysis. However, product ions are not necessarily unique for a given explosive. In this study NO_2^+ is a product ion that comes from all of the nitrate esters. This product ion results from the formation of a hydroxyl group upon proton transfer and the subsequent elimination of a nitro group in the form of NO_2^+ :



where $\text{M} = \text{EGDN}$, NG , or PETN . However, the observation of it and the protonated parent makes it possible to identify explosives with a high level of confidence. An example of this is its use to discriminate between TNT and NG. These two compounds have the same nominal protonated mass. However, TNT reacts with H_3O^+ to produce only the protonated parent. The absence of an NO_2^+ product ion provides a simple method to distinguish between NG and

TNT (compare figures 5.5 and 5.6). Even if TNT and NG are both present, the unusual increase of the TNTH^+ signal with increasing E/N ,⁷ means that it is possible to determine if both compounds are present. This serves to demonstrate how changes in operational parameters can be used effectively to improve the instrumental selectivity.

5.5.2 TDU/PTR-MS instrumental limits of detection and comparisons with other instruments

The LoD values obtained for various explosives demonstrate that the TDU/PTR-MS system provides an analytical technique with sensitivities comparable to those achieved by ion mobility spectrometry.^{17,18} The actual LoD values we have obtained are either lower (TNT (150 pg)) or slightly higher (RDX (6 ng), PETN (600 pg) and NG (2 ng)) than those often found for IMS. For example, Fetterolf and Clark have reported IMS LoD for RDX, TNT and PETN of 200 pg and for NG 50 pg.¹⁹ Another study using electrospray ionisation (ESI)-IMS reported LoD values for TNT, TNB, RDX, and EGDN to be 15 ng, 1.54 ng, 40 ng and 190 ng, respectively.²⁰ More recently, an IMS was interfaced with solid phase microextraction (SPME),²¹ for which a LoD of 160 pg for TNT has been reported (PETN and RDX were detected by the SPME-IMS, but not reproducibly and hence no LoD values are provided in that paper). Using a corona discharge ionisation IMS system, Lee *et al.* report LoD values for RDX, TNT, and PETN to be 100 pg, 1 ng, and 500 pg, respectively.¹⁷ Lower LoD values are possible with other types of instrumentation such as those that use liquid chromatography combined with MS^n techniques. These can also provide superior selectivity compared to IMS and PTR-MS.^{22,23} However, improved sensitivity and selectivity come at the expense of simplicity and costs. Furthermore, MS^n techniques can only look for one compound at a time. Therefore, even leaving aside the added complexity and allowing for the fact that it is possible to switch mass peaks quite quickly, this will limit the number of targets that can be covered in a brief thermal desorption event. These MS^n techniques are further unsuitable for general use in security areas, because of the long detection cycle as a result of the chromatographic techniques involved. Thus chromatography and MS^n techniques will have limited practical use as analytical devices in security areas. In comparison, IMS and PTR-MS can be used as rapid analytical instruments for the detection of single or multiple threat agents.

5.5.3 Cycle times

High sensitivity and selectivity, discussed above, are necessary but not sufficient for an analytical instrument to be of use in security areas. Another key property for an instrument to have is a rapid cycle time, whereby desorption, transfer, ionization, detection and removal of explosives take place within tens of seconds. This requires that instrumental memory effects are of the same timescale. We have demonstrated that the combination of a purposely built TDU and short heated inlet lines leading to the reaction chamber of a PTR-MS have resulted in memory effects that are small (tens of seconds). The only exception we have found is for the explosive RDX. The longer memory effect found for RDX are not associated with the TDU, but is a result of the compound not being efficiently transferred to the drift tube owing to surface effects. (This was verified by removing the swab containing the RDX from the TDU and replacing it with a clean swab.) However, even for RDX, recovery times are not too severe, being approximately 1 minute. We are currently working on improvements to the heating of the inlet and drift tube to try to reduce this.

5.6. Conclusions

This study detailed the use of a novel thermal desorption system specifically designed for application with PTR-MS to detect compounds with low volatilities such as explosives. This has resulted in a step change in the performance of PTR-MS for use as a detector for traces of explosives. We have demonstrated that a first generation PTR-MS combined with a specifically designed and manufactured TDU has achieved sensitivities (nanograms) that are sufficiently low to meet current security application criteria.²⁴ However, recent improvements in the sensitivity of PTR-MS instruments, including the development of an ion funnel system,²⁵ means that even lower LoD should be possible with a TDU/PTR-MS system.

Given the size and pumping requirements for PTR-MS, IMS instrumentation is less expensive and easier to use, especially when portable compact analytical devices are all that are required. These give IMS some distinct advantages over PTR-MS. However, PTR-MS has the distinct advantage of being more selective. We have demonstrated in this paper how this selectivity can be enhanced by manipulating the ion chemistry via changes in the operational parameters of the instrument, such as E/N to modify ion-molecule collisional energies and hence the intensities of the product ions.²⁶

It is appreciated that for this study we have introduced an analyte under the most advantageous way possible. However, the important goal of this paper is to demonstrate the TDU/PTR-MS system in terms of its efficiency and cycle time, which has been achieved. It is necessary to characterise a new instrument using ideal conditions, before considering complicating factors such as real samples and real-world sampling. Additional further work now needs to be undertaken to investigate the complexity of working with “real-world” sampling. This includes testing the instrument by wiping surfaces contaminated with known quantities of an explosive, using interference tests and determining throughput rate. Other studies are also needed to determine whether thermal decomposition of an explosive occurs. Thus details on the ideal temperatures (or range of temperatures) at which the TDU/PTR-MS should be operated for optimal conditions for a given explosive would be obtained.

5.7. Acknowledgements

This collaborative research programme between KORE Technology Ltd. and the University of Birmingham, and the funding of the Early Stage Researcher (RGM) were supported through the PIMMS Initial Training Network, which in turn is supported by the European Commission’s 7th Framework Programme under Grant Agreement Number 287382. This project was also in part funded under the Innovative Research Call in Explosives and Weapons Detection 2010. This is a Cross-Government programme sponsored by a number of Departments and Agencies under the UK Government’s CONTEST strategy in partnership with the US Department of Homeland Security. The authors wish to thank Smiths Detection Ltd., Watford, UK, for the loan of a KORE PTR-ToF-MS.

5.8. References

1. Caygill, J. S.; Davis, F.; Higson, S. P. J., Current trends in explosive detection techniques. *Talanta* **2012**, *88* (0), 14-29.
2. Ewing, R. G.; Atkinson, D. A.; Eiceman, G. A.; Ewing, G. J., A critical review of ion mobility spectrometry for the detection of explosives and explosive related compounds. *Talanta* **2001**, *54* (3), 515-529.

3. Shen, C.; Li, J.; Han, H.; Wang, H.; Jiang, H.; Chu, Y., Triacetone triperoxide detection using low reduced-field proton transfer reaction mass spectrometer. *International Journal of Mass Spectrometry* **2009**, *285* (1–2), 100-103.
4. Mayhew, C. A.; Sulzer, P.; Petersson, F.; Haidacher, S.; Jordan, A.; Märk, L.; Watts, P.; Märk, T. D., Applications of proton transfer reaction time-of-flight mass spectrometry for the sensitive and rapid real-time detection of solid high explosives. *International Journal of Mass Spectrometry* **2010**, *289* (1), 58-63.
5. Jürschik, S.; Sulzer, P.; Petersson, F.; Mayhew, C. A.; Jordan, A.; Agarwal, B.; Haidacher, S.; Seehauser, H.; Becker, K.; Märk, T. D., Proton transfer reaction mass spectrometry for the sensitive and rapid real-time detection of solid high explosives in air and water. *Anal Bioanal Chem* **2010**, *398* (7-8), 2813-2820.
6. P. Sulzer, B. Agarwal, S. Jürschik, M. Lanza, A. Jordan, E. Hartungen, G. Hanel, L. Märk, T. D. Märk, R. González-Méndez, P. Watts and C. A. Mayhew, Applications of switching reagent ions in proton transfer reaction mass spectrometric instruments for the improved selectivity of explosive compounds. *International Journal of Mass Spectrometry International Journal of Mass Spectrometry*, **2013**, *354-355*, 123-128.
7. Sulzer, P.; Petersson, F.; Agarwal, B.; Becker, K. H.; Jürschik, S.; Märk, T. D.; Perry, D.; Watts, P.; Mayhew, C. A., Proton Transfer Reaction Mass Spectrometry and the Unambiguous Real-Time Detection of 2,4,6 Trinitrotoluene. *Analytical Chemistry* **2012**, *84* (9), 4161-4166.
8. Cordell, R. L.; Willis, K. A.; Wyche, K. P.; Blake, R. S.; Ellis, A. M.; Monks, P. S., Detection of Chemical Weapon Agents and Simulants Using Chemical Ionization Reaction Time-of-Flight Mass Spectrometry. *Analytical Chemistry* **2007**, *79* (21), 8359-8366.
9. Petersson, F.; Sulzer, P.; Mayhew, C. A.; Watts, P.; Jordan, A.; Märk, L.; Märk, T. D., Real-time trace detection and identification of chemical warfare agent simulants using recent advances in proton transfer reaction time-of-flight mass spectrometry. *Rapid Communications in Mass Spectrometry* **2009**, *23* (23), 3875-3880.
10. Agarwal, B.; Petersson, F.; Jürschik, S.; Sulzer, P.; Jordan, A.; Märk, T. D.; Watts, P.; Mayhew, C. A., Use of proton transfer reaction time-of-flight mass spectrometry for the analytical detection of illicit and controlled prescription drugs at room temperature via direct headspace sampling. *Anal Bioanal Chem* **2011**, *400* (8), 2631-2639.

11. Jürschik, S.; Agarwal, B.; Kassebacher, T.; Sulzer, P.; Mayhew, C. A.; Märk, T. D., Rapid and facile detection of four date rape drugs in different beverages utilizing proton transfer reaction mass spectrometry (PTR-MS). *Journal of Mass Spectrometry* **2012**, *47* (9), 1092-1097.
12. Ewing, R. G.; Waltman, M. J.; Atkinson, D. A.; Grate, J. W.; Hotchkiss, P. J., The vapor pressures of explosives. *TrAC Trends in Analytical Chemistry* **2013**, *42* (0), 35-48.
13. Blake, R. S.; Whyte, C.; Hughes, C. O.; Ellis, A. M.; Monks, P. S., Demonstration of Proton-Transfer Reaction Time-of-Flight Mass Spectrometry for Real-Time Analysis of Trace Volatile Organic Compounds. *Analytical Chemistry* **2004**, *76* (13), 3841-3845.
14. Ennis, C. J.; Reynolds, J. C.; Keely, B. J.; Carpenter, L. J., A hollow cathode proton transfer reaction time of flight mass spectrometer. *International Journal of Mass Spectrometry* **2005**, *247* (1-3), 72-80.
15. Miller, S. PhD Thesis "Application of Proton Transfer Mass Spectrometry to Analytical Science". Open University, UK, 2014.
16. Jordan, A.; Haidacher, S.; Hanel, G.; Hartungen, E.; Märk, L.; Seehauser, H.; Schottkowsky, R.; Sulzer, P.; Märk, T. D., A high resolution and high sensitivity proton-transfer-reaction time-of-flight mass spectrometer (PTR-TOF-MS). *International Journal of Mass Spectrometry* **2009**, *286* (2-3), 122-128.
17. Lee, J.; Park, S.; Cho, S. G.; Goh, E. M.; Lee, S.; Koh, S.-S.; Kim, J., Analysis of explosives using corona discharge ionization combined with ion mobility spectrometry-mass spectrometry. *Talanta* **2014**, *120* (0), 64-70.
18. Gary A. Eiceman, Z. K., Herbert H. Hill Jr., Ion Mobility Spectrometry. Third ed.; CRC Press: 2014. Chapter 12.
19. Fetterolf, D.D.; Clark T.D., Detection of trace explosive evidence by ion mobility spectrometry. *Journal of Forensic Sciences* **1993** (38), 28-39.
20. Reid Asbury, G.; Klasmeier, J.; Hill Jr, H. H., Analysis of explosives using electrospray ionization/ion mobility spectrometry (ESI/IMS). *Talanta* **2000**, *50* (6), 1291-1298.
21. Perr, J. M.; Furton, K. G.; Almirall, J. R., Solid phase microextraction ion mobility spectrometer interface for explosive and taggant detection. *Journal of Separation Science* **2005**, *28* (2), 177-183.

22. DeTata, D.; Collins, P.; McKinley, A., A fast liquid chromatography quadrupole time-of-flight mass spectrometry (LC-QToF-MS) method for the identification of organic explosives and propellants. *Forensic Science International* **2013**, *233* (1–3), 63-74.
23. Xu, X.; Koeberg, M.; Kuijpers, C.-J.; Kok, E., Development and validation of highly selective screening and confirmatory methods for the qualitative forensic analysis of organic explosive compounds with high performance liquid chromatography coupled with (photodiode array and) LTQ ion trap/Orbitrap mass spectrometric detections (HPLC-(PDA)-LTQOrbitrap). *Science & Justice* **2014**, *54* (1), 3-21.
24. Rhykerd, C. L.; Hannum, D. W.; Murray, D. W.; Parmeter, J. E., Guide for the Selection of Commercial Explosives Detection Systems for Law Enforcement Applications **1999**, NIJ Guide 100-99.
25. Barber, S.; Blake, R. S.; White, I. R.; Monks, P. S.; Reich, F.; Mullock, S.; Ellis, A. M., Increased Sensitivity in Proton Transfer Reaction Mass Spectrometry by Incorporation of a Radio Frequency Ion Funnel. *Analytical Chemistry* **2012**, *84* (12), 5387-5391
26. Andrew M. Ellis, Christopher. A. Mayhew, Proton Transfer Reaction Mass Spectrometry: Principles and Applications. First ed.; John Wiley and Sons: 2014

CHAPTER 6

ENHANCEMENT OF COMPOUND SELECTIVITY USING A RADIO FREQUENCY ION-FUNNEL PROTON TRANSFER REACTION MASS SPECTROMETER: IMPROVED SPECIFICITY FOR EXPLOSIVE COMPOUNDS

This chapter is a reformatted copy of my published article:

Analytical Chemistry, 2016, 88 (21), 10624-10630.

Ramón González-Méndez,^{1*} Peter Watts,¹ David Olivenza,¹ D. Fraser Reich,² Stephen J. Mullock,² Clive A. Corlett,² Stuart Cairns,³ Peter Hickey,³ Matthew Brookes,⁴ and Chris A. Mayhew^{1,5}

1. Molecular Physics Group, School of Physics and Astronomy, University of Birmingham, Edgbaston, Birmingham, B15 2TT, UK
2. Kore Technology Ltd, Cambridgeshire Business Park, Ely, Cambridgeshire CB7 4EA, UK
3. Defence Science and Technology Laboratory, Fort Halstead, Sevenoaks, Kent, TN14 7BP, UK
4. Defence Science and Technology Laboratory, Porton Down, Salisbury, Wilshire SP4 0JQ, UK
5. Institut für Atemgasanalytik, Leopold-Franzens-Universitaet Innsbruck, Innsbruck 6020, Austria

* Corresponding author: Tel.:+44 121 414 4668. E-mail R.GonzalezMendez@bham.ac.uk

Declaration of contribution

My contribution to the study described in this Chapter was designing the experiments, performing the experiments, interpreting the data and writing the manuscript jointly with the other co-authors.

The Density Functional Theory (DFT) calculations used to aid in the interpretation of the data were made by Dr. Peter Watts (Molecular Physics Research Group, University of Birmingham).

6.1. Abstract

A key issue with any analytical system based on mass spectrometry with no initial separation of compounds is to have a high level of confidence in chemical assignment. This is particularly true for areas of security, such as airports, and recent terrorist attacks have highlighted the need for reliable analytical instrumentation. Proton transfer reaction mass spectrometry is a useful technology for these purposes because the chances of false positives are small owing to the use of a mass spectrometric analysis. However, the detection of an ion at a given m/z for an explosive does not guarantee that that explosive is present. There is still some ambiguity associated with any chemical assignment owing to the presence of isobaric compounds and, depending on mass resolution, ions with the same nominal m/z . In this paper we describe how for the first time the use of a radio frequency ion-funnel in the reaction region (drift tube) of a proton transfer reaction – time-of-flight – mass spectrometer (PTR-ToF-MS) can be used to enhance specificity by manipulating the ion-molecule chemistry through collisional induced processes. Results for trinitrotoluene, dinitrotoluenes and nitrotoluenes are presented to demonstrate the advantages of this new RFIF-PTR-ToF-MS for analytical chemical purposes.

6.2. Introduction

Ion funnels (IF) have been used since the late 1990s in conjunction with several ionisation and mass spectrometric techniques with a key purpose of increasing ion transmission efficiency and hence instrumental sensitivity and dynamic range.^{1,2} Of relevance to our study, Schaffer et al. developed a radio-frequency (RF) IF for focussing and transmitting ions from relatively high pressure (> 1 Torr) ion sources to mass spectrometers.¹ Given that the typical operating pressure of a drift tube used in proton transfer reaction mass spectrometry (PTR-MS) is close to the optimum pressure for the operation of a RFIF, Kore Technology Ltd. designed and developed a RFIF to be incorporated into drift tubes in order to increase the instruments sensitivity.³ This compact drift tube can simultaneously operate as an ion funnel and a reaction region with a controllable reaction time (dependent on the voltage supplied across the tube). The funnel design and the supplied RF and DC fields act in such a way to channel reagent and product ions towards the exit orifice of the drift tube so that more ions leave the reaction region into the much lower pressure mass spectrometric region, thereby decreasing the loss of ions that occurs at the end of the drift tube. The proof-of principle study reported increases in sensitivity of this RFIF-PTR-ToF-MS system that were found to be dependent on the m/z of the product ions, but were typically between 1 and 2 orders of magnitude. For example enhancement factors of 45 and 200 were reported for protonated acetaldehyde and protonated acetone, respectively, at a reduced electric field of 120 Td (where this field refers to the DC voltage applied across the drift tube).³

Given that the RFIF forms part of the drift tube, we asked the question whether the high RF fields involved in the operation of an IF could be used to enhance collisions of the reagent and product ions with the buffer gas in the DT and hence change either the nature of the initial chemical ionisation process or induce collisional induced dissociation, respectively, occurring within the DT? We hypothesised that changes would result from raising the internal energy of the product ions and the energy of the reactions between reagent ions and neutral species through collisional processes as a result of the applied RF field. The real question is whether the RF collisional induced dissociation would lead to substantial fragmentation, or be more selective resulting in unique product ions that can be used to identify a chemical compound of interest with a higher specificity than that achievable just by using a standard drift tube at a given reduced electric field. Here we report details on a collaborative project involving KORE Technology Ltd. and the University of Birmingham which investigated the

application of a RFIF drift tube of a PTR-ToF-MS for improved selectivity using several explosives as illustrative compounds, namely 2,4,6-trinitrotoluene (TNT), 2,4-, 2,6- and 3,4-dinitrotoluene (DNT) and 2-, 3- and 4-nitrotoluene (NT). We will show how the application of a RFIF leads to a higher confidence in compound identification. We thus demonstrate for the first time that the addition of a RFIF to a PTR-ToF-MS results in a more multi-dimensional analytical instrument that improves the selectivity that can be achieved by operating a drift tube of a PTR-MS in DC mode only.

6.3. Methods

6.3.1 Experimental Details

A KORE Technology Ltd. RFIF Series I PTR-ToF-MS was used. Details of KORE's PTR-ToF-MS system with no IF has been described in detail elsewhere,⁴⁻⁶ and hence only the salient points of this instrument are provided here. Using a needle valve, water vapour is introduced into a hollow cathode discharge where, after ionisation via electron impact and subsequent ion-molecule processes, the terminal reagent ion is H_3O^+ .⁷ These ions are transferred from the ion source into the drift tube (the reaction region) of the PTR-ToF-MS, which is typically at a pressure of 1 mbar and temperature 100 °C, where they encounter the analyte. H_3O^+ ions react with the analyte M by donating their protons at the collisional rate, providing M has a proton affinity greater than that of water ($\text{PA}(\text{H}_2\text{O}) = 691 \text{ kJ mol}^{-1}$). This process can be non-dissociative (resulting in the protonated molecule MH^+) and/or dissociative. Dissociative proton transfer results in product ions which may be useful in the identification of a compound. Fragmentation may be spontaneous upon proton transfer or may require additional energy which is supplied through collisions with the buffer gas resulting during the migration of ions under the influence of the electric field, E . The ratio of E to the buffer gas number density, N , is an important parameter (known as reduced electric field) which determines the mean collisional energy of ions with the neutral buffer gas. Hence it is the parameter often referred to and changed for investigating product ion branching ratios.⁸⁻¹⁵

The IF (schematically shown in figure 6.1) consists of 29 stainless steel plates of 0.2 mm thickness, mounted on precision-machined ceramic rods at an even spacing of 3.2 mm per plate. Tabs on the electrodes permit a resistor chain on a ceramic strip to be connected in

addition to two capacitor stacks which allow the RF to be applied to the second half of the reactor. The orifice diameters of the plates through the first half of the stack is 40 mm, as used in the standard drift tube reactor. In the second half of the drift tube the orifice diameter steadily decreases to 6 mm at the final plate before the exit orifice. Across the complete ion-funnel a DC voltage is applied driving ions axially. When just operating with this voltage we shall refer to the instrument as operating in DC-only mode. In addition to this, to the second part of the drift tube a RF field can applied. The resonant frequency of the system is ~ 760 kHz and the amplitude selected for the majority of the studies (peak-to-peak) was 200 V, which is superimposed on the dc voltage gradient across the drift tube.

The main purpose of the RF field is to focus ions radially by creating repulsive effective potentials at the edges of the electrodes. However, in addition to this intended purpose, the RF results in ions oscillating between electrodes as they drift down the reactor. This gives ions higher collisional energies than those in the first half of the drift tube. We shall refer to operating the instrument with the RF on as RF-mode. At the end of the drift tube is a $400 \mu\text{m}$ orifice, through which ions enter the ion transfer region for ToF-MS.

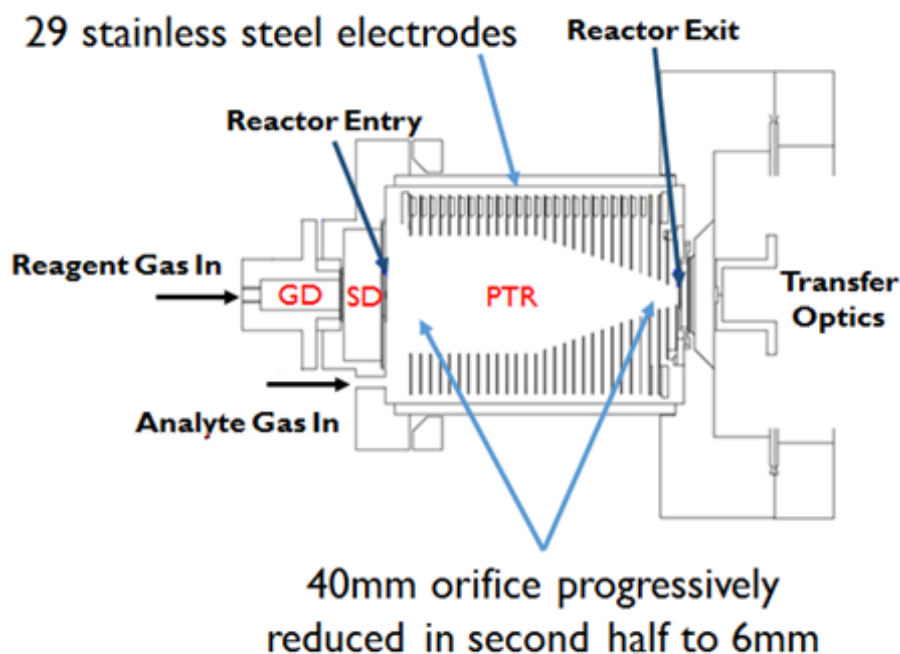


Figure 6.1. Schematic representation of the KORE Technology Ltd. radio frequency ion funnel drift tube (proton transfer reaction (PTR) region) used in this investigation. Also

shown is the ion source region (glow discharge GD), and a source drift (SD) region which is used to extract ions from the GD, aid in breaking-up protonated water clusters and to enhance production of H_3O^+ via additional ion-molecule reactions involving ions that can react with water. After exiting the drift tube the transfer optics guide the ions into the ToF-MS region.

The use of specifying a reduced electric field, E/N , is an appropriate parameter to use in DC-only mode, because it is well defined. In RF-mode (ion funnel on) the presence of DC and RF electric fields complicates the situation, because the electric field strength varies with distance from the RF electrodes, so that specifying a reduced electric field is not appropriate. Barber et al.³ simply adopted an empirical effective reduced electric field by finding operating conditions for the ion-funnel drift tube that matched the performance of the same drift tube when operated under DC-only mode. However, given that it is uncertain what the effective reduced electric field means, in this paper we refer to the DC voltage (V_{drift}) applied across the drift tube.

A thermal desorption unit (TDU) connected to the inlet of the drift tube was used to introduce the explosive samples, details of which have been given elsewhere.⁶ The TDU, connecting lines and drift tube were operated at a temperature of 150 °C. PTFE swabs (ThermoFisher Scientific) onto which known quantities of explosives were deposited were placed into the TDU. The swabs came prepared from the manufacturer mounted on rectangular cardboard for easy insertion into the TDU. Once a seal was created, a carrier gas (in this study laboratory air) is heated to the temperature of the TDU before it flows through a series of holes in a heated metal plate. This heated air then passes through the swab and into the inlet system driving any desorbed material through to the drift tube creating a temporal concentration “pulse” of typically between 10 – 20 seconds of an explosive in the drift tube.⁶ Each swab provided one measurement, which was replicated three times and then the results were averaged and any background signals were subtracted.

Explosive standards were purchased from AccuStandard Inc., New Haven, CT. Typically these standards contained 0.1 mg of the explosive compound in 1 ml of solvent. For TNT, 2,4- and 2,6-DNT, and the NTs this involved an acetonitrile:methanol (1:1) mix. 3,4-DNT was just mixed with methanol. These samples were diluted in the appropriate solvent(s) (HPLC grade) to provide the required quantity of an explosive. Typically 1 μl of a solvent containing the required mass of an explosive was spotted onto a PTFE swab.

6.3.2 Electronic Structure Calculations

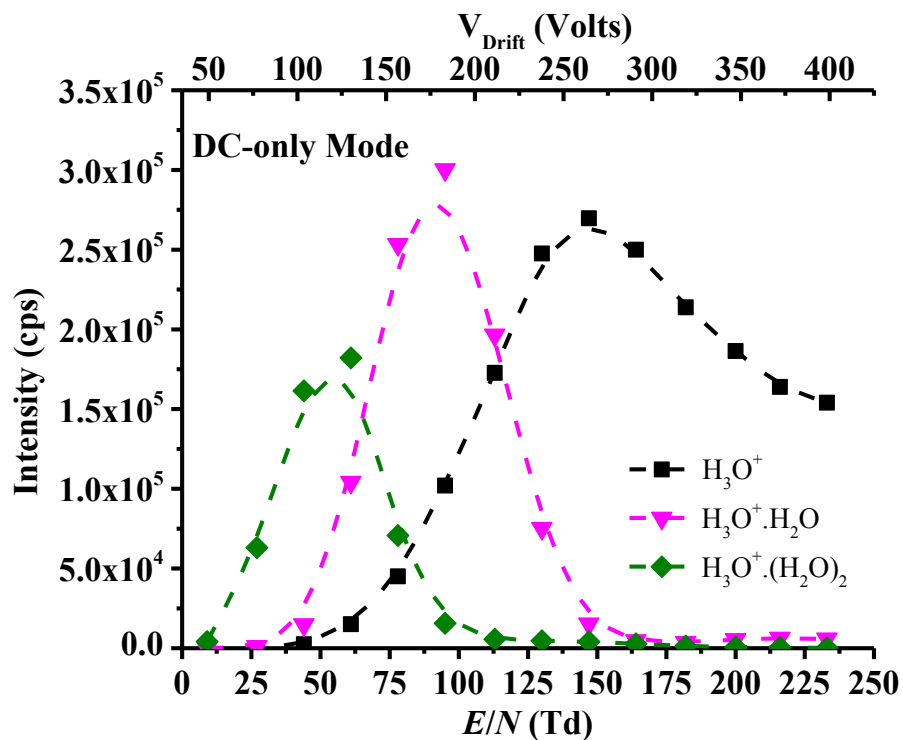
To aid in the interpretation of the experimental results a series of electronic structure calculations have been undertaken at 298 K. These involve density functional theory calculations using the GAUSSIAN09 PROGRAM with the GaussView 5 interface.¹⁶ The B3LYP functional with the 6-31+G(d,p) basis set was used throughout. Although it is appreciated that the drift tube temperature and the effective ion temperature are greater than 298 K, with the effective ion temperature being uncertain, the thermochemical calculations simply provide us with an indicator as to whether a reaction pathway is energetically possible or not.

6.4. Results and Discussion

6.4.1 Reagent ions

Before we begin discussing the results of the explosives, it is informative to present details on the reagent ion signal as a function of drift tube voltage, comparing intensities for DC-only mode (figure 6.2 (a)) and RF-mode (funnel-on) (figure 6.2(b)) under identical operating conditions of hollow cathode and drift tube pressures and temperature. The observed decrease of H_3O^+ reagent ion signal with decreasing drift tube voltage is predominantly a result of the clustering with water molecules in the drift tube, which are not broken-up through collisions at lower drift tube voltages. The marked decrease in total reagent ion signal below about 50 Td is considered to be a result of the low SD potential, which scales with the DC drift tube potential. As the SD voltage decreases we can expect that fewer reagent ions reach the reactor entry.

(a)



(b)

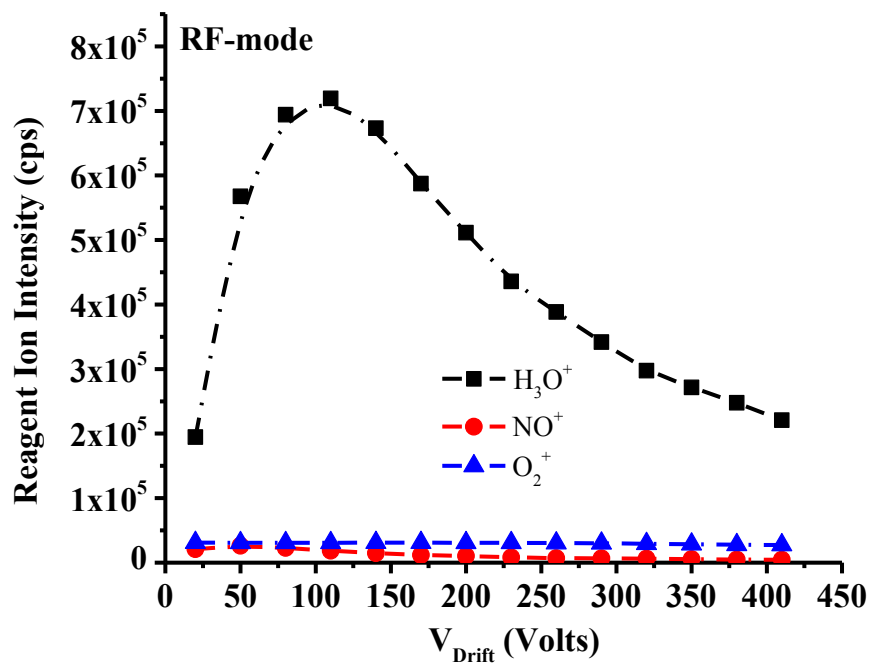


Figure 6.2. Ion intensities in counts per second (cps) of the water reagent ions present in the drift as a function of drift tube voltage (a) in DC-only mode and (b) in RF-mode (ion funnel

on). For (b) the ion signals at m/z 30 (NO^+) and 32 (O_2^+) are presented because although low intensity they are still significant and are observed as a result of the improved ion transmission in RF-mode. In DC-mode the signal intensities of these ions are negligible and are therefore not presented.

Figure 6.2(a) shows that by 100 Td the H_3O^+ reagent ion signal has reduced significantly and that the protonated water clusters start to dominate at the lowest reduced electric field corresponding to a voltage drop across the drift tube of about 200 V under the operational temperature and pressure values used. (The actual percentage of protonated water clusters for fixed E/N is also strongly dependent on the humidity of the buffer gas in the drift tube, which is dependent on the amount of forward flow of H_2O from the ion source into the drift tube and the humidity of the laboratory air.) In RF-mode no protonated water clusters are observed, because they are broken-up through collisions in the RFIF region of the drift tube. Furthermore, at about 120 V the H_3O^+ intensity is approximately at its maximum value. As the drift voltage decreases, the reagent ion signal decreases. However, even at a drift tube voltage of only 20 V (which in DC-only mode would correspond to a reduced electric field of only about 10 Td) there is still a significant reagent ion count. This enhancement of reagent ion signal at low drift tube voltages can only be a result of the trapping that the RF field provides thereby reducing the diffusional loss that occurs in DC-only mode under low drift tube voltages.

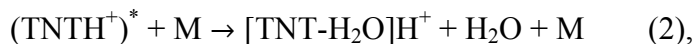
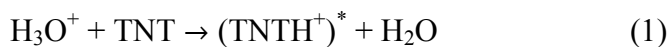
6.4.2. 2,4,6-trinitrotoluene (TNT)

Using both PTR-ToF-MS and PTR-Quad-MS systems Sulzer et al. have previously shown that there is an unusual dependence of the intensity of protonated TNT on the reduced electric field in that there is an increase in the sensitivity of detection with increasing E/N .^{9,17} This increase continues until a maximum is reached at about 180 Td, after which the signal intensity shows the more usual behaviour of decreasing with increasing E/N . This is opposite to what is commonly found in PTR-MS studies, because with reduced reaction times, fragmentation to non-specific product ions, and reduction in ion transmission the protonated molecule intensity reduces with increasing E/N . The explanation of this unusual intensity dependence for TNTH^+ has been described in detail.⁹ In brief, it is a result of a secondary reaction of $\text{TNTH}^+\cdot\text{H}_2\text{O}$ (which is

readily formed at low E/N) with H_2O leading to a terminal ion which does not contain TNT, namely $\text{H}_3\text{O}^+\cdot\text{H}_2\text{O}$.

In DC-only mode and when a product ion signal is detected, for all E/N values investigated only one product ion is observed that contains the explosive, namely protonated TNT at m/z 228. However, in RF mode, another fragment ion is found at m/z 210, the intensity of which increases with decreasing drift tube voltage (i.e. decreasing E/N in DC mode) down to values under which the PTR-ToF-MS does not perform in DC mode owing to a lack of sufficient transmission of ions to the mass spectrometer (figure 6.2(a)). Typical results obtained for TNT are shown in figure 6.3. That the fragment ion m/z 210 intensity increases with decreasing drift tube voltage (figure 6.3) is perhaps not what is expected given that decreasing DC voltage means lower collisional energies. However, that only applies in the first half of the drift tube. As the drift tube voltage is reduced more collisions in the RFIF region of the drift tube occur, which in turn enhances collisional induced dissociation.

Following proton transfer the protonated molecule gains sufficient internal energy through collisions in the RFIF section of the drift tube to eliminate H_2O :



where M is a buffer gas molecule. Thus specificity can be increased by either switching off and on the RFIF at a specific drift tube voltage or by switching the drift tube voltage. Note that a minor percentage of the observed m/z 210 results from the reaction of the O_2^+ (always present in low concentrations in the drift tube as an impurity ion) with TNT via a dissociative charge transfer process leading to the loss of OH from TNT^+ .¹²

That the reaction pathway leading to the elimination of H_2O is overall energetically favourable (table 6.1) but is only observed in RF mode, is an indication that there must be an energy barrier for pathway (2). Evidence of this is provided from the results obtained when investigating the effects of changing the RF amplitude at fixed drift tube voltages and fixed frequency. Figure 6.4 provides a summary of these measurements, which shows that as the RF peak-to-peak voltage is decreased the intensity of the m/z 210 decreases for all drift tube voltages.

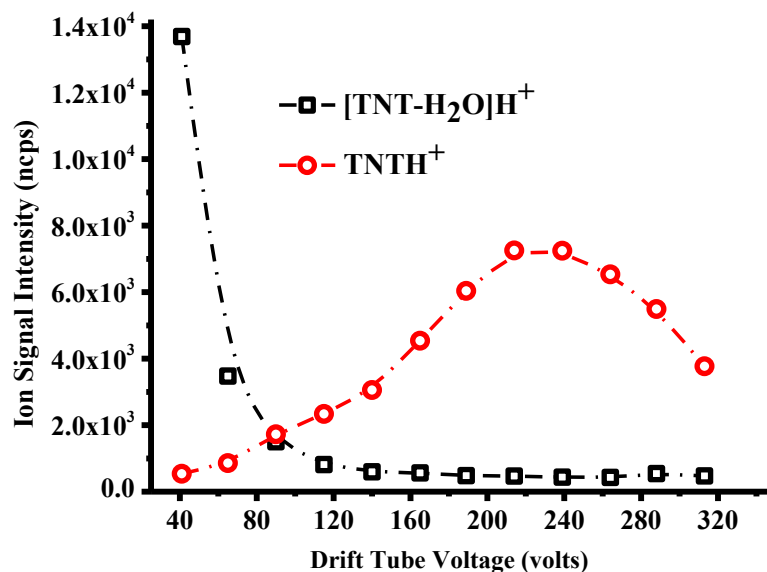


Figure 6.3. Product ion intensities as a function of drift tube voltage in RF mode. The data have been taken using 100 ng of TNT. The ion signals have been normalised to $10^6 \text{H}_3\text{O}^+$ reagent ions and drift times. (The lines used in all graphs are just a guide to the eye.)

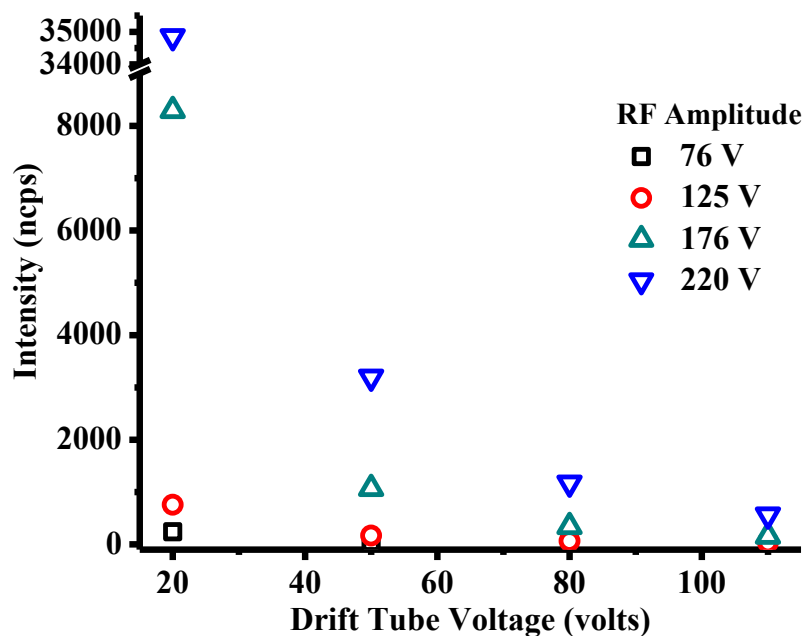


Figure 6.4. Intensities in ncps of the product ion $[\text{TNT-H}_2\text{O}]\text{H}^+$ as a function of drift tube voltage and RF amplitude (volts) with the frequency kept at 760 kHz ($\pm 3\%$).

The initial step leading to m/z 228 is the transfer of a proton from H_3O^+ to TNT. Protonation of TNT can occur on the nitro groups at the 2 and 4 positions, both having similar proton affinities, although as elimination of water from TNTH^+ will presumably involve the methyl group only protonation of the nitro group in the 2- position is of relevance. However, protonation on the 4 nitro will occur (the PA and GB are slightly greater than the 2 nitro) and this will reduce the amount of TNTH^+ available to lose water. Two configurations are possible for protonation in the 2 position as illustrated in figure 6.5, with the anti being slightly more stable by ca. 8 kJ mol^{-1} . The transition state energetics for interconversion are $\Delta H_{298}^\ddagger +46 \text{ kJ mol}^{-1}$ and $\Delta G_{298}^\ddagger +51 \text{ kJ mol}^{-1}$ above the anti conformation, but whichever is formed there is sufficient energy in the initial protonation to allow rapid interconversion (Table 6.1).

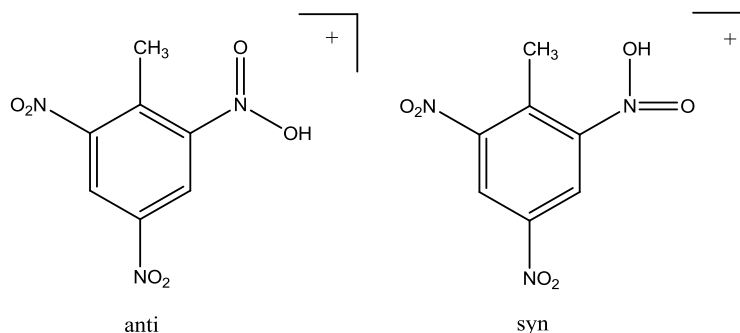


Figure 6.5. The two possible configurations resulting from protonation of TNT in the 2 position.

Table 6.1. Energetics for the proton transfer from H_3O^+ to TNT calculated using the B3LYP functional and the 6-31+G(d,p) basis set.

Products	$\Delta H_{298} \text{ kJ mol}^{-1}$	$\Delta G_{298} \text{ kJ mol}^{-1}$
$\text{TNTH}^+(2\text{NO}_2\text{syn}) + \text{H}_2\text{O}$	-46	-47
$\text{TNTH}^+(2\text{NO}_2\text{anti}) + \text{H}_2\text{O}$	-55	-55
$\text{TNTH}^+(4\text{NO}_2) + \text{H}_2\text{O}$	-68	-60
TS syn/anti + H_2O	-9	-5

There are three stable structures for the ion remaining after the elimination of water from TNTH^+ (figure 6.6). A fourth structure, similar to $\text{TNTH}^+ - \text{H}_2\text{O}$ (b) with the hydrogens

of the methylene group orthogonal to the ring, proved to be unstable and rearranged to $\text{TNTH}^+ - \text{H}_2\text{O}$ (a). The energetics for the transformation of TNTH^+ to $\text{TNTH}^+ - \text{H}_2\text{O}$ (a-c) + H_2O are given in Table 6.2.

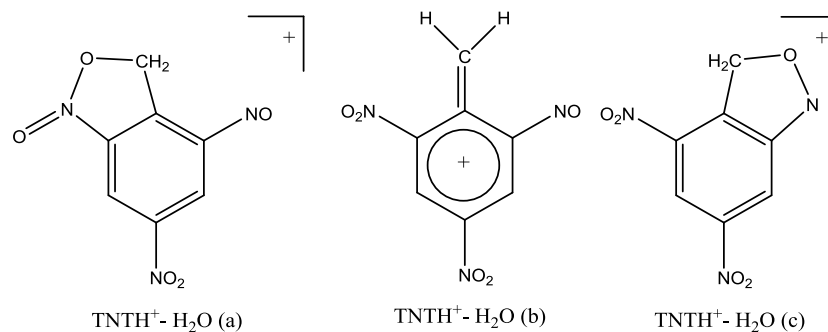


Figure 6.6. Stable structures of the $[\text{TNT-H}_2\text{O}]\text{H}^+$ ion.

Table 6.2. Energetics for the elimination of water from TNT following proton transfer from H_3O^+ for the three stable structures shown in figure 6.6.

Products	$\Delta\text{H}_{298} \text{ kJ mol}^{-1}$	$\Delta\text{G}_{298} \text{ kJ mol}^{-1}$
$\text{TNTH}^+ - \text{H}_2\text{O}$ (a) + $2\text{H}_2\text{O}$	-104	-145
$\text{TNTH}^+ - \text{H}_2\text{O}$ (b) + $2\text{H}_2\text{O}$	+47	-7
$\text{TNTH}^+ - \text{H}_2\text{O}$ (c) + $2\text{H}_2\text{O}$	-128	-168

Various attempts using the QST3 approach were made to find transition states for these possible reactions but all lead to $\text{TNTH}^+ - \text{H}_2\text{O}$ (c), though interestingly the transition state had a close resemblance to $\text{TNTH}^+ - \text{H}_2\text{O}$ (b). The transition state was characterised by one imaginary frequency and the internal reaction coordinate leading to $\text{TNTH}^+ - \text{H}_2\text{O}$ (c) in the forward direction and TNTH^+ with the proton on the 2-nitro group in the syn conformation in the reverse direction. The activation energies relative to $\text{TNT} + \text{H}_3\text{O}^+$ are $\Delta\text{H}_{298}^\ddagger + 158 \text{ kJ mol}^{-1}$ and $\Delta\text{G}_{298}^\ddagger + 162 \text{ kJ mol}^{-1}$.

The presumption that the elimination of water from protonated TNT can only occur when the methyl and nitro groups are adjacent to each other was readily tested by investigating isomers of DNT and NT. For those isomers that satisfy the condition of an adjacent nitro and methyl group, then $[\text{DNT-H}_2\text{O}]\text{H}^+$ and $[\text{NT-H}_2\text{O}]\text{H}^+$ fragment ions should be observed,

otherwise not. Thus we predicted to observe elimination of water from the 2,6-DNT, 2,4-DNT and 2-NT but not from 3,4-DNT, 3-NT or 4-NT following proton transfer in RF mode.

6.4.3 Dinitrotoluenes

In both RF-mode and DC-only mode for 3,4-DNT the only primary product ion that is observed with any significant intensity for all drift tube voltages is the protonated molecule. That no m/z 165 is observed, which would correspond to the elimination of water from the protonated molecule, is in agreement with our prediction, because neither nitro group are adjacent to the methyl group. With decreasing drift tube voltage the protonated 3,4-DNT clusters with H_2O , leading to a reduction in the $DNTH^+$ signal. Whilst this is particularly significant in DC-only mode, with $DNTH^+(H_2O)_n$ ($n = 1, 2$ and 3) ions becoming the dominant product ions by about 100 Td, some water clustering is still observed in RF-mode. For example at a drift tube voltage of 20 V the percentage branching ratios are approximately 70%, 20% and 10 % for $DNTH^+$, $DNTH^+ \cdot H_2O$, and $DNTH^+ \cdot (H_2O)_2$, respectively.

For the 2,4- and 2,6-DNT isomers, at low drift tube voltages in addition to an observed ion at m/z 201 corresponding to the $DNTH^+ \cdot H_2O$ in RF-mode a product ion is observed at m/z 165, which is $[DNT-H_2O]H^+$. Figure 6.7 illustrates this for 2,6-DNT, which shows that the probability for the elimination of water increases with decreasing drift tube voltage (the results for 2,4-DNT in RF-mode are similar, although the production for $[DNT-H_2O]H^+$ is less by about 10%). In DC-only mode, m/z 165 is also observed for 2,6-DNT, but its intensity only becomes significant when a high drift tube voltage is applied leading to reduced electric fields above about 180 Td, and even then the percentage ion product distribution is only approximately 10% (figure 6.8). However, this can explain the slight increase in the production of m/z 165 in figure 6.7 when the applied drift tube voltage is above about 275 V. With increasing drift tube voltage additional fragment ions are found at m/z 136 and 91, corresponding to an elimination of HONO and $2NO_2$, respectively, from the protonated molecule. These two ions are also found with significant intensities for 2,6-DNT when operating in DC-only mode when the reduced electric fields is greater than about 160 Td. That $DNTH^+ \cdot H_2O$ is observed in RF mode at low drift tube voltages, when no protonated water clusters are observed (figure 6.2 (b)), requires some explanation. We propose that following a collision the energy involved is distributed in more degrees of freedom for $DNTH^+ \cdot H_2O$ than for $H_3O^+ \cdot (H_2O)_n$ and hence it is less likely for energy to be concentrated into losing the water molecule.

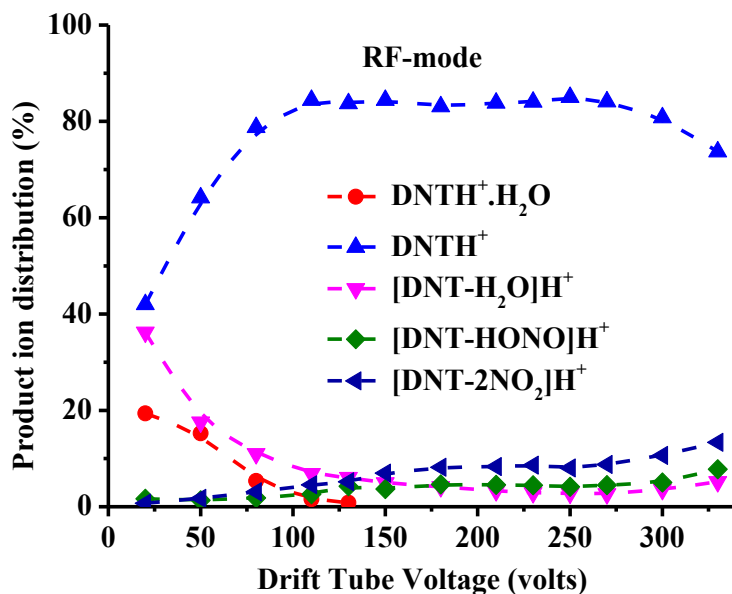


Figure 6.7. Percentage product ion distributions resulting from the reaction of H_3O^+ with 2,6-DNT in RF-mode including the secondary process resulting in the association of the protonated molecule with water as a function of supplied drift tube voltage.

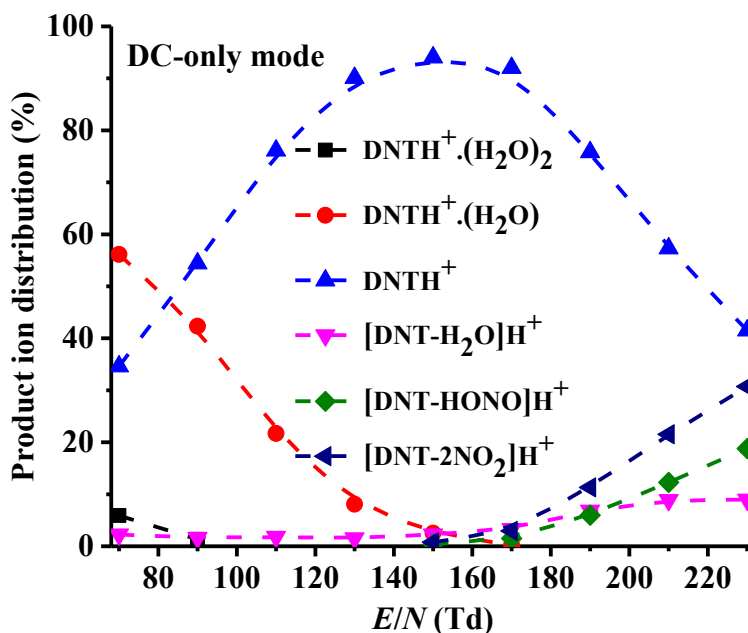


Figure 6.8. Percentage product ion distributions resulting from the reaction of H_3O^+ with 2,6-DNT in DC-only mode including the secondary process resulting in the association of the protonated molecule with water as a function reduced electric field.

Building on the comprehensive investigation of the TNT system we can go straight to the salient structures and energetics for the loss of water from 2,4-DNT and 2,6-DNT following proton transfer from H_3O^+ . These calculations are given in table 6.3 (a) and (b), respectively.

Table 6.3. Energetics for the elimination of water from (a) 2,4-DNT and (b) 2,6-DNT following proton transfer from H_3O^+ .

(a)

Products	ΔH_{298} kJ mol ⁻¹	ΔG_{298} kJ mol ⁻¹
2,4-DNTH ⁺ (syn) + H ₂ O	-89	-87
2,4-DNTH ⁺ (anti) + H ₂ O	-96	-95
TS syn/anti + H ₂ O	-21	-16
TS for loss of H ₂ O + H ₂ O	+126	+130
2,4-DNT-H ₂ O(c) + 2H ₂ O	-146	-187

(b)

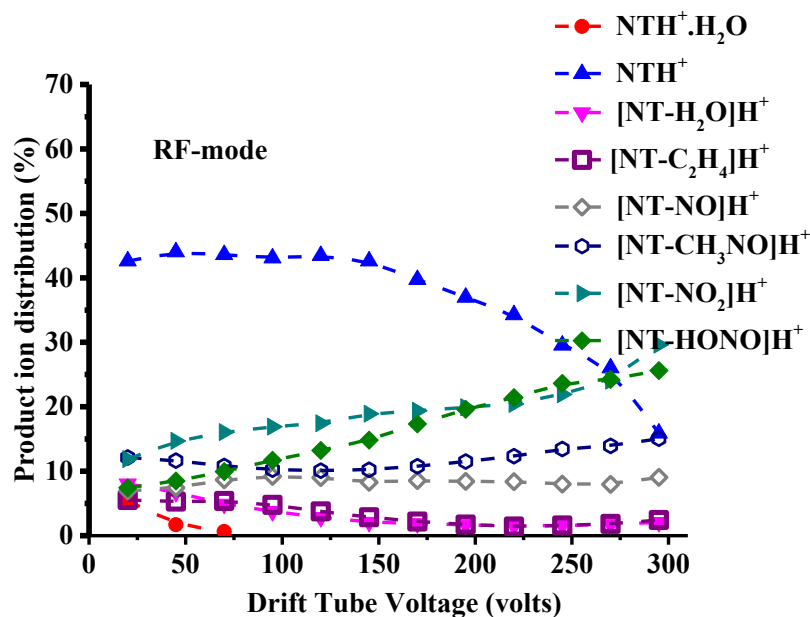
Products	ΔH_{298} kJ mol ⁻¹	ΔG_{298} kJ mol ⁻¹
2,6-DNTH ⁺ (syn) + H ₂ O	-87	-88
2,6-DNTH ⁺ (anti) + H ₂ O	-95	-95
TS syn/anti + H ₂ O	-42	-38
TS for loss of H ₂ O + H ₂ O	+117	+120
2,6-DNT-H ₂ O(c) + 2H ₂ O	-177	-217

6.4.4 Nitrotoluenes

In order to further investigate the requirement of methyl and nitro functional groups to be adjacent in order to facilitate the elimination of water when using the RFIF, the three isomers of nitrotoluene have been investigated. We can expect in RF-mode that only 2-NT should have a reaction pathway which would lead to the elimination of water following proton transfer from H_3O^+ . For 3-NT and 4-NT no such elimination should occur. A review of the resulting mass spectra for all three isomers shows that that is the case. However, the nitrotoluenes are more complicated than TNT and the DNTs, because other product ions are observed even at the lowest drift tube voltage. The NT isomers show significant fragmentation following proton transfer. This is found to occur in not only RF-mode but also

DC-only mode. In addition to the elimination of water, which is not the dominant product ion, channels corresponding to the elimination of C_2H_4 , NO , CH_3NO , NO_2 and $HONO$ are observed in both modes. This is illustrated in figure 6.9 for 2-NT when operating (a) in RF-mode and (b) in DC-only mode. At low drift tube voltages $NTH^+ \cdot H_2O$ is observed (figure 6.9(a)) in RF mode, presumably for reasons described above for DNT.

(a)



(b)

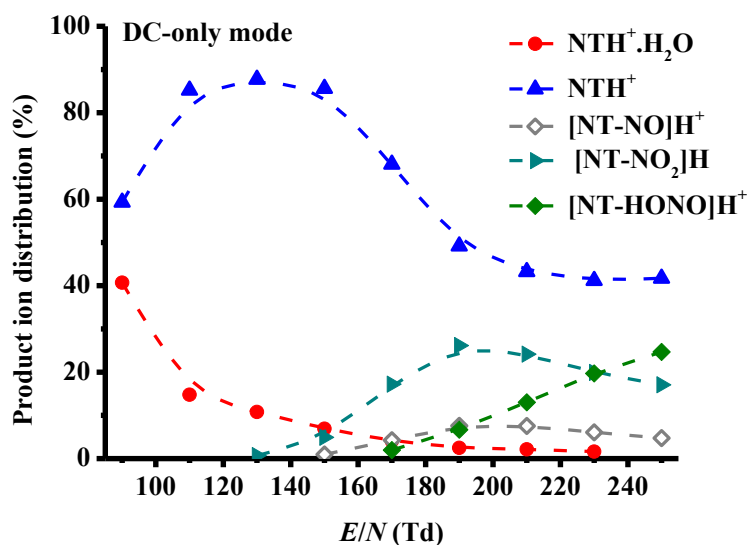


Figure 6.9. Percentage product ion distributions resulting from the reaction of H_3O^+ with 2-NT in (a) RF-mode and (b) DC-only mode as a function drift tube voltage. Included are the

secondary ion-molecule processes resulting in the association of the protonated molecule with water.

Table 6.4 presents the DFT energetics calculations for the elimination of water for 2-NT following proton transfer from H_3O^+ .

Table 6.4. Energetics for the elimination of water from 2-NT following proton transfer from H_3O^+ .

Products	ΔH_{298} kJ mol ⁻¹	ΔG_{298} kJ mol ⁻¹
2-NTH ⁺ (syn) + H ₂ O	-132	-138
2-NTH ⁺ (anti) + H ₂ O	-105	-110
TS syn/anti + H ₂ O	-71	-76
TS for loss of H ₂ O + H ₂ O	+82	+78
2-NT-H ₂ O + 2H ₂ O	-93	-126

6.5. Conclusions

A PTR-ToF-MS equipped with a radio frequency ion funnel, originally designed to improve sensitivity, has been used in an unusual way to induce fragmentation of product ions through changes in collisional induced dissociation. We have illustrated how this can be used to improve compound specificity by monitoring the ion signal in RF-mode. We propose that the rapid switching between RF and DC modes would be the best method to enhance selectivity. We are currently developing the instrument to achieve this, and this will be the subject of another paper. The key point of this work is that in place of major and costly changes in instrumental design to improve chemical specificity, such as having a high mass resolution time-of-flight mass spectrometer or adding a pre-separation technique, which also makes the instrument unacceptable for use in security areas, a new analytical method has been described which at its heart manipulates the ion chemistry.

6.6. Acknowledgements

We thank the Defence Science and Technology Laboratory for funding RGM. This project was in part supported by the PIMMS and IMPACT ITNs which are in turn supported by the

European Commission's 7th Framework Programme under Grant Agreement Numbers 287382 and 674911, respectively.

6.7. References

1. S. A. Shaffer, K. Tang, G. A. Anderson, D. C. Prior, H. R. Udseth and R. D. Smith, *Rapid Comm. Mass Spectrom.* **1997**, *11*, 1813.
2. Kelly, R. T., et al., *Mass Spectrom. Rev.* **2010**, *29* (2), 294.
3. Barber, S., et al., *Anal. Chem.* **2012**, *84* (12), 5387.
4. R.S. Blake, C. Whyte, C.O. Hughes, A.M. Ellis, P.S. Monks *Anal. Chem.* **2004**, *76*, 3841.
5. C.J. Ennis, J.C. Reynolds, B.J. Keely, L.J. Carpenter, *Int. J. Mass Spectrom.* **2005**, *247* (1–3), 72.
6. R. González-Méndez, D. F. Reich, S. J. Mullock, C. A. Corlett and C. A. Mayhew, *Int. J. Mass Spectrom.* **2015**, 385, 13.
7. A.M. Ellis, C.A. Mayhew, *Proton Transfer Reaction Mass Spectrometry: Principles and Applications*, first ed., John Wiley and Sons, 2014.
8. P. Brown, P. Watts, T. D. Märk, C. A. Mayhew, *Int. J. Mass Spectrom.* **2010**, *294*, 103.
9. P. Sulzer, F. Petersson, B. Agarwal, K. H. Becker, S. Jürschik, T. D. Märk, D. Perry, P. Watts, and C. A. Mayhew *Anal. Chem.* **2012**, *84*, 4161.
10. S. Jürschik, B. Agarwal, T. Kassebacher, P. Sulzer, C. A. Mayhew, T. D. Märk, *Journal of Mass Spectrom.* **2012**, *47*, 1092.
11. T. Kassebacher, P. Sulzer, S. Jürschik, E. Hartungen, A. Jordan, A. Edtbauer, S. Feil, G. Hanel, S. Jaksch, L. Märk, C. A. Mayhew, T. D. Märk. *Rapid Comm. Mass Spectrom.* **2013**, *27*, 325.
12. P. Sulzer, L. Märk, M. Lanza, S. Jürschik, B. Agarwal, T. D. Märk, R. González P. Watts, and C. A. Mayhew, *Int. J. Mass Spectrom.* **2013**, *354*, 123.
13. B. Agarwal, R. González-Méndez, M. Lanza, P. Sulzer, T. D. Märk, N. Thomas, and C. A. Mayhew *J. Phys. Chem. A* **2014**, *118*, 8829.
14. W. J. Acton, M. Lanza, B. Agarwal, S. Jurschik, P. Sulzer, K. Breiev, A. Jordan, E. Hartungen, G. Hanel, L. Märk, C. A. Mayhew, and T. D.Märk *Int. J. Mass Spectrom.* **2014**, *360*, 28.
15. M. Lanza, W. J. Acton, P. Sulzer, K. Breiev, S. Jürschik, A. Jordan, E. Hartungen, G. Hanel, L. Märk, T. D. Märk, and C. A. Mayhew *J. Mass Spectrom.* **2015**, *50*, 427.

16. DFT calculations were performed using the Gaussian 03 programme with the GaussView interface. (Gaussian 09, Revision A.02, M. J. Frisch, G. W. Trucks, H. B. Schlegel, G. E. Scuseria, M. A. Robb, J. R. Cheeseman, G. Scalmani, V. Barone, B. Mennucci, G. A. Petersson, H. Nakatsuji, M. Caricato, X. Li, H. P. Hratchian, A. F. Izmaylov, J. Bloino, G. Zheng, J. L. Sonnenberg, M. Hada, M. Ehara, K. Toyota, R. Fukuda, J. Hasegawa, M. Ishida, T. Nakajima, Y. Honda, O. Kitao, H. Nakai, T. Vreven, J. A. Montgomery, Jr., J. E. Peralta, F. Ogliaro, M. Bearpark, J. J. Heyd, E. Brothers, K. N. Kudin, V. N. Staroverov, R. Kobayashi, J. Normand, K. Raghavachari, A. Rendell, J. C. Burant, S. S. Iyengar, J. Tomasi, M. Cossi, N. Rega, J. M. Millam, M. Klene, J. E. Knox, J. B. Cross, V. Bakken, C. Adamo, J. Jaramillo, R. Gomperts, R. E. Stratmann, O. Yazyev, A. J. Austin, R. Cammi, C. Pomelli, J. W. Ochterski, R. L. Martin, K. Morokuma, V. G. Zakrzewski, G. A. Voth, P. Salvador, J. J. Dannenberg, S. Dapprich, A. D. Daniels, O. Farkas, J. B. Foresman, J. V. Ortiz, J. Cioslowski, and D. J. Fox, Gaussian, Inc., Wallingford CT, 2009.
17. C. A. Mayhew, P. Sulzer, F. Petersson, S. Haidacher, A. Jordan, L. Märk, P. Watts and T. D. Märk, *Int. J. Mass Spectrom.* **2010**, 289, 58.

CHAPTER 7

ENHANCING PROTON TRANSFER REACTION-MASS SPECTROMETRY SELECTIVITY USING RAPID REDUCED ELECTRIC FIELD SWITCHING

CONFIDENTIAL: Not for distribution.

For this study a paper is still in preparation. Presented here is a draft of the paper completed in February 2017.

Ramón González-Méndez,^{1*} P. Watts,¹ D. Fraser Reich,² Stephen J. Mullock,² Stuart Cairns,³ Peter Hickey,³ Matthew Brookes,⁴ and Chris A. Mayhew^{1,5}

1. Molecular Physics Group, School of Physics and Astronomy, University of Birmingham, Edgbaston, Birmingham, B15 2TT, UK
2. Kore Technology Ltd, Cambridgeshire Business Park, Ely, Cambridgeshire CB7 4EA, UK
3. Defence Science and Technology Laboratory, Fort Halstead, Sevenoaks, Kent, TN14 7BP, UK
4. Defence Science and Technology Laboratory, Porton Down, Salisbury, Wilshire SP4 0JQ, UK
5. Institut für Atemgasanalytik, Leopold-Franzens-Universität Innsbruck, Rathausplatz 4, 6850, Dornbirn, Austria

* Corresponding author: Tel.:+44 121 414 4668. E-mail: R.GonzalezMendez@bham.ac.uk.

Declaration of contribution

My contribution to the study described in this Chapter was designing the experiments, performing the experiments, interpreting the data and writing the manuscript jointly with the other co-authors.

7.1. Abstract

The fast response time and high sensitivity of Proton Transfer Reaction- Mass Spectrometry (PTR-MS) makes it a suitable analytical tool for detecting trace explosives. Selectivity is determined by the accuracy of determining the m/z of the product ions specific to a particular compound. In this paper we demonstrate how this specificity can be enhanced by changing the product ions produced (concentrations and types) by modifying the reduced electric field, which in turn modifies the collisional energies of the reagent and product ions. Further, we demonstrate a novel approach to rapidly change the reduced electric field, which permits any compound, such as an explosive, which will only be present in the reaction region for seconds to be thoroughly interrogated. We have specifically developed hardware and software which permits the reaction region's voltage to be rapidly switched (< 250 ms at a frequency of 0.1-5 Hz). We show how this technique provides a higher confidence in the identification of compounds than is possible by keeping to one reduced electric field value. Although demonstrated for explosives, this new technique has applications in other analytical areas and disciplines, and in particular where there could be rapid changes in a compounds concentration, e.g. in the atmosphere or in breath. Importantly it provides a method for improved selectivity without expensive instrumental changes.

7.2. Introduction

Proton Transfer Reaction-Mass Spectrometry (PTR-MS) is a broad-based technique that has proved its analytical use in many fields including atmospheric chemistry, food science, breath analysis and Homeland Security.¹ Within the Homeland Security area, PTR-MS is capable of detecting a wide range of dangerous substances, and a number of studies have been published dealing with chemical warfare agents, illicit drugs and explosives.²⁻¹⁸ A key criterion for any analytical instrumentation is sensitivity. The high sensitivity of PTR-MS, which can now reached levels of parts per quadrillion by volume in seconds, permits the relatively easy detection of many chemical compounds in trace amounts. Whilst high sensitivity is necessary, high selectivity is also required so that chemical compounds can be identified with a high level of confidence in real-time. High chemical specificity is of considerable importance to the military, to emergency responders and for applications in security areas such as airports, harbours and train stations.

Without a pre-separation stage (e.g. a fast GC stage), PTR-MS relies on the m/z of the product ions to identify a chemical compound. This of course results in uncertainty in identification. Fast GC systems are being developed for use with PTR-MS, but these take away a major advantage of PTR-MS, namely real-time measurements. A possible way to improve selectivity without losing the real time capability advantage of PTR-MS is to manipulate the ion chemistry occurring in the reaction chamber. Thus different product ions (or changes in their intensities) can be used to aid in the identification. A number of methods to achieve this have been proposed and adopted. One includes using different reagent ions, e.g. changing from H_3O^+ (proton transfer reactions) to O_2^+ (charge transfer),¹³ which is achieved by switching the reagent gas from water to air, although given that different product ions are observed there is no obvious advantage in switching reagent ions as is currently done, but to have both (or more) reagent ions injected into the reaction chamber simultaneously. A more recent proposition to improve selectivity is the use of a RF ion funnel system to enhance collisional induced dissociation.¹⁸ Changes in collisional induced dissociation can also be achieved by changing the reduced electric field, which is the key parameter in PTR-MS, and is the ratio of the electric field E in the drift tube to the total number density N . By changing the reduced electric field from a low value (e.g. 80 Td) to a high value (e.g. 200 Td), differences in product ion distributions, or vice versa, will occur, which can aid in the identification of the trace neutral responsible for those ions. This approach was used in the

early investigations using PTR-MS,^{19,20} where changes in the reduced electric field were used to distinguish isomeric compounds. More recent examples exploiting this technique can be found in the literature,²¹⁻²³ and this same approach was used by González-Méndez *et al.* to discriminate between nitro-glycerine (NG) and the isobaric compound 2,4,6-trinitrotoluene (TNT).¹⁷ For that study the drift tube voltage was changed manually. However, for the switching of the reduced electric field to be analytically useful, particularly for areas of applications where the samples are present in the reaction chamber of a PTR-MS for short periods of time, e.g. a breath sample or rapid (< 10 s) thermally desorbed materials, the reduced electric field needs to be changed rapidly (1 Hz or better). The simplest way to provide a rapid change in E/N is to alter the E field by quickly changing the voltage applied across the drift tube. In this paper we present details on a collaborative project involving KORE Technology Ltd. and the University of Birmingham on new hardware and software modifications for such a purpose. We illustrate the application of this new development to a number of explosive, or explosive related compounds, namely 2,4- and 2,6-dinitrotoluene (2,4- and 2,6-DNT, m/z 182, $C_7H_6N_2O_4$), hexamethylene triperoxide diamine (HMTD, m/z 208, $C_6H_{12}N_2O_6$), 1,3,5-trinitroperhydro-1,3,5-triazine (RDX, m/z 222, $C_3H_6N_6O_6$), and pentaerythritol tetranitrate (PETN, m/z 316, $C_5H_8N_4O_{12}$). Finally, the combined operation of a radio frequency ion-funnel PTR-MS and fast drift tube voltage switching is exemplified for 2,4,6-trinitrotoluene (TNT, m/z 227, $C_7H_5N_3O_6$).

7.3. Experimental Details

7.3.1 Proton Transfer Reaction Mass Spectrometry (PTR-MS)

A KORE Technology Ltd. Proton Transfer Reaction-Time of Flight-Mass Spectrometry (PTR-ToF-MS) was used, details of which have been comprehensively described elsewhere.^{24,25} In brief, a needle valve is used to introduce water vapour from a container into a hollow cathode discharge source where, after ionisation via electron impact and subsequent ion-molecule processes, the terminal reagent ions, H_3O^+ , are produced in high quantities. These ions are transferred from the ion source into the reaction chamber, the drift tube (DT), of the PTR-ToF-MS, where they encounter the analyte. H_3O^+ reacts with an analyte M through proton transfer, providing M has a proton affinity greater than that of water ($PA(H_2O) = 691 \text{ kJ mol}^{-1}$). This process can be non-dissociative (resulting in the protonated parent

molecule MH^+) and/or dissociative. Dissociative proton transfer results in product ions which, depending on their m/z values, may be useful for the identification of a compound. Fragmentation may be spontaneous upon proton transfer or may require additional energy which is supplied through collisions with the buffer gas during the migration of the product ions down the drift tube under the influence of the electric field, E .

This instrument's DT also incorporates a radio-frequency ion funnel (RFIF), described in detail elsewhere.^{18, 26} The RFIF consists of 29 stainless steel plates of 0.2 mm thickness, mounted on precision-machined ceramic rods at an even spacing of 3.2 mm per plate. Tabs on the electrodes permit a resistor chain on a ceramic strip to be connected in addition to two capacitor stacks which allow the RF to be applied to the second half of the reactor. The orifice diameters of the plates through the first half of the stack is 40 mm, as used in the standard drift tube reactor. In the second half of the DT the orifice diameter steadily decreases to 6 mm at the final plate before the exit orifice. Across the complete ion-funnel a DC voltage is applied driving ions axially. When just operating with this voltage we shall refer to the instrument as operating in DC-only mode. To the second part of the drift tube a RF field can be applied. The resonant frequency used is ~760 kHz and the voltage amplitude (peak-to-peak) is 200 V. The RF field is superimposed on the DC voltage gradient across the complete drift tube. We shall refer to operating the instrument with the RF on as RF-mode. At the end of the drift tube is a 400 μm orifice, through which a sample of the reagent and product ions enter the ion transfer region to the time-of-flight mass spectrometer for detection.

7.3.2 Fast reduced electric field switching

New electronics were developed by Kore Technology for the purpose of providing fast reduced electric field switching that could be retrofitted onto the Kore PTR-ToF-MS. The fast reduced electric field switching is accomplished by software control of a programmable +500 volts power supply unit (PSU) which can be controlled over the range 50 to 450 volts (covering typically the E/N range of between approximately 10 and 250 Td). It is possible to switch the output voltage according to the two required E/N values. This output voltage is computer controlled by using a serial digital-to-analogue converter to convert the binary signal from the computer into a control voltage for the power supply. In addition to the voltage control, the software also provides the facility to alter the frequency of switching between two voltages, whereby the first E/N value initially appears as a binary number on the

serial port of the computer. This is then converted by the serial digital-to-analogue converter to the control voltage required to cause the output voltage of the PSU to give the first required E/N value. After a time delay, set by the switching frequency (up to 5 Hz), a second binary value is then outputted onto the serial port to similarly provide a second E/N value. In addition to this, a floating +300 volts PSU provides the voltage gradient for the source drift (SD) region of the PTR source. This is required owing to the change in power supply configuration to drive the PTR entry voltage directly. The software automatically switches between two pre-set E/N values, and the data acquisition system records the intensity of the selected ions at the E/N values as a function of time.

7.3.3 Operational parameters

Sampling of the explosives was done through the use of PTFE swabs (ThermoFisher Scientific) and a Kore Technology Ltd. thermal desorption unit (TDU), specifically designed for use with PTR-MS, connected to the inlet of the drift tube. Details of the TDU have been given elsewhere.¹⁷ PTFE swabs, onto which known quantities of explosives were deposited, were placed into the TDU. The swabs came prepared from the manufacturer mounted on rectangular cardboard for easy insertion into the TDU. Once a seal was created, a carrier gas (in this study laboratory air) is heated to the temperature of the TDU before it flows through a series of holes in a heated metal plate. This heated air then passes through the swab and into the inlet system driving any desorbed material through to the drift tube creating a concentration “pulse” of typically between 10 – 20 seconds of an explosive in the drift tube.¹⁷ Triplicated averaged measurements, background subtracted, have been used all throughout.

Passivated (Silkonert®) stainless steel inlet lines were used in order to minimise adsorption effects. All measurements were taken under the same operational conditions. The TDU, inlet tubing and drift tube were maintained at 150°C. The drift tube pressure was set at 1.1 mbar. The only variable was the operating drift tube voltage, which was changed to provide the appropriate reduced electric fields to yield the product ion(s) of interest for each explosive investigated.

The acquisition time per point was set to 40 msec. Such short acquisition times imply that ion counts fluctuations will be at the level of 15 to 20% due to ion count statistics. For each individual cycle averaged values has been represented.

7.3.4 Explosive compounds

Explosive standards were purchased from AccuStandard Inc., New Haven, CT. and diluted in the appropriate solvent(s) (HPLC grade) to provide the required quantity that was then spotted onto the swabs prior to their insertion into the TDU.

7.4. Results and Discussion

7.4.1 Reagent ions

Before introducing an analyte using a thermal desorption unit containing a swab that is contaminated with a trace of an explosive, it is important to know the time constants associated with the rise and decay in ion signal intensities given that the drift tube voltage is rapidly (< 1 microsecond, μs) switched. It is to be expected that there will be an electronic time constant owing to the resistors and capacitors used in the drift tube. To investigate this we examined the temporal profile of the protonated water H_3O^+ (m/z 19) and the dimer and trimer water clusters, $\text{H}_3\text{O}^+\cdot\text{H}_2\text{O}$ (m/z 37) and $\text{H}_3\text{O}^+\cdot(\text{H}_2\text{O})_2$ (m/z 55), respectively. These were chosen because their individual concentrations in the drift tube are very sensitive to the E/N value used. For example at 90 Td protonated water clusters are the dominant reagent ions, whereas at 180 Td these have negligible intensities because the collisions occurring in the drift tube are sufficient to break-up protonated water clusters to the H_3O^+ monomer. Figure 1 shows an average of 2 cycles of measurements, switching between 180 Td and 80 Td at a frequency of approximately 1 Hz, starting with 180 Td at $t = 5\text{s}$. The relative ion intensities in this figure (and all subsequent ones) are obtained by averaging the product ion intensities over a cycle once the signal has reached its maximum intensity (plateau region). The figure shows that although the supply voltage can be changed rapidly (1 micro second) the drift tube does not respond on that timescale, as apparent from ions distributions. As mentioned above this is a result of a RC time constant associated with the drift tube. The reactor electrode stack is biased via a string of 1 M Ω resistors and there are a number of coupling capacitors for the RF funnel operation. This time constant (around 200 ms) limits the switching frequency to about 5 Hz. However, we will demonstrate that that is more than adequate for applications to explosive detection.

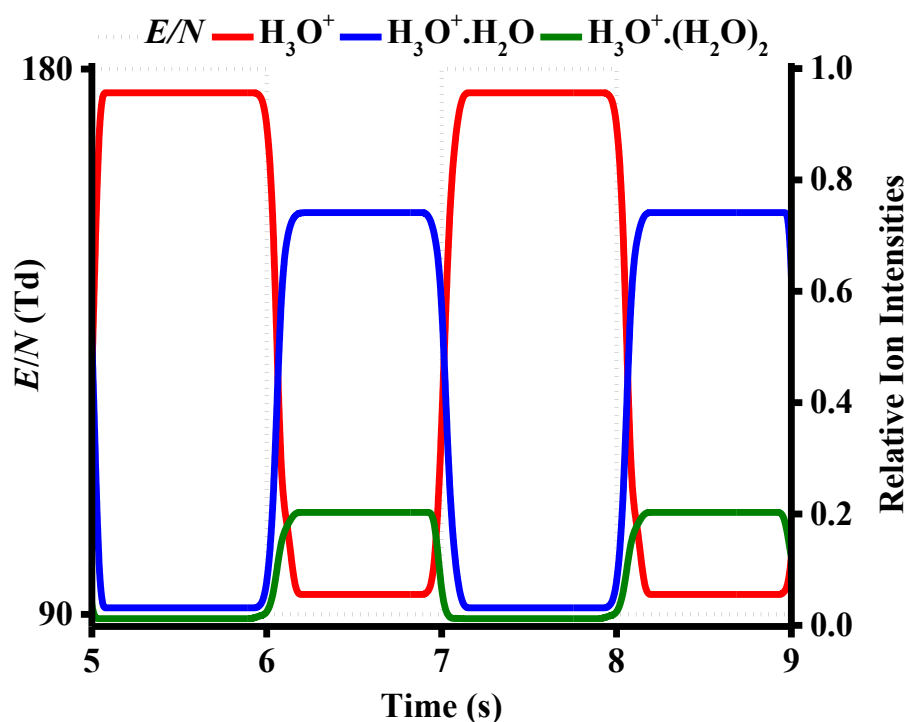


Figure 7.1. Changes in the protonated water and protonated water clusters intensities as E/N is switched between 180 Td and 90 Td at a frequency of 1 Hz. The rise and decay times of the reagent ions are greater than the time it takes to switch the voltage supply (less than a microsecond) owing to an RC time constant associated with the drift tube.

7.4.2 Explosive compounds

For any given explosive, it is necessary to ascertain the dependence of the product ion intensities as a function of E/N , and hence determine which two E/N values should be used to enhance selectivity. The dependences of the product ion distributions (PID) on E/N are reported for 2,4-DNT, HMTD, RDX and PETN.

7.4.2.1. 2,4- and 2,6 dinitrotoluene ($C_7H_6N_2O_4$)

Figure 2 shows the percentage product ion distribution (PID) plot as a function of E/N for (a) 2,4-DNT and (b) 2,6-DNT. (The product ion branching ratios for 2,6-DNT have recently been published in another paper dealing with the applications of a radio frequency field in the drift tube.¹⁸ However, for ease of comparison with the 2,4-DNT isomer the results are reproduced

in this paper. The only difference is that second water cluster ($2,6\text{-DNTH}^+(\text{H}_2\text{O})_2$) is not shown in figure 2(b), because its intensity is insignificant.) From figures 2(a) and (b) it can be seen that monitoring the two product ions at m/z 183 (the protonated parent) and 201 ($\text{DNTH}^+\text{H}_2\text{O}$) is sufficient for assigning 2,4-DNT, but that the presence of m/z 136 (elimination of HONO) and 91 (elimination of two nitro groups) at the high E/N setting indicates the presence of 2,6-DNT. The common ion at m/z 165 results from the elimination of H_2O from the protonated parent, observed for both isomers at high reduced electric field values, cannot be used to differentiate the isomers.¹⁸ Using selected ions a summary of results from the fast switching experiment for 2,4-DNT and 2,6-DNT are shown in figure 3.

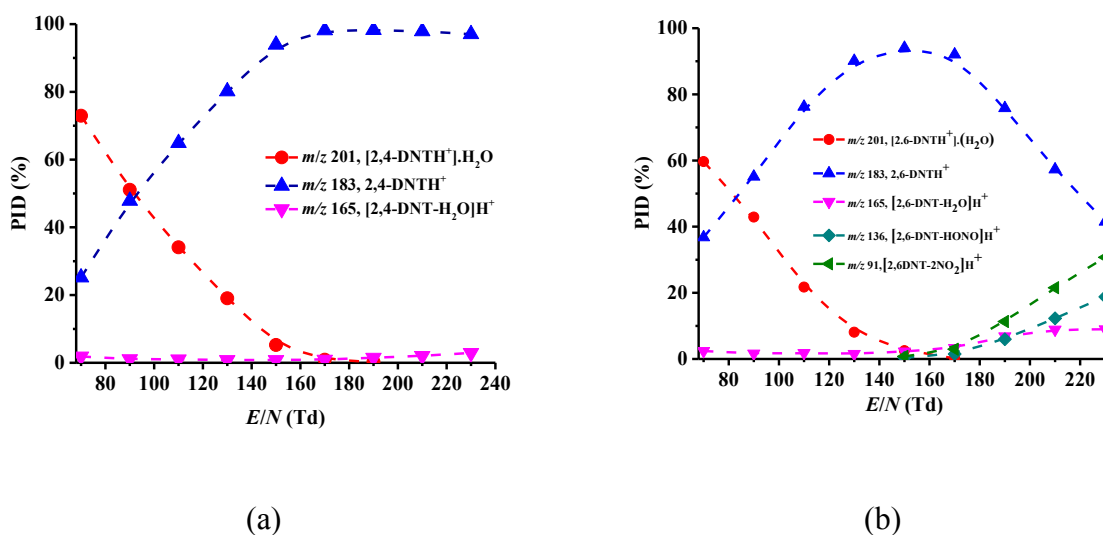


Figure 7.2. (a) Percentage product ion distribution (PID) results for (a) 2,4-DNT and (b) 2,6-DNT as a function of reduced electric field (70 to 230 Td).

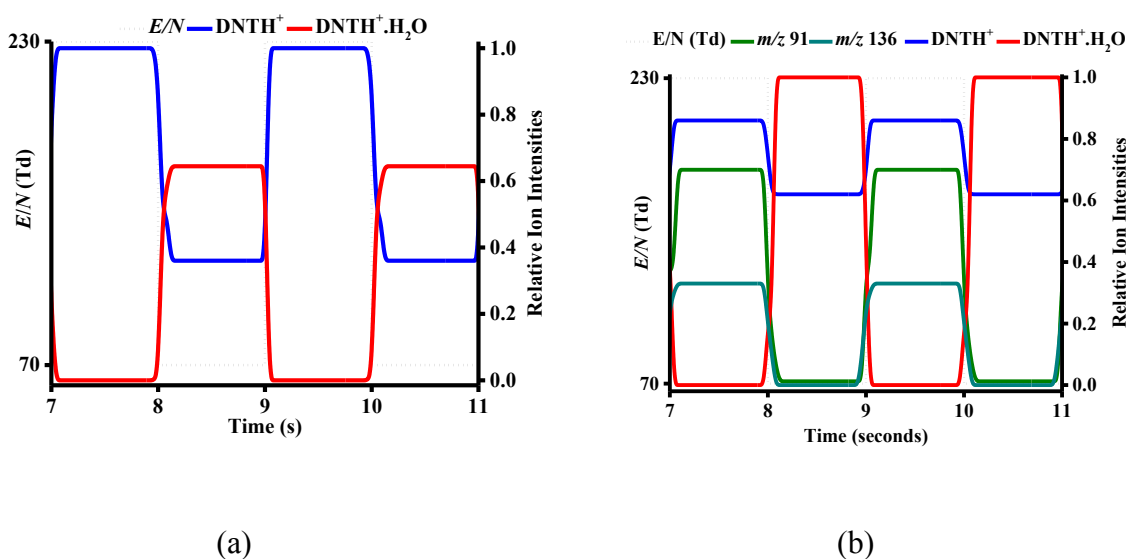


Figure 7.3. 1 Hz E/N switching between 70 Td and 230 Td for (a) 2,4-DNT and (b) 2,6-DNT.

7.4.2.2- HMTD ($C_6H_{12}N_2O_6$)

Figure 4 (a) shows the PID for HMTD as a function of the reduced electric field. Product ions are observed at m/z 46, 74, 88, 179 and 209. The ions at m/z 88 and m/z 179 have negligible intensities at all E/N values. m/z 209 is the protonated parent, but has a reasonable intensity at low E/N (90 Td). m/z 179 corresponds to the loss of formaldehyde (CH_2O) from the protonated parent, leaving a $C_5H_{10}N_2O_5H^+$ ion. m/z 88 corresponds to $C_3H_6NO_2^+$ and m/z 74 to $C_2H_4NO_2^+$. The ions that dominate are m/z 46 (CH_4NO^+) and m/z 74 ($C_2H_4NO_2^+$). Note that we can rule out m/z 46 being NO_2^+ , because its m/z is at 46.006, whereas the m/z for CH_4NO^+ is 46.029, which we can separate because of the mass resolution available with the time of flight mass spectrometer used. From the PID we propose that it is sufficient to monitor m/z 46, 74 and 209 for assignment of HMTD. The switching results for these three product ions are shown in figure 4(b).

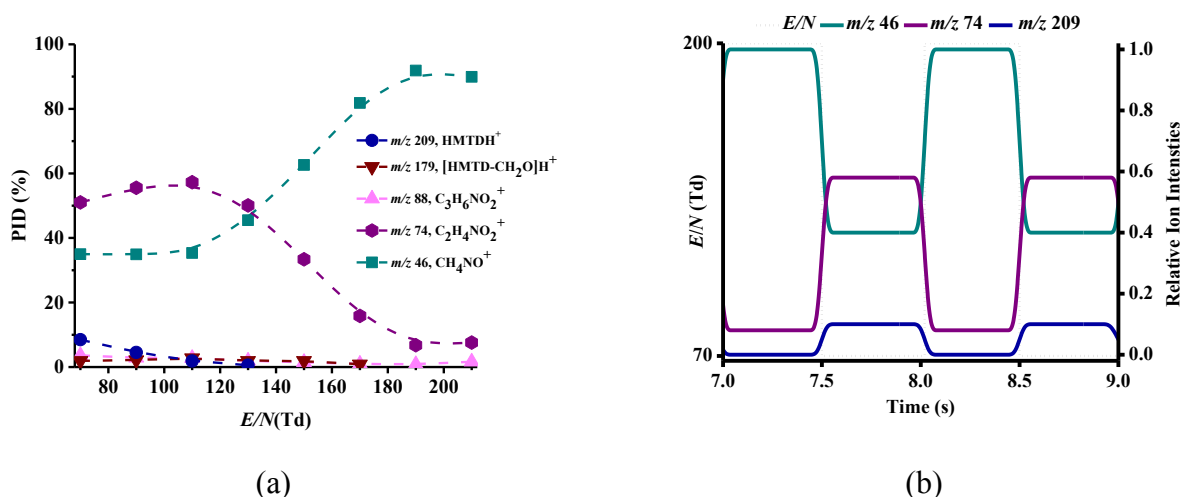


Figure 7.4.(a) PID as a function of reduced electric field covering the range 70-210 Td and (b) reduced electric field 2 Hz switching plots for HMTD.

7.4.2.3- RDX (C₃H₆N₆O₆)

Figure 5 (a) shows the PID for RDX as a function of E/N . Major product ions are observed are at m/z 46 (NO₂⁺) and m/z 75 (CH₃N₂O₂⁺). m/z 75 dominates at low E/N whereas m/z 46 dominates at high E/N . Another product ion is also observed at m/z 176 ([RDX-HONO]H⁺), but at a low intensity compared to the other two product ions. At the lowest E/N an ion is observed at m/z 241, which is RDXH⁺.H₂O. It is surprising that no protonated monomer is observed. We propose that as the reduced electric field is increased to the stage where no clustering occurs the protonated parent has too much internal energy for it to survive before detection. We found that the relative intensities of the RDX product ions are very sensitive to the operating temperatures, and hence product ion branching ratios would have to be obtained for different operating temperatures. For our operating conditions, we conclude that m/z 46, 75 and 241 are sufficient to detect the presence of RDX. Figure 5(b) shows the reduced electric field switching results for 70 Td and 170 Td.

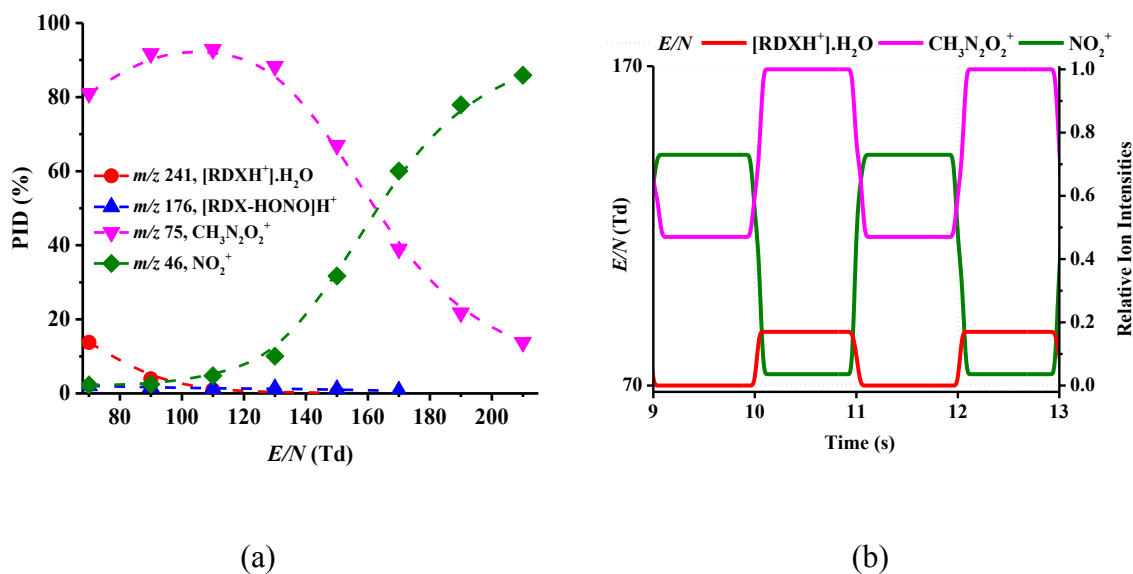


Figure 7.5. (a) PID as a function of reduced electric field covering the range 70-210 Td and (b) reduced electric field 1 Hz switching plots for RDX

7.4.2.4- PETN ($\text{C}_5\text{H}_8\text{N}_4\text{O}_{12}$)

The dominant product ions resulting from the reaction of H_3O^+ with PETN are the protonated parent at m/z 317 and NO_2^+ at m/z 46. Other product ions are observed at m/z 85, 87 and 182. m/z 85 and 87 ion intensities are low (less than about 3%) and are therefore not included in the PID for PETN (figure 6(a)). m/z 182 is assigned to be $\text{C}_4\text{H}_8\text{NO}_7^+$, which requires the elimination of HONO, NO_2 and CNO from the protonated parent. The results of the fast reduced electric field switching for PETN using the product ions at m/z 317, 182 and 46 are summarised in figure 6(b).

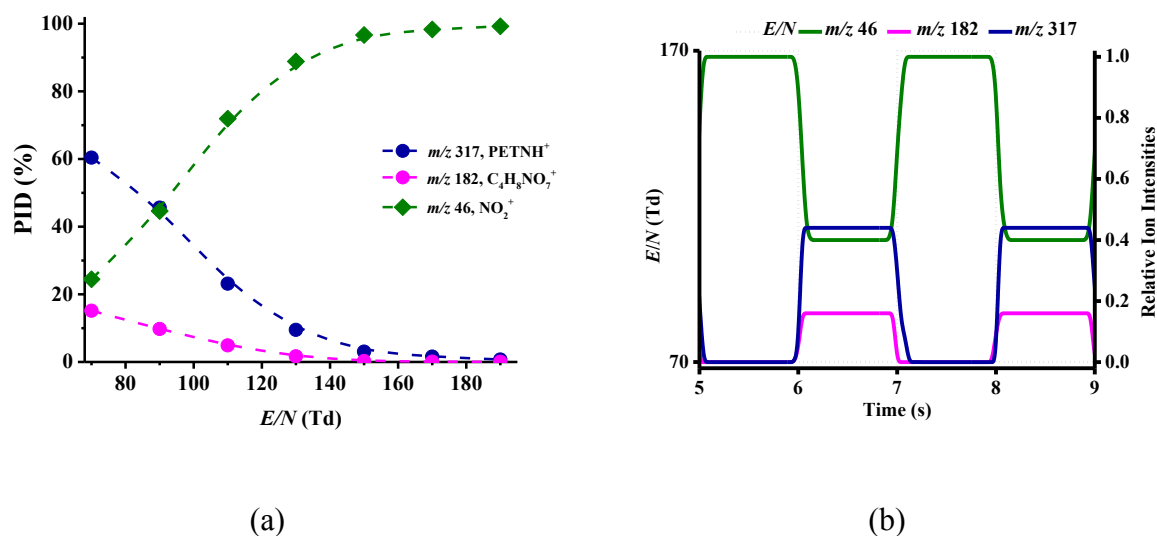


Figure 7.6. (a) PID as a function of reduced electric field covering the range 70-190 Td and (b) reduced electric field 1 Hz switching plots for PETN.

7.4.3 Combination of switching the drift tube DC voltage and the radio frequency ion funnel: an application to TNT

Recently, a radio frequency ion funnel-drift tube (RFIF-DT) has been employed in a novel way to modify the product ions resulting from the reaction of H_3O^+ with TNT through collisional induced dissociation.¹⁸ In DC-only mode, and for all E/N values investigated, TNT leads to only one product ion, namely protonated TNT at m/z 228.⁸ However, in RF-mode, another fragment ion is observed at m/z 210, corresponding to the elimination of water from the protonated parent,¹⁸ the intensity of this product ion increases relative to the protonated parent with decreasing drift tube voltage (i.e. decreasing E/N in DC mode) down to values under which the PTR-ToF-MS does operate in DC mode. The dominance of m/z 210 at low drift tube voltages is a result of the protonated molecule spending a longer time in the RF region of the drift tube. Through collisional processes this allows it to gain sufficient internal energy until it can eliminate H_2O . Here we illustrate how improved selectivity can be achieved by combining RF-mode with fast drift tube voltage switching for TNT (figure 7). We propose that by combining the RFIF and drift tube voltage switching techniques an even higher confidence in the assignment of an analyte in complex chemical environments is possible.

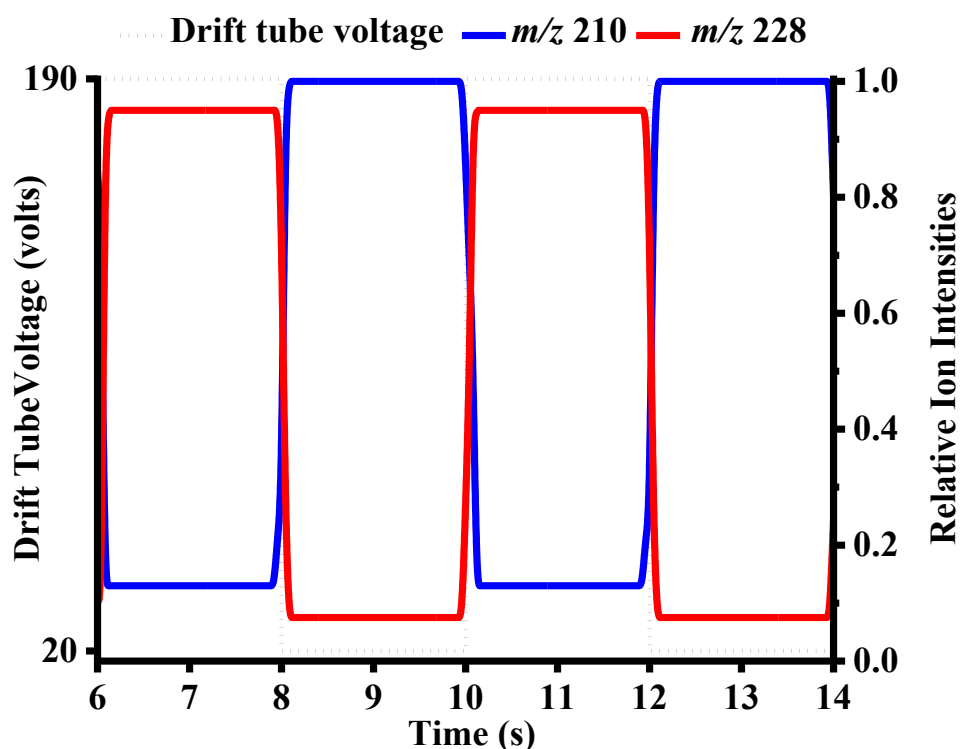


Figure 7.7. Application of combining radio frequency and fast drift tube voltage switching at 0.5 Hz between 20 and 190 V (equivalent to 30 and 180 Td in DC-mode only) for TNT.

7.5. Conclusions

We have successfully implemented a new hardware and software development for the rapid switching of the reduced electric field, E/N , within 200-250 ms at frequencies of 0.5-5 Hz in the drift tube of a KORE Technology PTR-ToF-MS. This results in the modification of product ions from the reactions of reagent ions with chemicals through changes in collisional energies. We have demonstrated in this paper how this technique provides an improved selectivity for explosives, thereby leading to a higher confidence in their identification in complex chemical environments. This switching of reduced electric field makes full use of the real-time measurement capabilities of PTR-MS and adds a new dimension to the analytical technique.

Although demonstrated for explosive compounds, this innovation has applications outside of those for homeland security and can be used for any other sampling protocol.

Finally, we have shown how the combination of the new drift tube voltage switching capabilities with RFIF provides further improvement in selectivity for TNT. This combination of switching capabilities and RFIF to PTR-MS opens up other possibilities for improved selectivity at little cost to the manufacture of the PTR-MS instrument.

7.6. Acknowledgements

We thank the Defence Science and Technology Laboratory for funding RGM under DSTL R-Cloud–Contract Number: DSTLX-1000096588 (Task Number: R1000100031). This research is part supported through a Marie Skłodowska-Curie Actions Innovative Training Network “IMPACT” supported by the European Commission’s HORIZON 2020 Programme under Grant Agreement Number 674911. The authors wish to thank Mahroz Mirzahekmati for producing the graphical abstract.

7.7. References

1. Andrew M. Ellis, Chris A. Mayhew., *Proton Transfer Reaction Mass Spectrometry: Principles and Applications*. 1st ed.; Wiley: 2014; p 336.
2. Cordell, R. L.; Willis, K. A.; Wyche, K. P.; Blake, R. S.; Ellis, A. M.; Monks, P. S., Detection of Chemical Weapon Agents and Simulants Using Chemical Ionization Reaction Time-of-Flight Mass Spectrometry. *Analytical Chemistry* **2007**, *79* (21), 8359-8366.
3. Shen, C.; Li, J.; Han, H.; Wang, H.; Jiang, H.; Chu, Y., Triacetone triperoxide detection using low reduced-field proton transfer reaction mass spectrometer. *International Journal of Mass Spectrometry* **2009**, *285* (1–2), 100-103.
4. Petersson, F.; Sulzer, P.; Mayhew, C. A.; Watts, P.; Jordan, A.; Märk, L.; Märk, T. D., Real-time trace detection and identification of chemical warfare agent simulants using recent advances in proton transfer reaction time-of-flight mass spectrometry. *Rapid Communications in Mass Spectrometry* **2009**, *23* (23), 3875-3880.
5. Mayhew, C. A.; Sulzer, P.; Petersson, F.; Haidacher, S.; Jordan, A.; Märk, L.; Watts, P.; Märk, T. D., Applications of proton transfer reaction time-of-flight mass spectrometry for the sensitive and rapid real-time detection of solid high explosives. *International Journal of Mass Spectrometry* **2010**, *289* (1), 58-63.

6. Jürschik, S.; Sulzer, P.; Petersson, F.; Mayhew, C. A.; Jordan, A.; Agarwal, B.; Haidacher, S.; Seehauser, H.; Becker, K.; Märk, T. D., Proton transfer reaction mass spectrometry for the sensitive and rapid real-time detection of solid high explosives in air and water. *Anal Bioanal Chem* **2010**, *398* (7-8), 2813-2820.
7. Agarwal, B.; Petersson, F.; Jürschik, S.; Sulzer, P.; Jordan, A.; Märk, T. D.; Watts, P.; Mayhew, C. A., Use of proton transfer reaction time-of-flight mass spectrometry for the analytical detection of illicit and controlled prescription drugs at room temperature via direct headspace sampling. *Anal Bioanal Chem* **2011**, *400* (8), 2631-2639.
8. Sulzer, P.; Petersson, F.; Agarwal, B.; Becker, K. H.; Jürschik, S.; Märk, T. D.; Perry, D.; Watts, P.; Mayhew, C. A., Proton Transfer Reaction Mass Spectrometry and the Unambiguous Real-Time Detection of 2,4,6 Trinitrotoluene. *Analytical Chemistry* **2012**, *84* (9), 4161-4166.
9. Jürschik, S.; Agarwal, B.; Kassebacher, T.; Sulzer, P.; Mayhew, C. A.; Märk, T. D., Rapid and facile detection of four date rape drugs in different beverages utilizing proton transfer reaction mass spectrometry (PTR-MS). *Journal of Mass Spectrometry* **2012**, *47* (9), 1092-1097.
10. Sulzer, P.; Jürschik, S.; Agarwal, B.; Kassebacher, T.; Hartungen, E.; Edtbauer, A.; Petersson, F.; Warmer, J.; Holl, G.; Perry, D.; Mayhew, C.; Märk, T., Designer Drugs and Trace Explosives Detection with the Help of Very Recent Advancements in Proton-Transfer-Reaction Mass Spectrometry (PTR-MS). In *Future Security*, Aschenbruck, N.; Martini, P.; Meier, M.; Tölle, J., Eds. Springer Berlin Heidelberg: 2012; Vol. 318, pp 366-375.
11. Kassebacher, T.; Sulzer, P.; Jürschik, S.; Hartungen, E.; Jordan, A.; Edtbauer, A.; Feil, S.; Hanel, G.; Jaksch, S.; Märk, L.; Mayhew, C. A.; Märk, T. D., Investigations of chemical warfare agents and toxic industrial compounds with proton-transfer-reaction mass spectrometry for a real-time threat monitoring scenario. *Rapid Communications in Mass Spectrometry* **2013**, *27* (2), 325-332.
12. Lanza, M.; Acton, W. J.; Jürschik, S.; Sulzer, P.; Breiev, K.; Jordan, A.; Hartungen, E.; Hanel, G.; Märk, L.; Mayhew, C. A.; Märk, T. D., Distinguishing two isomeric mephedrone substitutes with selective reagent ionisation mass spectrometry (SRI-MS). *Journal of Mass Spectrometry* **2013**, *48* (9), 1015-1018.
13. Sulzer, P.; Agarwal, B.; Jürschik, S.; Lanza, M.; Jordan, A.; Hartungen, E.; Hanel, G.; Märk, L.; Märk, T. D.; González-Méndez, R.; Watts, P.; Mayhew, C. A., Applications of

switching reagent ions in proton transfer reaction mass spectrometric instruments for the improved selectivity of explosive compounds. *International Journal of Mass Spectrometry* **2013**, 354–355 (0), 123-128.

14. Acton, W. J.; Lanza, M.; Agarwal, B.; Jürschik, S.; Sulzer, P.; Breiev, K.; Jordan, A.; Hartungen, E.; Hanel, G.; Märk, L.; Mayhew, C. A.; Märk, T. D., Headspace analysis of new psychoactive substances using a Selective Reagent Ionisation-Time of Flight-Mass Spectrometer. *International Journal of Mass Spectrometry* **2014**, 360 (0), 28-38.

15. Agarwal, B.; González-Méndez, R.; Lanza, M.; Sulzer, P.; Märk, T. D.; Thomas, N.; Mayhew, C. A., Sensitivity and Selectivity of Switchable Reagent Ion Soft Chemical Ionization Mass Spectrometry for the Detection of Picric Acid. *The Journal of Physical Chemistry A* **2014**, 118 (37), 8229-8236.

16. Lanza, M.; Acton, W. J.; Sulzer, P.; Breiev, K.; Jürschik, S.; Jordan, A.; Hartungen, E.; Hanel, G.; Märk, L.; Märk, T. D.; Mayhew, C. A., Selective reagent ionisation-time of flight-mass spectrometry: a rapid technology for the novel analysis of blends of new psychoactive substances. *Journal of Mass Spectrometry* **2015**, 50 (2), 427-431.

17. González-Méndez, R.; Reich, D. F.; Mullock, S. J.; Corlett, C. A.; Mayhew, C. A., Development and use of a thermal desorption unit and proton transfer reaction mass spectrometry for trace explosive detection: Determination of the instrumental limits of detection and an investigation of memory effects. *International Journal of Mass Spectrometry* **2015**, 385, 13-18.

18. González-Méndez, R.; Watts, P.; Olivenza-León, D.; Reich, D. F.; Mullock, S. J.; Corlett, C. A.; Cairns, S.; Hickey, P.; Brookes, M.; Mayhew, C. A., Enhancement of compound selectivity using a radio frequency ion-funnel proton transfer reaction mass spectrometer: improved specificity for explosive compounds. *Analytical Chemistry* **2016**, 88 (21), 10624-10630.

19. Hansel, A.; Jordan, A.; Holzinger, R.; Prazeller, P.; Vogel, W.; Lindinger, W., Proton transfer reaction mass spectrometry: on-line trace gas analysis at the ppb level. *International Journal of Mass Spectrometry and Ion Processes* **1995**, 149–150 (0), 609-619.

20. Lindinger, W.; Hansel, A.; Jordan, A., On-line monitoring of volatile organic compounds at pptv levels by means of proton-transfer-reaction mass spectrometry (PTR-MS) medical applications, food control and environmental research. *International Journal of Mass Spectrometry and Ion Processes* **1998**, 173 (3), 191-241.

21. Fortner, E. C.; Knighton, W. B., Quantitatively resolving mixtures of isobaric compounds using chemical ionization mass spectrometry by modulating the reactant ion composition. *Rapid Communications in Mass Spectrometry* **2008**, *22* (16), 2597-2601.
22. Shen, C.; Li, J.; Wang, Y.; Wang, H.; Han, H.; Chu, Y., Discrimination of isomers and isobars by varying the reduced-field across drift tube in proton-transfer-reaction mass spectrometry (PTR-MS). *International Journal of Environmental Analytical Chemistry* **2011**, *92* (3), 289-301.
23. Misztal, P. K.; Heal, M. R.; Nemitz, E.; Cape, J. N., Development of PTR-MS selectivity for structural isomers: Monoterpenes as a case study. *International Journal of Mass Spectrometry* **2012**, *310*, 10-19.
24. Ennis, C. J.; Reynolds, J. C.; Keely, B. J.; Carpenter, L. J., A hollow cathode proton transfer reaction time of flight mass spectrometer. *International Journal of Mass Spectrometry* **2005**, *247* (1-3), 72-80.
25. Blake, R. S.; Whyte, C.; Hughes, C. O.; Ellis, A. M.; Monks, P. S., Demonstration of Proton-Transfer Reaction Time-of-Flight Mass Spectrometry for Real-Time Analysis of Trace Volatile Organic Compounds. *Analytical Chemistry* **2004**, *76* (13), 3841-3845.
26. Barber, S.; Blake, R. S.; White, I. R.; Monks, P. S.; Reich, F.; Mullock, S.; Ellis, A. M., Increased Sensitivity in Proton Transfer Reaction Mass Spectrometry by Incorporation of a Radio Frequency Ion Funnel. *Analytical Chemistry* **2012**, *84* (12), 5387-5391.

PART III: CONCLUSIONS AND FUTURE WORK

CHAPTER 8

CONCLUDING REMARKS

Driven by the questions that arose from the initial works on proton transfer reaction-mass spectrometry (PTR-MS) and its application to the detection of explosive compounds,^{1,2} and the weaknesses of the technology at the beginning of this PhD programme, the present thesis had the demanding aim of overcoming a number of limitations to make the PTR-MS technique more multidimensional and applicable to real life scenarios. For such purposes, the work presented in this thesis investigated new analytical methodologies and instrumental developments to improve selectivity and sensitivity in the detection of explosive related compounds when using PTR-MS as the detection technology. More specifically the purpose of this thesis covered three aspects related to these developments:

1. In collaboration with Ionicon Analytik GmbH we investigated improvements in selectivity by using different reagent ions other than H_3O^+ , such as O_2^+ , NO^+ and Kr^+ . We explored their reactivity to a series of explosive compounds and more specifically to picric acid.
2. In collaboration with KORE Technology Ltd. we developed a new inlet PTR-MS system for particulate matter to be used with commercial swabs that allow efficient fast cycle times and use for low volatile compounds thereby improving sensitivity to be comparable to that of ion mobility spectrometry (IMS).
3. In collaboration with KORE Technology Ltd. and Dstl we have demonstrated how selectivity can be enhanced by changing product ions and/or their intensities through collisional induced dissociation processes either with a novel radio-frequency ion funnel implemented drift tube or by quickly switching the reduced electric field. KORE Technology Ltd. designed and developed the hardware and associated software.

This Chapter summarises the key findings from the empirical studies described in Part II (pages 67-165) of this thesis and identifies practical implications and general limitations that arise from the work done. This leads onto Chapter 9 (pages 175-180), which discusses possible directions for future work.

8.1. Summary of Research Findings and their Implications

8.1.1. Use of different reagent ions

In order to investigate improvements in the selectivity of PTR-MS for the detection of explosive compounds, namely TNT, 1,3,5-TNB, PETN and RDX, using different reagent ions, an Ionicon SRI-PTR-ToF-MS instrument,^{3,4} was used. This instrument allowed us to quickly (within seconds) switch between different reagent ions, namely H_3O^+ , O_2^+ and NO^+ . This is possible because the recombination energies of O_2^+ and NO^+ are less than the ionisation potential of H_2O . Rapid switching of reagent ions is not possible if the recombination energy of a reagent ion is greater than that of water or the major constituents of air. The use of different reagent ions leads to the production of different product ions owing to the different reaction channels. We have demonstrated how this enhances compound assignment. Furthermore, this work has shown that this technique could be used in security areas owing to the speed at which switching can occur.

The observed reaction processes for the compounds studied are:

- non-dissociative charge transfer between O_2^+ and TNT and 1,3,5-TNB
- dissociative charge transfer for O_2^+ with TNT
- adduct formation for NO^+ with PETN and RDX
- O_2^+ does not react with PETN and RDX, and neither does TNB with NO^+ .

Under the experimental conditions used only a small signal for $\text{TNT}\cdot\text{NO}^+$ was observed.

Although it might be useful to quickly switch reagent ions and therefore have different product ions for each reagent ion, it could be just as advantageous (if not more so) to have both (or more) reagent ions injected into the reaction chamber simultaneously.^{5,6} Thus, different product ions from different reagent ions would be observed simultaneously.

In Chapter 4 the use of different reagent ions, namely, NO^+ , H_3O^+ , O_2^+ and Kr^+ were applied to PiA using an Ionicon SRI-PTR-ToF-MS.⁷ This work was relevant as PiA and TNT and TNB structures are very similar and could mirror the interesting ion chemistry observed for these two explosives. NO^+ forms a simple adduct ion, $\text{PiA}\cdot\text{NO}^+$. H_3O^+ reactions showed that PiA reacts via non-dissociative proton transfer to form PiAH^+ . Both O_2^+ and Kr^+ react with PiA by non-dissociative charge transfer to ultimately produce PiA^+ . However, when using

Kr^+ , dissociation of PiA occurred, leading to NO_2^+ with a branching percentage of approximately 40% across the 60-110 Td range investigated. For the reagent ions H_3O^+ and O_2^+ (using laboratory air as the carrier gas), intensities of PiAH^+ and PiA^+ ions both exhibit a peak at a given drift-tube voltage (which is humidity dependent).⁷ Aided by electronic-structure calculations and previous studies of TNT and TNB,⁸ it is suggested that once $\text{PiAH}^+\cdot\text{H}_2\text{O}$ and $\text{PiA}^+\cdot\text{H}_2\text{O}$ are able to be formed, secondary ion reactions with water lead to a product ion ($\text{H}_3\text{O}^+\cdot\text{H}_2\text{O}$) that no longer contains picric acid.⁸ This unusual behaviour implies a peak in the detection sensitivity of PiA as a function of the drift-tube voltage.

8.1.2. New thermal desorption unit inlet system

An innovative thermal desorption unit (TDU) was purposely designed, developed and tested for trace detection of explosives using PTR-MS. This hardware add-on was applied to EGDN, 1,3-DNB, 3,4-DNT, HMTD, 1,3,5-TNB, RDX, NG, TNT and PETN showing the possibility of analysing low volatility explosive compounds. The TDU/PTR-MS showed for them all instrumental limits of detection in the traces (nanograms or less) region. Memory effects were also investigated and shown to be acceptable in relation to possible use in a security area, namely the base line recovered in less than 60 seconds for all compounds, with the exception of RDX. The combination of TDU and PTR-MS offers an alternative friendly to use sampling method for analysing particulate matter which could also be contained in a liquid substrate. This opens up the possibility for the TDU-PTR-MS to be applied to other scientific areas such as atmospheric chemistry. The TDU unit desorbs any spotted particulate material on the surface of the swab within less than a second upon insertion into the TDU.⁹ For a short period of time (seconds) a concentration “pulse” of an explosive enters the drift (reaction) tube of the PTR-MS. This temporal concentration pulse of material is monitored in real-time by recording the protonated parent ion and/or product(s) ion(s) intensities for a given explosive. By changing the reduced electric field in the drift tube region of the PTR-MS selectivity can be improved, and this was illustrated for the isobaric compounds NG and TNT – this being the proof of principle for the fast E/N switching project. This study demonstrated that the TDU/PTR-MS instrument meets security application criteria in terms of sensitivity, selectivity and recovery times.¹⁰

An observed limitation is that there are still some memory effects for some of the less volatile explosive compounds. In IMS an analysis cycle time is around 10-15 seconds,^{11,12} and that is still not achievable with this system for some compounds. There is, however, still room

for improving this. For example at present the instrument's oven temperature is limited to 150 °C. Increasing this to 200 °C is possible.

8.1.3. Enhancing sensitivity and selectivity through changes to collisional induced dissociation processes

A key issue with any analytical system based on mass spectrometry with no pre-separation of compounds is to have a high level of confidence in chemical assignment. Proton transfer reaction mass spectrometry (PTR-MS) is a useful technology for these purposes because false positives are reduced compared to IMS owing to the use of a mass spectrometric analysis. However, the detection of an ion at a given m/z for an explosive does not guarantee that that explosive is present. There is still some ambiguity associated with any chemical assignment owing to the presence of isobaric compounds and isomers. A possible way to improve selectivity without losing the real time capability advantage of PTR-MS is to manipulate the ion chemistry occurring in the reaction chamber. Thus different product ions (or changes in their intensities) can be used to aid identification. A number of methods to achieve this have been proposed and adopted. One has already been discussed, and includes the use of different reagent ions. Other alternatives include making changes to the collisional induced dissociation processes. This can be achieved by different means, and we explored two methods:

- a) The use of a radio frequency ion-funnel (RFIF) system. The main purpose of the RF field is to focus ions radially by creating repulsive effective potentials at the edges of the electrodes. However, in addition to this intended purpose, the RF results in ions oscillating between electrodes as they drift down the reactor. This gives ions higher collisional energies than those in the first half of the drift tube. It is hypothesised that changes would result from raising the internal energy of the product ions and the energy of the reactions between reagent ions and neutral species through collisional processes as a result of the applied RF field. Results for a series of nitro-aromatic (mono-, di- and tri-nitrotoluene) compounds that exhibited the *ortho*-effect on their structures,¹³⁻¹⁵ were presented to demonstrate the advantages of this new RFIF-PTR-ToF-MS for analytical chemical purposes.
- b) Switching the reduced electric field, which is the key parameter in the operation of PTR-MS. By changing the reduced electric field from a low (approximately 80 Td) to a

high value (greater than 180 Td) differences in product ion distributions can occur, which can be used to aid in the identification of the trace neutral responsible for those ions. The simplest way to provide a rapid change in E/N is to alter the E field by quickly changing the voltage applied across the drift tube. Thus, hardware and software were developed by KORE Technology Ltd. to rapidly switch (< 250 ms at a frequency of 0.5-5 Hz) the reduced electric field, to improve instrumental selectivity, specifically focussing on explosive compounds, namely 2,4 and 2,6-DNT, HMTD, RDX, PETN. It has been shown how this technique provides an improved selectivity for explosives, thereby leading to a higher confidence in their identification in complex chemical environments than it would be possible by keeping only to one reduced electric field value. This switching of reduced electric field makes full use of the real-time measurement capabilities of PTR-MS and adds a new dimension to the analytical technique. Furthermore, the combination of the new drift tube voltage switching capabilities with RFIF provides further improvement in selectivity for TNT. This combination of switching capabilities and RFIF to PTR-MS opens up other possibilities for improved selectivity at little cost to the manufacture of the PTR-MS instrument.

In summary, the new analytical methodologies which have been proposed, developed and adopted have contributed to the development of the next PTR-MS generation of instruments. PTR-MS can only evolve further for security applications if a compact and cheaper system is developed. The work presented here provides useful tools for the development of low mass resolution instruments, transforming PTR-MS into a more versatile and multidimensional technique.

8.2. References

1. Mayhew, C. A.; Sulzer, P.; Petersson, F.; Haidacher, S.; Jordan, A.; Märk, L.; Watts, P.; Märk, T. D., Applications of proton transfer reaction time-of-flight mass spectrometry for the sensitive and rapid real-time detection of solid high explosives. *International Journal of Mass Spectrometry* **2010**, 289 (1), 58-63.
2. Jürschik, S.; Sulzer, P.; Petersson, F.; Mayhew, C. A.; Jordan, A.; Agarwal, B.; Haidacher, S.; Seehauser, H.; Becker, K.; Märk, T. D., Proton transfer reaction mass

spectrometry for the sensitive and rapid real-time detection of solid high explosives in air and water. *Anal Bioanal Chem* **2010**, 398 (7-8), 2813-2820.

3. Jordan, A.; Haidacher, S.; Hanel, G.; Hartungen, E.; Herbig, J.; Märk, L.; Schottkowsky, R.; Seehauser, H.; Sulzer, P.; Märk, T. D., An online ultra-high sensitivity Proton-transfer-reaction mass-spectrometer combined with switchable reagent ion capability (PTR + SRI – MS). *International Journal of Mass Spectrometry* **2009**, 286 (1), 32-38.

4. Jordan, A.; Haidacher, S.; Hanel, G.; Hartungen, E.; Herbig, J.; Märk, L.; Schottkowsky, R.; Seehauser, H.; Sulzer, P.; Märk, T. D., An online ultra-high sensitivity Proton-transfer-reaction mass-spectrometer combined with switchable reagent ion capability (PTR + SRI – MS). *International Journal of Mass Spectrometry* **2009**, 286 (1), 32-38.

5. González-Méndez, R.; Watts, P.; Olivenza-León, D.; Reich, D. F.; Mullock, S. J.; Corlett, C. A.; Cairns, S.; Hickey, P.; Brookes, M.; Mayhew, C. A., Enhancing proton transfer reaction-mass spectrometry selectivity using rapid reduced electric field switching. *In preparation*. **2017**.

6. Molecular Physics Research Group (University of Birmingham), Internal document. Simultaneous multiple reagent ions (MRI) PTR-MS. **2016**.

7. Agarwal, B.; González-Méndez, R.; Lanza, M.; Sulzer, P.; Märk, T. D.; Thomas, N.; Mayhew, C. A., Sensitivity and Selectivity of Switchable Reagent Ion Soft Chemical Ionization Mass Spectrometry for the Detection of Picric Acid. *The Journal of Physical Chemistry A* **2014**, 118 (37), 8229-8236.

8. Sulzer, P.; Petersson, F.; Agarwal, B.; Becker, K. H.; Jürschik, S.; Märk, T. D.; Perry, D.; Watts, P.; Mayhew, C. A., Proton Transfer Reaction Mass Spectrometry and the Unambiguous Real-Time Detection of 2,4,6 Trinitrotoluene. *Analytical Chemistry* **2012**, 84 (9), 4161-4166.

9. González-Méndez, R.; Reich, D. F.; Mullock, S. J.; Corlett, C. A.; Mayhew, C. A., Development and use of a thermal desorption unit and proton transfer reaction mass spectrometry for trace explosive detection: Determination of the instrumental limits of detection and an investigation of memory effects. *International Journal of Mass Spectrometry* **2015**, 385, 13-18.

10. Rhykerd, C. L.; Hannum, D. W.; Murray, D. W.; Parmeter, J. E., Guide for the Selection of Commercial Explosives Detection Systems for Law Enforcement Applications **1999**, NIJ Guide 100-99.

11. Zhou, Q.; Peng, L.; Jiang, D.; Wang, X.; Wang, H.; Li, H., Detection of Nitro-Based and Peroxide-Based Explosives by Fast Polarity-Switchable Ion Mobility Spectrometer with Ion Focusing in Vicinity of Faraday Detector. *Scientific Reports* **2015**, *5*, 10659.
12. Peng, L.; Hua, L.; Wang, W.; Zhou, Q.; Li, H., On-site Rapid Detection of Trace Non-volatile Inorganic Explosives by Stand-alone Ion Mobility Spectrometry via Acid-enhanced Evaporization. *Scientific Reports* **2014**, *4*, 6631
13. Fujita, T.; Nishioka, T., The analysis of the ortho effect. *Prog. Phys. Org. Chem* **1976**, *12*, 49-89.
14. Bulusu, S.; Axenrod, T., Electron impact fragmentation mechanisms of 2,4,6-trinitrotoluene derived from metastable transitions and isotopic labeling. *Organic Mass Spectrometry* **1979**, *14* (11), 585-592.
15. Gross, J. H., *Mass Spectrometry. A textbook*. 2nd ed.; Springer: 2011; p 305.

CHAPTER 9

FUTURE WORK

9.1. Potential new research lines

Based on the work presented, there are several potential directions for future projects. The key goal is to focus on developing new analytical protocols/methodologies and instrumental developments for enhancing sensitivity and chemical specificity by manipulating the ion/molecule chemistry occurring within a DT. Thus, it is possible to tailor the occurring chemistry to target a particular analyte without the need for expensive high resolution instruments to separate isobaric compounds and/or interferences. This is a step change in the analytical use of soft chemical ionisation mass spectrometry (SCIMS) suitable for commercial and research exploitation.

Among a number of possible ways forward there are several which are particularly worthy of highlighting:

- (i) Use of negative ion mode as a new way to generate different reagent ions. Once they are created new reaction mechanisms would result, leading to different product ions, which would aid identifying a targeted molecule. A proof-of-principle study by Shen *et al.*,¹ showed how a PTR-MS instrument can be run in negative ion mode, creating OH⁻ anions from water vapour in a conventional PTR-MS (no further modifications needed). OH⁻, as a proton acceptor, can extract a proton from the organic compound (denoted by M) to generate a product ion [M-H]⁻,^{2,3} following the chemical reaction $\text{OH}^- + \text{M} \rightarrow [\text{M-H}]^- + \text{H}_2\text{O}$. This can be either a dissociative or non-dissociative proton transfer extraction reaction.¹ We propose that fast switching from positive ion mode to negative ion mode and viceversa (similarly as shown in Chapter 7) would enhance selectivity. Although IMS routinely uses negative mode for the detection of explosives, to my knowledge, nobody has explored this mode for explosives in PTR-MS. In IMS DT, the high pressure results in complex, competing chemical ionisation reactions.^{4,5} At ~1 mbar pressure this will not be the case, and the reagent ion will be greatly in excess compared to the analyte. We are not aware of data produced from explosives in negative mode for chemical reactors having < 1 mbar pressure and this will open a new area of research.
- (ii) Improvements of the sensitivity and selectivity of PTR-MS instruments using an ion funnel. Preliminary, proof-of-concept studies (results shown in Chapter 6),⁶ are

encouraging and serve to illustrate how this new hardware development may be utilised to manipulate ion-molecule processes in a selective way, thus modifying fragmentation and hence increasing the selectivity of the PTR-MS instrument. Research is required to investigate whether the improved selectivity observed for some of the explosive compounds investigated in this thesis will be of general relevance. Combined with DC-only mode operation (switching modes between RF and DC), a much higher level of confidence in compound assignment is possible. Further investigations are required to probe the effects of RF field strength, frequency, different reagent ions and dependences on pressure and humidity. Changes in drift tube design need to be investigated. For example, there could be considerable advantage in having the whole drift tube as a RFIF rather than the current design which has only the last half to which an RF can be applied.

- (iii) Development of a multiple reagent ion mass spectrometer (MRI-MS) for use as a soft chemical ionisation analytical device to improve selectivity and deliver capabilities to have simultaneous detection of all analytes of interest. Most researchers in the field of PTR-MS have long advocated using selected reagent ions to increase the range of molecules that can be ionised by chemical ionisation reactions. The two most widely used reagent ion beams currently in use are H_3O^+ and O_2^+ (with NO^+ taking relevance recently^{7,8}). What is now being proposed is that we go forward and deliberately use two or more reagent ions simultaneously in the drift tube. The use of multiple reagent ions is possible because the reaction mechanisms are different: proton transfer (non-dissociative or dissociative) for H_3O^+ and non-dissociative/dissociative electron transfer from the neutral to O_2^+ . An ion source capable of generating simultaneously high currents of different reagent ions simultaneously would need to be developed. This is currently one of the proposals being investigated through a H2020 ITN called IMPACT.⁹
- (iv) Reducing memory effects further (particularly for RDX) and studying how transfer temperature from swabs into the DT of the instrument affects the performance of the measurements. A temperature dependent study would provide information as to when thermal decomposition of an explosive occurs and therefore optimize the ideal

temperature (or range of temperatures) at which the thermal desorption system should be operated.¹⁰

- (v) Extend PTR-MS for the high-sensitivity detection of other compounds of interest, such as drugs, CWAs and/or gun powders. There is a large list of banned substances, not only for baggage or persons, but also for cargo monitoring. Preliminary measurements investigating the basic components of gunpowder (methyl and ethylcentralite, diphenylamine, N-nitrosodiphenylamine, 2-nitrodiphenylamine and 4-nitrodiphenylamine) have been undertaken by us, and these show promising results.¹¹ Further work would potentially lead to a method to be applied for use in forensic analysis, i.e. after a firearm discharge.
- (vi) Sampling is one of the most crucial steps on any analytical protocol.¹² Therefore, ensuring that this step is done properly is vital. In security applications swabs are commonly used to sample particulates, but swabbing is not always possible as requires physical contact between sample and swab. In a variety of other applications trap tubes are used to sample vapours. Using trap tubes, with a chosen sorbent material (that can be Tenax®, Carbopack®, HayeSep® for naming a few), for security applications could be advantageous.¹³ The idea is that a combination of a pocket-size pumping system attached to, for example, a container vessel, goods pack or other enclosed goods would sample the air in contact with the goods for a set time before shutting off. After that a rapid desorption and screening method operating nearby would allow screening of the various items in a timely manner. This would not be only limited to trap tubes, but other alternative is the use of solid-phase microextraction fibers (SPME).¹⁴

9.2. References

1. Shen, C.; Niu, W.; Huang, C.; Xia, L.; Lu, Y.; Wang, S.; Wang, H.; Jiang, H.; Chu, Y., Proton-extraction-reaction mass spectrometry (PER-MS) for monitoring organic and inorganic compounds. *International Journal of Mass Spectrometry* **2014**, *371* (0), 36-41.

2. P. Spanel, M. Pavlik, D. Smith, Reactions of H_3O^+ and OH^- ions with some organic-molecules applications to trace gas analysis in air. *International Journal of Mass Spectrometry* **1995**, 145, 177–186.
3. R. Thomas, Y. Liu, C.A. Mayhew, R. Peverall, Selected ion flow tube studies of the gas-phase reactions of O^- , O_2^- and OH^- with a variety of brominated compounds. *International Journal of Mass Spectrometry* **1996**, 155, 163–183.
4. Watts, P., Studies on gas-phase negative ion/molecule reactions of relevance to ion mobility spectrometry: kinetic modelling of the reactions occurring in “clean” air. *International Journal of Mass Spectrometry and Ion Processes* **1992**, 121 (1–2), 141-158.
5. Bell, A.; Giles, K.; Moody, S.; Watts, P., Studies on gas-phase positive ion—molecule reactions of relevance to ion mobility spectrometry. The reactions of 2-methyl-2-propanol (t-butyl alcohol) with protonated water clusters in an ion mobility system. *International journal of mass spectrometry and ion processes* **1998**, 173 (1), 65-70.
6. González-Méndez, R.; Watts, P.; Olivenza-León, D.; Reich, D. F.; Mullock, S. J.; Corlett, C. A.; Cairns, S.; Hickey, P.; Brookes, M.; Mayhew, C. A., Enhancement of Compound Selectivity Using a Radio Frequency Ion-Funnel Proton Transfer Reaction Mass Spectrometer: Improved Specificity for Explosive Compounds. *Analytical Chemistry* **2016**, 88 (21), 10624-10630.
7. Koss, A. R.; Coggon, M. M.; Veres, P. R.; de Gouw, J. A., Evaluation of NO^+ reagent ion chemistry for online measurements of atmospheric volatile organic compounds. *Atmospheric Measurement Techniques* **2016**, 9 (7), 2909.
8. Inomata, S.; Tanimoto, H.; Yamada, H., Mass Spectrometric Detection of Alkanes Using NO^+ Chemical Ionization in Proton-transfer-reaction Plus Switchable Reagent Ion Mass Spectrometry. *Chemistry Letters* **2014**, 43 (4), 538-540.
9. Marie Skłodowska-Curie Actions. Horizon 2020. Innovative Training Network “IMPACT”. <http://impact-h2020itn.com/> (accessed 20-010-2017).
10. Najarro, M.; Morris, M. E. D.; Staymates, M. E.; Fletcher, R.; Gillen, G., Optimized thermal desorption for improved sensitivity in trace explosives detection by ion mobility spectrometry. *Analyst* **2012**, 137 (11), 2614-2622.
11. González-Méndez, R.; Watts, P., Mayhew, C. A. Unpublished data from Molecular Physics Research Group (University of Birmingham), **2017**.

12. Mitra, S., *Sample preparation techniques in analytical chemistry*. John Wiley & Sons: 2004; Vol. 237.
13. Grate, J. W.; Ewing, R. G.; Atkinson, D. A., Vapor-generation methods for explosives-detection research. *TrAC Trends in Analytical Chemistry* **2012**, *41*, 1-14.
14. Lai, H.; Leung, A.; Magee, M.; Almirall, J. R., Identification of volatile chemical signatures from plastic explosives by SPME-GC/MS and detection by ion mobility spectrometry. *Analytical and Bioanalytical Chemistry* **2010**, *396* (8), 2997-3007.

APPENDICES

[Redacted]

[Redacted]

[Redacted]

[Redacted]

[Redacted]

[Redacted]

[Redacted]

[Redacted]

[Redacted]

[Redacted]

[Redacted]



[Redacted]

[Redacted]

[Redacted]

[Redacted]

[Redacted]

[Redacted]

[Redacted]

[Redacted]

[Redacted]

[Redacted]

[Redacted]

[Redacted]

[Redacted]

[Redacted]

[Redacted]

[Redacted]

[Redacted]

[Redacted]

[Redacted]

[Redacted]

[Redacted]

[Redacted]

[Redacted]

[Redacted]

[Redacted]

[Redacted]

[Redacted]

[Redacted]

[Redacted]

[Redacted]

[Redacted]

[Redacted]

[Redacted]

[Redacted]

[Redacted]

[Redacted]

[Redacted]

[Redacted]

[Redacted]

[Redacted]

[Redacted]

[Redacted]

[Redacted]

[Redacted]

[Redacted]

[REDACTED]

[REDACTED]

[REDACTED]

- [REDACTED]
- [REDACTED]
- [REDACTED]

[REDACTED]

[REDACTED]

[REDACTED]

[REDACTED]

[REDACTED]

